PCB TMDL MODEL FOR THE POTOMAC RIVER ESTUARY

Draft Final Report on Hydrodynamic/Salinity and PCB Transport and Fate Models

EPA Contract No. 68-C-03-041
Work Assignment No. 4-34

September 19, 2007

Prepared for:

Region III
U.S. Environmental Protection Agency
Water Management Division
Office of Watersheds (3WP12)
1650 Arch Street
Philadelphia, PA 19103

Through:

Oceans and Coastal Protection Division
U.S. Environmental Protection Agency
1200 Pennsylvania Ave., NW
Washington, D.C. 20460

Prepared by:

LimnoTech
2109 Rolling Road
Greensboro, NC 27403
(336) 274-2688
E-mail: vbierman@limno.com

Through:

BATTELLE
397 Washington Street
Duxbury, MA 02332
(781) 934-0571

TABLE OF CONTENTS

ABBREVIATIONS

ADF	Advection factor
AFL	Above fall line
ANAC	Anacostia spatial zone
ANS	Academy of Natural Sciences, Philadelphia
BAF	Bioaccumulation factor
BAT	Battelle Laboratory
BFL	Below fall line
BIC	Biotic (algal) carbon
BOD	Biological oxygen demand
CBL	University of Maryland Chesapeake Biological Laboratory
CBP	Chesapeake Bay Program
CBWQM	Chesapeake Bay Water Quality Model
C:CHL	Carbon to chlorophyll *a* ratio
CFD	Cumulative frequency distribution
cfs	Cubic feet per second
CH3D	Chesapeake Bay Hydrodynamic Model
Chl *a*	Chlorophyll *a* concentration
CSO	Combined sewer overflow
CWA	Clean Water Act
DC	District of Columbia
DCDOE	District of Columbia Department of the Environment
DC WASA	District of Columbia Water and Sewer Authority
DD	Direct drainage
DEM	Dynamic Estuary Model
DOC	Dissolved organic carbon
DRBC	Delaware River Basin Commission
DYNHYD	Dynamic Estuary Hydrodynamic Model
EPA	U.S. Environmental Protection Agency
ERDC	Engineer Research and Development Center, Vicksburg, MS
ETM	Estuarine turbidity maximum
FIPS	Federal Information Processing Standard
GERG	Geochemical and Environmental Research Group, Texas A&M
GMU	George Mason University
GPP	Gross primary production
g/yr	Grams per year
H	Henry's Law Constant
HOC	Hydrophobic organic chemical
HOT	Head of tide
ICPRB	Interstate Commission on the Potomac River Basin
IS	Inorganic solids
Kdoc	Partition coefficient to dissolved organic carbon
Koc	Partition coefficient to particulate organic carbon
LA	Load allocation
LOWESS	Locally weighted least squares

LPOTMH	Lower Potomac mesohaline spatial zone
LPOTTF	Lower Potomac tidal fresh spatial zone
LTCP	Long Term Control Plan (District of Columbia)
LTI	LimnoTech
MD	State of Maryland
MDE	Maryland Department of the Environment
MDNR	Maryland Department of Natural Resources
MOS	Margin of Safety
MS4	Municipal Separate Storm Sewer Systems
MW	Molecular weight
MWCOG	Metropolitan Washington Council of Governments
ng/g	Nanograms per gram
ng/l	Nanograms per liter
NOAA	National Oceanic and Atmospheric Administration
NPDES	National Pollutant Discharge Elimination System
NSWC	Indian Head Naval Surface Warfare Center at Indian Head
PC	Particulate carbon
PCB	Polychlorinated biphenyls
PCB3+	Sum of PCB homologs 3-10
PDC	Particulate detrital carbon
PMP	Pollutant Minimization Plans (Virginia)
POC	Particulate organic carbon (sum of BIC and PDC)
POTMH	Potomac mesohaline spatial zone
POTOH	Potomac oligohaline spatial zone
POTPCB	Potomac PCB model
POTTF	Potomac tidal fresh spatial zone
ppb	Parts per billion
ppt	Parts per thousand (salinity)
RM	River mile
RUSLE2	Revised Universal Soil Loss Equation, Version 2
SOD	Sediment oxygen demand
SPMD	Semi-Permeable Membrane Device
SWMP	Stormwater Management Plan (District of Columbia)
TMDL	Total maximum daily load
TOC	Total organic carbon (sum of POC and DOC)
TOXI5	Toxic chemical module in WASP
TRIB	Minor Tributaries spatial zone
TS	Total solids
TSCA	Toxic Substances Control Act (Virginia)
TSP	Total suspended particulates
TSS	Total suspended solids
UOSA	Upper Occoquan Sanitation Authority Wastewater Treatment Plant
UPOTMH	Upper Potomac mesohaline spatial zone
UPOTTF	Upper Potomac tidal fresh spatial zone
USACE	U.S. Army Corps of Engineers
USDA	U.S. Department of Agriculture

USGS	U.S. Geological Survey
VA	Commonwealth of Virginia
VADCR	Virginia Department of Conservation and Recreation
VADEQ	Virginia Department of Environmental Quality
VEERF	Virginia Environmental Emergency Response Fund
WASP	Water Quality Analysis Simulation Program
WLA	Wasteload Allocation
WM5	Chesapeake Bay Watershed Model, Phase 5
WQA	Water quality analysis
WQBEL	Water quality based effluent limit
WQLS	Water Quality Limited Segment
WQS	Water quality standard
WRAS	Watershed Restoration Action Strategy Program (Maryland)
WSE	Water surface elevation (tidal height)
wt	Weight
WWTP	Wastewater treatment plan

EXECUTIVE SUMMARY

The Potomac River estuary was listed as impaired under Section 303(d) of the Clean Water Act due to the levels of polychlorinated biphenyls (PCBs) in the tissues of resident fish species. The impaired region includes the tidal freshwater portions of the Anacostia and Potomac rivers, and extends approximately 118 miles downstream to the mouth of the Potomac Estuary at Chesapeake Bay. As per a court order, a Total Maximum Daily Load (TMDL) for PCBs needs to be developed by the District of Columbia (DC), and approved by EPA no later than September, 2007. This project was complicated by many factors including the complexity of the system, limited available data on loadings and ambient concentrations, limited resources, and a very ambitious schedule.

This report describes the development, calibration and validation of a PCB water quality model for the tidal freshwater portions of the Potomac and Anacostia rivers that was used to determine the PCB TMDL. The principal goals of the modeling effort were scientific understanding and management utility. The first goal involved gaining an understanding of the principal environmental processes influencing the transport and fate of PCBs in the Potomac and Anacostia. The second goal involved assessment of various PCB load reduction scenarios to determine the external PCB loads that can enter the system and still meet the applicable TMDL targets. To meet these goals the model must be scientifically credible and satisfy all regulatory requirements.

The overall conceptual approach was an integrated modeling framework that includes hydrodynamics, salinity, sorbent dynamics and PCB transport and fate. The underlying premise is that the transport and fate of toxic chemicals, especially hydrophobic organic chemicals (HOCs) like PCBs, are strongly influenced by sorption to organic carbon and interactions between the water column and bedded sediments. In this framework, separate balances are conducted in series for water, salinity, sorbents (as organic carbon) and PCBs.

The water quality model is two dimensional in the horizontal direction and includes 257 discrete spatial segments that encompass the tidal Potomac and Anacostia rivers, their tidal tributaries, and numerous embayments. The model spatial grid includes separate representation of the main channel (Maryland waters), the DC portion of the main channel, and various embayments, tributaries and coves in both Virginia (VA) and Maryland (MD) waters. This detailed spatial representation was required because there are different water quality standards for PCBs in each of these three jurisdictions.

Hydrodynamic and salinity calibrations were conducted for 1996-1997 and 2002-2005. Sorbent and PCB calibrations were conducted for 2002-2005. Selection of these calibration periods was based primarily on availability of data for model inputs and for comparisons of computed results with observations.

The calibration strategy was to specify as many external inputs and internal parameters as possible using site-specific data or independent measurements, and only a minimal number of parameters through model calibration. Another part of the strategy was that parameters determined through model calibration were held spatially and temporally constant unless there

was supporting information to the contrary. Model parameters were not permitted to assume arbitrary values in order to obtain the best "curve fits" in a strictly mathematical sense. Where necessary, sensitivity analyses were conducted for model parameters over ranges consistent with the scientific literature, other modeling studies and best professional judgment to obtain optimal agreement between computed and observed values.

The assessment of model calibration results was a weight-of-evidence approach that relied on a suite of quantitative metrics and best professional judgment. No single metric provides sufficient information by itself to completely evaluate model calibration results. The metrics used here included cumulative frequency distributions, bivariate plots with lines of 1:1 correspondence, regression statistics, time series plots at fixed locations, spatial profiles at fixed points in time, comparisons of seasonal median values, and comparisons of computed first-order PCB loss rates with those from available historical data for PCB body burdens in benthic feeding fish.

Sensitivity analyses were conducted with the calibrated model to help identify the model inputs and parameters to which computed results for water column PCB concentrations were most sensitive. Results from these analyses provided greater understanding of the relative importance of controlling environmental processes. Sensitivity analyses were conducted for PCB mass loads from the Potomac River at Chain Bridge, and from direct drainage areas, combined sewer overflows (CSOs), point source discharges, and atmospheric wet and dry deposition to the water surface. Sensitivity analyses were also conducted for downstream boundary PCB concentrations, initial conditions for PCB concentrations in the sediments, and sediment-water mass transfer rates for dissolved phase PCBs.

The TMDL design conditions correspond to quasi-steady state, dynamic equilibrium among external PCB mass loads, and concentrations in the water column and sediments. Under these conditions there is no net flux of PCB across the air-water interface, and both the surface and deep sediment layers are net sinks for PCB, not sources. Diagnostic simulations were conducted with the calibrated model to evaluate the impact of legacy contamination in the sediments on current PCB concentrations in the water column, and the time required to achieve dynamic equilibrium. Results from these simulations indicated that approximately 50 years or more is required to reach the TMDL design conditions of quasi-steady state, dynamic equilibrium.

To better understand the sources, transport and fate pathways for PCBs in the system, results from the calibrated model were used to construct mass balance components for the principal spatial zones in the Potomac and Anacostia rivers. These components are organized in terms of external mass loads, net exchanges with external boundaries, and internal exchanges between the water column and sediments.

Given the model assumptions and the available data for model inputs and ambient water quality conditions, results from the calibrated model are a reasonable representation of seasonal magnitudes and spatial distributions for water surface elevation, salinity, organic carbon sorbents, and PCBs in the tidal Potomac and Anacostia Rivers. In consideration of the overall weight-of-evidence, the PCB TMDL Steering Committee judged that the model was scientifically credible and acceptable for use in developing the PCB TMDL.

1. INTRODUCTION

1.1 Background

The Potomac River estuary was listed as impaired under Section 303(d) of the Clean Water Act due to the levels of polychlorinated biphenyls (PCBs) in the tissues of resident fish species. The impaired region includes the tidal freshwater portions of the Anacostia and Potomac rivers, and extends approximately 118 miles downstream to the mouth of the Potomac Estuary at Chesapeake Bay (Figure 1). As per a court order, a Total Maximum Daily Load (TMDL) for PCBs needs to be developed by the District of Columbia (DC), and approved by EPA no later than September, 2007. As agreed by the States, the Interstate Commission on the Potomac River Basin (ICPRB) had the lead to develop the TMDL, working collaboratively with the States, EPA and local stakeholders ("The Parties") through the Potomac PCB TMDL Steering Committee.

This project is complicated by many factors including the complexity of the system, limited available data on loadings and ambient concentrations, limited resources, and a very ambitious schedule. A PCB water quality model was developed, calibrated, validated and applied to determine the PCB TMDL for the tidal freshwater portions of the Potomac and Anacostia rivers. Battelle Team member, LimnoTech, had the lead in conducting the PCB modeling work. In collaboration with the Steering Committee, ICPRB used results from forecast scenarios with the calibrated/validated model to develop the actual PCB TMDL. LimnoTech provided scientific and technical guidance/assistance to ICPRB and the Parties during the TMDL development process.

As a first step, LimnoTech was tasked by EPA to develop and summarize at least two options for the PCB modeling approach. LimnoTech considered options for approaches that vary in complexity from simple one-dimensional models to more complex multi-dimensional models (LimnoTech 2005). LimnoTech recommended a one-dimensional branched version of the DYNHYD5 hydrodynamic model, coupled to DELPCB, a modified version of the EPA WASP5/TOXI5 model that was applied to penta-PCBs in the Delaware River Estuary to support development of a Stage 1 TMDL (DRBC 2003a, 2003b, 2003c, 2003d).

These recommendations were approved by the Potomac PCB TMDL Steering Committee on September 29, 2005. The key criteria in approving these recommendations were sound science, data availability, use of the least complex tool that can answer the principal management questions, and maximizing the likelihood of success given the time frame and available resources.

1.2 Purpose of Report

This report describes the development and calibration of a coupled hydrodynamic, salinity, sorbent dynamics, and PCB mass balance model for the tidal portions of the Potomac and Anacostia rivers. It also includes results for sensitivity and diagnostic analyses, and mass balance components, to better understand the environmental processes underlying the observed ambient data.

1.3 Report Organization and Format

In terms of report organization, all tables are contained in Appendix A and all figures are contained in Appendix B.

The contents of the individual sections are as follows:

- Section 1 provides the report introduction;
- Section 2 presents the overall conceptual approach and descriptions of the individual models;
- Section 3 presents the physical data and hydrology used by the models;
- Section 4 presents results for calibration of the hydrodynamic model;
- Section 5 presents results for calibration of the mass balance model for salinity;
- Section 6 presents summaries of input mass loads for organic carbon sorbents and PCBs;
- Section 7 presents summaries of the ambient monitoring data used for model inputs and calibration targets;
- Section 8 presents results for calibration of the mass balance model for sorbents (organic carbon) and PCBs;
- Section 9 presents results for selected sensitivity analyses with the calibrated water quality model;
- Section 10 presents results for long-term diagnostic analyses with the calibrated water quality model; and,
- Section 11 presents results for mass balance components analyses for PCBs in the water column and sediments.

1.4 Modeling Goals and Objectives

The principal goals of this modeling effort were scientific understanding and management utility. The first goal involved gaining an understanding of the principal environmental processes influencing the transport and fate of PCBs in the tidal portions of the Potomac and Anacostia rivers. The second goal involved assessment of various PCB load reduction scenarios to determine the external PCB loads that can enter the system and still meet the applicable TMDL targets. To meet these goals the model must be scientifically credible and satisfy all regulatory requirements.

The specific objectives of this modeling effort were the following:

- Develop a mass balance model for PCB concentrations in the water column and bedded sediments of the tidal Potomac and Anacostia rivers;

- Calibrate the mass balance model to available historical data, including data collected to support this modeling effort;

- Conduct forecast simulations with the calibrated model to estimate responses of water column and sediment PCB concentrations to a range of scenarios for reductions in external PCB mass loads; and,

- Estimate the magnitudes and spatial distributions of external mass loads of PCBs that will meet the TMDL targets under the specified TMDL conditions.

2. MODELING APPROACH

2.1 Integrated Modeling Framework

The overall conceptual approach is an integrated modeling framework that includes hydrodynamics, sorbent dynamics and PCB transport and fate (Figure 2). The underlying premise is that the transport and fate of toxic chemicals, especially hydrophobic organic chemicals (HOCs) like PCBs, are strongly influenced by sorption to organic carbon and interactions between the water column and bedded sediments. In this framework, separate balances are conducted in series for water, salinity, sorbents (as organic carbon) and PCBs.

The first operational step is calibration of the hydrodynamic model to data for tidal heights, and confirmation using the computed hydrodynamics to drive a mass balance model for salinity. The computed hydrodynamics, in terms of flows and tidal mixing coefficients, are then used as a "hydraulic chassis" to drive a mass balance model for sorbent dynamics. The sorbent dynamics model is calibrated to data for two different forms of particulate organic carbon and the computed sorbent dynamics, in terms of settling, resuspension and net burial, are then used as a "sorbent dynamics chassis" to drive a mass balance model for PCBs.

2.1.1 Conceptual Approach for Sorbent Dynamics

The conventional mass balance modeling approach is to represent total solids concentrations, often in terms of fine-grain (silt and clay) and coarse-grain (sand and gravel) size classes, and assign constant fractions of organic carbon to each class. Disadvantages of this approach are that much effort can be expended on determination of external solids loadings and sediment transport dynamics, and the required data are often not available to support such an approach. In addition, it is primarily fine-grain and not coarse-grain solids that are the important sorbents for HOCs. This is because fine-grain solids typically have much higher fractions of organic carbon than course-grain solids.

Another disadvantage of this conventional approach is that a large proportion of the organic carbon in aquatic systems can be produced internally by algal primary production, which is not represented in conventional models for total solids. One solution is to model both inorganic and algal-derived organic solids. A comprehensive approach requires inclusion of total external solids loadings, solids interactions with the sediment bed, primary production, and a sediment diagenesis model that represents transformation and ultimate fate of organic carbon.

For the sorbent dynamics model of the Potomac and Anacostia, a simplified approach is used that accounts for the principal organic carbon sorbents in the water column and sediments, and for net burial of solids and ultimate fate of organic carbon in the sediments (Figure 3). This approach builds upon the integrated exposure model for PCBs in Green Bay, Lake Michigan, developed by Bierman et al. (1992). Mass balances are conducted for biotic carbon (BIC) in the water column and particulate detrital carbon (PDC) in the water column and sediments. BIC represents particulate organic carbon contained in live algal biomass. PDC represents particulate detrital carbon derived from algal decomposition and allochthonous (watershed) sources.

Simplifications in the water column include external specification of dissolved organic carbon (DOC) concentrations and BIC loadings from primary production. DOC is included as a sorbent compartment in the water column and sediments, but is not included explicitly in the carbon mass balance equations. Simplifications in the sediment include external specification of temporally constant values for solids porosity and fraction organic carbon, and a first-order decay rate for PDC. The currency in this conceptual approach is organic carbon and not solids. This approach builds upon DePinto et al. (1993) by linking organic carbon and solids concentrations in the sediments. It accounts for net solids burial and losses of organic carbon to diagenesis, and constrains the relationship between these parameters to be consistent with observed sediment properties and sediment oxygen demand (SOD). It also allows translation of net organic carbon burial rates to equivalent net solids burial rates for comparison of model results to observed net deposition rates from dated sediment cores.

Model process mechanisms include BIC decay in the water column, PDC decay in the water column and sediments, BIC net settling, and PDC gross settling and resuspension. It is assumed that BIC is transformed to PDC when it enters the surface sediment by net settling. It is assumed that BIC decays to PDC but that PDC decay constitutes a loss of organic carbon from the system. This is because concentrations of DOC in the water column and sediments are not included in the carbon mass balance equations. That is, loss of organic carbon upon PDC decay is not explicitly represented as gain of organic carbon by DOC. Depending on the existence and direction of concentration gradients, diffusion of DOC can occur across the sediment-water interface and between sediment layers.

2.1.2 Sediment Sorbent Properties

Sediment sorbent properties are represented by the following equations:

$$TS = IS + PDC \tag{1}$$

$$foc = \frac{PDC}{TS} = \frac{PDC}{IS + PDC} \tag{2}$$

$$TS = \rho_s (1 - \phi) \cdot 10^6 = IS + PDC \tag{3}$$

where TS = total solids, mg/l;
IS = inorganic solids, mg/l;
PDC = organic solids, mg/l;
foc = mass fraction organic carbon, dimensionless
ρ_s = solids density, g/cm^3; and,
ϕ = porosity (water volume/bulk volume), dimensionless.

Solids density, porosity and fraction organic carbon are externally specified from site-specific data. Sediment PDC decay rate is determined using site-specific data for SOD which represents loss of organic carbon due to diagenesis. Constant solids density and porosity are equivalent to constant total solids concentration. Inorganic solids (IS) is a "pseudo" state variable whose only function is to serve as an adjustment parameter to maintain a constant fraction of organic carbon.

Sediment volume is variable and is used as an adjustment parameter to maintain constant porosity, or total solids concentration.

2.1.3 Conceptual Approach for PCBs

The conceptual framework for the PCB model (Figure 4) builds upon the organic carbon sorbents model. A mass balance is conducted for total PCB, a group of homologs, or an individual homolog or congener. Using equilibrium partitioning relationships, total PCB concentration is separated into four components, a freely dissolved aqueous phase and components sorbed to three types of organic carbon: biotic carbon (BIC), particulate detrital carbon (PDC) and dissolved organic carbon (DOC). Operationally, total dissolved PCB is the sum of the freely dissolved aqueous and DOC-bound phases. Process mechanisms for PCBs include fluxes of gas phase PCBs across the air-water interface and diffusion of PCBs across the sediment-water interface and between sediment layers. Diffusion of PCB can occur for both the freely dissolved and DOC-bound phases.

2.2 Model Implementation

2.2.1 Hydrodynamics

Hydrodynamics was implemented for the tidal Potomac and Anacostia rivers using a 1D branched version of DYNHYD5 (Ambrose et al. 1993a) coupled to a modified version of WASP5/TOXI5 (Ambrose et al. 1993b). This implementation closely followed the successful model implementation used for transport and fate of penta-PCBs in the Delaware River Estuary. Results from the Delaware modeling effort were judged acceptable by an expert panel of independent scientists and modeling practitioners, and the model was used to develop a Stage 1 TMDL for PCBs that was subsequently approved by EPA Regions 2 and 3. Complete results for the Delaware hydrodynamic and salinity models are presented in Delaware River Basin Commission (DRBC) (2003a). Complete results for the organic carbon sorbents and PCB models are presented in DRBC (2003b, 2003c) and summarized in Bierman et al. (2004a, 2004b, 2005).

DYNHYD5 is a link-node hydrodynamic model that is the successor to the Dynamic Estuary Model (DEM). DYNHYD5 solves the one-dimensional equations of continuity and momentum for a branching or channel-junction (link-node) computational network. The resulting unsteady predictions of hydraulic conditions are averaged over larger user-specified time intervals and stored in an output file that can be subsequently linked as the hydrodynamic driver to a WASP5-based water quality model (Ambrose et. al. 1993a, 1993b). The equation of motion, based on the conservation of momentum, computes water velocities and flows. The equation of continuity, based on the conservation of volume, computes water heights (heads) and volumes.

The one-dimensional framework of the model requires that the effects of the Coriolis force and other accelerations normal to the direction of flow be neglected. Other simplifications assume that hydraulic conditions can be adequately represented by wide rectangular channels and that bottom slopes are moderate. The equations of continuity and motion are solved at alternating grid points within the model network, providing velocities (U) and heads (H) throughout the water body over the period of simulation. At each time step, the equation of motion is solved for each channel, and the equation of continuity is solved at the junctions. For the linkage to

WASP5, the computed channel velocities and junction heads (or water surface elevations) are integrated over each water quality time step and converted to flows and volumes in order to provide the balanced advective flow conditions that serve as the "hydraulic chassis" for driving mass balance model calculations.

2.2.2 Water Quality

To represent organic carbon sorbent dynamics in the water column and sediments, the three existing solids state variables in WASP5/TOXI5 were converted to represent BIC, PDC and IS. The conversion involved changing these state variables from conservative to non-conservative in accordance with the kinetics in the organic carbon sorbent dynamics model (Figure 3 and Equations 1-3). DOC was externally specified and not included as a model state variable. Although IS is a "pseudo" state variable in this application, it is represented explicitly in the computer code because it is used as an adjustment parameter to maintain a constant fraction organic carbon in the sediments. The WASP5 variable volume option is used for the surface sediment layer to maintain constant porosity.

The computational approach consists of the following sequential steps:

1. When gross settling flux of organic carbon (from water column BIC and PDC) exceeds resuspension flux plus decay of sediment PDC, then PDC in the surface sediment layer increases due to net deposition.

2. Additional inorganic solids (IS) are added to the surface sediment layer to maintain a constant value of fraction organic carbon (Equation 2).

3. Volume of the surface sediment layer is increased to maintain a constant value of porosity (total solids concentration). This increase in volume affects only porosity and not fraction organic carbon.

4. Increase in surface sediment layer volume divided by sediment surface area corresponds to net deposition rate of total sediment solids.

This approach accounts for net solids burial and losses of organic carbon to diagenesis, and constrains the relationship between these parameters to be consistent with observed sediment properties. It also allows translation of net organic carbon burial rates to equivalent net solids burial rates for comparison of model results to observed net deposition rates from dated sediment cores.

It should be noted that apart from any limitations due to available data for model inputs or model calibration, this modeling approach has the following inherent limitations:

- One dimensional and vertically averaged;

- No representation of lateral spatial gradients within the main channel and/or within embayments, tributaries and coves;

- No representation of potential differences in sediment-water exchanges between the main channel and nearshore areas;

- No representation of the complex physical processes in the vicinity of the estuarine turbidity maximum (ETM);

- No representation of vertical stratification in the lower estuary; and,

- No explicit representation of sediment transport or suspended solids mass balance.

3. PHYSICAL DATA AND HYDROLOGY

3.1 Introduction

This section presents the sources for all physical data and hydrology required by the hydrodynamic, salinity, sorbents and PCB models. Water quality data requirements for the sorbent and PCB models are presented in Section 7.

Hydrodynamic and salinity model calibrations were conducted for 1996-1997 and 2002-2005. Sorbent and PCB model calibrations were conducted only for 2002-2005. Selection of these calibration periods was based primarily on availability of data for model inputs and comparisons of computed results with observations. The period 1996-1997 provided the best coverage for tidal observations because at least one NOAA tidal gage was operational in the Anacostia for a portion of 1996, and it also captured some tidal data in the lower Potomac that were not available in 2002-2005. Data for PCBs in the water column were available only for 2002 in the Anacostia and primarily for 2005 in the Potomac, although limited PCB data were also available in the Potomac for 2003 and 2003.

Bathymetry and freshwater inflows are needed for both the DYNHYD5 hydrodynamic and WASP5/TOXI5 water quality models. Data for water surface elevation (WSE), or tidal height, are needed to calibrate the hydrodynamic model. Air temperature and wind speed are needed as external inputs for the process mechanisms representing fluxes of gas phase PCBs across the air-water interface. Water temperature is needed for various chemical-biological reactions in the sorbent dynamics model.

3.2 Bathymetry

The coupled DYNHYD5/WASP5/TOXI5 model in this application, known as POTPCB, provides separate spatial representation of the main channel (Maryland waters), the DC portion of the main channel, and various embayments, tributaries and coves in both Virginia (VA) and Maryland (MD) waters. This detailed spatial representation is required because there are different water quality standards for PCBs in each of these three jurisdictions.

An important objective in designing the model spatial grid was to maintain as much consistency as possible among the various existing model spatial grids and available bathymetry data sets. Most of the POTPCB spatial grid is a superset of the spatial grid for the 57,000 cell (57K) version of the Chesapeake Bay Water Quality Model (CBWQM) currently being developed by the U.S. EPA Chesapeake Bay Program (EPA/CBP). This 57K version is a refinement to the 2002 Chesapeake Bay Eutrophication Model (Cerco and Noel 2004). The bathymetry for the Potomac portion of this grid is shown in Figure 5. Spatial grids from the TAM/WASP model of the Anacostia River (Mandel and Schultz 2000) and the Potomac version of the DEM (U.S. EPA 1979) were also used to provide higher spatial resolution in the vicinity of Washington, DC.

Bathymetry data were also obtained from the EPA/CBP (ftp://ftp.chesapeakebay.net/gis/bathymetry/). The original source for these data was NOAA bathymetry soundings for the Chesapeake Bay and tidal tributaries. These data contained no information on the reference vertical datum and were intended to be used only for depths of two

meters or less. These data were used to refine the model spatial grid for tidal portions of the VA tributaries.

3.3 Freshwater Inflows

For the Potomac River near head of tide, daily average flows measured at the USGS gage at Little Falls, VA, were used to specify freshwater inflows for the model. The periods of record for this station, along with those from the other gaging stations in the upper Potomac, are summarized in Table 1. Daily average flows at Little Falls, the largest source to the Potomac, are shown in Figures 6 and 7 for 1996-1997 and 2002-2005, respectively.

All other freshwater inflows from the watershed, including those from the Northeast (NE) and Northwest (NW) Branches of the Anacostia, were specified using output from the Phase 5 Watershed Model (WM5) and discharge information from point sources (Haywood and Buchanan 2007, Appendix A). WM5 inflows were mapped to the DYNHYD5 model segments by ICPRB and daily flow time series were provided to LimnoTech. These daily time series were used to specify daily freshwater inflows to all model junctions downstream of the fall line boundaries for the 1996-1997 and 2002-2005 calibration periods.

3.4 Water Surface Elevation

Available data for WSE were obtained from NOAA (http://www.co-ops.nos.noaa.gov/data_res.html). Four tide stations with verified observed hourly tidal heights were located within the model domain for at least some portions of the two model calibration periods. These gages are located at Lewisetta, Colonial Beach, and the Washington DC Ship Channel in the Potomac, and at Bladensburg in the Anacostia (Figure 8). Hourly tidal heights were downloaded based on Local Standard Time (LST), units of meters, and Mean Lower Low Water (MLLW) datum. Water surface elevation data sets were then converted to the NAVD88 datum. A summary of the available water surface elevation data with DYNHYD5 model junction information is contained in Table 2.

Data from the Lewisetta gage were used to specify the downstream tidal boundary condition for the DYNHYD5 model. This gage is located approximately 8.5 miles above the mouth of the Potomac River Estuary, so the hourly tidal data required adjustment to reflect this distance. NOAA has developed regression methods which are used to provide high and low tide predictions at locations within estuarine systems that are based upon reference gages. In the Potomac, the Washington Ship Channel gage serves as the reference gage for prediction of tidal conditions at other locations within the estuary.

The NOAA relationships between this reference gage and the other locations within the Potomac were evaluated with respect to both the phasing and the magnitude of high and low tide, as described in Table 3. This assessment revealed a strong correlation between distance from the reference gage and the timing of low and high tide, but no predictable correlation for the tidal range. Therefore, the DYNHYD5 downstream boundary condition was determined by shifting the observed hourly tidal heights at Lewisetta backwards in time by 34.778 minutes, but no vertical adjustment of the hourly observations was made.

3.5 Salinity

The EPA/CBP water quality database (http://www.chesapeakebay.net/data/index.htm) was the primary source for the required external forcing conditions and ambient monitoring data for salinity. These EPA/CBP monitoring stations extend for almost the entire length of the estuary (Figure 8) and are sampled bi-weekly each year, generally from late April or early May through October or early November. An additional monitoring station at Piney Point (Figure 8) from the Maryland Department of Natural Resources (MDNR) Eyes on the Bay Program (http://mddnr.chesapeakebay.net/eyesonthebay/index.cfm) was used to supplement the EPA/CBP database. Data were available at this station for April-October in 2004 and 2005 at approximately daily intervals. Table 4 contains descriptive information for each of these monitoring stations.

Station LE 2.3 is less than 1 mile upstream of the mouth of the Potomac and was used to represent the downstream tidal boundary condition. All of the other stations upstream were used for model calibration targets. All salinity data were vertically-averaged because the POTPCB model is one-dimensional vertically in the water column.

3.6 Temperatures and Wind Speed

Daily air temperatures for 2002-2005 were obtained from the National Weather Service Station in Washington, DC, Reagan National Airport.

Daily water temperatures for 2002-2005 for the tidal fresh, oligohaline and mesohaline portions of the Potomac were estimated by linear interpolation using bi-weekly measurements from the EPA/CBP water quality database.

Wind speed for 2002-2005 was estimated using a spatially and temporally constant value of 5 m/sec (11 mph).

4. HYDRODYNAMIC MODEL CALIBRATION

4.1 Spatial Grid Development

The discrete spatial domain for the Potomac River Estuary DYNHYD5 model application is represented by 258 junctions and 257 inter-connecting channels which encompass the entire mainstem and its tidal tributaries and embayments (Figure 9). The DYNHYD5 junction-channel grid is shown in more detail for each of the principal sub-regions (Figures 10-13). Figure 14 contains a schematic diagram of the DYNHYD5 spatial segmentation grid for the entire Potomac River estuary and shows junction numbers and river mile locations. Tables 5 and 6 contain summaries of the DYNHYD5 junction and channel geometries, respectively.

The model grid represents the mainstem Potomac as one-dimensional using 97 junctions which extend from the fall line near Chain Bridge (RM 118.1) to the confluence with Chesapeake Bay (RM 0). The mainstem junction and channel geometry is a superset of the 57K CBWQM horizontal spatial grid from the mouth up to the confluence of the Potomac and Anacostia rivers. Between the Potomac fall line and the Anacostia River, the mainstem segmentation is also based upon the CBWQM, but the spatial resolution was increased by splitting the CBWQM model cells in half to better represent local gradients in water quality.

The CBWQM also represents many of the tidal embayments and tributaries that flow into the Potomac, but with varying degrees of spatial resolution. In the tidal Anacostia River, the CBWQM is one-dimensional in the longitudinal direction and the spatial scale is relatively coarse. To better represent local gradients in water quality, the existing TAM/WASP model grid was integrated within the DYNHYD5 model network. TAM/WASP represents the Anacostia River as one-dimensional, but its longitudinal spatial resolution is approximately four times finer than the CBWQM model grid. In this adaptation of the TAM/WASP grid, the segmentation for the DYNHYD5 model represents the Anacostia River with 38 junctions, including separate representation of the NE and NW branches up to their approximate fall line locations.

It should be noted that the bathymetry for most of the included tributaries, especially those in Virginia, is relatively coarse. Furthermore, most of these tributaries do not have sufficient data for model calibration. Nonetheless, they were included in the model spatial grid at the request of the Parties because they are listed as impaired and need to be included in development of the PCB TMDL.

4.2 Calibration Approach

As described above, DYNHYD5 was calibrated to data for water surface elevation WSE (tidal height) and confirmed using the computed hydrodynamics to drive a mass balance model for salinity. The principal calibration parameters were Manning's N coefficient for DYNHYD5 and dispersive mixing coefficients between the model spatial segments for the salinity mass balance model. The large spatial gradient between very low salinity freshwater inflows at the fall lines and higher salinity tidally-driven flow entering the mouth of the estuary from Chesapeake Bay allows salinity to serve as a conservative tracer for confirmation of the computed hydrodynamics.

There were two calibration periods for the DYNHYD5 hydrodynamic model, 1996-1997 and 2002-2005. Prior to each of these periods the model was run for three months to "spin up" and establish initial conditions relative to freshwater inflows and boundary conditions. The model calibration was conducted in a stepwise fashion, beginning with parameter adjustments to match computed and observed WSE in order to constrain advection-driven flows. The next step was linkage of the hydrodynamic computations to the water quality model for calibration of dispersive-driven mass transport using salinity as a conservative tracer.

The DYNHYD5 model was calibrated using observed WSEs for the tidal gages at Colonial Beach, Washington DC Ship Channel, and Bladensburg (Figure 8) for 1996-1997, and for Colonial Beach and Washington DC Ship Channel in 2002-2005. Initial values for the Manning's N were taken from Mandel and Schultz (2000) and U.S. EPA (1979). These initial values were then adjusted to obtain optimal agreement with observed WSEs.

Data for current velocities were collected during two intensive, 3-day studies in August 2004 and September 2005 (Cartwright and Friedrichs 2006). A series of vertical profiles across the channel were obtained using an acoustic doppler current profiler (ADCP) mounted on a boat. Data were collected over full tidal cycles for each vertical profile but no discrete points in time were reported with the measurements. The DYNHYD5 model is 1D in the vertical and operates at an hourly time scale. The appropriate spatial scale for model-data comparisons would be the entire channel cross section and the appropriate temporal scale would be hourly. Consequently, it was not possible to compare these current velocity data to model results because of spatial-temporal incompatibilities.

A computational time step of 5 seconds was required to maintain numerical stability for the DYNHYD5 simulation during high flow events over the calibration period. A complete simulation for the two calibration periods required approximately 10 hours of real time.

4.3 Calibration Results

The assessment of model calibration results was a weight-of-evidence approach that relied on multiple quantitative metrics and best professional judgment. No single metric provides sufficient information by itself to completely evaluate model calibration results. The metrics used for the DYNHD5 calibration include cumulative frequency distributions (CFDs), bivariate plots with lines of 1:1 correspondence, regression statistics, and time series plots for different flow conditions at the locations of individual tidal gages.

Cumulative frequency distributions for WSE were developed using paired hourly computations and observations that were matched in location and time. The mean error of the distribution indicates whether the model over- or under-computes the observations, on average. The mean error can achieve its ideal value, zero, while large discrepancies exist between individual computations and observations. The absolute mean error is a measure of the characteristic difference between individual computations and observations. An absolute mean error of zero indicates the model perfectly matches each observation. The relative error is the absolute mean error normalized by the mean concentration. Relative error provides a statistic that can be used to compare results among different variables in a model or among different models. A statistical summary of all calibration results for the hydrodynamic model is presented in Table 7.

The Manning's N coefficient is the key parameter for determining water movement in DYNHYD5 and was the only model parameter adjusted during model calibration. Model results indicated that larger Manning's coefficients slowed tidal propagation and decreased tidal amplitude (or range). Smaller Manning's coefficients increased the speed of tidal propagation and the tidal amplitude. Various combinations of adjustments to the Manning's coefficients were tested to optimize correspondence between computed and observed WSEs. The calibrated Manning's N coefficients are shown in Figure 15 for the DYNHYD5 model junction schematic.

Figures 16 and 17 show CFDs for computed and observed hourly WSE at all gage locations combined and at individual gage locations, respectively, for 1996-1997. Overall, the model performance is very good and is better in the lower portion of the estuary than in the upper portion. There is good correspondence between computed and observed medians, but with a tendency for over-computation at low WSE and under-computation at high WSE, especially in the upper portion of estuary.

Mean error for all gages combined is 0.032 meters and ranges from 0.010 to 0.073 for individual tidal gages (Table 7). Absolute mean error for all gages combined is 0.091 meters and ranges from 0.056 to 0.209 for individual tidal gages. The relative error statistic is not as useful for WSE as it is for other model calibration parameters. An inherent difficulty with this statistic is that it behaves poorly at low observed values. In the case of WSE most of the observations are centered on zero except those that represent very high flows and/or storm events.

Figures 18 and 19 contain bivariate plots with lines of 1:1 correspondence for computed versus observed hourly WSE at all gage locations combined and at individual gage locations, respectively, for 1996-1997. Model performance is very good in the lower portion of the estuary at Colonial Beach but tends to under-compute WSE in the upper portion of the estuary near Washington, DC. The model explains 76 percent of the variability in hourly WSE for all gages combined and between 63 and 90 percent of the variability in hourly WSE at the three individual gage locations.

Figures 20-22 show comparisons between computed and observed hourly WSE for three 7-day periods during 1996-1997 that represent high, moderate and low flow conditions, respectively. These flow conditions span a range of almost a factor of seven. In general, the model reproduces the observed temporal phasing in the estuary, but tends to under-compute the magnitudes of observed WSE ranges in the upper portion of the estuary near Washington DC and Bladensburg.

Figures 23 and 24 show CFDs for computed and observed hourly WSE at both locations combined and at the two individual gage locations, respectively, for 2002-2005. The model performance is very good but is better at Colonial Beach in the lower portion of the estuary than in the upper portion at Washington, DC. Again, there is good correspondence between computed and observed medians, but a tendency for over-computation at low WSE and under-computation at high WSE in the upper portion of the estuary. Mean errors in meters are -0.014 for both gages combined, 0.003 for Colonial Beach, and -0.020 for Washington, DC (Table 7). The corresponding absolute mean errors in meters are 0.126, 0.041, and 0.157.

Figures 25 and 26 contain bivariate plots with lines of 1:1 correspondence for computed versus observed hourly WSE at both gage locations combined and at the individual locations, respectively, for 2002-2005. Again, model performance is very good in the lower portion of the estuary at Colonial Beach but tends to under-compute WSE in the upper portion near Washington, DC. The model explains 77 percent of the variability in hourly WSE for both gages combined, and 74 and 96 percent of the variability in hourly WSE at the two individual gage locations.

Figures 27-29 show comparisons between computed and observed hourly WSE for three 7-day periods during 2002-2005 that represent high, moderate and low flow conditions, respectively. These flow conditions span a range of almost a factor of seven. Again, the model reproduces the observed temporal phasing in the estuary, but tends to under-compute the magnitudes of observed WSE ranges in the upper portion of the estuary near Washington DC.

It should be noted that model performance reflects not only the capabilities and limitations of the model itself, but also those of the model inputs. For example, boundary conditions at the fall lines are daily average flows, but boundary conditions at mouth of estuary are hourly average WSEs. This is probably the main reason why there tend to be higher discrepancies between computed and observed values in the upper portion of the estuary than in the lower portion. Observed hourly average WSEs in upper portion of estuary may be influenced by higher-frequency variations in flows than are represented in the daily average upstream boundary conditions. With respect to use of the hydrodynamic model to drive the PCB mass balance model, this is not a significant flaw because the relevant time scales for water column PCB concentrations are daily or longer.

No standard criteria exist for judging acceptable model performance. One approach is to compare performance with other similar model applications using comparable metrics. In that regard, the comparisons between computed and observed WSEs for the present model calibration are consistent with those for validation and application of the second generation, three dimensional hydrodynamic model of Chesapeake Bay (Wang and Johnson 2000).

5. SALINITY MODEL CALIBRATION

5.1 Spatial Segmentation and Linkage to DYNHYD5

The spatial grid for the POTPCB model is the same for salinity, sorbents (organic carbon) and PCBs. Consequently, the advective flows and dispersive mixing coefficients from the salinity calibration also provide the transport "chassis" for sorbents and PCBs. The water column segmentation for POTPCB is based on a 1:1 mapping to the segmentation of the DYNHYD5 hydrodynamic model. The WASP5/TOXI5 model drops the boundary junctions in the mapping process in order to provide a linkage for external flows to the water quality model segments. Therefore, the total number of water column segments for the POTPCB model is 257, which is one less than the total number of DYNHYD5 junctions.

The full model spatial grid for the WASP5/TOXI5 component of the POTPCB water quality model is shown in Figure 30. The spatial grid is shown in more detail for each of the principal sub-regions (Figures 31-34). Figure 35 contains a schematic diagram of the POTPCB spatial segmentation grid for the entire Potomac River estuary and shows model segment numbers and river mile locations.

5.2 Calibration Approach

The only additional external forcing conditions required by the salinity model are salinity concentrations for upstream freshwater inflows and at the mouth of the estuary. The salinity concentration for upstream freshwater inflows was specified at a constant, nominal value of 0.1 ppt. Care must be taken in specification of salinity at the downstream boundary because the Potomac Estuary does not extend to the ocean where salinity is well-characterized. Another confounding factor is that the available salinity data for specification of the downstream boundary, as well as for model calibration, are temporally sparse.

For this calibration, the available bi-weekly salinity data for Station LE 2.3 were used to specify downstream boundary salinity concentrations. Linear interpolation was used to fill in the gaps in time between the bi-weekly monitoring cruises. No adjustments to the measured salinities were made to account for the distance from the location of Station LE 2.3 to the estuary mouth because the data were sparse and because this station is only approximately 1 mile from the confluence with Chesapeake Bay.

When advection-driven transport computed by the hydrodynamic model is linked to a mass balance water quality model, numerical dispersion is introduced as an inherent consequence of the finite difference numerical solution technique. The amount of numerical dispersion depends on the size of the spatial segments, the computational time step, and a user-specified advection factor. For this model application, the spatial scale of the model segmentation and the computational time step used introduce much less dispersion than is required to calibrate the non-advective bulk mixing. Consequently, as part of the calibration process, additional dispersive mixing was imposed in order for computed salinities to match observed spatial and temporal distributions.

A computational time step of 1 minute for the POTPCB salinity simulation was required to ensure numerical stability and mass conservation. This time step is 12 times larger than the 5 second DYNHYD5 time step, so the hydrodynamic linkage between DYNHYD5 and POTPCB reflects hydrodynamic conditions that are integrated over this 1 minute time scale at 5 second intervals. DYNHYD5 allows the linkage to be integrated over less frequent intervals than 5 seconds, but test simulations indicated that the loss of accuracy this may cause was an unnecessary liability, and not worth the small reduction in model run times.

There are two parameters that can be adjusted to calibrate the model for salinity: the advection factor (ADF) and the longitudinal dispersion or mixing coefficients. In this application the ADF was held constant at the WASP5-default value of 0.0 and was not used as a calibration parameter. A non-zero ADF can help reduce numerical dispersion produced by particular combinations of velocity, channel length, and time step. However, a non-zero ADF can also cause numerical instabilities to occur. For this application, additional user-specified dispersive mixing was required for the salinity calibration, hence it was not necessary to specify a non-zero value for ADF.

5.3 Calibration Results

As with the hydrodynamic model, the assessment of model calibration results for salinity was a weight-of-evidence approach that relied on multiple quantitative metrics and best professional judgment. No single metric provides sufficient information by itself to completely evaluate model calibration results. The metrics used for the salinity calibration include cumulative frequency distributions, bivariate plots with lines of 1:1 correspondence, regression statistics, time series plots at fixed locations, and spatial profiles at fixed points in time. A statistical summary of all calibration results for the salinity model is presented in Table 7.

To calibrate the model for salinity, dispersion (or mixing) coefficients were adjusted to achieve optimal agreement between computed and observed bi-weekly values. Emphasis was placed on reproducing the observed longitudinal salinity profiles in the estuary, and the observed temporal variations at individual monitoring stations. The calibrated dispersion coefficients are shown in Figure 36 for the POTPCB model segmentation schematic. A unified set of dispersion coefficients was determined that produced the best correspondence between computed and observed values for both the 1996-1997 and 2002-2005 calibration periods.

Figures 37 and 38 show CFDs for computed and observed daily average salinity for all stations combined and three representative monitoring stations, respectively, in different regions of the estuary for 1996-1997. Stations TF2.4, RET2.4 and LE2.2 are located, respectively, in the tidal fresh, river-estuary transition, and lower estuary zones (Figure 8). Overall, the model performance is very good. There is good correspondence between computed and observed values with the sole exception of some over-computation in the upper 20th percentile of salinities at Station RET2.4.

For 1996-1997, the mean error for all salinity monitoring stations combined is -0.177 parts per thousand (ppt) and ranges from -0.718 to 0.146 ppt for the three representative stations in Figure 38. Absolute mean error for all stations combined is 0.965 ppt and ranges from 0.718 to 1.25 ppt

for the three representative stations. Relative error for all stations combined is 0.159 and ranges from 0.071 to 0.666 for the three representative stations.

Figures 39 and 40 contain bivariate plots with lines of 1:1 correspondence for computed versus observed daily average salinity for all stations combined and the three representative stations, respectively, for 1996-1997. The model explains 92 percent of the variability in daily salinity for all stations combined, and from 58 to 88 percent of the variability at the three representative stations. Model performance is very good in the lower estuary and in the river-estuarine transition zone, but declines in the tidal fresh portion at Station TF2.4. The reasons are that observed salinities are very low at this location and available data are sparse. Results for this station are only included to demonstrate that model computations are consistent with the lowest observed salinities in the estuary.

Figures 41 and 42 show time series plots for computed and observed salinity at the three representative stations. In general, model results are a reasonable representation of the magnitudes and temporal distributions in observed salinities. Note that the results shown for portions of 1995 are model "spin up" conditions and were not part of the model calibration.

Figures 43 and 44 show spatial profiles of computed and observed daily average salinity during 1996-1997 that represent high, moderate and low flow conditions. These flow conditions span a range of almost a factor of 60. Computed results are shown for daily average, daily minimum and daily maximum salinity values. All of the salinity observations correspond to point-in-time grab samples. Depending on the upstream freshwater inflow, the salinity intrusion point ranges between approximately RMs 45 (high flow) and 85 (low flow). There is good correspondence between computed and observed salinities across this range of flow conditions.

Figures 45 and 46 show CFDs for computed and observed daily average salinity for all stations combined (Figure 45) and all stations combined except Piney Point (Figure 46) for 2002-2005. There are many more salinity observations for 2002-2005 (n = 308) than for 1996-1997 (n = 110), not including the large number of measurements (n = 397) at Piney Point. Results are shown separately with and without the Piney Point data because observations at Piney Point represent 56 percent of the total observations for 2002-2005 and tend to skew the calibration results.

For 2002-2005, mean error for all salinity monitoring stations combined (excluding Piney Point) is 0.110 ppt and ranges from -0.162 to 0.480 ppt for the three representative stations (Table 7). Absolute mean error for all stations combined (excluding Piney Point) is 1.01 ppt and ranges from 0.480 to 1.56 ppt for the three representative stations. Relative error for all stations combined (excluding Piney Point) is 0.163 ppt and ranges from 0.081 to 0.295 for the three representative stations.

Overall, the model performance is very good. For all stations combined (excluding Piney Point) there is good correspondence between computed and observed salinities over the entire range of the CFD (Figure 46). When Piney Point observations are included, the model over-computes observed salinities between the 30^{th} and 90^{th} percentiles of the CFD (Figure 45). For individual stations (Figure 47), the model tends to under-compute observed salinities in the lower 50^{th}

percentile of the CFD at Station LE2.2. Correspondence between computed and observed medians is good at Station RET2.4, but the model under-computes at lower salinities and over-computes at higher salinities. The model over-computes observed salinities at Piney Point except for salinities in the highest 10^{th} percentile of the CFD.

Figures 48 and 49 contain bivariate plots with lines of 1:1 correspondence for computed versus observed salinity for all stations combined (Figure 48) and all stations combined except Piney Point (Figure 49) for 2002-2005. Figure 50 contains the corresponding results for the three representative stations and Piney Point. Model performance is very good at the three representative stations, but declines at the Piney Point station. The model explains 93 percent of the variability in daily salinity for all stations combined (excluding Piney Point), and from 81 to 89 percent of the variability at the three representative stations. Although the model explains 81 percent of the variability at Piney point, the model over-computes observed salinities and the intercept of the regression line is 3.31 ppt, substantially larger than those for all other stations combined or the three representative stations.

Figures 51 and 52 show time series plots for computed and observed salinity at the three representative stations and Piney Point. In general, model results are a reasonable representation of the magnitudes and temporal distributions in observed salinities, with the exception of Piney Point. Consistent with the above results, computed results are systematically higher than observations at Piney Point. Note that the results shown for portions of 2001 are model "spin up" conditions and were not part of the model calibration.

Figures 53 and 54 show spatial profiles of computed and observed daily average salinity during 2002-2005 that represent high, moderate and low flow conditions. These flow conditions span a range of approximately a factor of 60. Computed results are shown for daily average, daily minimum and daily maximum salinity values. All of the salinity observations correspond to point-in-time grab samples. Depending on the upstream freshwater inflow, the salinity intrusion point ranges between approximately RMs 55 (high flow) and 85 (low flow). Again, there is good correspondence between computed and observed salinities across a wide range of flow conditions.

It is difficult to evaluate the significance, if any, of the salinity model performance relative to the observations at Piney Point. These observations represent different methods, a much higher sampling frequency (daily), and only a single location, relative to observations from the 10 EPA/CBP monitoring stations.

Although no standard criteria exist for judging acceptable model performance, it is informative to compare these salinity model calibration results to those for the second generation CBWQM (Cerco and Noel 2004). From the CFD statistics (Table 7) the relative errors for the salinity model calibration were 15.9 and 16.3 percent, respectively, for 1996-1997 and 2002-2005. The relative error for salinity in the CBWQM was 22.5 percent in the Potomac River estuary for a 10-year calibration period from 1985-1994.

5.4 Tracer Analysis for External Boundaries

Sensitivity analyses were conducted with the calibrated salinity model to investigate the relative impacts of external boundaries on the Potomac and Anacostia. These analyses were conducted by setting each of the external boundaries, in turn and in combination, at a salinity concentration of 100 ppt. Figures 55 and 56 show spatial profiles of the computed salinities in the Potomac and Anacostia, respectively. These results are informative because they illustrate the influence of all external boundaries normalized to the same source strength. That is, the value of 100 ppt can be viewed as a source strength of 100 percent.

The upstream boundary at head of tide (HOT) near Chain Bridge dominates the upper and middle portions of the Potomac (Figure 55). Computed salinity concentrations remain above 50 percent from Chain Bridge downstream to just below RM 50. The downstream boundary at Chesapeake Bay dominates the lower portion of the Potomac, with computed salinity concentrations that remain above 50 percent from the mouth of the Potomac upstream to approximately RM 40. None of the other boundaries, either alone or in combination, produce computed salinity concentrations greater than 20 percent anywhere in the Potomac. The upstream boundaries at the NE and NW Anacostia have only a minor influence on the Potomac mainstem due to the large difference in flow between the Anacostia and Potomac rivers.

In contrast, the upstream boundaries at the NE and NW Anacostia are the dominant influences within the tidal Anacostia River (Figure 56). It is significant to note that the boundary at Chain Bridge influences the Anacostia for approximately 4-5 upstream from its confluence with the Potomac. This is due to tidal mixing with the mainstem Potomac and the large difference in flow between the Potomac and Anacostia rivers.

6. MASS LOADS FOR SORBENTS AND PCBs

6.1 Introduction

The ICPRB gathered, compiled and organized the available data for the tidal Potomac and Anacostia rivers, and maintains the overall project database. This database includes physical and geographical data for the watershed, freshwater inflows, and ambient monitoring data for the water column and sediments.

The ICPRB, in collaboration with EPA/CBP, developed the required model inputs for freshwater inflows and external mass loads of organic carbon and PCBs for most of the loading sources (Haywood and Buchanan 2007, Appendix A). The primary data for this effort included historical data, recently collected data to support this PCB TMDL modeling effort, literature values, and results from the EPA/CBP Phase 5 Watershed Model (WM5).

The ICPRB provided external mass loadings for organic carbon sorbents and/or PCBs to LimnoTech for the following source categories:

- Potomac above fall line (AFL) at head of tide (near Chain Bridge)
- All other tidal tributaries
- Direct drainage
- Combined sewer overflows (CSOs)
- Point source discharges
- Atmospheric wet/dry deposition to the water surface
- Contaminated sites

Because the Potomac monitoring station at Chain Bridge was the location for determination of all AFL mass loads, these loads will be referred to as Potomac River loads at Chain Bridge throughout this report. LimnoTech, in collaboration with ICPRB, EPA/CBP, and the U.S. Army Corps of Engineers (USACE) Engineer Research and Development Center (ERDC), developed organic carbon loadings for algal primary productivity, marshes and shoreline bank erosion.

To provide spatial context and facilitate understanding of relationships between external loadings and transport and fate within the estuary, mass loadings were organized in terms of seven operational zones:

- UPOTTF - Upper Potomac Tidal Fresh
- LPOTTF - Lower Potomac Tidal Fresh
- POTOH - Potomac Oligohaline
- UPOTMH - Upper Potomac Mesohaline
- LPOTMH - Lower Potomac Mesohaline
- ANAC - Anacostia
- TRIB - Tributaries

These zones are pictured in Figures 57 through 61 and shown in the form of a schematic diagram of the POTPCB model spatial segmentation grid in Figure 62.

For spatial aggregation of results from the CBWQM and application to water quality criteria, the EPA/CBP delineated three Chesapeake Bay Criteria Segments in the Potomac River estuary (http://www.chesapeakebay.net/pubs/segmentscheme.pdf): (1) Potomac Tidal Fresh (POTTF); (2) Potomac Oligohaline (POTOH); and, (3) Potomac Mesohaline (POTMH). The spatial zones used here are consistent with these CBP segments, the differences being that POTTF was split into separate UPOTTF and LPOTTF portions, and the POTMH was split into separate UPOTMH and LPOTMH portions to better represent watershed loadings and ambient conditions relevant to the PCB TMDL.

A noteworthy point is that the boundary between UPOTTF and LPOTTF is just above the confluence of the Anacostia with the Potomac. Water quality conditions in UPOTTF are strongly influenced by freshwater inflows and mass loads from AFL near Chain Bridge, while those in LPOTTF are influenced by downstream flows from both the Potomac and Anacostia. Note that although all tributaries except the Potomac and Anacostia are included in the TRIB spatial zone, this zone actually represents a group of non-contiguous model spatial segments throughout the spatial domain of the model. This was done to ensure completeness and capture all of the mass loads in the model spatial domain in the various tables and figures.

6.2 Internal Primary Production

An important source of organic carbon to aquatic systems is internal loading directly to the water column from algal primary productivity. This is the principal source of biotic carbon (BIC) for the sorbent dynamics model. One way to determine internal loading of BIC is by direct measurements of algal primary productivity as was done for the PCB TMDL model for the Delaware River Estuary using a spatially extensive, 25-year dataset (Delaware River Basin Commission 2003c). Although there are measurements for primary productivity during the 2002-2005 model calibration period, they represent only three monitoring stations in the Potomac and none in the Anacostia.

Another way to determine internal loading of BIC is to apply an eutrophication model and use its computed results for gross algal primary productivity. The schedule and available resources for this PCB modeling effort precluded such an application. However, as part of an ongoing, long-term federal agency program, EPA/CBP and USACE/ERDC have already developed first- and second-generation eutrophication models for Chesapeake Bay (Modeling Subcommittee 2000) and are currently developing a third-generation model to support development of bay-wide TMDLs for nutrients and solids in 2011.

The calibration period for the second-generation CBWQM (Cerco and Noel 2004) was 1985-1994 and that for the third-generation model will be 1994-2005, thus encompassing the 2002-2005 calibration period for the PCB TMDL model. Unfortunately, results from the third-generation CBWQM are not scheduled to become available until after the September 2007 deadline for the PCB TMDL. Under the circumstances, the only reasonable approach was to use results from the second-generation model for 1985-1994 as the best available estimates for internal loading of BIC in the Potomac and Anacostia.

The EPA/CBP provided depth integrated, daily, gross primary productivity results from the second-generation CBWQM for the entire spatial domain of the PCB TMDL model for 1985-1994. These results were temporally aggregated into daily average values and then spatially mapped on to the 257 vertically-mixed water column segments in the POTPCB model spatial grid (Figure 35). They were then spatially aggregated into the Potomac and Anacostia spatial zones (Figure 62) and the individual tributary model segments. Finally, they were temporally aggregated into monthly internal BIC mass loads for each spatial zone and tributary model segment. It was judged that these spatial-temporal scales were appropriate in extrapolating average conditions for 1985-1994 to estimate those during the PCB TMDL model calibration period for 2002-2005.

6.3 Wetlands and Marsh Areas

The ICPRB used the WM5 to provide daily flows and generate estimates of organic carbon and PCB mass loads from tidal tributaries and direct drainage areas (Haywood and Buchanan 2007, Appendix A). The WM5 does not include organic carbon loads from wetlands or marsh areas. These loads were determined using the same uniform carbon export value (0.3 gm C/m^2/day) as Cerco and Noel (2004) and wetland-marsh areas delineated in a file from the USGS National Hydrography Dataset obtained by ICPRB (Figure 63).

Cerco and Noel (2004) assumed that organic carbon loads from wetland-marsh areas were split equally into dissolved organic carbon (DOC), and labile particulate and refractory particulate organic carbon. For the Potomac PCB TMDL model, DOC is externally specified as water column and sediment concentrations not as organic carbon mass loading. It was assumed that PDC mass loads from wetland-marsh areas were equivalent to the sum of labile particulate and refractory particulate organic carbon, as defined by Cerco and Noel (2004), and that BIC loads from these areas were negligible. These PDC loads were determined separately for each spatial zone and the tributaries, but the loads for UPOTMH and LPOTMH were spatially aggregated during the model calibration process to provide more even spatial distribution and avoid sediment bed scour in some of the tributaries.

6.4 Shoreline Bank Erosion

Another potentially important source of organic carbon mass loads is shoreline bank erosion. Total organic carbon (TOC) loads from bank erosion were determined by Cerco and Noel (2004) for the second-generation CBWQM. These loads were provided to LimnoTech in electronic form for the Potomac tidal fresh, oligohaline, and mesohaline portions of the estuary. It was assumed that these loads represented PDC loads for the PCB TMDL model because they were completely in the particulate form.

6.5 Design Conditions for TMDL

All external mass loads from the watershed are organized into two time periods, 2002-2005 which corresponds to the model calibration period, and 2005 which represents the design conditions used for the PCB TMDL (Haywood and Buchanan 2007, Appendix C). The TMDL design conditions correspond to quasi-steady state, dynamic equilibrium among external PCB mass loads and exposure concentrations in the water column and sediments. Under these

conditions there is no net flux of PCBs across the air-water interface, and both the surface and deep sediment layers are net sinks for PCBs.

Forecast simulations with the calibrated model to determine the external PCB mass loads that will achieve the TMDL targets could require 50 to 100 years to reach dynamic equilibrium. This is because water column PCB concentrations in rivers or estuaries typically respond to changes in external loadings on time scales of days to weeks; however, sediment PCB concentrations typically respond on time scales of years to decades because PCBs are much less mobile in bedded sediments.

EPA TMDL guidance for toxic substances where the human health impact is based on lifetime accumulation recommends using the harmonic mean flow as the TMDL design flow. The most feasible way to implement this TMDL design flow in long-term forecast simulations is to select a year for which the harmonic mean flow is close to the long term harmonic mean flow and repeatedly cycle this flow sequence until the model reaches dynamic equilibrium. It is highly desirable to select a cycling year that lies within the model calibration period for two reasons. First, it is not possible to evaluate model performance outside the model calibration period. Second, additional sets of freshwater inflows, mass loads, and other external forcing functions would need to be developed in order to even run the model outside this period.

The ICPRB conducted an analysis of historical flows for the Potomac River at Little Falls (Haywood and Buchanan 2007, Appendix C). The long-term (1931-2005) harmonic mean flow was found to be 4,700 cfs and is compared with recent annual harmonic mean flows in Figure 64. Harmonic mean flow in calendar 2005 (5,485 cfs) approximates both the long term harmonic mean and the long term cumulative frequency distribution for the Potomac River at Little Falls (Haywood and Buchanan 2007, Appendix C). The harmonic mean flow in 2002 is lower than the long term harmonic mean, and the harmonic mean flows in 2003 and 2004 are much higher. The calendar year ending on December 31, 2005, is the 365-day period wholly within the model calibration period with a harmonic mean flow that most closely matches the long-term harmonic mean. Given the project schedule and available resources, the PCB TMDL Steering Committee decided to use model inputs for calendar year 2005 as the TMDL design conditions.

6.6 Summaries of Organic Carbon and PCB3+ Mass Loads

Tables 8-16 contain summaries of all mass loads for BIC, PDC and POC (derived as the sum of BIC and PDC). Tables 17-24 contain summaries of all mass loads for PCB expressed as the sum of PCB homologs 3-10 (PCB3+), the calibration target used for the PCB model. The rationale for selection of this PCB form as the model calibration target is presented in Section 7.

Results in Table 8 and Figure 65 indicate that UPOTTF receives 72 percent of the PDC loads to the whole system during the model calibration period. Almost all (98 percent) of this PDC load is delivered to UPOTTF by the Potomac River at Chain Bridge (Table 10). The PDC loads for UPOTTF plus the sum of all PDC loads delivered by other tributaries represents 87 percent of the total PDC loads to the whole system during the model calibration period. No other spatial zone contributes more than 4 percent of the total PDC load during this period.

Results in Table 9 and Figure 66 indicate that organic carbon loads of BIC from internal primary productivity are much greater than external PDC loads. Total BIC load is 96 percent of the total POC load to the whole system for the model calibration period. Most of the BIC load enters the system in the lower estuary, with LPOTMH and UPOTMH accounting for 62 percent of the total BIC load to the whole system during the model calibration period. This is intuitively reasonable because these zones have large surface areas compared to other zones and are highly productive. The only zone in which PDC load is greater than BIC load is UPOTTF (Table 9) because loads to this zone are dominated by the Potomac River at Chain Bridge.

To summarize, most of the organic carbon load to the system (62 percent) is to the lower estuary (Figure 66) and almost 100 percent of this load is BIC from internal primary productivity (Table 9). Contrasting situations exist at opposite ends of the estuary with respect to organic carbon loading sources. Most of the organic carbon load to UPOTTF (86 percent) is from PDC (Table 9), almost all of it from the Potomac at Chain Bridge, while almost 100 percent of the organic carbon load to LPOTMH is BIC from internal primary productivity.

PDC loads to the ANAC (Table 15) are dominated by the NE and NE Branches (72 percent) and direct drainage (21 percent) during the model calibration period. On a whole system scale, PDC loads from marshes and shoreline bank erosion are small, accounting for only 11 percent of the total PDC load during this period (Figure 65). In contrast, PDC loads from these sources can be important at local scales and dominate the total PDC loads in POTOH, UPOTMH and LPOTMH in the middle and lower portions of the estuary (Tables 12-14).

Results in Table 17 and Figure 67 indicate that UPOTTF receives 71 percent of the PCB3+ loads to the whole system during the model calibration period. Almost all (94 percent) of this PCB3+ load is delivered to the UPOTTF by the Potomac River at Chain Bridge (Table 18). Together, the PCB3+ loads delivered at Chain Bridge and to the Anacostia account for 85 percent of the PCB3+ loads delivered to the whole system during the model calibration period. The two largest sources for PCB3+ loads to the whole system (Figure 67) are the Potomac at Chain Bridge (66 percent) and direct drainage (17 percent).

Results in Table 23 indicate that most (78 percent) of the PCB3+ loads to the Anacostia during the model calibration period are from direct drainage. The largest other loading source is CSOs (12 percent). Together, the NE and NW Branches deliver only about 9 percent of the total PCB3+ load to the Anacostia. Although PCB3+ loads to the whole system from atmospheric wet and dry deposition (Figure 67) are small (6.7 percent), they account for almost all (approximately 97 percent) of the PCB3+ loads to POTOH, UPOTMH and LPOTMH in the middle and lower portions of the estuary (Tables 20-22).

For the overall model calibration period (2002-2005) mass loads for PDC and PCB3+ from flow-dependent sources (tributaries, direct drainage and CSOs) are higher than those in 2005. The reason is that PDC and PCB3+ loads were both estimated using regression of TSS on flow, and TSS concentrations are generally higher at higher flows. The magnitudes of internal mass loads of BIC are the same for each year of the calibration period. The impacts of these mass loads differ among the individual calibration years because 2002 was a dry year, 2003 and 2004 were very wet years, and 2005 was close to an average year.

For all of these mass loads and source categories there remain questions and uncertainties. The magnitude and timing of freshwater inflows are not well-quantified at the scales of the model spatial segmentation grid. Sampling frequencies for sorbent and PCB3+ concentrations low, especially for the Potomac at Chain Bridge and for nonpoint sources. With the available information, it is not possible to accurately quantify mass loads directly or develop accurate statistical relationships between flow and observed concentrations for solids, organic carbon and PCBs. These uncertainties are discussed in more detail in Appendix A of Haywood and Buchanan (2007).

7. AMBIENT MONITORING DATA

7.1 Introduction

The ICPRB gathered, compiled and organized the available data for the tidal Potomac and Anacostia rivers, and maintains the overall project database. This database includes physical and geographical data for the watershed, freshwater inflows, and ambient monitoring data for the water column and sediments.

Data sources included historical data, recently collected data to support this PCB TMDL modeling effort, information from various government agency reports and databases, and the published scientific literature. Copies of the project database may be obtained directly from ICPRB. The complete database will eventually be made available on the ICPRB web page (www.potomacriver.org).

7.2 Water Column Data

The water column monitoring stations used to obtain data for sorbents and PCBs are listed in Table 25. Table 26 lists the water quality parameters measured at each station and the laboratories responsible for the analyses. Figures 68-72 show the locations of these monitoring stations in the tidal Potomac and Anacostia Rivers.

7.3 Development of Model Calibration Targets for Sorbents

Model calibration targets for BIC and PDC are not measured directly but must be derived from paired measurements for particulate organic carbon (POC) and chlorophyll *a* (Chl *a*) concentrations, and application of a carbon:chlorophyll *a* (C:CHL) ratio. Direct measurements were available only for particulate carbon (PC) and not particulate organic carbon (POC). For lack of an alternative, it was assumed that POC was approximated by PC.

The available data for DOC could not be used due to apparent analytical problems. Many of the reported DOC values were greater than or equal to reported total organic carbon (TOC) values. After consultation with Ms. Mary Ellen Ley, Quality Assurance Coordinator, USGS/CBP, it was decided to derive the components of TOC using observations for TOC and PC and determining DOC by difference.

The computational approach for deriving BIC and PDC was the following:

BIC = Chl *a* x C:CHL

PDC = POC – BIC

where C:CHL = carbon to chlorophyll *a* ratio
Chl *a* = Chlorophyll a, mg/L
BIC = Biotic carbon, mg/L
POC = Particulate organic carbon, mg/L
PDC = Particulate detrital carbon, mg/L.

To estimate an appropriate C:CHL ratio, available paired concentrations for POC and Chl *a* were compiled and the resultant BIC values computed for a range of assumed C:CHL values. Two criteria were used to select the most appropriate C:CHL ratio for the Potomac. First, the ratio should not result in BIC values greater than POC because BIC is a component of POC, and second, the selected ratio should result in BIC concentrations that are approximately 15-25 percent of POC.

Cerco and Noel (2004) conducted an analysis of C:CHL ratios in Chesapeake Bay using actual phytoplankton and Chl *a* observations and reported that more than 70 percent of values were less than 75 and the most common values were between 25 and 50. Here, BIC values were computed for a range of assumed C:CHL values from 30 to 50 and it was judged that a value of 30 produced the most reasonable results (Figure 73). This ratio produced no negative values for PDC and median values for the ratio BIC/POC that ranged from 0.11 in the tidal fresh portion to 0.21 in the mesohaline portion of the estuary. This range is reasonable and is consistent with higher external loadings of "dirt" in the upper portion of the estuary that would result in lower ratios of algal solids to non-algal solids.

7.4 Sediment Data

The sediment database is extensive and includes 52 stations in the Potomac mainstem and 129 stations in the Anacostia mainstem. Measurements for PCBs and fraction organic carbon were obtained at these stations by George Mason University, Academy of Natural Sciences (Philadelphia), and the University of Maryland Chesapeake Biological Laboratory. Sediment porosity data were obtained from Cartwright and Friedrichs (2006). Copies of the sediment database may be obtained directly from ICPRB. The complete database will eventually be made available on the ICPRB web page (www.potomacriver.org).

7.5 Selection of PCB3+ as Model Calibration Target for PCBs

7.5.1 Background

PCBs are a class of synthetic compounds that were typically manufactured through the progressive chlorination of batches of biphenyl to achieve a target percentage of chlorine by weight. PCBs are not a unique chemical compound. Individual PCB compounds called congeners can have up to 10 chlorine atoms attached to a basic biphenyl structure consisting of two connected rings of six carbon atoms each. There are 209 patterns in which chlorine atoms may be attached, resulting in 209 possible compounds. These compounds can be grouped into "homologs" defined by the number of chlorine atoms attached to the carbon rings. For example, PCB compounds that contain five chlorine atoms comprise a homolog referred to as pentachlorobiphenyls or penta-PCBs. PCBs are hydrophobic and tend to bind to organic particles in sediments and soils, and accumulate in the tissues of aquatic organisms, including fish.

7.5.2 PCB TMDL Targets

The PCB TMDL targets in DC, MD and VA waters are expressed in terms of total PCBs for the protection of human health from carcinogenic effects. The underlying water quality standards (WQS) are expressed as total PCB concentrations in the water column and/or in fish tissue. This

is consistent with the EPA human health national criteria for PCBs which are expressed in terms of total PCBs, applied to both water and fish consumption. Although there may be differences in homolog distributions among sources, ambient conditions and impacted resources in a particular system, the current EPA criteria are still based on total PCB.

7.5.3 Technical Issues

The basic issue stems from the fact that "total PCB" is not a unique chemical compound but is the sum of 209 separate compounds, or congeners. From a regulatory standpoint, all that matters is total PCBs but from a transport and fate modeling standpoint, it is practically impossible to model all 209 individual congeners. It is possible to represent total PCBs as a single variable by taking the grand averages of the physical-chemical properties of all 209 congeners and assigning them to a single state variable in the model. This approach would be scientifically unsound because the physical-chemical properties (e.g., octanol-water partition coefficients) of PCBs can vary over approximately four orders of magnitude from mono-PCBs to deca-PCBs. Consequently, such a "total PCB" state variable could only be characterized with low precision and large uncertainty.

An alternate approach would be to aggregate the 209 congeners into 10 homologs, model each homolog, and then sum the results to form total PCBs. This would substantially decrease the range of uncertainty because the physical-chemical properties of individual homolog groups could be defined much more precisely than those of total PCBs. While technically feasible, this approach would involve 10 separate models and would be extremely intensive in terms of data, resources and schedule.

Another alternate approach would be to identify a surrogate homolog or group of homologs for total PCBs. In the ideal case, the concentrations of the surrogate would be proportional to total PCB concentrations and it would include a small enough number of homologs so that the physical-chemical properties of the grouping could be reasonably well characterized. The feasibility of this approach is highly site-specific and depends on the spatial-temporal distributions of the various homolog groups among the sources, ambient conditions and impacted resources, and the adequacy of the database.

7.5.4 Analysis of Potomac and Anacostia Data

Refer to Haywood and Buchanan (2007), Appendix B, for a detailed analysis of PCB homolog data for the Potomac and Anacostia because only summary results are presented here. Figure 74 shows the normalized frequency of homolog distributions among the different media for the Potomac and Anacostia. There is great variability in homolog distributions among sources (below fall line tributaries and WWTPs), ambient conditions (sediments and water column particulates) and impacted resources (filets of bottom feeding fish) in the Potomac and Anacostia. Large peaks are apparent for homologs 3-7, with lower percentages occurring in the tails of the distribution.

Figure 75 shows median percent distributions of each homolog in the various tributaries to the tidal Potomac and Anacostia. In addition, results are shown separately for five different laboratories. Overall, homologs 3-6 contribute 10 percent or more to the total PCB

concentrations in each tributary. However, there is high variability among the tributaries for each of these four homolog groups and no single group stands out as being representative.

Confounding this variability among tributaries is the analytical variability among laboratories, especially between CBL and the other four laboratories. For the CBL data, homologs 1 and 2 contribute greater than 10 percent to the total PCB concentrations in several different tributaries. The corresponding results for all of the other laboratories are less than 10 percent. Still another confounding factor is that the GMU data for PCB do not even include homologs 1 and 2.

Figure 76 shows the percent contributions of each homolog to total PCBs in fish filets of bottom feeders in the Potomac and Anacostia rivers. Homologs 4-7 represent most of the total PCBs in these fish. Homologs 3 and 8 contribute small percentages, and homologs 1, 2, 9 and 10 are not significant contributors.

7.5.5 Rationale for Selection of Homologs 3-10 (PCB3+)

From the results in Figures 74-76, no single homolog appears to stand out as an appropriate surrogate for total PCB concentrations. Furthermore, identification of a single homolog group as a surrogate is confounded by analytical differences among the five individual laboratories. The CBL data for homologs 1 and 2 are suspect because they do not appear to be compatible with corresponding results from any of other four laboratories, and the GMU data do not include homologs 1 and 2.

There are also scientific reasons for excluding homologs 1 and 2 in a surrogate for total PCBs. Due to their physical-chemical properties, homologs 1 and 2 behave very differently than other homolog groups. They have very low partitioning to solids and very high volatility, compared to other homologs, and very low accumulation levels in fish tissue. For example, although octanol-water partition coefficients of PCBs vary over approximately four orders of magnitude from homologs 1 through 10, they vary over a range that is six times smaller for homologs 3 through 10 (PCB3+). Consequently, PCB3+ can be characterized with much greater precision and lower uncertainty than total PCBs.

It could be argued that homologs 9 and 10 should also be excluded because of their small contributions to sources, ambient conditions and impacted resources. As a practical matter, however, this would involve additional data processing steps beyond excluding homologs 1 and 2, and would not significantly affect the results.

If the goal is to select a surrogate for total PCB concentrations that represents all sources, ambient conditions and impacted resources, then PCB3+ is the most reasonable choice, given the site-specific conditions in the Potomac and Anacostia. A disadvantage of PCB3+ is that there will be more uncertainty in specification of physical-chemical properties than with a smaller group of homologs. This does not mean it will be impossible to develop a scientifically credible model. For example, PCB3+ (also called Tri+ PCB) was the surrogate variable for total PCBs in the transport and fate model for the Upper Hudson River RI/FS, and results from this model were approved by an Expert Panel of independent scientists and accepted by EPA Region 2.

7.6 Development of Sediment Initial Conditions

The PCB model requires that sediment concentrations for PDC and PCB3+ be specified at the beginning of the model simulation. The available sediment data for the Potomac and Anacostia showed high degrees of spatial variability and were processed using the locally weighted scatter plot smooth (LOWESS) algorithm in Matlab. LOWESS was applied to the porosity data from Cartwright and Friedrichs (2006) to estimate solids concentrations in the sediment. These results were brought forward into the analysis of the available data for sediment organic carbon and PCB3+ to estimate bulk volumetric concentrations for PDC and PCB3+ required for input to the PCB model.

Figures 77 and 78 show the spatially processed results for the Potomac and Anacostia mainstems, respectively. These results were mapped on to the model spatial segmentation grid and used to specify sediment initial conditions. These spatially-smoothed initial conditions prevented the introduction of fine-scale artifacts in the model computations that were not justified by the available data.

8. PCB MODEL CALIBRATION

8.1 Calibration Strategy

The U.S. EPA (2003) recommended best practices for evaluation of environmental models to help determine when a model, despite its uncertainties, can be appropriately used to inform a management decision. The proposed "tools" or best practices emphasized by U.S. EPA include model corroboration, and sensitivity and uncertainty analysis. Model corroboration is the use of quantitative and qualitative methods to evaluate the degree to which a model corresponds to reality. In practical terms, it is the process of "confronting models with data." Model corroboration has also been called model calibration or validation. The evaluation of the PCB TMDL model for the tidal Potomac and Anacostia rivers was consistent with this U.S. EPA guidance on evaluation of environmental models.

The calibration strategy was to specify as many external inputs and internal parameters as possible using site-specific data or independent measurements, and only a minimal number of parameters through model calibration. Another part of the strategy was that parameters determined through model calibration were held spatially and temporally constant unless there was supporting information to the contrary. Model parameters were not permitted to assume arbitrary values in order to obtain the best "curve fits" in a strictly mathematical sense. Where necessary, sensitivity analyses were conducted for model parameters over ranges consistent with the scientific literature, other modeling studies and best professional judgment to obtain optimal agreement between computed and observed values. Calibration results were interpreted using a suite of different quantitative metrics that were used collectively in a weight-of-evidence approach.

The following were the principal operational steps in calibration of the organic carbon dynamics model:

1. Specify a constant net settling rate for BIC.

2. Specify a constant gross settling rate for PDC.

3. Specify temperature-dependent PDC and BIC decay rates in the water column.

4. Specify a temperature-dependent PDC decay rate in the sediments, consistent with available data for SOD.

5. Adjust PDC resuspension rates for each spatial zone to achieve optimal agreement between computed and observed results for water column PDC concentrations and net solids burial rates.

The calibrated sorbent dynamics model was used to drive the transport and fate mass balance model for PCB3+. All external inputs and internal model parameters for PCB3+ were specified using site specific data or independent measurements. No PCB3+ model parameters were determined through model calibration. Furthermore, there was only feed-forward from the sorbents calibration, not feed-back from the PCB3+ calibration. That is, results from the PCB3+

simulations were not used to retroactively adjust any of the model parameters in the sorbents calibration.

As with the hydrodynamic and salinity models, the assessment of model calibration results for sorbents and PCB3+ was a weight-of-evidence approach that relied on multiple quantitative metrics and best professional judgment. No single metric provides sufficient information by itself to completely evaluate model calibration results. The metrics used for the sorbent and PCB3+ calibrations include cumulative frequency distributions, time series plots at fixed locations, spatial profiles at fixed points in time, comparisons of seasonal median values, and comparisons of computed first-order loss rates with those from available historical data for PCB body burdens in benthic feeding fish.

8.2 Incompatibilities Among Ambient Datasets

An over-arching factor that confounded attempts to calibrate the PCB model was the apparent incompatibility of PCB3+ data for the Potomac at Chain Bridge for determining mass loads, and PCB3+ data immediately downstream for representing ambient conditions. Figure 79 illustrates the crux of the problem. There is a total of 11 CBL and Battelle data at Chain Bridge with a mean concentration of 0.67 ng/L and a median of 0.39 ng/L. There are eight ANS data within the first eight miles downstream, two at each of four different stations. These data have a mean concentration 1.35 ng/L and a median of 1.39 ng/L. Depending on whether the mean or the median is used, the ANS data are 200-360 percent greater than the combined CBL and Battelle data at Chain Bridge.

There is no independent evidence for accepting or rejecting the CBL, Battelle, or the ANS data. However, if all three data sets are correct they imply a large, unaccounted source of PCB3+ to the Potomac within the first few miles downstream of Chain Bridge. This source would need to be either external (watershed) or internal (sediments). Given the locations of Rock Creek and the Anacostia (Figure 79) relative to the ANS sampling stations, it is unlikely that large "missing loads" would be coming from these sources. It also seems unlikely that there could be a large unaccounted watershed source, especially between 0.60 (ANS PR-1) and 3.3 (ANS PR-2) miles downstream of Chain Bridge because the watershed in this region is primarily forested. The available sediment data in this region are not sufficient to further inform this investigation.

It was not possible to fully resolve these data incompatibilities within the present modeling study. Haywood and Buchanan (2007) discuss these and other data issues, describes the various investigations and analyses that were conducted, and documents the assumptions, rationale, and methods used to develop the final mass loads and calibration targets for this PCB TMDL modeling effort.

8.3 Apparent Outliers for Ambient PCB3+ Concentrations

Several apparent outliers for ambient PCB3+ concentrations in the middle and lower portions of the Potomac also confounded calibration of the PCB model. Figure 80 shows all of the available data for ambient PCB3+ concentrations in the Potomac for the model calibration period 2002-2005. There are 36 total data with a mean value of 1.34 ng/L and a standard deviation of 1.04 ng/L. There is a general spatial trend of higher concentrations in the upper portion of the estuary in the vicinity of DC and a decline with distance downstream, except for the three data values at

RMs 77.83, 48.62 and 18.11. These three data values are unique because they are all greater than the highest reported PCB3+ concentration in the vicinity of DC, they are all approximately 2-4 times greater than the standard deviation of 1.04 ng/L, and they were all taken on June 27, 2003.

There is no independent evidence for accepting or rejecting these three apparent outlier values. It is possible they reflect sampling and/or analytical errors or other QA/QC problems. Another possibility is that they represent a large loading event that was not captured in development of the external PCB3+ mass loads. This is unlikely because these three data represent locations that are almost 60 miles apart in the longitudinal direction. The magnitude of such an external loading event, or an internal sediment resuspension event, would need to be unrealistically enormous. The mean flow of the Potomac River on June 27, 2003, was 19,500 cfs and was approximately equal to the mean flow for the 12-month period ending on July 5, 2003 (19,755 cfs) (Haywood and Buchanan 2007, Appendix C).

8.4 Calibration Results

8.4.1 Introduction

Table 27 presents the model calibration parameters for sorbents and PCB3+ and includes numerical values, physical units and sources of information. Partition coefficients, Henry's Law Constant and Molecular Weight for PCB3+ were determined as the sum of the weighted averages for the individual homologs that were present. These weighted averages were derived using the average percent sample detection distribution for each homolog in the combined ANS/CBL/GMU data set.

Table 28 presents zone specific calibration values for net solids burial rates that were derived as described above, and PDC resuspension and sediment decay rates. The calibration targets for net solids burial rates were the same (0.25 to 0.50 cm/year) as those used by Cerco and Cole (1994) and derived from measurements by Brush (1989). The model was calibrated to produce positive median net burial rates in all sediment spatial segments during 2005 that closely matched this observed range. The reasons for constraining model results for 2005 were that harmonic mean flow for 2005 most closely matched the long-term harmonic mean, and that all TMDL forecast simulations were conducted by repeated cycling of 2005 flows. It was assumed that net erosion was not a realistic, sustainable condition in any of the model spatial segments, nor were there any data to support such a long-term condition.

Table 29 presents a statistical summary of model calibration results for sorbents and PCB3+ for the whole Potomac and each of the six spatial zones in Figures 57-62. Interpretation and assessment of model calibration results requires much judgment and an understanding of context. It was noted in Section 6 that there remain questions and uncertainties in freshwater inflows and mass loads, especially at the scales of the model spatial segmentation grid. Another over-arching factor is the large disparity in the number of observations available to constrain the model calibration. For example, during the period 2002-2005 in the Potomac there are 421 observations for BIC and PDC but only 36 observations for PCB3+. For the same period in the Anacostia there are only 26 observations for BIC and PDC, and 36 observations for PCB3+. Furthermore, most of the data for BIC and PDC were collected at different stations and times,

and by different agencies, than the data for PCB3+ hence very few of the sorbent and PCB3+ data are synoptic.

8.4.2 Sorbents and PCB3+ in the Potomac

Figures 81-85 show CFDs for computed and observed daily average sorbent and total PCB3+ concentrations for the whole Potomac. Particulate organic carbon (POC) is not a model state variable but is derived as the sum of BIC and PDC and is reported here for completeness. Overall, results appear reasonable given the model assumptions and available data for model inputs and ambient water quality conditions. In particular, recall that mass loads for BIC, the major source of organic carbon, are based on average conditions for 1985-1994 not for the model calibration period of 2002-2005. Furthermore, the same BIC mass loads are repeatedly cycled for each of the four calibration years and do not reflect the substantial differences in inter-annual flows.

The CFDs for BIC and PDC (Figures 81-82) are characterized by relatively flat distributions until approximately the 80th percentiles, then by very high values in the highest 10th percentiles for both computed and observed values. Median values are over-computed for BIC but computed and observed values are in close agreement for PDC and POC. The observations span a range of 0-3 mg/L for BIC and 0-20 mg/L for PDC, thus most of the observed POC consists of PDC. Consequently, the over-computation of BIC does not have a large impact on the overall results for organic carbon (Figure 83). The statistical results for BIC (Table 29) indicate a mean error of -0.07 mg/L, an absolute mean error of 0.26 mg/L, and a relative error of 83 percent. The corresponding results for PDC are -0.10 mg/L, 0.65 mg/L, and 54 percent.

For PCB3+, computed values are compared with all data and all data except the three apparent outliers discussed above. For all data (Figure 84), computed and observed median values are in close agreement, but the model under-computes observations in the upper 50th percentile of the CFD. There is also some over-computation in the lower 20th percentile of the CFD. For all data except the three apparent outliers (Figure 85), computed and observed median values are still in close agreement, but there is now much closer agreement in the upper 50th percentile of the CFD.

The statistical results for PCB3+ versus all data indicate a mean error of 0.33 ng/L, an absolute mean error of 0.81 ng/L, and a relative error of 56 percent. Statistical results for PCB3+ versus all data except the three apparent outliers (Table 29) indicate a mean error of 0.08 ng/L, an absolute mean error of 0.61 ng/L, and a relative error of 50 percent.

Figure 86 shows CFDs for computed and observed daily average particulate and dissolved phase PCB3+ concentrations for the whole Potomac (excluding apparent outliers). The results closely mirror those for total PCB3+ in Figure 85. There is good agreement between computed and observed medians but under-computation for the upper 50th percentile of the CFDs. These results indicate good representation of the partitioning of total PCB3+ concentration into its dissolved and particulate phase components.

Figures 87-91 show CFDs for computed and observed daily average sorbent and total PCB3+ concentrations for the individual spatial zones in the Potomac. The vertical scales for each state variable are the same on all CFDs for the whole Potomac and the individual spatial zones to

facilitate cross-comparisons. Table 29 contains statistical summaries for each state variable and spatial zone.

Results are reasonable in UPOTTF (Figure 87) for sorbents and PCB3+ with the exception of some under-computation of PCB3+ in the upper 50th percentile of the CFD. The most data-rich zone is LPOTTF (Figure 88). Results for sorbents and PCB3+ show similar patterns as those for the whole Potomac. The model consistently over-computes BIC in POTOH (Figure 89) but computed and observed values are in good agreement for PDC and POC. Results for PCB3+ are generally good except for some under-computation of the highest observation. There are insufficient observations for PCB3+ in UPOTMH (Figure 90) and LPOTMH (Figure 91) to construct CFDs. The model consistently over-computes BIC in UPOTMH and under-computes it in LPOTMH. Results for PDC and POC are generally reasonable in both zones.

Figures 92-99 show time series plots for computed and observed daily average BIC and PDC concentrations for the eight monitoring stations that include most of the available data. The same vertical scales are used at each station to illustrate trends with distance downstream. Results for BIC tend to increase and those for PDC tend to decrease with distance downstream. This is consistent with results in Figure 73 showing higher ratios of BIC to POC in the lower portion of the estuary.

Computed results for BIC show similar patterns each year because the same internal BIC mass loads are repeatedly cycled each year during the calibration. Differences in responses among years occur because freshwater inflows differ among the individual years. Computed values for PDC are characterized by storm-driven events, especially during the wet years 2003-2004. Few of the observations for PDC capture these events. The magnitude and frequency of these events attenuate with distance downstream.

Figures 100-105 show time series plots for computed and observed daily average total PCB3+ concentrations at the 12 monitoring stations for which there are at least two data. Computed results are characterized by the same storm-driven events as PDC, especially during the wet years 2003-2004. Most of the observations are confined to UPOTTF and LPOTTF and few of them capture these events. The magnitude and frequency of these events attenuate with distance downstream.

Figures 106-109 show spatial profiles of computed and observed daily average BIC and PDC concentrations that represent typical winter, spring, summer, and fall conditions. Computed BIC tends to increase with distance downstream, but the observations do not reveal a clear spatial structure. Observed PDC tends to decrease with distance downstream but computed PDC shows little spatial structure.

Figures 110-112 show spatial profiles of computed and observed total PCB3+ concentrations at the six points in time for which there are at least two data. Most of the PCB3+ observations occur on only two days, April 12 and July 27, 2005. On April 12 the model under-computes observations in UPOTTF and is well below observations in LPOTTF immediately below the confluence with the Anacostia at RM 110.3. There are no more observations downstream on April 12 with which to evaluate model performance. On July 27 there is good agreement

between computed and observed values in UPOTTF, but again the model falls well below observations in UPOTTF near to and below the confluence with the Anacostia. There are insufficient observations on the other four dates for quantitative evaluation of model performance.

The high degree of small-scale variability due to storm-driven events confounds quantitative evaluation of model results using regression analysis. There is frequently little or no one-to-one correspondence between daily average computations and instantaneous observed values. This is because the available data for external mass loads and ambient water quality conditions are not always in phase at the spatial-temporal scales at which the model operates. Under these circumstances, it is more appropriate to evaluate model performance using CFDs and not regressions.

Although no standard criteria exist for judging acceptable model performance, it is informative to compare these model calibration results to similar results for the second generation CBWQM (Cerco and Noel 2004). No CBWQM statistics were reported for organic carbon, total suspended solids (TSS) or inorganic suspended solids (ISS). Statistics were reported for chlorophyll *a* concentration, which is proportional to BIC, and for total phosphorus concentration which can be viewed as a surrogate for PCB3+ because both are conserved and strongly sorb to solids.

From the CFD statistics (Table 29) the relative errors for BIC, PDC and PCB3+ for the whole Potomac were 83, 54 and 50 percent, respectively. The relative errors for surface chlorophyll *a* and total phosphorus concentrations in the Potomac portion of the CBWQM were 80 and 59 percent, respectively, for a 10-year calibration period from 1985-1994.

8.4.3 Sorbents and PCB3+ in the Anacostia

Figure 113 shows CFDs for computed and observed daily average sorbent and total PCB3+ concentrations for the Anacostia. Given the assumptions and available data, there is reasonable agreement for computed and observed median values. However, there is substantial divergence of computed BIC below observations, beginning at the 70th percentile of the CFD and substantial divergence of computed PCB3+ above the observations, beginning at approximately the 40th percentile of the CFD. There is also some over-computation of PDC in the upper 15th percentile of the CFD.

Evaluation of model performance in the Anacostia is confounded by the strong influence of storm-driven loading events. Such events exert much stronger influence on the Anacostia than the Potomac because a large proportion (78 percent) of PCB3+ mass loads to the Anacostia are from direct drainage (Table 23) and receiving water flows are much smaller than those in the Potomac.

Figure 114 shows time series plots for computed and observed daily average BIC and PDC concentrations at RM 3.39, one of the principal sampling locations in the Anacostia. There is a repeating annual pattern for computed BIC concentrations and very strong event-driven behavior for PDC, especially in the wet years 2003-2004. Observations are sparse and confined to only 2002. Figure 115 shows the corresponding results for PCB3+ at this same location. As with

computed PDC, there is strong event-driven behavior, especially in 2003-2004. Again, observations are sparse, confined to only 2002, and do not capture events.

It is informative to further explore the under-sampling of flow events and its impact on the ability to evaluate model performance. Figure 116 shows CFDs for daily average flow and flow for days on which ambient conditions and direct drainage loads were sampled in the Anacostia. Sampling for both ambient conditions (green line) and direct drainage loads (red line) was biased towards low flows, relative to actual daily flows (dark blue line). This is significant because PDC and PCB3+ mass loads were estimated using regressions of TSS concentrations on flow, and TSS concentrations are generally greater at higher flows. Consequently, mass input loads to the model correspond to higher flows than those for which there are observations of ambient conditions.

Figures 117-119 show spatial profiles of computed and observed daily average BIC and PDC concentrations for the principal sampling events in the Anacostia. Results for May 6 and August 31, 2002, appear reasonable, but computed BIC and PDC values for June 24 are not in good agreement with observations.

Figures 120 and 121 show spatial profiles of computed and observed daily average PCB3+ concentrations for the four principal sampling events in the Anacostia during 2002. Along with results in Figure 116, these results highlight the confounding influence of storm-driven loading events in evaluation of model performance. In particular, comparisons between computed and observed PCB3+ concentrations are strongly influenced by two large flow events that occurred on August 29 and October 16 (Haywood and Buchanan 2007, Appendix A), just prior to the sampling events whose results are shown in Figure 121. The August 29 event delivered the highest daily mass load of PCB3+ to the Anacostia for the entire year. There are 14 total observations for these two days which constitute 54 percent of the 26 total observations for the whole Anacostia. Consequently, comparison of computed and observed daily average PCB3+ concentrations on these two days skews the entire CFD for 2002.

8.4.4 PCB3+ in the Tributaries

Figure 122 shows time series plots for computed and observed daily average PCB3+ concentration in Occoquan Bay, and Figure 123 shows the same results for Mattawoman Creek. There are only three data for water column PCB3+ during 2002-2005 for model segments representing minor tributaries, coves or embayments, one in Occoquan Bay and two in Mattawoman Creek. Although the available data are not sufficient to draw definitive conclusions, the comparisons between computed and observed PCB3+ concentrations appear reasonable.

8.4.5 PCB3+ Seasonal Medians

A useful metric for evaluating model performance is comparison between computed and observed seasonal medians and ranges. This metric tends to compensate for the influence of flow-driven events and corresponds more closely to how the model will be used to determine the TMDL. EPA TMDL guidance for toxic substances where the human health impact is based on lifetime accumulation recommends using annual median exposure concentrations.

Figures 124-129 show comparisons between computed and observed seasonal medians and ranges for PCB3+ concentrations in the five Potomac spatial zones and the Anacostia. Note that all plots are auto-scaled and have different vertical scales. Overall, computed and observed medians show close agreement except for summer in UPOTMH and LPOTMH (Figures 127 and 128) when only a single datum is available in each zone. In sharp contrast to the CFD results in Figure 113, there is good agreement between computed and observed PCB3+ concentrations in the Anacostia (Figure 129). Note that while comparisons of computed and observed median values are in good agreement, model results are generally characterized by much higher ranges than the data. This is a direct reflection of the under-sampling of ambient conditions during flow-driven events.

8.5 Evaluation of PCB3+ Attenuation Rates

Model calibration involved continuous dynamic simulations with the sorbent and PCB transport and fate models over a relatively short-term simulation period from 2002 to 2005. Apart from issues related to data quality, quantity and representativeness, this calibration approach is necessary but not sufficient to constrain all of the controlling environmental processes. The reason is that water column PCB concentrations in rivers or estuaries typically respond to changes on time scales of days to weeks; however, sediment PCB concentrations typically respond on time scales of years to decades because PCBs are much less mobile in bedded sediments. Consequently, it is advisable to evaluate model performance over longer time scales if the required data are available.

It is not possible to conduct longer-term simulations for the tidal Potomac and Anacostia rivers because historical data to support these simulations do not exist. An alternative is to conduct an independent consistency check on the calibration by comparing model response trajectories to available time series data for fish body burdens. The reasoning is that fish are good extractors of PCBs from the water column and sediments, through the pelagic and benthic good chains, and fish body burdens tend to mirror environmental exposure concentrations. Two advantages of this approach are that fish body burden data are generally more available than data for mass loadings or ambient concentrations, and that fish are good integrators of spatial variability, thus increasing the potential for detection of temporal trends.

Figure 130 shows lipid-normalized total PCB body burdens in benthic feeding fish species (channel catfish and gizzard shad) in the tidal Potomac and Anacostia from 1999 to 2005 (ICPRB Database). These species can be expected to mirror temporal trends in sediment PCB concentrations. Although the data are highly variable, they appear to be declining with time. Regression analysis was used to confirm that there are significant downward trends and to determine first-order loss rates in the Potomac tidal fresh, oligohaline and lower estuary regions, and in the Anacostia.

Figure 131 shows comparisons of first-order loss rates for PCB3+ expressed as model medians and ranges for sediment concentrations over 2002-2005, and body burdens in benthic feeders over 1999-1005. For all results combined, model medians range between 0.029 and 0.156 per year, and body burden medians range between 0.014 and 0.171 per year. The range of model medians is fully encompassed within the range of body burden medians for all results combined

and for three of the four spatial regions. The only exception is the lower Potomac estuary for which the model range is higher than the estimated body burden value.

The half-times corresponding to these first-order loss rates range between 4.4 and 24 years for the model results, and between 4 and 50 years for the body burden data. Model results imply greater rates of decline in all three regions of the Potomac than in the Anacostia. Body burden results imply greater rates of decline in the tidal fresh and oligohaline portions of the Potomac than in the lower Potomac estuary and the Anacostia.

Given all of the assumptions involved, computed results are in close agreement with the available observations. This conclusion should be qualified by noting that the data are highly variable, they represent only a relatively short period of record, and the spatial correspondence between computed and observed loss rates is only approximate. Nonetheless, the favorable comparison of computed loss rates with those determined from independent information serves to strengthen the scientific basis for the model calibration.

9. SENSITIVITY ANALYSES

9.1 Introduction

Sensitivity analysis evaluates the effects of changes in external model inputs or internal parameters on model results. Uncertainty analysis investigates the effects of lack of knowledge and other potential sources of error in the model, and when conducted in combination with sensitivity analysis, allows a model user to be adequately informed about the confidence that can be placed in model results. It is not practical to conduct formal, quantitative uncertainty analyses with complex, deterministic environmental models. U.S. EPA (2003) recommends sensitivity analysis as the principal evaluation tool for characterizing the most and least important sources of uncertainty in environmental models.

Sensitivity analyses were conducted with the calibrated PCB TMDL model to help identify the model inputs and parameters to which computed results for water column PCB3+ concentrations were most sensitive. Results from these analyses help to provide greater understanding of the relative importance of controlling environmental processes. These analyses were conducted for the following model inputs and parameters:

- Mass loads for PCB3+ from the Potomac at Chain Bridge;
- Mass loads for PCB3+ from direct drainage areas;
- Mass loads for PCB3+ from CSOs;
- Mass loads for PCB3+ from point source discharges;
- Mass loads for PCB3+ from atmospheric wet and dry deposition to the water surface;
- Downstream boundary concentration for PCB3+;
- Sediment initial conditions for PCB3+ concentrations; and,
- Sediment-water mass transfer rate for dissolved phase PCB3+.

Calibration values for each of these model inputs or parameters were varied by plus and minus 30 percent, and results compared to those for the base model calibration. A constant percent change normalizes results across the different cases and a value of 30 percent generally produces responses with sufficient magnitudes for meaningful interpretation.

Results for all sensitivity analyses are compared to base model calibration results for 2005 because these conditions were used for the TMDL forecast simulations. Specifically, all sensitivity results are presented for June 13, 2005, because Potomac flows on this day closely approximate the annual harmonic mean value. It should be noted that model responses to changes in external inputs or internal parameters are a function of flow and will not be exactly the same for different flow conditions.

9.2 External Mass Loads

9.2.1 Potomac River at Chain Bridge

Figure 132 shows the sensitivity of model calibration results to plus/minus 30 percent changes in PCB3+ mass loads from the Potomac at Chain Bridge. The primary impact is on UPOTTF. This is consistent with the spatial distribution of PCB3+ mass loads. The PCB3+ mass load from the

Potomac at Chain Bridge in 2005 is 44 percent of the total load to the system (Figure 67) and 83 percent of the total load to UPOTTF (Table 18). Advective flow and tidal mixing propagate this influence downstream into LPOTTF and POTOH. The influence of this perturbation declines with distance downstream and is not evident at the mouth because PCB3+ concentrations at this location are controlled primarily by the downstream boundary condition and tidal mixing. Changes in PCB3+ mass loads from the Potomac at Chain Bridge have a minor impact on the lower portion of the Anacostia due to tidal mixing with the Potomac mainstem.

9.2.2 Direct Drainage

Figure 133 shows the sensitivity of model calibration results to plus/minus 30 percent changes in PCB3+ mass loads from direct drainage areas. The primary impact is on the LPOTTF. Again, this is consistent with the spatial distribution of PCB3+ mass loads. Direct drainage loads in 2005 are 29 percent of the total load to the system (Figure 67) and 20 percent of the total load to LPOTTF. This spatial zone has the highest percent contribution of PCB3+ mass loads from direct drainage of all the Potomac zones. There is also a major impact on the Anacostia because direct drainage loads of PCB3+ during 2005 were 76 percent of the total PCB3+ load to the Anacostia (Table 23).

9.2.3 CSOs

Figure 134 shows the sensitivity of model calibration results to plus/minus 30 percent changes in PCB3+ mass loads from CSOs. Again, the primary impact is on LPOTTF. CSO loads of PCB3+ in 2005 are 8.4 percent of the total load to the whole system (Figure 67) and 20 percent of the total load to LPOTTF (Table 19). This is the highest percentage contribution of PCB3+ mass loads from CSOs among all Potomac spatial zones. There is also some impact on the Anacostia because PCB3+ loads from CSOs in 2005 were 15 percent of the total PCB3+ load to the Anacostia (Table 23).

9.2.4 Point Source Discharges

Figure 135 shows the sensitivity of model calibration results to plus/minus 30 percent changes in PCB3+ mass loads from point source discharges. The primary impact is on LPOTTF but the magnitude of this impact is small. The reason is that although loads of PCB3+ from point source discharges in 2005 are 25 percent of the total load to LPOTTF (Table 19), the total PCB3+ load from this source category is only 2 percent of the total load to the whole system (Figure 67). Consequently, a plus/minus 30 percent change in PCB3+ mass loads from point source discharges does not translate into a large change in mainstem PCB3+ concentrations.

9.2.5 Atmospheric Wet/Dry Deposition

Figure 136 shows the sensitivity of model calibration results to plus/minus 30 percent changes in PCB3+ mass loads from atmospheric wet plus dry deposition to the water surface. There are only small impacts on the Potomac and the Anacostia. Atmospheric wet/dry deposition contributes only 9 percent of the total PCB3+ mass load to the whole system in 2005 (Figure 67) and this contribution is spatially distributed over the entire water surface. It should be noted that although this source contributes greater than 95 percent of the total PCB3+ mass loads to POTOH, UPOTMH and LPOTMH (Tables 20-22), the magnitudes of these contributions are small. Mass loads from atmospheric wet/dry deposition are not significant during the model

calibration, but become relatively more important under TMDL conditions of reduced external loadings of PCB3+ from the watershed.

9.3 Downstream Boundary Concentration

Figure 137 shows the sensitivity of model calibration results to plus/minus 30 percent changes in the PCB3+ downstream boundary concentration. There is a substantial relative impact on LPOTMH and this impact propagates upstream into UPOTMH due to tidal mixing. Impacts in the upper and middle portions of the Potomac and in the Anacostia are not significant.

9.4 Sediment Initial Conditions

Figure 138 shows the sensitivity of model calibration results to plus/minus 30 percent changes in the PCB3+ sediment initial conditions. There are substantial impacts on both the Potomac and the Anacostia because sediment conditions were changed in all spatial zones. There is little impact on UPOTTF because PCB3+ concentrations in this zone are dominated by mass loads from the Potomac at Chain Bridge, the largest loading source to the whole system. The largest relative impact is in POTOH and declines with distance downstream. The lowest impact occurs at the downstream boundary because PCB3+ concentrations at this location are controlled primarily by the downstream boundary concentration and tidal mixing. These results illustrate that current PCB3+ concentrations in the water column are driven not only by external mass loads, but also by legacy contamination in the sediments.

9.5 Sediment-Water Mass Transfer Rate

The sediment-water mass transfer rate represents sediment-water mass flux of PCB3+ under non-resuspension conditions due to bioturbation-enhanced diffusive mass transfer (Thibodeaux and Bierman 2003). Bioturbation is an in-bed particle translocation mechanism driven by the activity of bottom-living animals that moves sediment-bound pollutants and homogenizes surface layers. This process is separate and completely distinct from flow-driven resuspension of sediment solids. Bioturbation-enhanced diffusion was found to be the dominant mechanism for sediment-water mass transfer of PCBs in the Upper Hudson River (U.S. EPA 2000; Erickson et al. 2005).

Figure 139 shows the sensitivity of model calibration results to plus/minus 30 percent changes in the PCB3+ sediment-water mass transfer rate. There are impacts on both the Potomac and the Anacostia because this rate was changed in all spatial zones. The spatial pattern of these impacts is similar to that for the impacts of changes in sediment initial conditions, and for essentially the same reasons.

10. DIAGNOSTIC SIMULATIONS

10.1 Approach

Water column PCB concentrations are influenced by external sources from the watershed and atmospheric wet/dry deposition, as well as legacy contamination in the sediments. The PCB mass balance model includes both the water column and sediments, and explicitly includes the influence of sediment PCBs on water column PCB concentrations. Diagnostic simulations were conducted to evaluate the impact of legacy contamination in the sediments on current PCB3+ concentrations in the water column and the time required to achieve dynamic equilibrium. Results from these simulations helped to inform the design of the TMDL forecast scenarios.

The TMDL conditions correspond to quasi-steady state, dynamic equilibrium among external PCB3+ mass loads, and concentrations in the water column and sediments. Under these conditions there is no net flux of PCB3+ across the air-water interface, and both the surface and deep sediment layers are net sinks for PCB3+ not sources. It can not be assumed that water column and sediment PCB3+ concentrations are currently in dynamic equilibrium because the long-term histories of external mass loads and ambient exposure concentrations are not known.

Two long-term (100 years) forecast simulations were conducted with the calibrated model. The first was a baseline simulation driven by repeated cycling of 2005 flows and external mass loads. The second was a "washout" run also driven by repeated cycling of 2005 conditions, but with all external PCB3+ loads set to zero. This run included zero values for the downstream boundary concentration, atmospheric wet/dry deposition to the water surface, and PCB3+ gas phase concentration. If it is assumed that future PCB3+ mass loads will never exceed those in 2005, then these two forecast simulations will bound the future response trajectories of the system.

To represent current conditions, results are shown for mid-June in the first year of the 100-year forecast simulations. Potomac River flow during this period approximates the annual harmonic mean value for 2005 that was used as the TMDL flow condition. Note that results from these forecast simulations do not correspond to those on June 13, 2005, of the model calibration period due to different simulation periods and time sequences for flows and mass loads. The calibration simulations used actual 2002-2005 flows and mass loads, and the 100-year forecast simulations used repeated cycling of 2005 flows and mass loads.

10.2 Impacts of Sediments on Current Conditions

Figure 140 shows spatial profiles of computed daily average PCB3+ concentrations in the Potomac water column for 2005. Results for the "washout" case represent only the sediment contribution to the water column concentrations, and results for the baseline case represent the contributions of both external mass loads and the sediments. The difference between these two profiles (red arrow) is the contribution from only external mass loads.

Water column PCB3+ concentrations are driven primarily by external mass loads in UPOTTF and most of LPOTTF. There is a downstream transition from dominance by external mass loads to dominance by sediment contributions in POTOH, UPOTMH and LPOTMH. These results are

consistent with the dominant influence of PCB3+ mass loads from the Potomac at Chain Bridge in the upper portion of the Potomac (Figure 132).

Figure 141 shows corresponding results for the Anacostia. Water column PCB3+ concentrations are driven primarily by external loads for most of the river, but are influenced by both the sediments and external mass loads from the NE and NW tributary branches at the upstream end. The decline in concentrations at the downstream end is due to tidal mixing with the Potomac which has lower PCB3+ concentrations.

10.3 Evaluation of Long-Term Responses

Figure 142 shows long-term results for PCB3+ concentrations in the Potomac and Anacostia sediments at two locations, RMs 92.58 and 3.39, respectively. Sediment concentrations are a better indicator of long-term responses than water column concentrations because they have lower small-scale temporal variability. Results indicate that approximately 50 years or more is required to reach quasi-steady state, dynamic equilibrium conditions. Note that these results are only illustrative because time to dynamic equilibrium depends partly on the magnitude of the change in external mass loads and on spatial location in the river.

For the baseline run, sediment PCB3+ concentrations asymptote to values that are at dynamic equilibrium with 2005 external mass loads. These quasi-steady state, dynamic equilibrium conditions are the same as the TMDL conditions, but for 2005 external mass loads, not the reduced external loads that will be required to reach the TMDL targets. Results indicate that surface sediment PCB3+ concentrations decline by approximately 80 percent in the Potomac and increase by approximately 10 percent in the Anacostia in the noted locations.

Inspection of results for other locations in the Potomac indicates that computed surface sediment PCB3+ concentrations decline with time in all model spatial segments. For the Anacostia, computed concentrations decline with time between RMs 8.31 and 4.66, increase with time between RMs 4.41 and 1.31, and then again decline with time between RM 1.13 and the confluence with the Potomac. These results are consistent with migration of sediment PCB3+ from upstream to downstream over time. While this is not unreasonable, the available data for external loadings and ambient conditions are not sufficient to confirm such a conclusion.

For the “washout” run, surface sediment PCB3+ concentrations asymptote to zero in both the Potomac and Anacostia. This is because the only PCB3+ mass in the system is the PCB3+ mass present in the sediments at the beginning of the simulation. All of this PCB3+ mass eventually attenuates due to net burial into deep sediment layers, volatilization within the Potomac and Anacostia, and transport downstream to Chesapeake Bay.

11. MASS BALANCE COMPONENTS ANALYSIS

11.1 Introduction

To better understand the sources, transport and fate pathways for PCB3+, results from the calibrated model were used to construct mass balance components for the principal spatial zones in the Potomac and Anacostia rivers. These components are organized in terms of external mass loads, net exchanges with external boundaries, and internal exchanges between the water column and sediments.

11.2 Mass Loads and Boundary Fluxes

Figure 143 is a conceptual representation of the principal PCB3+ mass loads and fluxes in the tidal Potomac and Anacostia rivers. External loads are unidirectional and include inputs from the Potomac at Chain Bridge, the NE and NW Branches of the Anacostia, direct drainage, CSOs, point source discharges, contaminated sites, and atmospheric wet/dry deposition to the water surface. Exchanges with external boundaries can be bidirectional and include tidal tributaries, the downstream boundary with Chesapeake Bay, and air-water gas phase exchange. Finally, internal fluxes represent exchanges across the sediment-water interface and can also be bidirectional. The actual directions of these boundary exchanges depend on the relative PCB3+ concentrations on opposing sides of the boundaries and, for tidal tributaries and the downstream boundary, on the combined effects of water flow and tidal mixing.

11.3 Mass Balance Components for PCB3+

Figure 144 is a schematic diagram showing PCB3+ external mass loads, boundary fluxes and sediment-water mass transfers for the five Potomac spatial zones over the model calibration period 2002-2005. For each zone results are presented for the water column and surface sediment layers. The category labeled “External Loads” includes direct drainage, CSOs, point source discharges, contaminated sites, atmospheric wet/dry deposition, and net inputs from tidal tributaries. Note that net inputs from tidal tributaries can be negative because they include both advective inflows and mass exchanges due to dispersion at the interfaces between tributary mouths and the mainstem.

Results indicate that most of the PCB3+ mass enters the system from the Potomac at Chain Bridge and is either transported downstream to Chesapeake Bay or lost to gas phase flux (volatilization). Note that except for UPOTTF, the surface sediments are sources to the water column not sinks. This is intuitively reasonable for a system that has received large external loadings of PCB3+ in the past and accumulated a large internal sediment reservoir, but which is now receiving much lower external loadings. It should be noted that both the magnitude and direction of the net sediment flux in UPOTTF are uncertain due mainly to the paucity of data for sediment initial conditions in this zone.

Results also indicate net burial of PCB3+ from surface to deep sediments in all spatial zones. This is consistent with net burial of PCB3+ by "cleaner" solids in current external PCB3+ mass loads, as opposed to more contaminated solids that likely existed in historical external loads. There is no contradiction in the result that surface sediments can lose PCB3+ mass to both the overlying water column and to deep sediment layers. This implies that surface sediment PCB3+

concentrations are attenuating due to processes at both interfaces: (1) solids cycling (settling and resuspension) and bio-enhanced diffusion of PCB3+ across the sediment-water interface; and (2) net solids burial to the deep sediment layers. Surface sediments in all spatial zones in the Potomac show net losses of PCB3+ mass. This is consistent with the computed temporal declines in surface sediment PCB3+ concentrations in all model spatial segments noted in Section 10.3.

Figure 145 shows PCB3+ mass balance components for the Anacostia over the model calibration period 2002-2005. Results indicate that most of the PCB3+ mass enters the system from external loads and is transported downstream to the Potomac. The two other fate pathways are losses to volatilization and net flux to the surface sediment. It was noted in Section 10.3 that for the Anacostia, computed surface sediment PCB3+ concentrations decline with time upstream and increase with time downstream. For the whole system, however, results for mass balance components indicate there is net PCB3+ mass flux from the water column to the surface sediments and net burial of PCB3+ from surface to deep sediments. Because the PCB3+ mass loss to deep sediments is greater than the mass gain from the water column, surface sediment PCB3+ concentrations for the Anacostia as a whole are declining with time.

Comparison of results in Figures 144 and 145 indicates that surface sediments are sources of PCB3+ to the water column for most of the Potomac, but sinks of PCB3+ from the water column in the Anacostia. One implication of these results is that external loadings of PCB3+ to the Anacostia have not declined enough from their historical values for the internal sediment reservoir to become a source to the water column. While this is not unreasonable, the available data for external loadings and ambient conditions are not sufficient to confirm such a conclusion.

REFERENCES

Ambrose, R.B., Wool, T.A., and Martin, J.L. 1993a. The Dynamic Estuary Model Hydrodynamics Program, DYNHYD5 Documentation and User Manual. US Environmental Protection Agency.

Ambrose, R.B., T.A. Wool and J.A. Martin. 1993b. The Water Quality Analysis Simulation Program WASP5, Part A: Model Documentation, Version 5.10, U.S. Environmental Protection Agency, Environmental Research Laboratory, Athens, Georgia.

Banks, R.B. and F.F. Herrera. 1977. Effects of wind and rain on surface reaeration. Journal of Environmental Engineering, American Society of Civil Engineers. 103(EE3):489-504.

Bierman, V.J., Jr., S.C. Hinz, N.S. Suk, S.-L. Liao, J.R. Yagecic and T.J. Fikslin. 2005. Dynamics of PCBs in the Delaware River Estuary: existing conditions and loading reductions required for achievement of water quality standards. Proceedings of TMDL 2005, Water Environment Federation, Philadelphia, Pennsylvania, June 26-29, 2005.

Bierman, V.J., Jr., S.C. Hinz, J.V. DePinto, S.-L. Liao, N.S. Suk and T.J. Fikslin. 2004a. Conceptual modeling framework for the PCB TMDL in the Delaware River Estuary. Proceedings of WEFTEC04, Water Environment Federation, New Orleans, Louisiana, October 2-6, 2004.

Bierman, V.J., Jr., S.C. Hinz, S.-L. Liao, N.S. Suk, J.R. Yagecic, T.J. Fikslin and J.V. DePinto. 2004b. A simplified mass balance modeling framework for toxics TMDLs: application to PCBs in the Delaware River Estuary. Proceedings of Watershed 2004, Water Environment Federation, Dearborn, Michigan, July 11-14, 2004.

Bierman, V.J., Jr., J.V. DePinto, T.C. Young, P.W. Rodgers, S.C. Martin and R. Raghunathan. 1992. Development and Validation of an Integrated Exposure Model for Toxic Chemicals in Green Bay, Lake Michigan. Final Report to U.S. Environmental Protection Agency, Large Lakes and Rivers Research Branch, Grosse Ile, Michigan.

Boynton, W.R., J.M. Barnes, B.J. Weaver, L.L. Magdeburger and P. Sampou. 1996. Sediment-Water Fluxes and Sediment Analyses in Chesapeake Bay: Tidal Fresh Potomac River and Maryland Main Stem. Contract Report W-96-1, U.S. Army Corps of Engineers, Waterways Experiment Station, Vicksburg, MS.

Boynton, W., W. Kemp, J. Garber and J. Barnes. 1986. Ecosystem Processes Component (EPC) Level 1 Data Report No. 3. UMCEES CBL Reference No. 85-86. University of Maryland Center for Environmental and Estuarine Studies, Solomons, MD.

Brunciak, P.A., J. Dachs, T.P. Franz, C.L. Gigliotti, E.D. Nelson, B.J. Turpin and S.J. Eisenreich. 2001. Polychlorinated biphenyls and particulate organic/elemental carbon in the atmosphere of Chesapeake Bay, USA. Atmospheric Environment. 35:5663-5667.

Brush, G.S. 1989. Rates and patterns of estuarine sediment accumulation. Limnology and Oceanography. 34(7):1235-1246.

Cartwright, G.M. and C.T. Friedrichs. 2006. Development of a Sediment Transport Model for the Chesapeake Bay: Supporting Physical Data from VIMS Potomac River Intensive Surveys August 19-28, 2004 and September 20-23, 2005. VIMS Report CHSD-2006-02. Virginia Institute of Marine Science, Gloucester Point, VA. Draft Version July 2006.

Cerco, C.F. and M.R. Noel. 2004. The 2002 Chesapeake Bay Eutrophication Model. Technical Report EPA 903-R-04-004, Chesapeake Bay Program Office, U.S. Environmental Protection Agency, Annapolis, MD.

Cerco, C.F. and T.M. Cole. 1994. Three-Dimensional Eutrophication Model of Chesapeake Bay. Volume 1: Main Report. Technical Report EL-94-4. U.S. Army Corps of Engineers, Waterways Experiment Station, Vicksburg, MS.

Chapra, S.C. 1997. Surface Water-Quality Modeling. McGraw-Hill, Boston, MA.

Delaware River Basin Commission. 2003a. DYNHYD5 Hydrodynamic Model (Version 2.3) and Chloride Water Quality Model for the Delaware Estuary. Delaware River Basin Commission, West Trenton, New Jersey.

Delaware River Basin Commission. 2003b. PCB Water Quality Model for Delaware Estuary (DELPCB). Delaware River Basin Commission, West Trenton, New Jersey.

Delaware River Basin Commission. 2003c. Calibration of the PCB Water Quality Model for the Delaware Estuary for Penta-PCBs and Carbon. Delaware River Basin Commission, West Trenton, New Jersey.

Delaware River Basin Commission. 2003d. U.S. Environmental Protection Agency Regions II and III. Total Maximum Daily Loads for Polychlorinated Biphenyls (PCBs) for Zones 2-5 of the Tidal Delaware River. Delaware River Basin Commission, West Trenton, New Jersey.

DePinto, J.V., R. Raghunathan, V.J. Bierman, Jr., P.W. Rodgers, T.C. Young and S.C. Martin. 1993. Analysis of organic carbon sediment-water exchange in Green Bay, Lake Michigan, USA. Water Science and Technology. 28(8-9):149-159.

Di Toro, D.M. 2000. Sediment Flux Modeling. John Wiley & Sons, Inc., Hoboken, NJ.

Eadie, B.J., N.R. Morehead, J.V. Klump and P.F. Landrum. 1992. Distribution of hydrophobic organic compounds between dissolved and particulate organic matter in Green Bay waters. Journal of Great Lakes Research. 18(1):91-97.

Eadie, B.J., N.R. Morehead and P.F. Landrum. 1990. Three-phase partitioning of hydrophobic organic compounds in Great Lakes waters. Chemosphere. 20(1-2):161-178.

Erickson, M.J., C.L. Turner and L.J. Thibodeaux. 2005. Field observation and modeling of dissolved fraction sediment-water exchange coefficients for PCBs in the Hudson River. Environmental Science and Technology. 39:549-556.

Hansen, B.G., A.B. Paya-Perez, M. Rahman and B.R. Larsen. 1999. QSARs for Kow and Koc of PCB congeners: a critical examination of data, assumptions and statistical approaches. Chemosphere. 39(13):2209-2228.

Haywood, H.C. and C. Buchanan. 2007. Total Maximum Daily Loads of Polychlorinated Biphenyls (PCBs) for Tidal Portions of the Potomac and Anacostia Rivers in the District of Columbia, Maryland, and Virginia. Interstate Commission on the Potomac River Basin. ICPRB Report 07-07. Rockville, MD. September 2007.

LimnoTech. 2005. Recommendations for Potomac PCB TMDL Modeling Approach. EPA Contract No. 68-C-03-041. Work Assignment No. 2-34, Amendment 1. Prepared for Battelle by Limno-Tech, Inc. September 30, 2005.

Mackay, D., W. Shiu and K Ma. 2000. Physical-Chemical Properties and Environmental Fate Handbook. Section 4.2. CRC Press LLC.

Mandel, R. and C. S. Schultz. 2000. The TAM/WASP Model: A Modeling Framework for the Total Maximum Daily Load Allocation in the Tidal Anacostia River – Final Report. Prepared by the Interstate Commission on the Potomac River Basin for the District of Columbia, Department of Health, Environmental Health Administration. Washington, DC.

Modeling Subcommittee. 2000. Chesapeake Bay Watershed Model Land Uses and Linkages to the Airshed and Estuarine Models. Report of the Modeling Subcommittee, Chesapeake Bay Program Office, Annapolis, MD.

O'Connor, D.J. and W.E. Dobbins. 1958. Mechanisms of reaeration in natural streams. Transactions American Society of Sanitary Engineering, American Society of Civil Engineers. SA4:955-975.

Thibodeaux, L.J. and V.J. Bierman, Jr. 2003. The bioturbation-driven chemical release response. Environmental Science and Technology. 37(13):252A-253A.

U.S. Environmental Protection Agency. 2003. Draft Guidance on the Development, Evaluation, and Application of Regulatory Environmental Models. Prepared by the Council for Regulatory Environmental Modeling, Office of Science Policy, Office of Research and Development, Washington, DC.

U.S. Environmental Protection Agency. 2000. Further Site Characterization and Analysis, Volume 2D – Revised Baseline Modeling Report, Books 1 and 2. Hudson River PCBs

Reassessment RI/FS. Prepared for USEPA by Limno-Tech, Inc., Menzie-Cura & Associates, Inc., and Tetra-Tech, Inc., January 2000.

U.S. Environmental Protection Agency. 1979. User's Manual for the Dynamic (Potomac) Estuary Model. Technical Report 63. By Stephen E. Roesch, Leo J. Clark, and Molly M. Bray. Annapolis Field Office, Region III, U.S. Environmental Protection Agency.

Wang, H.V. and B.H. Johnson. 2000. Validation and application of the second generation three dimensional hydrodynamic model of Chesapeake Bay. Water Quality and Ecosystem Modeling. 1:51-90.

PCB TMDL MODEL FOR THE POTOMAC RIVER ESTUARY

Draft Final Report on Hydrodynamic/Salinity and PCB Transport and Fate Models

APPENDIX A

TABLES

Table 1. Summary of Upper Potomac Estuary Fall Line USGS Discharge Stations.

Site Name	Site Number	Latitude (deg)	Longitude (deg)	Total Period of Flow Records	Drainage Area (sq mile)	HUC
Little Falls Pump Station near Washington, DC	01646500	38.949778	-77.127639	3/1/1930 - 12/31/2005	11560.0	2070008
North East Branch Anacostia River at Riverdale, MD	01649500	38.960250	-76.925972	8/1/1938 - 12/31/2005	72.8	2070010
North West Branch Anacostia River near Hyattsville, MD	01651000	38.952333	-76.966056	7/1/1938 - 12/31/2005	49.4	2070010
Piscataway Creek at Piscataway, MD	01653600	38.705778	-76.966194	10/1/1965 - 12/31/2005	39.5	2070010
Zekiah Swamp Run near Newtown, MD	01660920	38.490583	-76.927083	6/14/1983 - 12/31/2005	79.9	2070011
St Clement Creek near Clements, MD	01661050	38.333306	-76.725000	10/1/1968 - 12/31/2005	18.5	2070011
St Marys River at Great Mills, MD	01661500	38.241750	-76.503667	6/21/1946 - 12/31/2005	24.0	2070011
Watts Branch at Washington, DC	01651800	38.901111	-76.942194	6/19/1992 - 12/31/2005	3.3	2070010
Fourmile Run at Alexandria, VA	01652500	38.843446	-77.079145	10/1/1951 - 12/31/2005	13.8	2070010
Beaverdam Run near Garrisonville, VA	01660500	38.507068	-77.428872	5/1/1951 - 12/31/2005	12.7	2070011

Table 2. Summary of NOAA Tidal Observation Stations in the Potomac Estuary in Operation over the 1996-2005 Calibration Period.

Station Name	Station ID	Latitude (deg)	Longitude (deg)	River Mile	DYNHYD5 Junction	Overall Period of Record	Vertical Datum Adjustment, MLLW – NAVD88 (m)
Lewisetta, Potomac R.	8635750	37.995000	-76.465000	9.61	4	1/1/96 - 4/30/06	-0.253
Colonial Beach, Potomac R.	8635150	38.251667	-76.960000	42.33	20	1/1/96 - 9/18/03	-0.301
Washington, DC Ship Channel	8594900	38.873333	-77.021667	112.03	250	4/15/31 - 10/04/06	-0.425
Bladensburg, Anacostia R.	8579997	38.933333	-76.938333	118.58	244	9/1/95 - 8/13/96	-0.427

Table 3. Summary of NOAA Tidal Height Prediction Relationships in the Potomac Estuary.

Tide Station	Latitude (deg, min)	Longitude (deg, min)	Mean Range (ft)	Spring Range (ft)	Mean Tide Level (ft)	Time Adjustment		Height Multiplier		River Mile	Miles From Ship Channel
						High Tide (min)	Low Tide (min)	High Tide (ft)	Low Tide (ft)		
Lewisetta, VA	37° 59.7'	76° 27.9'	1.25	1.42	0.74	-403	-389	0.46	0.80	8.50	103.25
Piney Point, MD	38° 08'	76° 32'	1.4	1.6	0.8	-372	-410	0.52	0.53	17.25	94.50
Colonial Beach, VA	38° 15.1'	76° 57.6'	1.63	1.79	0.96	-332	-347	0.61	0.93	51.50	60.25
Mathias Point, VA	38° 24'	77° 03'	1.2	1.4	0.7	-257	-190	0.45	0.45	56.50	55.25
Maryland Point Light, MD	38° 21'	77° 12'	1.1	1.3	0.7	-192	-142	0.41	0.41	65.25	46.50
Indian Head, MD	38° 36'	77° 11'	1.8	2	1	-26	-32	0.66	0.65	88.75	23.00
Wash. Ship Channel, DC	38° 52.3'	77° 01.2'	2.77	3.07	1.55	0	0	0	0	111.75	0.00
Potomac Estuary Mouth										0	111.75

Log-linear regressions for time adjustments versus distance from the Washington Ship Channel -

High Tide Time Adjustment: $TA_{High} = -251.63 * Ln(Distance) + 754.23$ $r^2 = 0.96$

Low Tide Time Adjustment: $TA_{Low} = -264.29 * Ln(Distance) + 817.43$ $r^2 = 0.88$

Note: No correlation was found for height adjustment versus distance

Table 4. Water Column Monitoring Stations for Salinity

Station ID	Station Location	Potomac Basin	CBP 2003 Segment	Latitude (deg)	Longitude (deg)	HUC
TF2.0	POTOMAC RIVER AT CHAIN BRIDGE	POTOMAC RIVER	POTTF	38.929554	-77.116920	2070010
TF2.1	AT FL BOUY 77 OFF MOUTH OF PISCATAWAY CREEK; CHARACTERIZES TIDAL FRESH ZONE	MIDDLE POTOMAC RIVER	POTTF	38.706505	-77.048590	2070010
TF2.2	BOUY 67 OFF MOUTH OF PISCATAWAY CREEK; CHARACTERIZES TIDAL FRESH ZONE	MIDDLE POTOMAC RIVER	POTTF	38.690670	-77.111090	2070010
TF2.3	BOUY N 54 MID-CHANNEL OFF INDIANHEAD; CHARACTERIZES TIDAL FRESH ZONE	LOWER POTOMAC RIVER	POTTF	38.608173	-77.173870	2070011
TF2.4	BOUY 44 BETWEEN POSSUM POINT AND MOSS POINT; CHARACTERIZES TIDAL FRESH/TRANSITION ZONE	LOWER POTOMAC RIVER	POTTF	38.529842	-77.26526	2070011
RET2.1	BUOY 27 SOUTHWEST OF SMITH POINT; CHARACTERIZES TRANSITION ZONE	LOWER POTOMAC RIVER	POTOH	38.403458	-77.26915	2070011
RET2.2	BOUY 19 MID-CHANNEL OFF MARYLAND POINT; CHARACTERIZES TRANSITION ZONE	LOWER POTOMAC RIVER	POTOH	38.35207	-77.20442	2070011
RET2.3	BOUY 13 OFF MOUTH OF NANJEMOY CREEK; CHARACTERIZES TRANSITION ZONE	LOWER POTOMAC RIVER	POTOH	38.38818	-77.13053	2070011
RET2.4	MID-CHANNEL AT MORGANTOWN BRIDGE (U.S. ROUTE 301); CHARACTERIZES LOWER ESTUARINE	LOWER POTOMAC RIVER	POTMH	38.362625	-76.99053	2070011
LE2.2	POTOMAC RIVER OFF RAGGED POINT AT BUOY 51B; LOWER ESTUARINE ZONE	LOWER POTOMAC RIVER	POTMH	38.166794	-76.583015	2070011
Piney Point	POTOMAC RIVER NEAR PINEY POINT POINT, MARYLAND WESTERN SHORE	LOWER POTOMAC RIVER	POTMH	38.1378	-76.5058	2070011
LE2.3	MOUTH OF POTOMAC RIVER; BOUNDARY BETWEEN CB5 AND LE2; RIVER CHANNEL	LOWER POTOMAC RIVER	POTMH	38.021515	-76.347725	2070011

Table 5. Potomac Estuary DYNHYD5 Model Grid Junction Geometry.

Junction Number	Mile Point	Location	Surface Area (m^2)	Bottom Elevation (m, NAVD88)	1st Linked Channel	2nd Linked Channel	3rd Linked Channel	4th Linked Channel
1	2.24	Potomac R.	3.89E+07	-10.439	1	0		
2	4.82	Potomac R.	4.62E+07	-9.721	1	2	251	
3	7.16	Potomac R.	5.05E+07	-9.341	2	3	97	
4	9.66	Potomac R.	4.53E+07	-8.74	3	4	101	103
5	11.71	Potomac R.	2.52E+07	-9.533	4	5		
6	13.62	Potomac R.	2.64E+07	-10.198	5	6	120	
7	15.45	Potomac R.	1.92E+07	-11.337	6	7		
8	17.93	Potomac R.	2.51E+07	-9.652	7	8		
9	19.88	Potomac R.	2.69E+07	-8.576	8	9		
10	22.25	Potomac R.	2.36E+07	-7.898	9	10		
11	24.22	Potomac R.	2.85E+07	-6.708	10	11	128	
12	25.80	Potomac R.	1.47E+07	-6.725	11	12		
13	27.51	Potomac R.	3.36E+07	-6.764	12	13	131	136
14	29.74	Potomac R.	2.95E+07	-6.039	13	14	139	
15	31.59	Potomac R.	1.33E+07	-7.337	14	15		
16	33.42	Potomac R.	3.67E+07	-6	15	16		
17	35.73	Potomac R.	3.95E+07	-6.292	16	17	143	
18	38.30	Potomac R.	3.92E+07	-5.697	17	18		
19	40.28	Potomac R.	1.80E+07	-5.893	18	19	151	
20	42.49	Potomac R.	2.73E+07	-6.599	19	20		
21	45.18	Potomac R.	2.82E+07	-5.84	20	21	254	
22	47.00	Potomac R.	1.29E+07	-6.148	21	22	153	
23	48.59	Potomac R.	7.49E+06	-7.872	22	23		
24	50.18	Potomac R.	7.60E+06	-8.054	23	24		
25	52.50	Potomac R.	1.22E+07	-6.46	24	25		
26	54.04	Potomac R.	1.01E+07	-5.361	25	26	155	
27	55.15	Potomac R.	7.66E+06	-5.284	26	27		
28	56.94	Potomac R.	1.12E+07	-4.757	27	28		
29	58.32	Potomac R.	8.35E+06	-5.535	28	29		
30	59.55	Potomac R.	7.17E+06	-6.231	29	30	159	
31	60.75	Potomac R.	6.29E+06	-6.233	30	31		
32	61.97	Potomac R.	4.78E+06	-6.493	31	32		
33	63.16	Potomac R.	5.35E+06	-6.252	32	33		
34	64.46	Potomac R.	5.66E+06	-6.01	33	34		
35	65.98	Potomac R.	7.03E+06	-5.626	34	35		
36	67.36	Potomac R.	9.23E+06	-4.656	35	36		
37	68.40	Potomac R.	7.34E+06	-4.061	36	37	164	
38	69.47	Potomac R.	8.22E+06	-4.268	37	38		
39	71.05	Potomac R.	1.43E+07	-4.488	38	39	167	
40	72.64	Potomac R.	9.42E+06	-4.303	39	40		

Table 5. Potomac Estuary DYNHYD5 Model Grid Junction Geometry - Continued

Junction Number	Mile Point	Location	Surface Area (m^2)	Bottom Elevation (m, NAVD88)	1st Linked Channel	2nd Linked Channel	3rd Linked Channel	4th Linked Channel
41	73.87	Potomac R.	1.01E+07	-3.997	40	41		
42	75.07	Potomac R.	9.49E+06	-4.115	41	42		
43	76.27	Potomac R.	8.53E+06	-4.311	42	43		
44	77.51	Potomac R.	6.79E+06	-4.696	43	44		
45	78.72	Potomac R.	6.04E+06	-5.319	44	45	256	
46	79.85	Potomac R.	3.69E+06	-6.311	45	46		
47	80.72	Potomac R.	2.94E+06	-6.359	46	47	171	
48	81.52	Potomac R.	4.03E+06	-6.074	47	48	173	
49	82.46	Potomac R.	4.00E+06	-6.009	48	49		
50	83.41	Potomac R.	3.73E+06	-5.328	49	50		
51	84.10	Potomac R.	5.26E+06	-4.636	50	51	174	179
52	84.82	Potomac R.	5.37E+06	-4.301	51	52		
53	85.65	Potomac R.	5.60E+06	-4.654	52	53		
54	86.51	Potomac R.	6.50E+06	-4.158	53	54	186	
55	87.69	Potomac R.	6.20E+06	-4.269	54	55		
56	89.21	Potomac R.	4.43E+06	-5.197	55	56		
57	90.48	Potomac R.	6.47E+06	-4.265	56	57		
58	91.72	Potomac R.	3.14E+06	-5.891	57	58		
59	92.58	Potomac R.	3.21E+06	-5.108	58	59		
60	93.77	Potomac R.	4.18E+06	-4.96	59	60	194	
61	95.16	Potomac R.	3.21E+06	-4.795	60	61		
62	96.33	Potomac R.	2.34E+06	-5.852	61	62	199	
63	97.23	Potomac R.	1.86E+06	-7.162	62	63		
64	98.06	Potomac R.	2.43E+06	-5.742	63	64		
65	98.96	Potomac R.	2.60E+06	-5.282	64	65	200	203
66	100.02	Potomac R.	1.30E+06	-6.164	65	66		
67	100.79	Potomac R.	1.14E+06	-6.39	66	67		
68	101.64	Potomac R.	1.45E+06	-5.894	67	68		
69	102.50	Potomac R.	2.26E+06	-5.615	68	69	204	
70	103.40	Potomac R.	2.46E+06	-3.625	69	70		
71	104.18	Potomac R.	1.42E+06	-4.107	70	71		
72	105.02	Potomac R.	2.30E+06	-3.846	71	72	205	206
73	105.90	Potomac R.	1.44E+06	-3.563	72	73		
74	106.58	Potomac R.	1.23E+06	-3.649	73	74	207	
75	107.20	Potomac R.	9.99E+05	-3.734	74	75		
76	107.86	Potomac R.	1.14E+06	-3.737	75	76		
77	108.55	Potomac R.	1.17E+06	-3.617	76	77	209	
78	109.22	Potomac R.	8.72E+05	-4.107	77	78		
79	109.78	Potomac R.	1.08E+06	-4.863	78	79	210	
80	110.33	Potomac R.	7.25E+05	-5.195	79	80		

Table 5. Potomac Estuary DYNHYD5 Model Grid Junction Geometry - Continued

Junction Number	Mile Point	Location	Surface Area (m^2)	Bottom Elevation (m, NAVD88)	1st Linked Channel	2nd Linked Channel	3rd Linked Channel	4th Linked Channel
81	110.87	Potomac R.	7.17E+05	-5.218	80	81		
82	111.38	Potomac R.	4.90E+05	-4.233	81	82		
83	111.87	Potomac R.	4.52E+05	-4.157	82	83		
84	112.35	Potomac R.	3.79E+05	-4.131	83	84		
85	112.77	Potomac R.	3.65E+05	-4.174	84	85		
86	113.15	Potomac R.	3.91E+05	-3.717	85	86		
87	113.51	Potomac R.	4.22E+05	-3.611	86	87		
88	113.85	Potomac R.	3.02E+05	-4.765	87	88		
89	114.31	Potomac R.	3.10E+05	-4.623	88	89		
90	114.78	Potomac R.	1.69E+05	-4.605	89	90		
91	115.14	Potomac R.	1.44E+05	-4.724	90	91		
92	115.56	Potomac R.	1.79E+05	-4.163	91	92		
93	116.01	Potomac R.	1.87E+05	-4.147	92	93		
94	116.49	Potomac R.	8.61E+04	-4.722	93	94		
95	117.01	Potomac R.	7.60E+04	-4.722	94	95		
96	117.52	Potomac R.	7.39E+04	-4.722	95	96		
97	118.06	Potomac R.	7.58E+04	-4.722	96	0		
98		Smith Cr.	8.31E+05	-1.674	97	98		
99		Smith Cr.	6.18E+05	-3.198	98	99	100	
100		Smith Cr.	8.68E+05	-1.674	99	0		
101		Jutland Cr.	1.16E+06	-1.674	100	0		
102		Coan Cr.	2.42E+06	-1.674	101	102		
103		Coan Cr.	2.95E+06	-1.674	102	0		
104		St. Mary's R.	4.44E+06	-5.143	103	104	114	
105		St. Mary's R.	2.59E+06	-4.803	104	105		
106		St. Mary's R.	2.27E+06	-4.862	105	106		
107		St. Mary's R.	2.43E+06	-4.728	106	107	118	
108		St. Mary's R.	1.67E+06	-4.722	107	108	119	
109		St. Mary's R.	1.45E+06	-3.198	108	109		
110		St. Mary's R.	1.66E+06	-3.198	109	110		
111		St. Mary's R.	1.94E+06	-3.198	110	111		
112		St. Mary's R.	1.63E+06	-3.198	111	112		
113		St. Mary's R.	1.83E+06	-1.674	112	113		
114		St. Mary's R.	3.09E+06	-1.674	113	0		
115		St. George Cr.	1.87E+06	-1.674	114	115		
116		St. George Cr.	1.46E+06	-1.674	115	116		
117		St. George Cr.	1.41E+06	-1.674	116	117		
118		St. George Cr.	1.51E+06	-1.674	117	0		
119		Carthagena Cr.	1.10E+06	-1.674	118	0		
120		Inigoes Cr.	1.41E+06	-3.198	119	0		

Table 5. Potomac Estuary DYNHYD5 Model Grid Junction Geometry - Continued

Junction Number	Mile Point	Location	Surface Area (m^2)	Bottom Elevation (m, NAVD88)	1st Linked Channel	2nd Linked Channel	3rd Linked Channel	4th Linked Channel
121		Yeocomico R.	3.10E+06	-2.579	120	121		
122		Yeocomico R.	1.88E+06	-2.468	121	122		
123		Yeocomico R.	1.76E+06	-1.674	122	123	125	127
124		Yeocomico R.	1.40E+06	-1.674	123	124		
125		Yeocomico R.	1.51E+06	-1.674	124	0		
126		Yeocomico R.	1.55E+06	-1.674	125	126		
127		Yeocomico R.	1.78E+06	-1.674	126	0		
128		Yeocomico R.	2.05E+06	-1.674	127	0		
129		L. Machodoc Cr.	3.24E+06	-1.674	128	129		
130		L. Machodoc Cr.	1.61E+06	-1.674	129	130		
131		L. Machodoc Cr.	1.74E+06	-1.674	130	0		
132		Breton Bay	2.08E+06	-3.198	131	132		
133		Breton Bay	2.45E+06	-3.198	132	133		
134		Breton Bay	3.08E+06	-3.198	133	134		
135		Breton Bay	2.75E+06	-3.198	134	135		
136		Breton Bay	1.92E+06	-1.674	135	0		
137		Nomini Bay	3.96E+06	-1.674	136	137		
138		Nomini Bay	2.32E+06	-1.674	137	138		
139		Nomini Bay	2.04E+06	-1.674	138	0		
140		St. Clement Bay	1.97E+06	-3.198	139	140		
141		St. Clement Bay	2.28E+06	-3.198	140	141		
142		St. Clement Bay	2.52E+06	-3.198	141	142		
143		St. Clement Bay	3.10E+06	-1.674	142	0		
144		Wicomico R.	5.70E+06	-3.198	143	144		
145		Wicomico R.	5.01E+06	-3.198	144	145		
146		Wicomico R.	6.84E+06	-3.198	145	146		
147		Wicomico R.	4.80E+06	-1.674	146	147		
148		Wicomico R.	4.19E+06	-1.674	147	148	150	
149		Wicomico R.	3.99E+06	-1.674	148	149		
150		Wicomico R.	3.31E+06	-1.674	149	0		
151		Wicomico R.	2.98E+06	-1.674	150	0		
152		Mattox Cr.	3.29E+06	-1.674	151	152		
153		Mattox Cr.	2.20E+06	-1.674	152	0		
154		U. Machodoc Cr.	1.96E+06	-1.674	153	154		
155		U. Machodoc Cr.	1.26E+06	-1.674	154	0		
156		Port Tobacco R.	2.77E+06	-1.674	155	156		
157		Port Tobacco R.	1.92E+06	-1.674	156	157		
158		Port Tobacco R.	1.38E+06	-1.674	157	158		
159		Port Tobacco R.	6.55E+05	-1.674	158	0		
160		Nanjemoy Cr.	3.28E+06	-1.674	159	160		

Table 5. Potomac Estuary DYNHYD5 Model Grid Junction Geometry - Continued

Junction Number	Mile Point	Location	Surface Area (m^2)	Bottom Elevation (m, NAVD88)	1st Linked Channel	2nd Linked Channel	3rd Linked Channel	4th Linked Channel
161		Nanjemoy Cr.	2.49E+06	-1.674	160	161		
162		Nanjemoy Cr.	1.72E+06	-1.674	161	162		
163		Nanjemoy Cr.	1.45E+06	-1.674	162	163		
164		Nanjemoy Cr.	1.44E+06	-1.674	163	0		
165		Potomac Cr.	3.27E+06	-1.674	164	165		
166		Potomac Cr.	2.71E+06	-1.674	165	166		
167		Potomac Cr.	2.49E+06	-1.674	166	0		
168		Aquia Cr.	2.39E+06	-1.674	167	168		
169		Aquia Cr.	2.10E+06	-1.674	168	169		
170		Aquia Cr.	1.59E+06	-1.674	169	170		
171		Aquia Cr.	1.05E+06	-1.674	170	0		
172		Quantico Cr.	1.32E+06	-1.674	171	172		
173		Quantico Cr.	1.32E+06	-1.674	172	0		
174		Chicamuxen Cr.	1.49E+06	-1.674	173	0		
175		Mattawoman Cr.	1.66E+06	-1.674	174	175		
176		Mattawoman Cr.	1.58E+06	-1.674	175	176		
177		Mattawoman Cr.	1.24E+06	-1.674	176	177		
178		Mattawoman Cr.	9.05E+05	-1.674	177	178		
179		Mattawoman Cr.	1.02E+06	-1.674	178	0		
180		Powells Cr.	1.28E+06	-1.674	179	0		
181		Neabsco Cr.	5.57E+05	-1.674	180	181		
182		Neabsco Cr.	4.84E+05	-1.674	181	182		
183		Neabsco Cr.	4.80E+05	-1.674	182	183		
184		Neabsco Cr.	2.79E+05	-1.674	183	0		
185		Occoquan R.	1.25E+05	-1.674	184	0		
186		Belmont Bay	3.11E+05	-1.674	185	0		
187		Occoquan Bay	4.03E+06	-1.674	180	186	187	
188		Occoquan Bay	3.74E+06	-1.674	187	188		
189		Occoquan Bay	3.40E+06	-1.674	188	189		
190		Occoquan Bay	1.74E+06	-1.674	189	190	192	
191		Occoquan R.	1.69E+06	-1.674	190	191		
192		Occoquan R.	4.60E+05	-1.674	191	184		
193		Belmont Bay	2.25E+06	-1.674	192	193		
194		Belmont Bay	1.62E+06	-1.674	193	185		
195		Gunston Cove	2.48E+06	-1.674	194	195		
196		Gunston Cove	1.70E+06	-1.674	195	196		
197		Gunston Cove	1.11E+06	-1.674	196	197	198	
198		Pohick Cr.	1.43E+06	-1.674	197	0		
199		Accotink Cr.	1.04E+06	-1.674	198	0		
200		Dogue Cr.	2.15E+06	-1.674	199	0		

Table 5. Potomac Estuary DYNHYD5 Model Grid Junction Geometry - Continued

Junction Number	Mile Point	Location	Surface Area (m^2)	Bottom Elevation (m, NAVD88)	1st Linked Channel	2nd Linked Channel	3rd Linked Channel	4th Linked Channel
201		Piscataway Cr.	1.31E+06	-1.674	200	201		
202		Piscataway Cr.	9.15E+05	-1.674	201	202		
203		Piscataway Cr.	6.55E+05	-1.674	202	0		
204		Little Hunting Cr.	1.02E+06	-1.674	203	0		
205		Henson Cr.	1.79E+06	-1.674	204	0		
206		Potomac R.	1.27E+06	-1.674	205	0		
207		Cameron Run	1.44E+06	-1.674	206	0		
208		Oxon Run	4.89E+05	-1.674	207	208		
209		Oxon Run	2.54E+05	-1.674	208	0		
210		Four Mile Run	8.32E+05	-1.674	209	0		
211	0.38	Anacostia R.	1.78E+05	-4.204	210	211		
212	0.61	Anacostia R.	1.52E+05	-4.204	211	212	248	
213	0.89	Anacostia R.	1.52E+05	-4.348	212	213		
214	1.13	Anacostia R.	1.34E+05	-4.759	213	214		
215	1.31	Anacostia R.	1.18E+05	-5.229	214	215		
216	1.50	Anacostia R.	1.18E+05	-5.369	215	216		
217	1.70	Anacostia R.	1.16E+05	-5.227	216	217		
218	1.90	Anacostia R.	1.17E+05	-5.144	217	218		
219	2.05	Anacostia R.	1.14E+05	-4.981	218	219		
220	2.24	Anacostia R.	1.20E+05	-4.62	219	220		
221	2.51	Anacostia R.	7.97E+04	-4.156	220	221		
222	2.77	Anacostia R.	1.08E+05	-3.281	221	222		
223	3.07	Anacostia R.	1.12E+05	-2.395	222	223		
224	3.39	Anacostia R.	9.95E+04	-1.955	223	224		
225	3.65	Anacostia R.	8.78E+04	-1.92	224	225		
226	3.89	Anacostia R.	9.04E+04	-1.761	225	226		
227	4.14	Anacostia R.	8.05E+04	-1.454	226	227	247	
228	4.41	Anacostia R.	6.98E+04	-1.313	227	228		
229	4.66	Anacostia R.	5.91E+04	-1.49	228	229		
230	4.90	Anacostia R.	5.48E+04	-1.724	229	230		
231	5.13	Anacostia R.	4.77E+04	-1.714	230	231		
232	5.40	Anacostia R.	5.06E+04	-1.488	231	232		
233	5.67	Anacostia R.	4.30E+04	-1.483	232	233		
234	5.93	Anacostia R.	3.18E+04	-1.738	233	234		
235	6.17	Anacostia R.	2.96E+04	-1.967	234	235		
236	6.36	Anacostia R.	2.42E+04	-2.015	235	236		
237	6.57	Anacostia R.	2.45E+04	-2.014	236	237		
238	6.78	Anacostia R.	2.34E+04	-1.959	237	238		
239	6.96	Anacostia R.	2.89E+04	-1.848	238	239		
240	7.12	Anacostia R.	2.82E+04	-1.819	239	240		

Table 5. Potomac Estuary DYNHYD5 Model Grid Junction Geometry - Continued

Junction Number	Mile Point	Location	Surface Area (m^2)	Bottom Elevation (m, NAVD88)	1st Linked Channel	2nd Linked Channel	3rd Linked Channel	4th Linked Channel
241	7.30	Anacostia R.	2.90E+04	-1.911	240	241		
242	7.54	Anacostia R.	2.80E+04	-2.076	241	242		
243	7.81	Anacostia R.	2.61E+04	-1.880	242	243		
244	8.09	Anacostia R.	5.06E+04	-1.385	243	244		
245	8.31	Anacostia R.	4.09E+04	-0.998	244	245	246	
246	8.88	NW Anacostia	5.47E+04	-0.954	245	0		
247	9.00	NE Anacostia	5.47E+04	-0.954	246	0		
248		Kingman Lake	2.00E+05	-1.274	247	0		
249		Wash. Ship Ch.	3.34E+05	-6.559	248	249		
250		Wash. Ship Ch.	2.97E+05	-7.171	249	250		
251		Wash. Ship Ch.	1.49E+05	-7.477	250	0		
252		Hull Cr.	2.25E+05	-1.480	251	252		
253		Hull Cr.	7.28E+05	-1.480	252	253		
254		Hull Cr.	2.61E+05	-1.360	253	0		
255		Rosier Cr.	6.21E+05	-1.380	254	255		
256		Rosier Cr.	7.56E+05	-1.000	255	0		
257		Chopawamsic Cr.	2.42E+05	-2.640	256	257		
258		Chopawamsic Cr.	1.24E+06	-1.000	257	0		

Table 6. Potomac Estuary DYNHYD5 Model Grid Channel Geometry.

Channel Number	Location	Length (m)	Width (m)	Initial Depth (m)	Manning's N	1st Linked Junction	2nd Linked Junction
1	Potomac R.	4246.2	9816.8	10.74	0.024	1	2
2	Potomac R.	3716	12921.2	10.159	0.024	2	3
3	Potomac R.	3709.1	12966.1	9.688	0.024	3	4
4	Potomac R.	4239.5	8612.4	9.589	0.024	4	5
5	Potomac R.	2296.8	11300.4	10.562	0.024	5	6
6	Potomac R.	3148.5	7152.5	11.335	0.024	6	7
7	Potomac R.	4469.3	5081.1	10.848	0.024	7	8
8	Potomac R.	2345.5	11136.5	9.659	0.024	8	9
9	Potomac R.	3785.3	6716.5	8.904	0.024	9	10
10	Potomac R.	3306.7	7833.4	7.888	0.024	10	11
11	Potomac R.	2717.7	8760.7	7.321	0.024	11	12
12	Potomac R.	2805.8	9479.1	7.367	0.024	12	13
13	Potomac R.	3661.4	8817.8	7.043	0.024	13	14
14	Potomac R.	2761	8832.1	6.881	0.024	14	15
15	Potomac R.	3434.5	8686.3	6.784	0.024	15	16
16	Potomac R.	3404.1	11233.9	6.784	0.024	16	17
17	Potomac R.	4038.8	9763.9	6.599	0.024	17	18
18	Potomac R.	2666.1	13414.1	6.323	0.024	18	19
19	Potomac R.	3931.7	5859.3	6.955	0.024	19	20
20	Potomac R.	4758.8	5827	6.83	0.024	20	21
21	Potomac R.	2585.9	8285.1	6.532	0.024	21	22
22	Potomac R.	2741.3	3770.2	7.351	0.024	22	23
23	Potomac R.	2817.5	2684.9	8.601	0.024	23	24
24	Potomac R.	3949.2	2865.7	7.284	0.024	24	25
25	Potomac R.	1875.5	6026.5	6.631	0.024	25	26
26	Potomac R.	2209.1	3959.2	5.933	0.024	26	27
27	Potomac R.	3035.2	3314.3	5.495	0.024	27	28
28	Potomac R.	2321	4066.7	5.79	0.024	28	29
29	Potomac R.	1788.4	4263.7	6.547	0.024	29	30
30	Potomac R.	1831.8	3644	6.842	0.024	30	31
31	Potomac R.	2363.1	2356.9	6.95	0.02	31	32
32	Potomac R.	1761.3	2880.1	6.973	0.02	32	33
33	Potomac R.	1859.3	2956.2	6.745	0.02	33	34
34	Potomac R.	3218.6	2009.8	6.373	0.02	34	35
35	Potomac R.	2083	4148.3	5.476	0.02	35	36
36	Potomac R.	1303	6143.5	4.913	0.02	36	37
37	Potomac R.	1694.6	4662.8	4.808	0.02	37	38
38	Potomac R.	2652.5	4706.4	5.053	0.02	38	39
39	Potomac R.	2354.8	5247.7	5.04	0.02	39	40
40	Potomac R.	2004	4871.1	4.76	0.02	40	41

Table 6. Potomac Estuary DYNHYD5 Model Grid Channel Geometry - Continued

Channel Number	Location	Length (m)	Width (m)	Initial Depth (m)	Manning's N	1st Linked Junction	2nd Linked Junction
41	Potomac R.	1792.9	5492.9	4.658	0.02	41	42
42	Potomac R.	2277.4	3946.6	4.822	0.02	42	43
43	Potomac R.	1925.1	3891.7	5.129	0.02	43	44
44	Potomac R.	1831.5	3492.9	5.613	0.02	44	45
45	Potomac R.	1800.9	2765	6.26	0.02	45	46
46	Potomac R.	1639.9	2005.4	6.944	0.02	46	47
47	Potomac R.	1218.9	3059.6	6.746	0.02	47	48
48	Potomac R.	1316.8	3048.7	6.65	0.02	48	49
49	Potomac R.	1754.9	2207.3	6.306	0.02	49	50
50	Potomac R.	1394.2	3393.4	5.435	0.02	50	51
51	Potomac R.	1243.4	4296.5	4.998	0.02	51	52
52	Potomac R.	1349.3	4100.6	5.167	0.02	52	53
53	Potomac R.	1305.1	4793.9	4.886	0.02	53	54
54	Potomac R.	1775.5	3561.1	4.83	0.02	54	55
55	Potomac R.	2127.6	2666.1	5.093	0.02	55	56
56	Potomac R.	2400.3	2215.9	5.314	0.02	56	57
57	Potomac R.	1885.1	2853.2	5.187	0.02	57	58
58	Potomac R.	1521.2	2087.4	6.133	0.02	58	59
59	Potomac R.	2075.9	1834.8	5.618	0.02	59	60
60	Potomac R.	2137.4	1713.2	5.493	0.02	60	61
61	Potomac R.	1939.8	1468.6	5.764	0.017	61	62
62	Potomac R.	1463.9	1440.9	7.023	0.017	62	63
63	Potomac R.	1571.1	1442.2	6.692	0.017	63	64
64	Potomac R.	1178.3	2170.2	6.002	0.017	64	65
65	Potomac R.	1603.6	1214.4	6.185	0.017	65	66
66	Potomac R.	1245	978.2	6.882	0.017	66	67
67	Potomac R.	1327.1	979.9	6.716	0.017	67	68
68	Potomac R.	1403.6	1364.6	6.314	0.017	68	69
69	Potomac R.	1460.5	1616.4	5.183	0.017	69	70
70	Potomac R.	1276.2	1617.1	4.361	0.017	70	71
71	Potomac R.	1387.4	1443.6	4.519	0.017	71	72
72	Potomac R.	1409.1	1369.3	4.365	0.017	72	73
73	Potomac R.	1136.1	1167.3	4.214	0.017	73	74
74	Potomac R.	943.7	1172.3	4.299	0.017	74	75
75	Potomac R.	1042.1	1035	4.345	0.017	75	76
76	Potomac R.	1069.5	1080.9	4.287	0.017	76	77
77	Potomac R.	1120.5	938.7	4.387	0.017	77	78
78	Potomac R.	874.7	1107.4	5.115	0.017	78	79
79	Potomac R.	918.6	1006.9	5.585	0.017	79	80
80	Potomac R.	898.3	802.6	5.816	0.017	80	81

Table 6. Potomac Estuary DYNHYD5 Model Grid Channel Geometry - Continued

Channel Number	Location	Length (m)	Width (m)	Initial Depth (m)	Manning's N	1st Linked Junction	2nd Linked Junction
81	Potomac R.	841.9	729.6	5.472	0.017	81	82
82	Potomac R.	753.8	623.8	4.805	0.017	82	83
83	Potomac R.	804.8	518.7	4.756	0.017	83	84
84	Potomac R.	701.7	530.4	4.762	0.017	84	85
85	Potomac R.	588.4	645.1	4.517	0.017	85	86
86	Potomac R.	578.3	701.7	4.273	0.017	86	87
87	Potomac R.	440.4	861.8	4.543	0.014	87	88
88	Potomac R.	866.6	352.5	5.306	0.014	88	89
89	Potomac R.	735.4	349.3	5.228	0.014	89	90
90	Potomac R.	633.9	248.3	5.266	0.014	90	91
91	Potomac R.	646.5	255.2	4.969	0.014	91	92
92	Potomac R.	763.5	239.8	4.765	0.014	92	93
93	Potomac R.	760.6	165.9	4.994	0.014	93	94
94	Potomac R.	811.9	100	5.332	0.014	94	95
95	Potomac R.	861.8	86.9	5.332	0.014	96	95
96	Potomac R.	877.6	85.3	5.332	0.014	97	96
97	Smith Cr.	8225.8	5812.7	9.943	0.014	3	98
98	Smith Cr.	1011.5	709.9	2.981	0.014	98	99
99	Smith Cr.	1441.4	546.7	2.666	0.014	99	100
100	Jutland Cr.	1173.7	869.1	2.527	0.014	99	101
101	Coan Cr.	6349.1	6189.3	9.288	0.014	4	102
102	Coan Cr.	1891.9	1432.7	2.284	0.014	102	103
103	St. Mary's R.	7614.2	5266.6	9.299	0.014	4	104
104	St. Mary's R.	984.5	3224.7	5.562	0.014	104	105
105	St. Mary's R.	970.4	2448.2	5.451	0.014	105	106
106	St. Mary's R.	1175.8	2013.1	5.386	0.014	106	107
107	St. Mary's R.	855.4	2224.6	5.334	0.014	107	108
108	St. Mary's R.	1177.8	1306.9	4.488	0.014	108	109
109	St. Mary's R.	1209	1288.7	3.808	0.014	109	110
110	St. Mary's R.	1494.7	1220.1	3.808	0.014	110	111
111	St. Mary's R.	1556.8	1147.2	3.808	0.014	111	112
112	St. Mary's R.	1671.4	1038.1	2.988	0.014	112	113
113	St. Mary's R.	2200.9	1181.9	2.284	0.014	113	114
114	St. George Cr.	2445	1522.9	5.27	0.014	104	115
115	St. George Cr.	1649.6	1005.2	2.284	0.014	115	116
116	St. George Cr.	1768.2	810.3	2.284	0.014	116	117
117	St. George Cr.	1832.2	801.5	2.284	0.014	117	118
118	Carthagena Cr.	1908.5	1022.5	4.718	0.014	107	119
119	Inigoes Cr.	1893.5	814.1	4.636	0.014	108	120
120	Yeocomico R.	5146.2	4896.2	10.758	0.014	6	121

Table 6. Potomac Estuary DYNHYD5 Model Grid Channel Geometry - Continued

Channel Number	Location	Length (m)	Width (m)	Initial Depth (m)	Manning's N	1st Linked Junction	2nd Linked Junction
121	Yeocomico R.	1304.2	2043.1	3.16	0.014	121	122
122	Yeocomico R.	883	2062.1	2.701	0.014	122	123
123	Yeocomico R.	1420.4	1089.1	2.284	0.014	123	124
124	Yeocomico R.	1690	860.5	2.284	0.014	124	125
125	Yeocomico R.	1638.6	1016.9	2.284	0.014	123	126
126	Yeocomico R.	1849.9	902.4	2.284	0.014	126	127
127	Yeocomico R.	2079.3	925.5	2.284	0.014	123	128
128	L. Machodoc Cr.	4704.2	5644	7.27	0.022	11	129
129	L. Machodoc Cr.	2053.7	1234.2	2.284	0.022	129	130
130	L. Machodoc Cr.	2186.3	774.8	2.284	0.022	130	131
131	Breton Bay	5297.4	5588.6	7.344	0.022	13	132
132	Breton Bay	1622.2	1418.9	3.808	0.022	132	133
133	Breton Bay	1541.3	1808.2	3.808	0.022	133	134
134	Breton Bay	2420.6	1205.7	3.808	0.022	134	135
135	Breton Bay	2241.4	1077.4	3.322	0.022	135	136
136	Nomini Bay	5126.1	5963.4	7.293	0.022	13	137
137	Nomini Bay	1713.2	1716.4	2.284	0.022	137	138
138	Nomini Bay	2160.8	1008.6	2.284	0.022	138	139
139	St. Clement Bay	5231	4906.1	6.619	0.022	14	140
140	St. Clement Bay	1800.9	1193.2	3.808	0.022	140	141
141	St. Clement Bay	2271.9	1066.7	3.808	0.022	141	142
142	St. Clement Bay	2809.8	898.3	3.808	0.022	142	143
143	Wicomico R.	6147.2	5724.9	6.836	0.022	17	144
144	Wicomico R.	2516.3	2141.6	3.808	0.022	144	145
145	Wicomico R.	2450.7	2511.2	3.808	0.022	145	146
146	Wicomico R.	2536.4	2364	3.303	0.022	146	147
147	Wicomico R.	1913.7	2348.5	2.284	0.022	147	148
148	Wicomico R.	2347.6	1738.5	2.284	0.022	148	149
149	Wicomico R.	3022.5	1210.7	2.284	0.022	149	150
150	Wicomico R.	2502.3	1451.2	2.284	0.022	148	151
151	Mattox Cr.	4416.2	3632.2	6.385	0.022	19	152
152	Mattox Cr.	2812.1	969.3	2.284	0.022	152	153
153	U. Machodoc Cr.	3803.3	2715.7	6.557	0.022	22	154
154	U. Machodoc Cr.	1300	1240.3	2.284	0.022	154	155
155	Port Tobacco R.	4066.1	2088.9	5.704	0.022	26	156
156	Port Tobacco R.	1954.6	1161.9	2.284	0.022	156	157
157	Port Tobacco R.	1905.2	862.2	2.284	0.022	157	158
158	Port Tobacco R.	1820.3	596.4	2.284	0.022	158	159
159	Nanjemoy Cr.	2875.8	1854	5.952	0.022	30	160
160	Nanjemoy Cr.	2113.8	1393.7	2.284	0.022	160	161

Table 6. Potomac Estuary DYNHYD5 Model Grid Channel Geometry - Continued

Channel Number	Location	Length (m)	Width (m)	Initial Depth (m)	Manning's N	1st Linked Junction	2nd Linked Junction
161	Nanjemoy Cr.	1666	1292.7	2.284	0.022	161	162
162	Nanjemoy Cr.	1316.5	1204.7	2.284	0.022	162	163
163	Nanjemoy Cr.	1501.1	963.4	2.284	0.022	163	164
164	Potomac Cr.	3312.5	1867	4.314	0.022	37	165
165	Potomac Cr.	2179.7	1372.4	2.284	0.022	165	166
166	Potomac Cr.	2280.8	1134.4	2.284	0.022	166	167
167	Aquia Cr.	3003.9	3873.2	4.967	0.022	39	168
168	Aquia Cr.	2452	919.2	2.284	0.022	168	169
169	Aquia Cr.	1902.8	982.2	2.284	0.022	169	170
170	Aquia Cr.	2175	606.9	2.284	0.022	170	171
171	Quantico Cr.	2117.7	1122.8	6.061	0.022	47	172
172	Quantico Cr.	2139.6	616.7	2.284	0.022	172	173
173	Chicamuxen Cr.	2105.3	1540.5	6.058	0.022	48	174
174	Mattawoman Cr.	2753.3	1690.8	5.067	0.022	51	175
175	Mattawoman Cr.	1623	998.1	2.284	0.022	175	176
176	Mattawoman Cr.	1420	997.9	2.284	0.022	176	177
177	Mattawoman Cr.	1684.1	651.3	2.284	0.022	177	178
178	Mattawoman Cr.	1643.7	591.4	2.284	0.022	178	179
179	Powells Cr.	3136.3	1359.4	5.022	0.022	51	180
180	Neabsco Cr.	2430.9	1515.5	2.284	0.035	187	181
181	Neabsco Cr.	884.4	584.8	2.284	0.035	181	182
182	Neabsco Cr.	798.7	603.2	2.284	0.035	182	183
183	Neabsco Cr.	743.7	542.1	2.284	0.035	183	184
184	Occoquan R.	1687.3	213.3	2.284	0.022	192	185
185	Belmont Bay	1176.6	986.6	2.284	0.022	194	186
186	Occoquan Bay	1803.2	3562	4.726	0.022	54	187
187	Occoquan Bay	981.2	4067	2.284	0.022	187	188
188	Occoquan Bay	1389.7	2617	2.284	0.022	188	189
189	Occoquan Bay	1982.6	1243.4	2.284	0.022	189	190
190	Occoquan R.	1778.9	959.2	2.284	0.022	190	191
191	Occoquan R.	2547	452.5	2.284	0.022	191	192
192	Belmont Bay	1058.8	1902.9	2.284	0.022	190	193
193	Belmont Bay	1173	1623.7	2.284	0.022	193	194
194	Gunston Cove	1528.3	2297.3	4.657	0.022	60	195
195	Gunston Cove	1307.1	1627.6	2.284	0.035	195	196
196	Gunston Cove	1149	1233.9	2.284	0.035	196	197
197	Pohick Cr.	1461.4	903.3	2.284	0.035	197	198
198	Accotink Cr.	1623.8	661.7	2.284	0.035	197	199
199	Dogue Cr.	1746.1	1285.1	4.374	0.022	62	200
200	Piscataway Cr.	1760.9	1244.6	5.213	0.022	65	201

Table 6. Potomac Estuary DYNHYD5 Model Grid Channel Geometry - Continued

Channel Number	Location	Length (m)	Width (m)	Initial Depth (m)	Manning's N	1st Linked Junction	2nd Linked Junction
201	Piscataway Cr.	1509.1	762	2.284	0.035	201	202
202	Piscataway Cr.	1335	604.5	2.284	0.035	202	203
203	Little Hunting Cr.	2395.9	761.8	4.905	0.035	65	204
204	Henson Cr.	1643.2	1229.4	4.432	0.022	69	205
205	Potomac R.	1019.4	1928.7	3.999	0.022	72	206
206	Cameron Run	1061.5	1845.3	3.824	0.02	72	207
207	Oxon Run	937.5	1019.7	3.889	0.02	74	208
208	Oxon Run	767.9	480.6	2.284	0.022	208	209
209	Four Mile Run	806.1	1282.6	3.601	0.022	77	210
210	Anacostia R.	764.1	1251.9	5.457	0.024	79	211
211	Anacostia R.	345	479.8	4.814	0.025	211	212
212	Anacostia R.	353	428.3	4.886	0.025	212	213
213	Anacostia R.	360	396.7	5.15	0.025	213	214
214	Anacostia R.	338	375.6	5.589	0.025	214	215
215	Anacostia R.	328	357.1	5.909	0.025	215	216
216	Anacostia R.	335	349.3	5.908	0.025	216	217
217	Anacostia R.	335	347.9	5.795	0.025	217	218
218	Anacostia R.	329	349.9	5.673	0.025	218	219
219	Anacostia R.	338	349.8	5.405	0.025	219	220
220	Anacostia R.	359	292.3	5.044	0.025	220	221
221	Anacostia R.	413	227.2	4.261	0.025	221	222
222	Anacostia R.	460	239.2	3.441	0.025	222	223
223	Anacostia R.	458	232.4	2.797	0.025	223	224
224	Anacostia R.	448	211	2.548	0.025	224	225
225	Anacostia R.	440	202.5	2.449	0.025	225	226
226	Anacostia R.	438	194.8	2.226	0.025	226	227
227	Anacostia R.	430	175.2	1.998	0.025	227	228
228	Anacostia R.	400	161.3	2.004	0.025	228	229
229	Anacostia R.	375	151.9	2.212	0.025	229	230
230	Anacostia R.	414	128.5	2.329	0.025	230	231
231	Anacostia R.	449	109.3	2.208	0.025	231	232
232	Anacostia R.	445	105.7	2.096	0.025	232	233
233	Anacostia R.	408	92.8	2.201	0.025	233	234
234	Anacostia R.	388	79.3	2.458	0.025	234	235
235	Anacostia R.	359	74.8	2.599	0.025	235	236
236	Anacostia R.	321	76.1	2.624	0.025	236	237
237	Anacostia R.	323	73.7	2.597	0.025	237	238
238	Anacostia R.	318	82.7	2.507	0.025	238	239
239	Anacostia R.	313	92.2	2.443	0.025	239	240
240	Anacostia R.	309	93.9	2.475	0.025	240	241

Table 6. Potomac Estuary DYNHYD5 Model Grid Channel Geometry - Continued

Channel Number	Location	Length (m)	Width (m)	Initial Depth (m)	Manning's N	1st Linked Junction	2nd Linked Junction
241	Anacostia R.	377	78.2	2.602	0.025	241	242
242	Anacostia R.	446	60.2	2.591	0.025	242	243
243	Anacostia R.	438	99.3	2.163	0.025	243	244
244	Anacostia R.	420	110.2	1.821	0.025	244	245
245	NW Anacostia	420	55.1	1.582	0.025	245	246
246	NE Anacostia	420	55.1	1.582	0.025	245	247
247	Kingman Lake	2000	1000	1.935	0.025	227	248
248	Wash. Ship Ch.	1036.3	289.6	1.921	0.025	212	249
249	Wash. Ship Ch.	1036.3	283.5	6.312	0.025	249	250
250	Wash. Ship Ch.	1066.8	274.3	7.47	0.025	250	251
251	Hull Cr.	6863.3	1280	9.31	0.024	2	252
252	Hull Cr.	986.2	1533	1.43	0.024	252	253
253	Hull Cr.	1372.5	1095	1.43	0.024	253	254
254	Rosier Cr.	3557.1	1945	5.52	0.022	21	255
255	Rosier Cr.	1241.3	945	0.91	0.022	255	256
256	Chopawamsic Cr.	1947.8	235	4.81	0.022	45	257
257	Chopawamsic Cr.	1189.8	779	0.81	0.022	257	258

Table 7. Statistical Summary of Model Calibration for Water Surface Elevation and Salinity

1996-1997	**Water Surface Elevation**				**Salinity**			
	All Stations	Colonial Beach	Washington	Bladensburg	All Stations	Station LE2.2	Station RET2.4	Station TF2.4
Mean Error	0.032	0.020	0.073	0.010	-0.177	0.146	-0.255	-0.718
Absolute Mean Error	0.091	0.056	0.209	0.154	0.965	0.773	1.25	0.718
Relative Error	1.00	0.928	1.08	1.54	0.159	0.071	0.247	0.666
Slope	0.709	0.887	0.607	0.664	0.984	0.960	1.15	1.08
Intercept	0.005	-0.013	0.003	0.024	0.275	0.292	-0.499	0.635
R^2	0.762	0.902	0.629	0.746	0.924	0.884	0.853	0.585
Number of observations	31,213	13,836	4,145	13,232	110	36	37	6
2002-2005	**Water Surface Elevation**				**Salinity**			
	All Stations	Colonial Beach	Washington	Bladensburg	All Stations (except Piney Point)	Station LE2.2	Station RET2.4	Station TF2.4
Mean Error	-0.014	0.003	-0.020	-	0.110	0.480	-0.115	-0.162
Absolute Mean Error	0.126	0.041	0.157	-	1.01	1.02	1.56	0.480
Relative Error	1.16	0.764	1.23	-	0.163	0.081	0.219	0.295
Slope	0.704	0.911	0.658	-	1.00	1.12	1.18	0.781
Intercept	0.046	0.002	0.064	-	-0.131	-1.94	-1.15	0.518
R^2	0.775	0.957	0.740	-	0.929	0.894	0.831	0.806
Number of observations	23,285	6,259	17,026	No data	308	78	78	20

Table 8. Whole System Loads for Particulate Detrital Carbon (PDC)

	Mass Load in Metric Tons						
Spatal Zone	**2002**	**2003**	**2004**	**2005**	**Percent of Total for 2005**	**2002-2005**	**Percent of Total for 2002-2005**
UPOTTF	13,017	126,888	43,371	23,947	52.0%	207,222	71.6%
LPOTTF	1,950	2,528	2,100	2,285	5.0%	8,863	3.1%
POTOH	1,662	1,781	1,735	1,759	3.8%	6,937	2.4%
UPOTMH	2,128	2,438	2,345	2,356	5.1%	9,268	3.2%
LPOTMH	1,501	1,660	1,664	1,579	3.4%	6,404	2.2%
ANAC	671	2,070	990	1,510	3.3%	5,241	1.8%
TRIBS	5,166	18,521	9,274	12,638	27.4%	45,599	15.7%
Totals	26,096	155,886	61,478	46,074	100.0%	289,534	100.0%

Table 9. Whole System Loads for Particulate Organic Carbon (POC) and Components for Biotic Carbon (BIC) and Particulate Detrital Carbon (PDC)

Zone	2005 Total (MT)				2002-2005 Total (MT)			
	BIC	PDC	POC	Percent POC of Total for 2005	BIC	PDC	POC	Percent POC of Total for 2002-2005
UPOTTF	1,754	23,947	25,701	5.1%	8,308	51,818	60,126	3.2%
LPOTTF	27,989	2,285	30,274	6.0%	111,957	2,216	114,172	6.0%
POTOH	45,307	1,759	47,066	9.4%	181,228	1,734	182,962	9.7%
UPOTMH	183,029	2,356	185,385	37.0%	732,115	2,317	734,432	38.8%
LPOTMH	106,886	1,579	108,465	21.7%	427,546	1,601	429,147	22.7%
ANAC	589	1,510	2,098	0.4%	2,354	1,310	3,665	0.2%
TRIBS	89,104	12,638	101,743	20.3%	356,418	11,400	367,817	19.4%
Total	454,658	46,074	500,732	100.0%	1,819,925	72,396	1,892,321	100.0%

Table 10. Loads for Particulate Detrital Carbon (PDC) in Upper Potomac Tidal Fresh (UPOTTF)

	Mass Load in Metric Tons						
Source	**2002**	**2003**	**2004**	**2005**	**Percent of Total for 2005**	**2002-2005**	**Percent of Total for 2002-2005**
Potomac at Chain Bridge	12,620	125,020	42,726	22,466	93.8%	202,833	97.9%
All Other Tributaries	334	1,732	570	1,348	5.6%	3,983	1.9%
Direct Drainage	32	93	40	78	0.3%	243	0.1%
CSOs	5	17	8	28	0.1%	58	0.0%
Point Sources	0	0	0	0	0.0%	0	0.0%
Marshes	0	0	0	0	0.0%	0	0.0%
Bank Erosion	26	26	26	26	0.1%	105	0.1%
Totals	13,017	126,888	43,371	23,947	100.0%	207,222	100.0%

Table 11. Loads for Particulate Detrital Carbon (PDC) in Lower Potomac Tidal Fresh (LPOTTF)

	Mass Load in Metric Tons						
Source	**2002**	**2003**	**2004**	**2005**	**Percent of Total for 2005**	**2002-2005**	**Percent of Total for 2002-2005**
Tributaries	0	0	0	0	0.0%	0	0.0%
Direct Drainage	127	512	201	407	17.8%	1,248	14.1%
CSOs	3	30	11	19	0.8%	63	0.7%
Point Sources	766	932	830	805	35.2%	3,333	37.6%
Marshes	573	573	574	573	25.1%	2,292	25.9%
Bank Erosion	481	481	483	481	21.1%	1,927	21.7%
Totals	1,950	2,528	2,100	2,285	100.0%	8,863	100.0%

Table 12. Loads for Particulate Detrital Carbon (PDC) in Potomac Oligohaline (POTOH)

	Mass Load in Metric Tons						
Source	**2002**	**2003**	**2004**	**2005**	**Percent of Total for 2005**	**2002-2005**	**Percent of Total for 2002-2005**
Tributaries	0	0	0	0	0.0%	0	0.0%
Direct Drainage	23	140	91	118	6.7%	372	5.4%
CSOs	0	0	0	0	0.0%	0	0.0%
Point Sources	2	3	2	3	0.2%	10	0.1%
Marshes	1,180	1,180	1,183	1,180	67.1%	4,723	68.1%
Bank Erosion	458	458	459	458	26.0%	1,832	26.4%
Totals	1,662	1,781	1,735	1,759	100.0%	6,937	100.0%

Table 13. Loads for Particulate Detrital Carbon (PDC) in Upper Potomac Mesohaline (UPOTMH)

	Mass Load in Metric Tons						
Source	**2002**	**2003**	**2004**	**2005**	**Percent of Total for 2005**	**2002-2005**	**Percent of Total for 2002-2005**
Tributaries	0	0	0	0	0.0%	0	0.0%
Direct Drainage	75	385	286	303	12.9%	1,049	11.3%
CSOs	0	0	0	0	0.0%	0	0.0%
Point Sources	0	0	0	0	0.0%	1	0.0%
Marshes	1,400	1,400	1,403	1,400	59.4%	5,602	60.4%
Bank Erosion	653	653	655	653	27.7%	2,615	28.2%
Totals	2,128	2,438	2,345	2,356	100.0%	9,268	100.0%

Table 14. Loads for Particulate Detrital Carbon (PDC) in Lower Potomac Mesohaline (LPOTMH)

	Mass Load in Metric Tons						
Source	**2002**	**2003**	**2004**	**2005**	**Percent of Total for 2005**	**2002-2005**	**Percent of Total for 2002-2005**
Tributaries	0	0	0	0	0.0%	0	0.0%
Direct Drainage	41	200	199	118	7.5%	558	8.7%
CSOs	0	0	0	0	0.0%	0	0.0%
Point Sources	0	0	0	0	0.0%	0	0.0%
Marshes	996	996	998	996	63.1%	3,985	62.2%
Bank Erosion	465	465	466	465	29.4%	1,861	29.1%
Totals	1,501	1,660	1,664	1,579	100.0%	6,404	100.0%

Table 15. Loads for Particulate Detrital Carbon (PDC) in Anacostia (ANAC)

	Mass Load in Metric Tons						
Source	**2002**	**2003**	**2004**	**2005**	**Percent of Total for 2005**	**2002-2005**	**Percent of Total for 2002-2005**
Other Tributaries	0	0	0	0	0.0%	0	0.0%
Direct Drainage	152	419	217	321	21.3%	1,109	21.2%
CSOs	13	33	19	47	3.1%	113	2.2%
Point Sources	0	0	0	0	0.0%	0	0.0%
Marshes	37	37	37	37	2.5%	149	2.8%
Bank Erosion	18	18	18	18	1.2%	71	1.4%
NE Branch	266	922	412	641	42.5%	2,241	42.8%
NW Branch	185	641	287	445	29.5%	1,558	29.7%
Totals	671	2,070	990	1,510	100.0%	5,241	100.0%

Table 16. Loads for Particulate Detrital Carbon (PDC) in Minor Tributaries (TRIBS)

	Mass Load in Metric Tons						
Source	**2002**	**2003**	**2004**	**2005**	**Percent of Total for 2005**	**2002-2005**	**Percent of Total for 2002-2005**
Upstream Inflow	1,829	11,132	4,262	6,744	53.4%	23,966	52.6%
Direct Drainage	1,415	5,402	3,055	3,938	31.2%	13,811	30.3%
CSOs	3	11	5	12	0.1%	31	0.1%
Point Sources	240	296	266	264	2.1%	1,067	2.3%
Marshes	1,083	1,083	1,085	1,083	8.6%	4,333	9.5%
Bank Erosion	597	597	599	597	4.7%	2,391	5.2%
Totals	5,166	18,521	9,274	12,638	100.0%	45,599	100.0%

Table 17. Whole System External Loads for PCB Homologs 3-10 (PCB3+)

	Mass Load in Grams						
Spatal Zone	**2002**	**2003**	**2004**	**2005**	**Percent of Total for 2005**	**2002-2005**	**Percent of Total for 2002-2005**
UPOTTF	9,845	74,596	28,513	18,234	52.9%	131,189	70.6%
LPOTTF	1,720	3,026	2,091	2,545	7.4%	9,382	5.0%
POTOH	264	276	271	273	0.8%	1,083	0.6%
UPOTMH	608	636	627	627	1.8%	2,498	1.3%
LPOTMH	428	442	442	434	1.3%	1,746	0.9%
ANAC	3,201	9,553	5,403	8,446	24.5%	26,602	14.3%
TRIBS	1,895	5,048	2,539	3,942	11.4%	13,424	7.2%
Totals	17,961	93,576	39,886	34,501	100.0%	185,924	100.0%

Table 18. External Loads for PCB Homologs 3-10 (PCB3+) in Upper Potomac Tidal Fresh (UPOTTF)

	Mass Load in Grams						
Source	**2002**	**2003**	**2004**	**2005**	**Percent of Total for 2005**	**2002-2005**	**Percent of Total for 2002-2005**
Potomac at Chain Bridge	8,952	71,415	27,214	15,118	82.9%	122,700	93.5%
All Other Tributaries	195	920	308	669	3.7%	2,092	1.6%
Direct Drainage	508	1,721	704	1,598	8.8%	4,531	3.5%
CSOs	125	473	221	784	4.3%	1,603	1.2%
Point Sources	0	0	0	0	0.0%	0	0.0%
Atmospheric wet/dry deposition	64	64	65	64	0.4%	258	0.2%
Contaminated Sites	1	1	1	1	0.0%	5	0.0%
Totals	**9,845**	**74,596**	**28,513**	**18,234**	**100.0%**	**131,189**	**100.0%**

Table 19. External Loads for PCB Homologs 3-10 (PCB3+) in Lower Potomac Tidal Fresh (LPOTTF)

	Mass Load in Grams						
Source	**2002**	**2003**	**2004**	**2005**	**Percent of Total for 2005**	**2002-2005**	**Percent of Total for 2002-2005**
Tributaries	0	0	0	0	0.0%	0	0.0%
Direct Drainage	146	589	246	508	20.0%	1,489	15.9%
CSOs	73	805	293	517	20.3%	1,689	18.0%
Point Sources	628	760	677	647	25.4%	2,712	28.9%
Atmospheric wet/dry deposition	872	872	874	872	34.2%	3,489	37.2%
Contaminated Sites	1	1	1	1	0.0%	4	0.0%
Totals	**1,720**	**3,026**	**2,091**	**2,545**	**100.0%**	**9,382**	**100.0%**

Table 20. External Loads for PCB Homologs 3-10 (PCB3+) in Potomac Oligohaline (POTOH)

	Mass Load in Grams						
Source	**2002**	**2003**	**2004**	**2005**	**Percent of Total for 2005**	**2002-2005**	**Percent of Total for 2002-2005**
Tributaries	0	0	0	0	0.0%	0	0.0%
Direct Drainage	2	14	9	11	4.1%	36	3.4%
CSOs	0	0	0	0	0.0%	0	0.0%
Point Sources	0	0	0	0	0.0%	0	0.0%
Atmospheric wet/dry deposition	261	261	262	261	95.8%	1,046	96.6%
Contaminated Sites	0	0	0	0	0.0%	0	0.0%
Totals	**264**	**276**	**271**	**273**	**100.0%**	**1,083**	**100.0%**

Table 21. External Loads for PCB Homologs 3-10 (PCB3+) in Upper Potomac Mesohaline (UPOTMH)

	Mass Load in Grams						
Source	**2002**	**2003**	**2004**	**2005**	**Percent of Total for 2005**	**2002-2005**	**Percent of Total for 2002-2005**
Tributaries	0	0	0	0	0.0%	0	0.0%
Direct Drainage	7	35	24	26	4.1%	92	3.7%
CSOs	0	0	0	0	0.0%	0	0.0%
Point Sources	0	0	0	0	0.0%	0	0.0%
Atmospheric wet/dry deposition	596	596	597	596	95.0%	2,385	95.5%
Contaminated Sites	5	5	5	5	0.9%	22	0.9%
Totals	**608**	**636**	**627**	**627**	**100.0%**	**2,498**	**100.0%**

Table 22. External Loads for PCB Homologs 3-10 (PCB3+) in Lower Potomac Mesohaline (LPOTMH)

	Mass Load in Grams						
Source	**2002**	**2003**	**2004**	**2005**	**Percent of Total for 2005**	**2002-2005**	**Percent of Total for 2002-2005**
Tributaries	0	0	0	0	0.0%	0	0.0%
Direct Drainage	4	18	17	10	2.4%	48	2.8%
CSOs	0	0	0	0	0.0%	0	0.0%
Point Sources	0	0	0	0	0.0%	0	0.0%
Atmospheric wet/dry deposition	424	424	425	424	97.6%	1,697	97.2%
Contaminated Sites	0	0	0	0	0.0%	0	0.0%
Totals	**428**	**442**	**442**	**434**	**100.0%**	**1,746**	**100.0%**

Table 23. External Loads for PCB Homologs 3-10 (PCB3+) in Anacostia (ANAC)

	Mass Load in Grams						
Source	**2002**	**2003**	**2004**	**2005**	**Percent of Total for 2005**	**2002-2005**	**Percent of Total for 2002-2005**
Other Tributaries	0	0	0	0	0.0%	0	0.0%
Direct Drainage	2,484	7,567	4,388	6,428	76.1%	20,867	78.4%
CSOs	371	925	520	1,300	15.4%	3,116	11.7%
Point Sources	0	0	0	0	0.0%	0	0.0%
Atmospheric wet/dry deposition	46	46	46	46	0.5%	185	0.7%
Contaminated Sites	3	3	3	3	0.0%	12	0.0%
NE Branch	175	597	263	394	4.7%	1,429	5.4%
NW Branch	122	415	183	274	3.2%	993	3.7%
Totals	**3,201**	**9,553**	**5,403**	**8,446**	**100.0%**	**26,602**	**100.0%**

Table 24. External Loads for PCB Homologs 3-10 (PCB3+) in Minor Tributaries (TRIB)

	Mass Load in Grams						
Source	**2002**	**2003**	**2004**	**2005**	**Percent of Total for 2005**	**2002-2005**	**Percent of Total for 2002-2005**
Upstream Inflow	413	1,986	662	1,291	32.8%	4,352	32.4%
Direct Drainage	536	1,913	867	1,458	37.0%	4,775	35.6%
CSOs	56	249	114	300	7.6%	719	5.4%
Point Sources	51	62	55	54	1.4%	221	1.6%
Atmospheric wet/dry deposition	835	835	837	835	21.2%	3,341	24.9%
Contaminated Sites	4	4	4	4	0.1%	17	0.1%
Totals	**1,895**	**5,048**	**2,539**	**3,942**	**100.0%**	**13,424**	**100.0%**

Table 25. Water Column Monitoring Stations for Sorbents and PCB3+

Station Name	RM	Description	Spatial Zone	POTPCB Model Segment	Laboratory	Latitude (deg)	Longitude (deg)
PRMCB	117.47	Chain Bridge	UPOTTF	95	CBL	38.9296	-77.1164
PR-1	116.98	Below Chain Bridge	UPOTTF	94	ANS	38.9246	-77.1121
PR-2	114.03	Key Bridge	UPOTTF	87	ANS	38.9021	-77.0693
PRM28	113.14	Below Roosevelt Bridge	UPOTTF	85	CBL	38.8914	-77.0563
PR-3	112.65	Below Memorial Bridge	UPOTTF	84	ANS	38.8849	-77.0534
PR-4	110.49	Above Hains Point	UPOTTF	79	ANS	38.8597	-77.0281
AR-8	109.90	Confluence with Anacostia	LPOTTF	78	ANS	38.8515	-77.0214
PR-5	108.82	Bolling AFB	LPOTTF	76	ANS	38.8363	-77.0256
PR-6	107.04	Oronoco Bay Park Alexandria	LPOTTF	74	ANS	38.8112	-77.0344
PR-7	106.45	Alexandria	LPOTTF	73	ANS	38.8112	-77.0344
PRM25	102.61	Off mouth of Broad Creek	LPOTTF	68	CBL	38.7468	-77.0341
TF2.1	99.57	FL Buoy 77 off mouth of Piscataway Creek	LPOTTF	65	CBP/MDNR	38.7065	-77.0486
TF2.2	96.32	Buoy 67 off mouth of Piscataway Creek	LPOTTF	61	CBP/MDNR	38.6907	-77.1111
PRM21	92.39	Hallowing Point	LPOTTF	58	CBL	38.6349	-77.1212
TF2.3	88.85	Buoy N 54 off Indianhead	LPOTTF	55	CBP/MDNR	38.6082	-77.1739
TF2.4	81.08	Buoy 44 between Possum Point and Moss Point	LPOTTF	46	CBP/MDNR	38.5298	-77.2653
PRM16	78.71	Quantico	POTOH	44	CBL	38.5043	-77.2975
CBTOX_A	77.83	Sandy Point	POTOH	43	CBL	38.4856	-77.2861
PRM15	77.53	Quantico	POTOH	43	CBL	38.4879	-77.3095
PRM10	72.22	Marlboro Point	POTOH	39	CBL	38.4068	-77.2883
RET2.1	71.53	Buoy 27 SW of Smith Point	POTOH	38	CBP/MDNR	38.4034	-77.2692
RET2.2	65.04	Buoy 19 off Maryland Point	POTOH	33	CBP/MDNR	38.3521	-77.2044

Table 25. Water Column Monitoring Stations for Sorbents and PCB3+ - Continued

Station Name	RM	Description	Spatial Zone	POTPCB Model Segment	Laboratory	Latitude (deg)	Longitude (deg)
RET2.4	49.60	Morgantown Bridge (US 301)	UPOTMH	23	CBP/MDNR	38.3626	-76.9905
CBTOX_B	48.62	Morgantown	UPOTMH	22	CBL	38.3476	-76.9807
LE2.2	20.47	Buoy 51B off Ragged Point	LPOTMH	8	CBP/MDNR	38.1668	-76.5830
CBTOX_C	18.11	Ragged Point	LPOTMH	7	CBL	38.1330	-76.5637
LE2.3	3.54	Potomac mouth	LPOTMH	1	CBP/MDNR	38.0215	-76.3477
PRM01	0.591	Potomac mouth	LPOTMH	1	CBL	37.9969	-76.3084
AR-NE (GMU)	0.248	NE Branch Anacostia Gauge	ANAC	246	GMU	38.9603	-76.9260
AR-NE (ANS)	0.248	NE Branch Anacostia Gauge	ANAC	246	ANS	38.9603	-76.9260
AR-1	8.18	Anacostia	ANAC	243	ANS	38.9350	-76.9398
AR-2	6.70	Anacostia	ANAC	237	ANS	38.9161	-76.9450
AR-3	5.62	Anacostia	ANAC	232	ANS	38.9059	-76.9584
AR-4/AR-CSX	3.75	Anacostia/CSX Bridge	ANAC	223	ANS	38.8797	-76.9710
AR-5	2.56	Anacostia	ANAC	220	ANS	38.8720	-76.9902
PRM27	1.78	S. Capitol St. Bridge	ANAC	216	CBL	38.8705	-77.0037
AR-6	1.78	Anacostia	ANAC	216	ANS	38.8705	-77.0039
AR-7	0.691	Anacostia	ANAC	211	ANS	38.8587	-77.0170
PRM18	0.00	Mattawoman Creek	TRIB	174	CBL	38.5602	-77.2040
MAT0035	0.00	Mattawoman Creek	TRIB	176	BAT	38.5686	-77.1765
PRM20	0.00	Occoquan Bay	TRIB	187	CBL	38.6235	-77.2135
1aWLB000.06	0.00	Mills Branch	TRIB	191	BAT	38.6808	-77.2519
1aOCC006.99	0.00	Occoquan River	TRIB	184	GERG	38.6861	-77.2624

Table 26. Primary Water Column Measurements

Parameter	Laboratory						
	ANS	BAT	CBL	CBL (CBTOX)	CBP/ MDNR	GERG	GMU
Temperature					X		
Total suspended particulates			X	X			X
Total suspended solids	X			X	X	X	
Total organic carbon					X		
Particulate carbon	X		X	X	X	X	
Dissolved organic carbon	X			X	X	X	
Chlorophyll *a*	X			X	X		
Sum of PCB homologs 3-10	X	X	X	X		X	X

Key:

ANS	Academy of Natural Sciences, Philadelphia
BAT	Battelle Laboratory
CBL	Chesapeake Biological Laboratory (2005)
CBL (CBTOX)	Chesapeake Biological Laboratory (2003)
CBP/MDNR	Chesapeake Bay Program/Maryland Department of Natural Resources
GERG	Geochemical and Environmental Research Group, Texas A&M
GMU	George Mason University

Table 27. Model Calibration Parameters for Sorbents and PCB3+

Parameter	Description	Value	Unit	Source
$Vs_{,BIC}$	BIC net settling velocity	0.10	m/day	Calibration
$Vs_{,PDC}$	PDC gross settling velocity	1.0	m/day	Calibration
Vr	PDC resuspension velocity	Zone specific (See Table 28)	mm/year	Calibration; constrained by site specific net burial rates from Brush 1989 and Cerco and Cole 1994
K_{BIC}	BIC decay rate	0.40	1/day	Calibration
K_{WPDC}	PDC water column decay rate	0.05	1/day	Calibration
K_{SPDC}	PDC sediment decay rate	Zone specific (See Table 28)	1/day	Estimated from site specific SOD data by Boynton et al. 1986 (tabulated in DiToro 2000); constrained by site specific net burial rates from Brush 1989 and Cerco and Cole 1994
ρ	Sediment solids density	2.65	g/cm^3	Chapra 1997
ø	Sediment porosity	Function of rivermile	dimensionless	LOWESS smoothing of data from Cartwright and Friedrichs 2006
foc	Mass fraction organic carbon in sediment	Function of rivermile	dimensionless	Derived from sediment porosity and CBL data for sediment organic carbon
log Kpoc	PCB3+ partition coefficient to particulate organic carbon	5.885	log(L/kg)	Hansen et al. 1999
log Kdoc	PCB3+ partition coefficient to dissolved organic carbon	4.885	log (L/kg/)	Estimated as 10% of log Koc (Eadie et al. 1990, 1992)
DOCw	DOC in water column	2.71	mg/L	Derived from CBL and CBP/MDNR data
DOCs	DOC in sediment	20.6 in LPOTTF, POTTF, ANAC 10.8 in POTOH, UPOTMH, LPOTMH	mg/L	Boynton et al. 1996
MW	PCB3+ molecular weight	319.6	gm/mole	Mackay et al. 2000
H	Henry's Law Constant for PCB3+	109.18	Pa m^3/mol	Mackay et al. 2000

Table 27. Model Calibration Parameters for Sorbents and PCB3+ - Continued

Parameter	Description	Value	Unit	Source
K_l	Air-water liquid film mass transfer rate	Formulation by O'Connor and Dobbins 1958	m/day	Documented in Chapra 1997
K_g	Air-water gas exchange mass transfer rate	Formulation by Banks and Herrera 1977	m/day	Documented in Chapra 1997
$PCB3+_{gas}$	Atmospheric gas phase PCB3+ concentration	506	pg/m^3	Brunciak et al. 2001 (Assumes PCB3+ is 92% of Total PCB)
Kf	PCB3+ sediment-water mass transfer rate	12.15	cm/day	Erickson et al. 2005
Ev	Vertical diffusion coefficient between surface and deep sediments	1.00E-10	m^2/sec	Assumed to be molecular diffusion rate
Wv1	Sediment particle mixing rate in surface layers	1.0E-10	m^2/sec	U.S. EPA 2000

Table 28. Zone Specific Values for Net Solids Burial and PDC Resuspension and Sediment Decay Rates

Zone	Median Burial Rate (cm/yr)		Minimum Burial Rate (cm/yr)		Maximum Burial Rate (cm/yr)		Sed. PDC decay @20C (day^{-1})	Vr, PDC (mm/yr)
	2002-2005	2005	2002-2005	2005	2002-2005	2005		
LPOTMH	0.58	0.49	0.55	0.43	0.65	0.62	8.89E-04	4
UPOTMH	0.83	0.49	0.67	0.38	0.97	0.58	8.89E-04	4
POTOH	0.80	0.45	0.47	0.03	1.04	0.78	3.81E-04	10
LPOTTF	1.05	0.29	0.90	0.20	1.50	0.46	3.81E-04	2
UPOTTF	1.28	0.18	1.15	0.08	1.46	0.32	3.81E-04	1
ANAC	0.54	0.61	0.16	0.10	2.92	2.25	3.81E-04	2

Table 29. Statistical Summary of Model Calibration for Sorbents and PCB3+

BIC, mg/L	Whole Potomac	UPOTTF	LPOTTF	POTOH	UPOTMH	LPOTMH	ANAC
Mean Error	-0.07	0.00	-0.06	-0.20	-0.11	0.12	0.30
Absolute Mean Error	0.26	0.03	0.24	0.27	0.41	0.23	0.43
Relative Error	0.83	0.19	0.83	1.11	0.89	0.52	0.63
Number of observations	421	8	214	88	57	54	26
PDC, mg/L	**Whole Potomac**	**UPOTTF**	**LPOTTF**	**POTOH**	**UPOTMH**	**LPOTMH**	**ANAC**
Mean Error	-0.10	-0.67	-0.34	0.31	0.02	0.12	-0.11
Absolute Mean Error	0.65	0.68	0.78	0.65	0.52	0.27	0.92
Relative Error	0.54	0.99	0.64	0.46	0.47	0.28	0.56
Number of observations	421	8	214	88	57	54	26
[1]PCB3+, ng/L	**Whole Potomac**	**UPOTTF**	**LPOTTF**	**POTOH**	**UPOTMH**	**LPOTMH**	**ANAC**
Mean Error	0.08	0.14	0.09	0.03	n/a	n/a	-5.85
Absolute Mean Error	0.61	0.34	0.94	0.47	n/a	n/a	6.10
Relative Error	0.50	0.28	0.65	0.49	n/a	n/a	2.40
Number of observations	33	10	14	7	Insufficient Data (1)	Insufficient Data (1)	36

[1]Excluding three apparent outliers in Potomac on 6/27/03

PCB TMDL MODEL FOR THE POTOMAC RIVER ESTUARY

Draft Final Report on Hydrodynamic/Salinity and PCB Transport and Fate Models

APPENDIX B

FIGURES

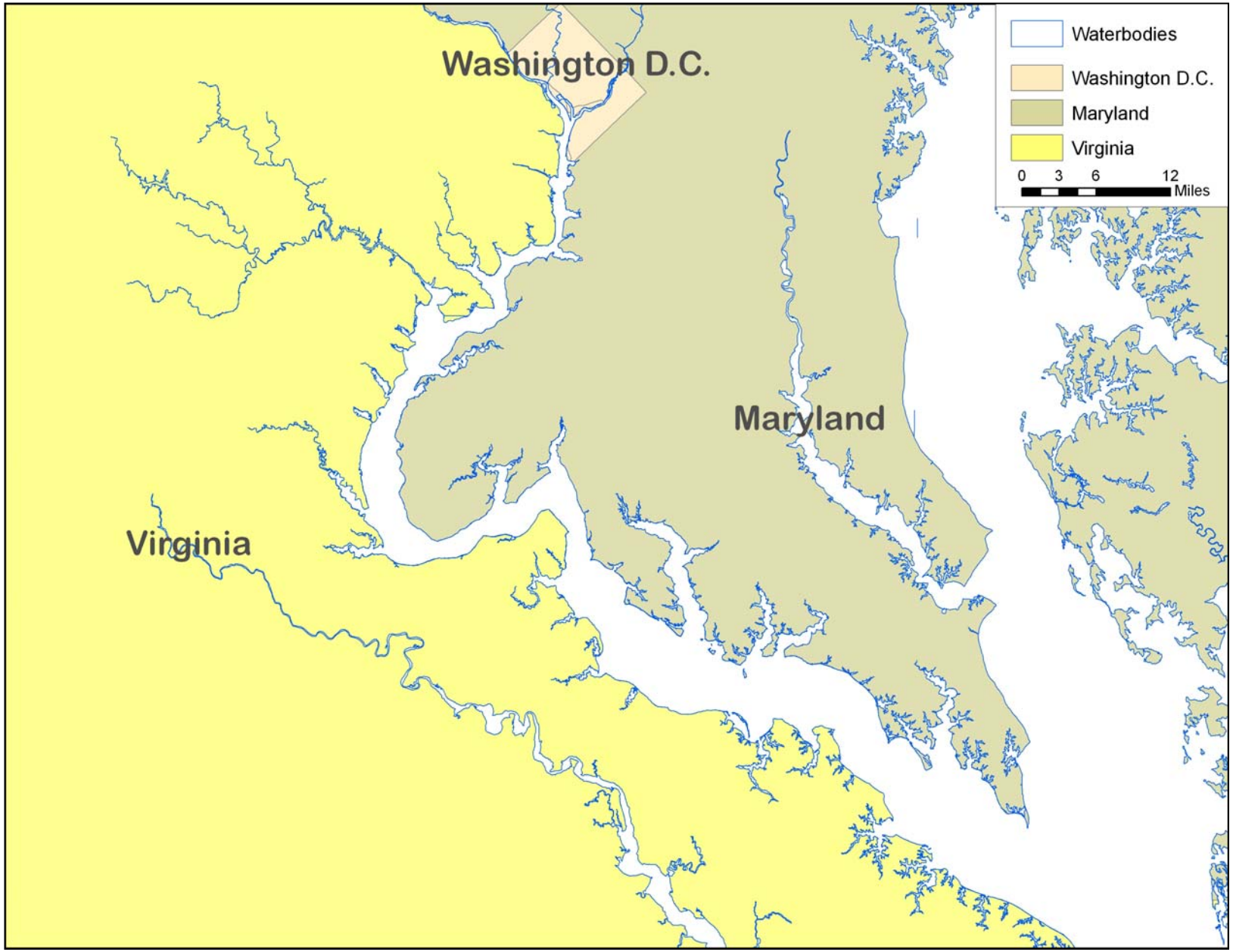

Figure 1. Map of Study Area

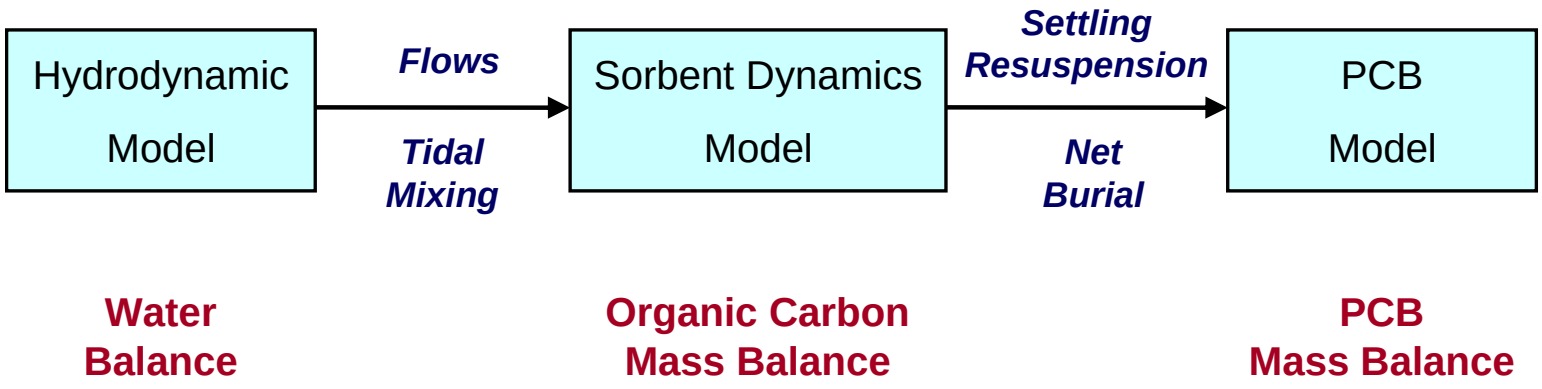

Figure 2. Integrated Modeling Framework

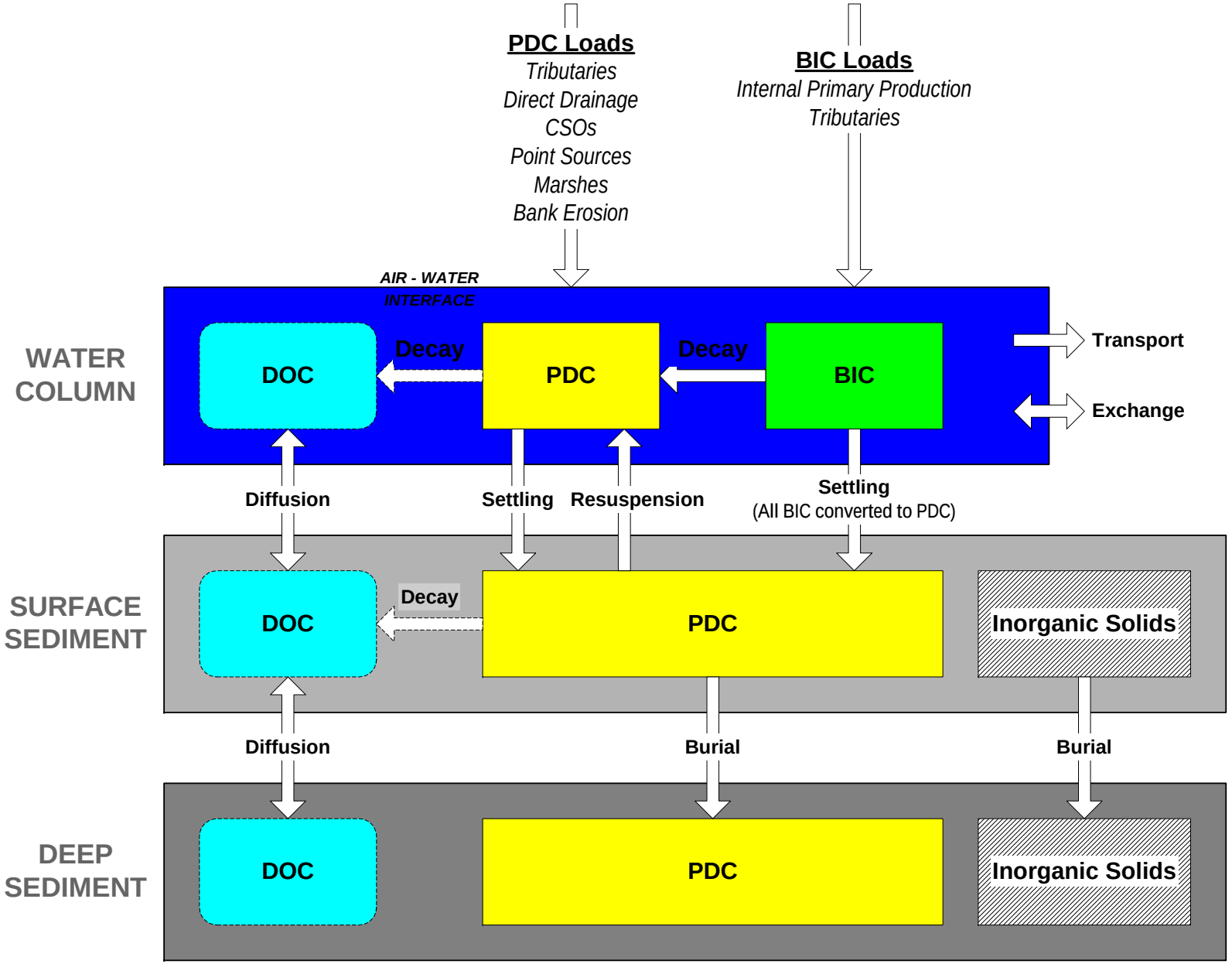

Figure 3. Conceptual Framework for Organic Carbon Sorbents Model

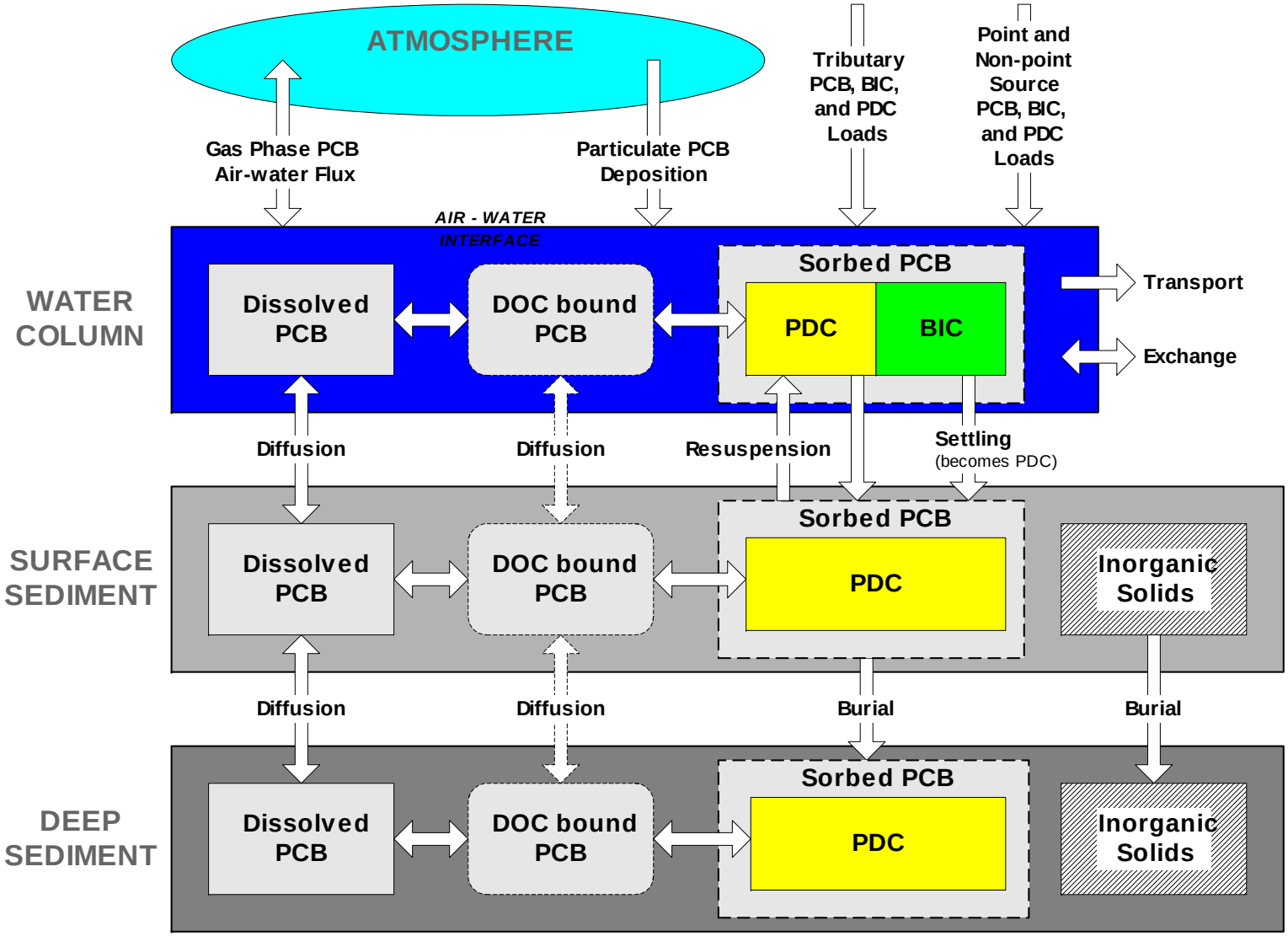

Figure 4. Conceptual Framework for PCB Model

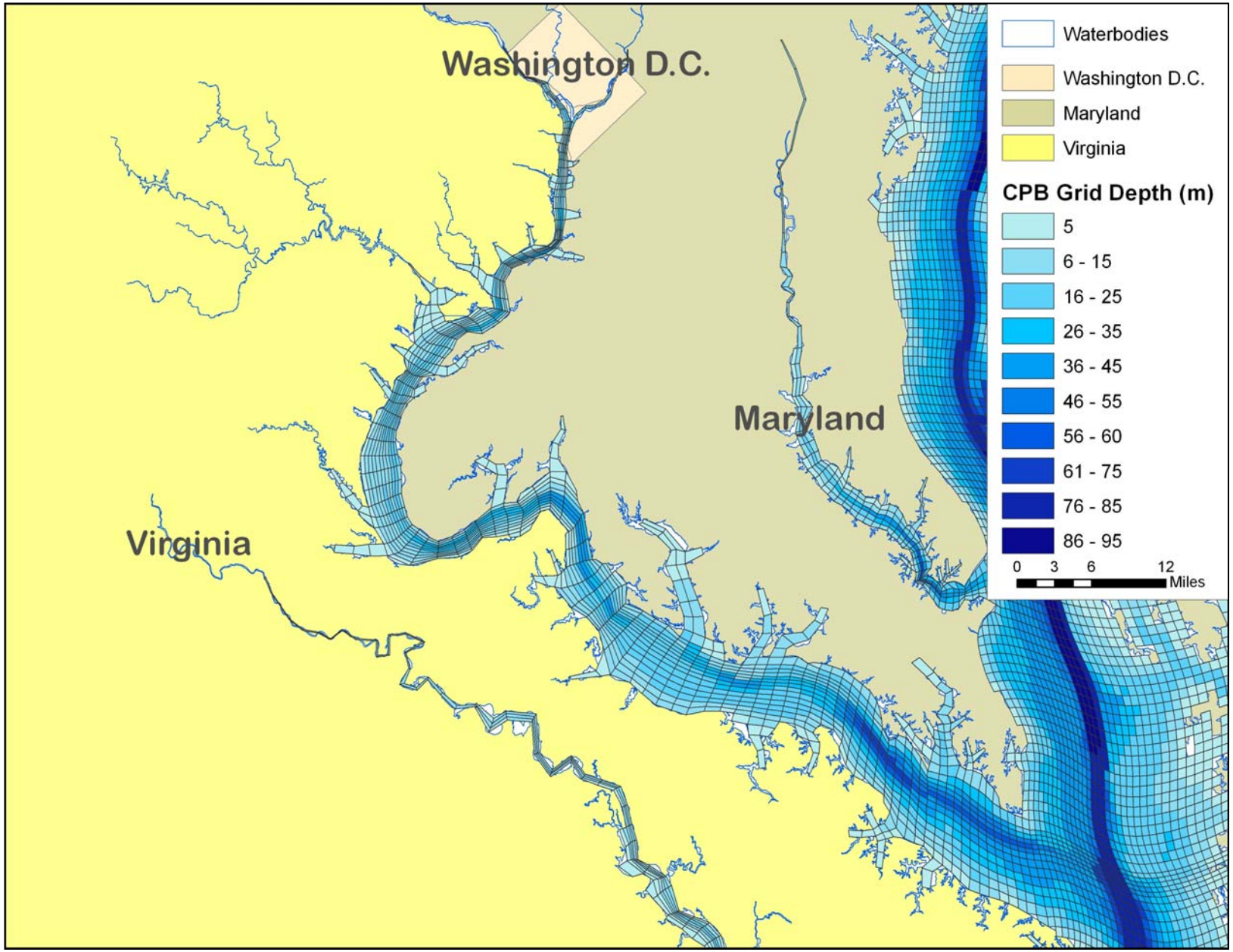

Figure 5. Bathymetry from 57K Chesapeake Bay Water Quality Model

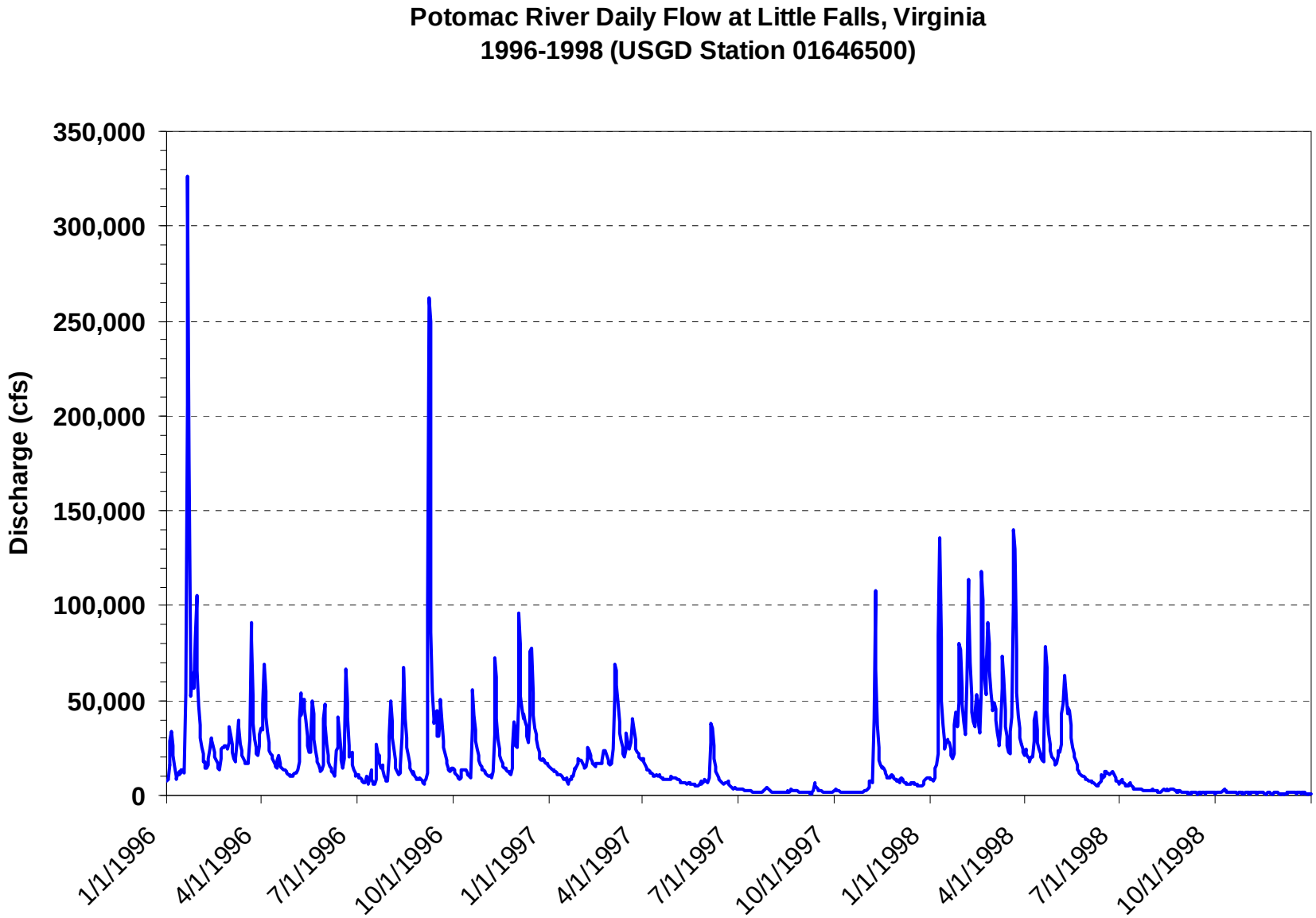

Figure 6. Daily Average Potomac River Flow at Little Falls, VA (1996-1997)

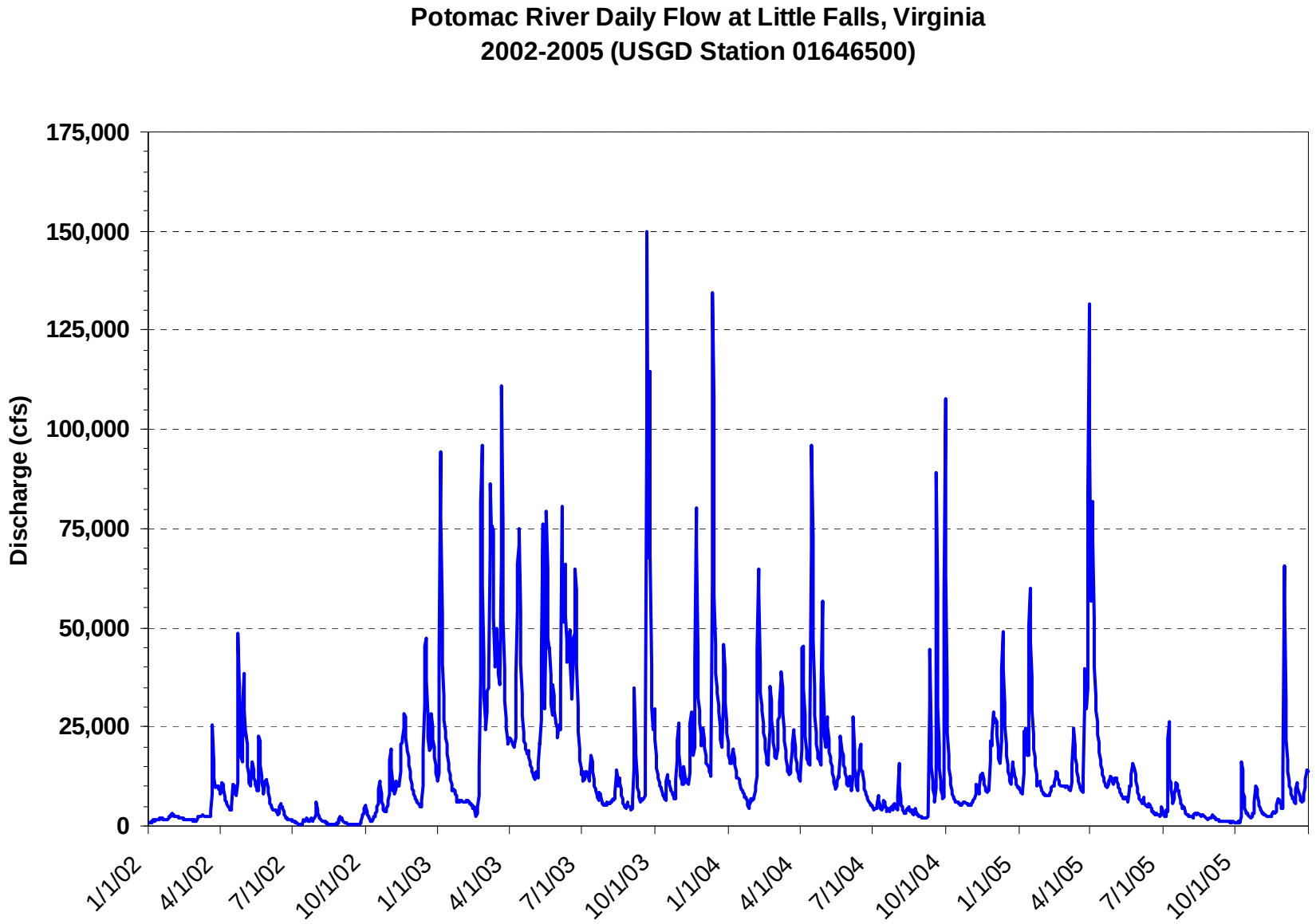

Figure 7. Daily Average Potomac River Flow at Little Falls, VA (2002-2005)

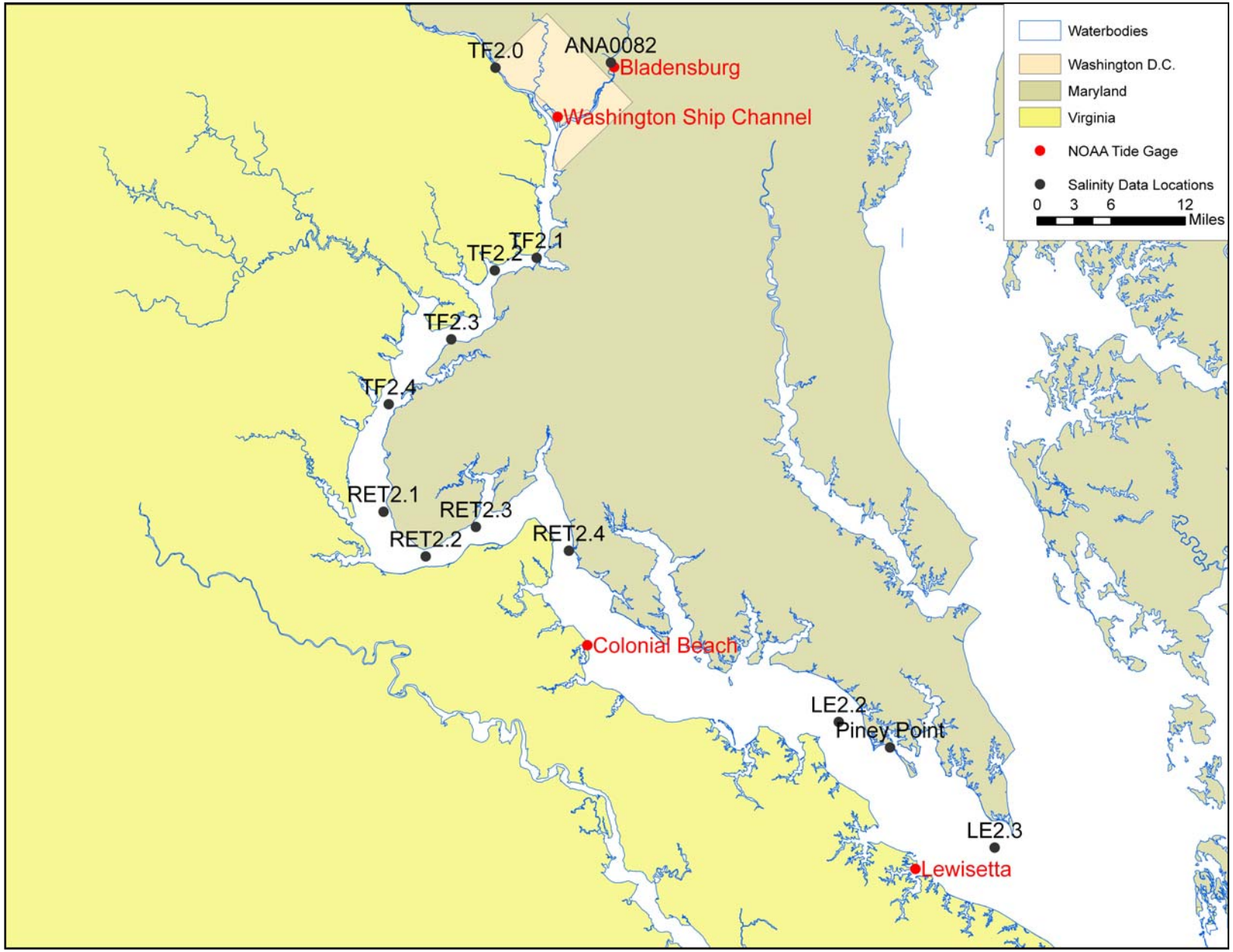

Figure 8. Locations of Salinity and Tide Gages

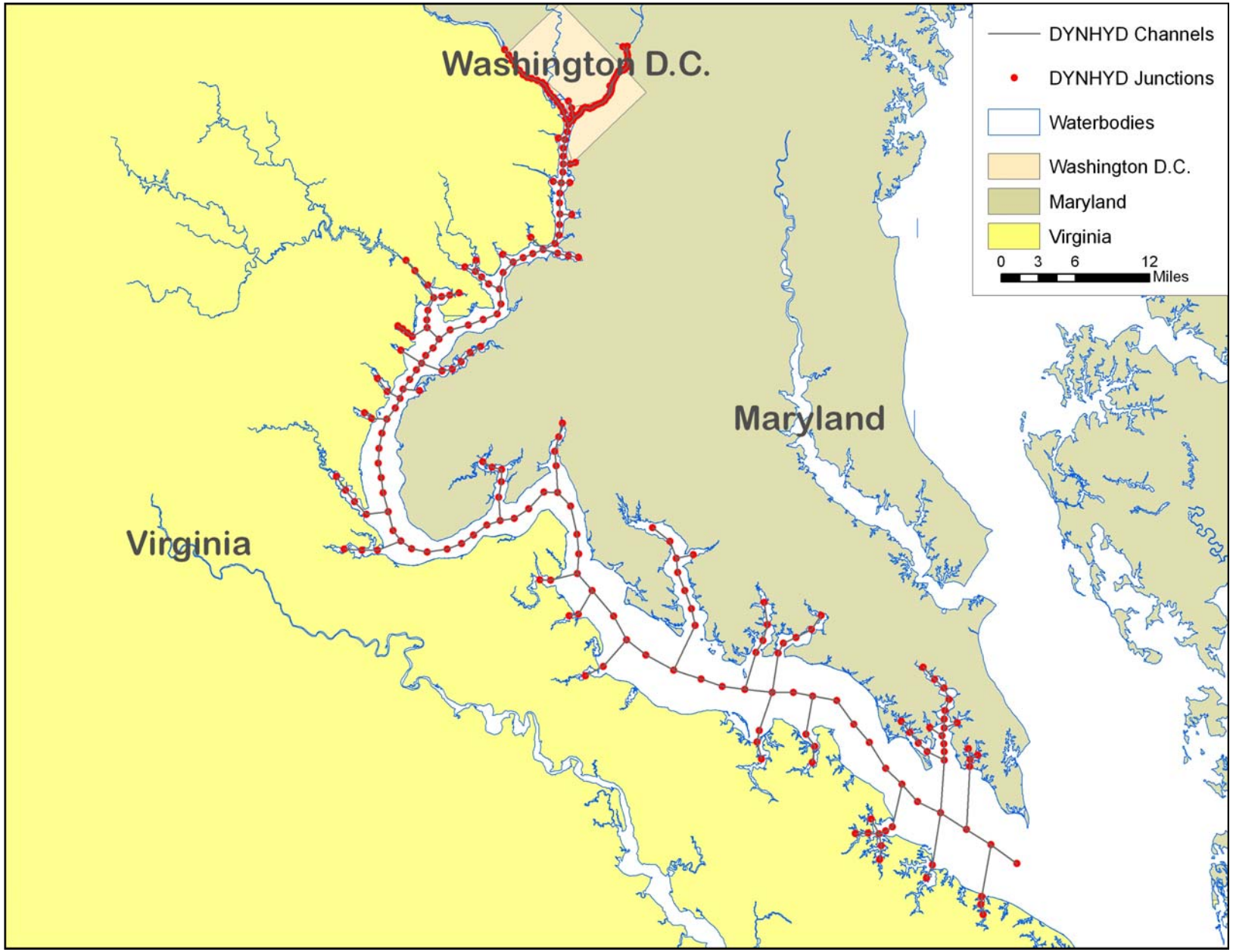

Figure 9. DYNHYD Junction-Channel Grid

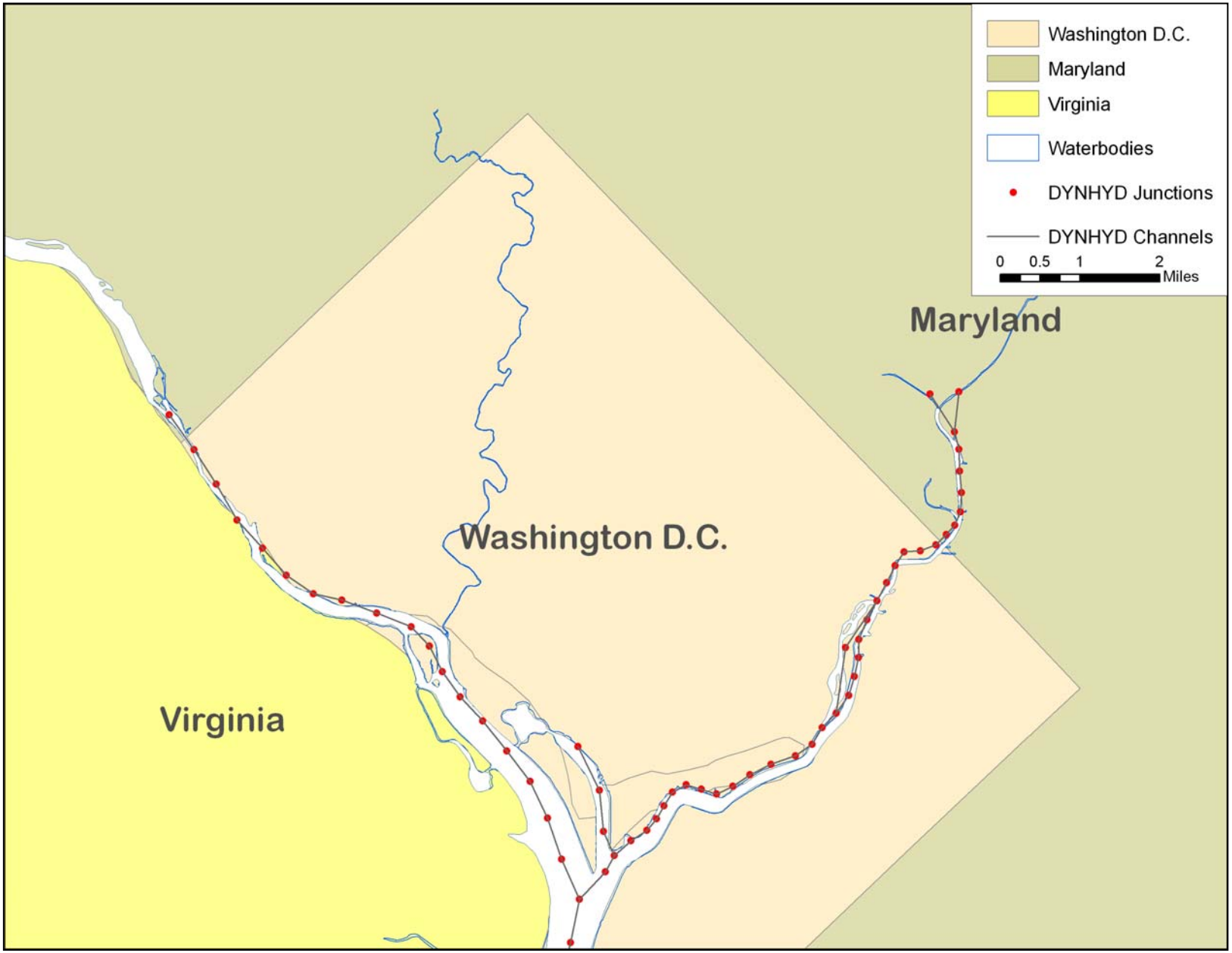

Figure 10. DYNHYD Junction-Channel Grid (Washington DC)

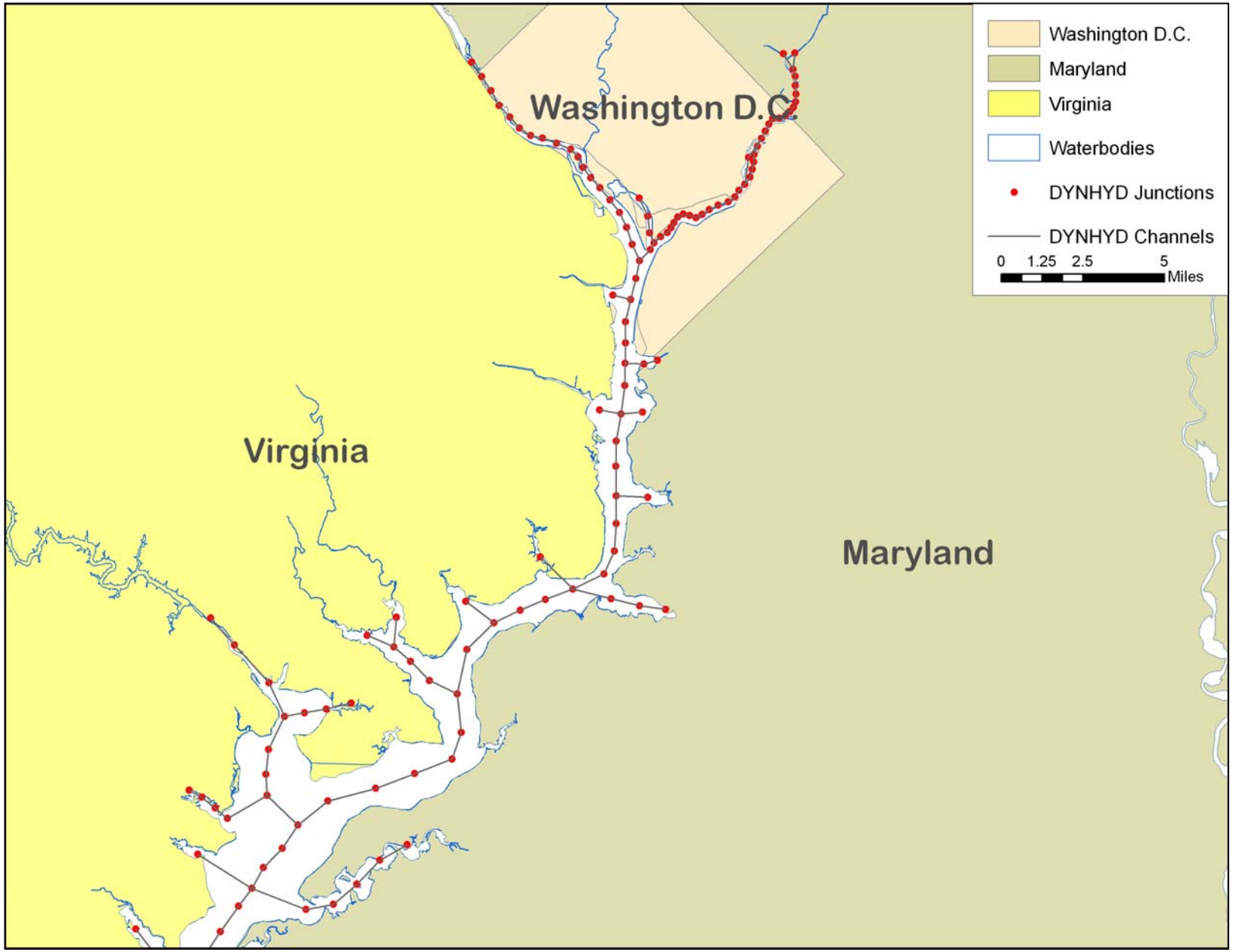

Figure 11. DYNHYD Junction-Channel Grid (Upper Potomac)

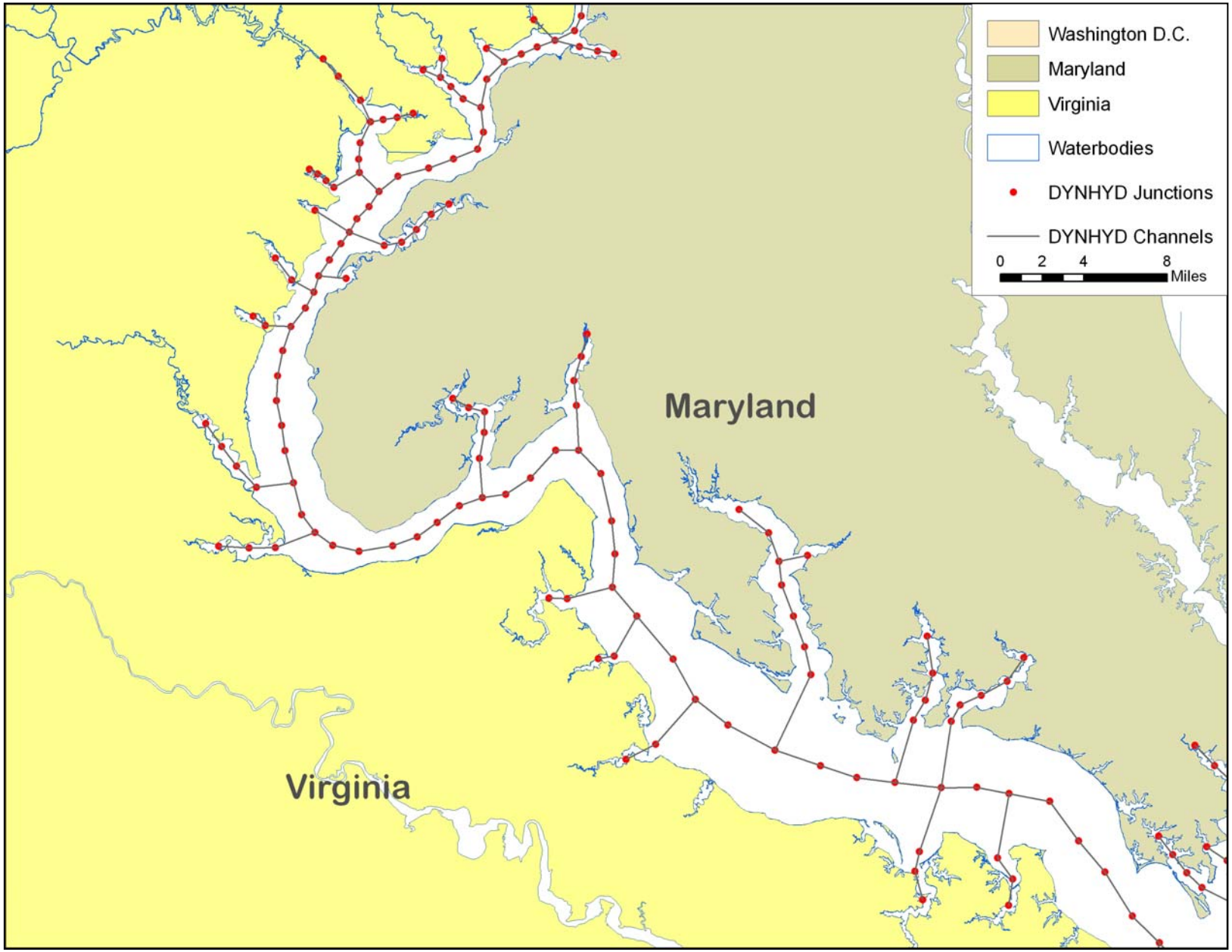

Figure 12. DYNHYD Junction-Channel Grid (Middle Potomac)

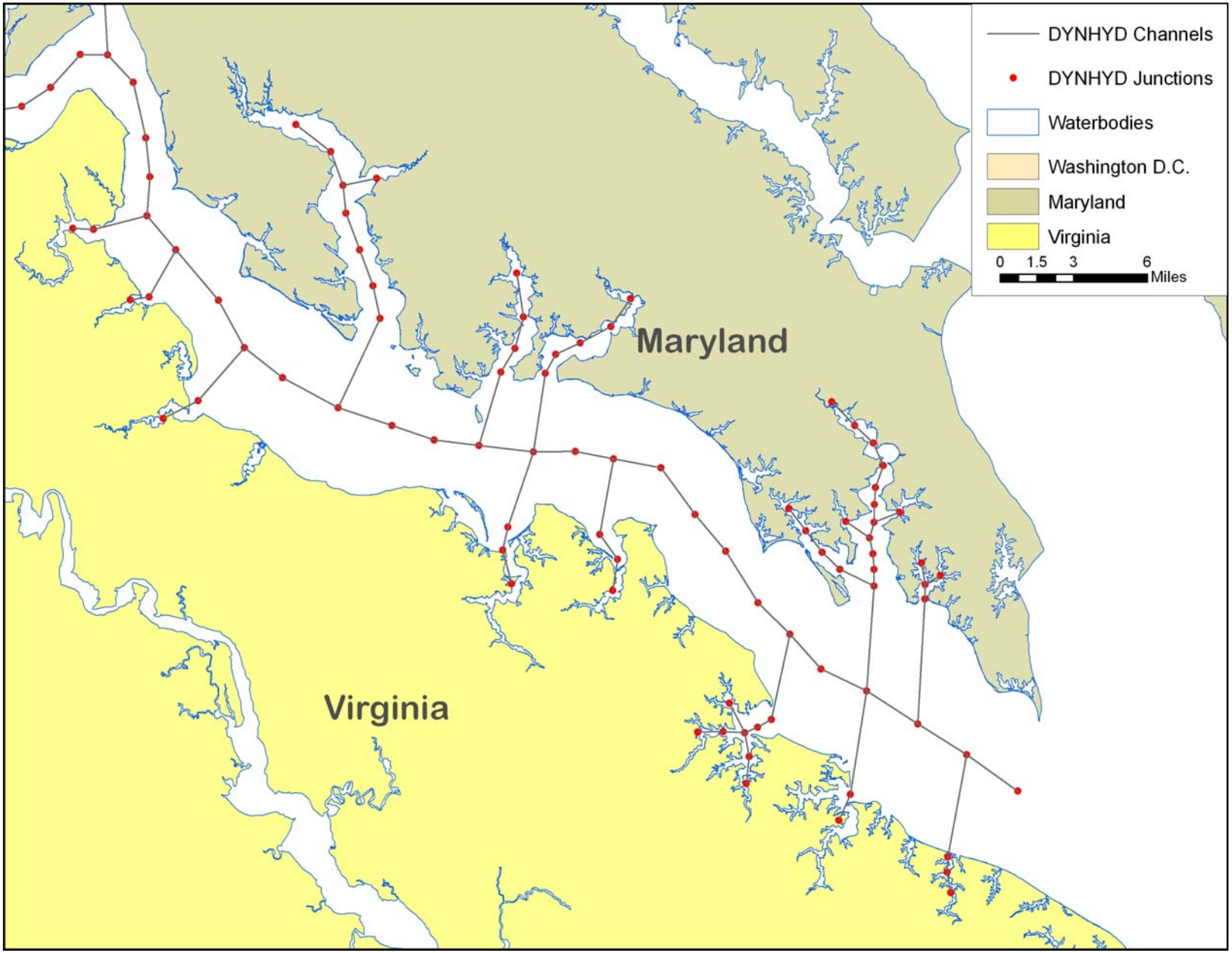

Figure 13. DYNHYD Junction-Channel Grid (Lower Potomac)

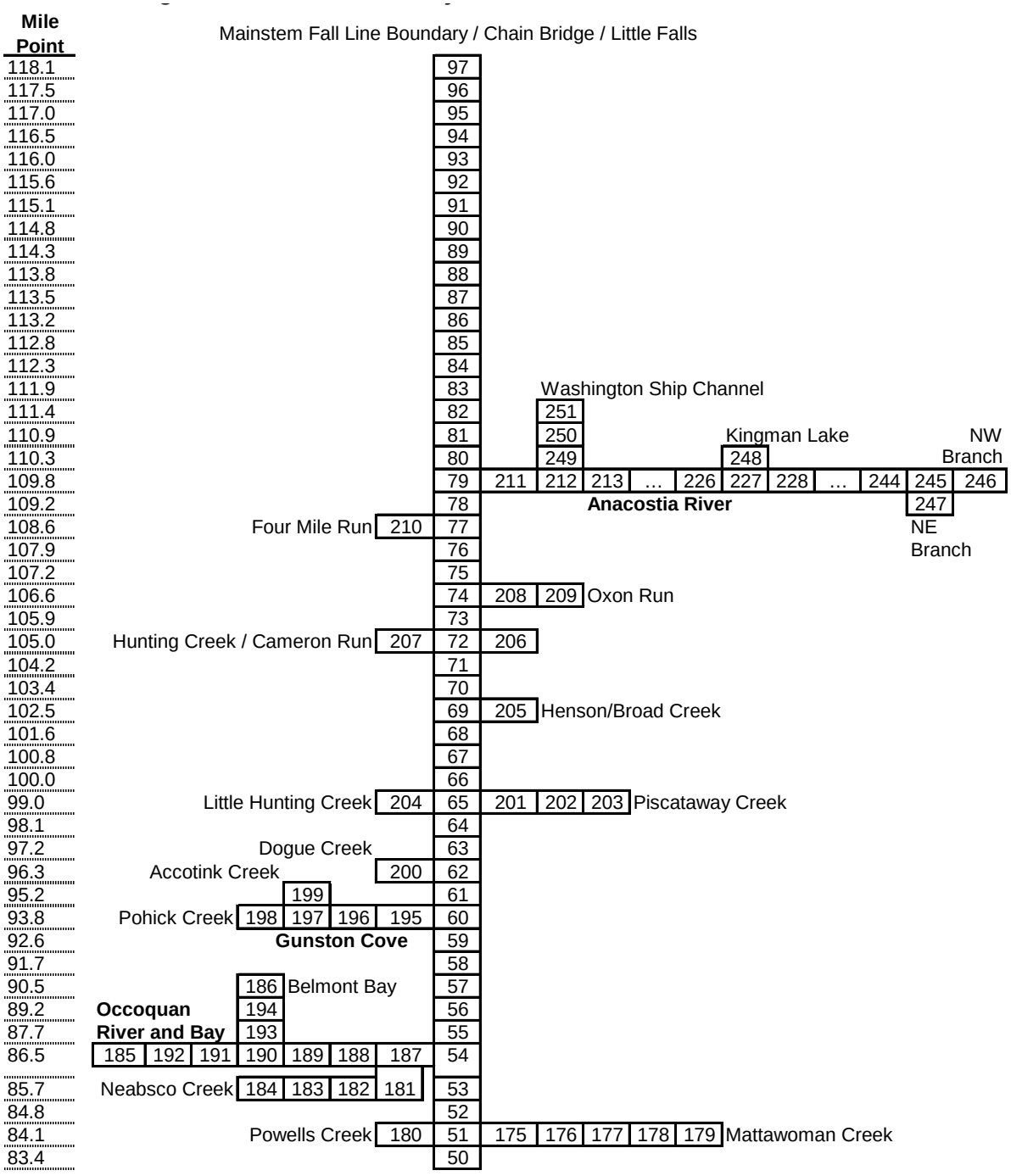

Figure 14. Potomac Estuary DYNHYD5 Model Junction Schematic

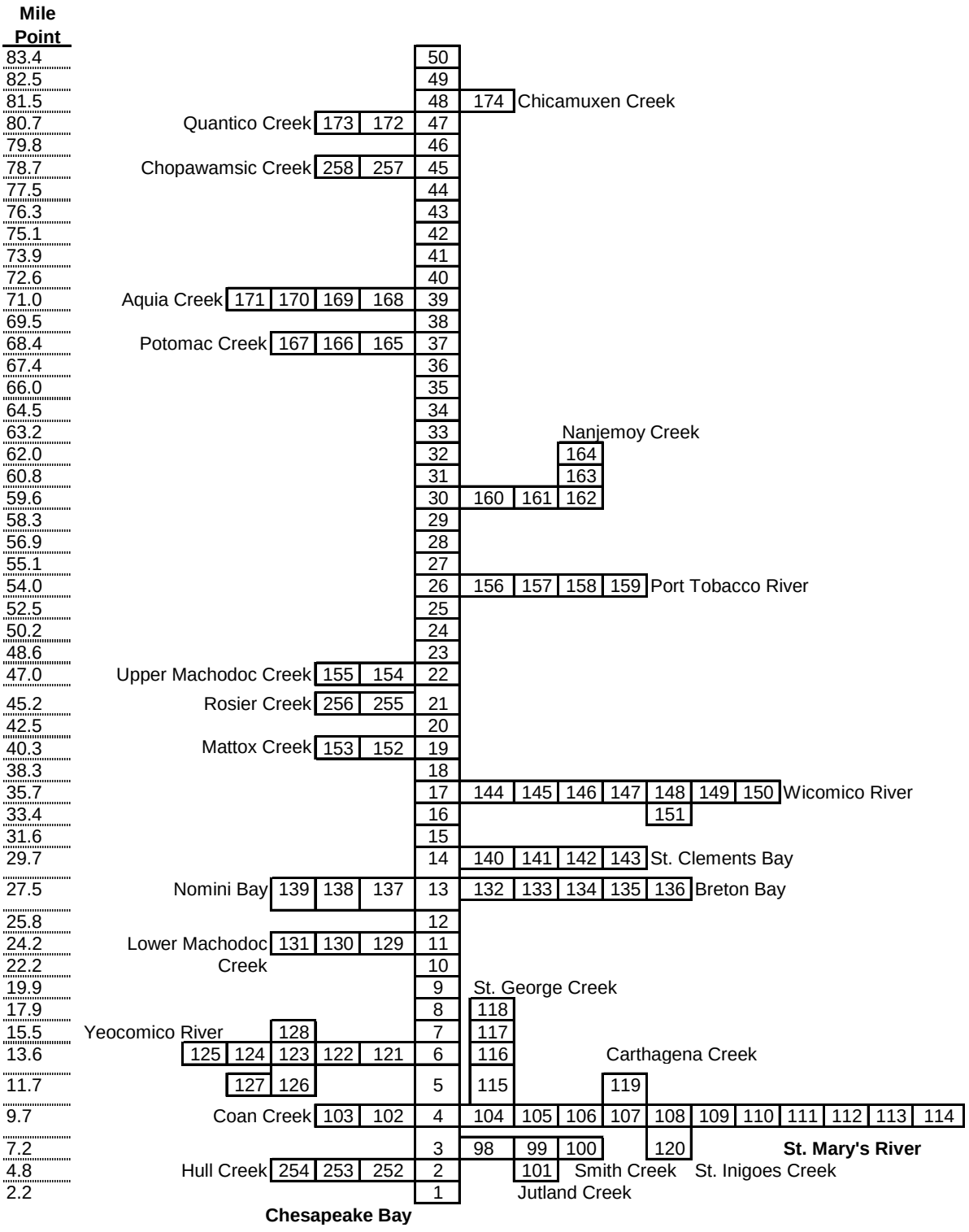

Figure 14. Potomac Estuary DYNHYD5 Model Junction Schematic (continued)

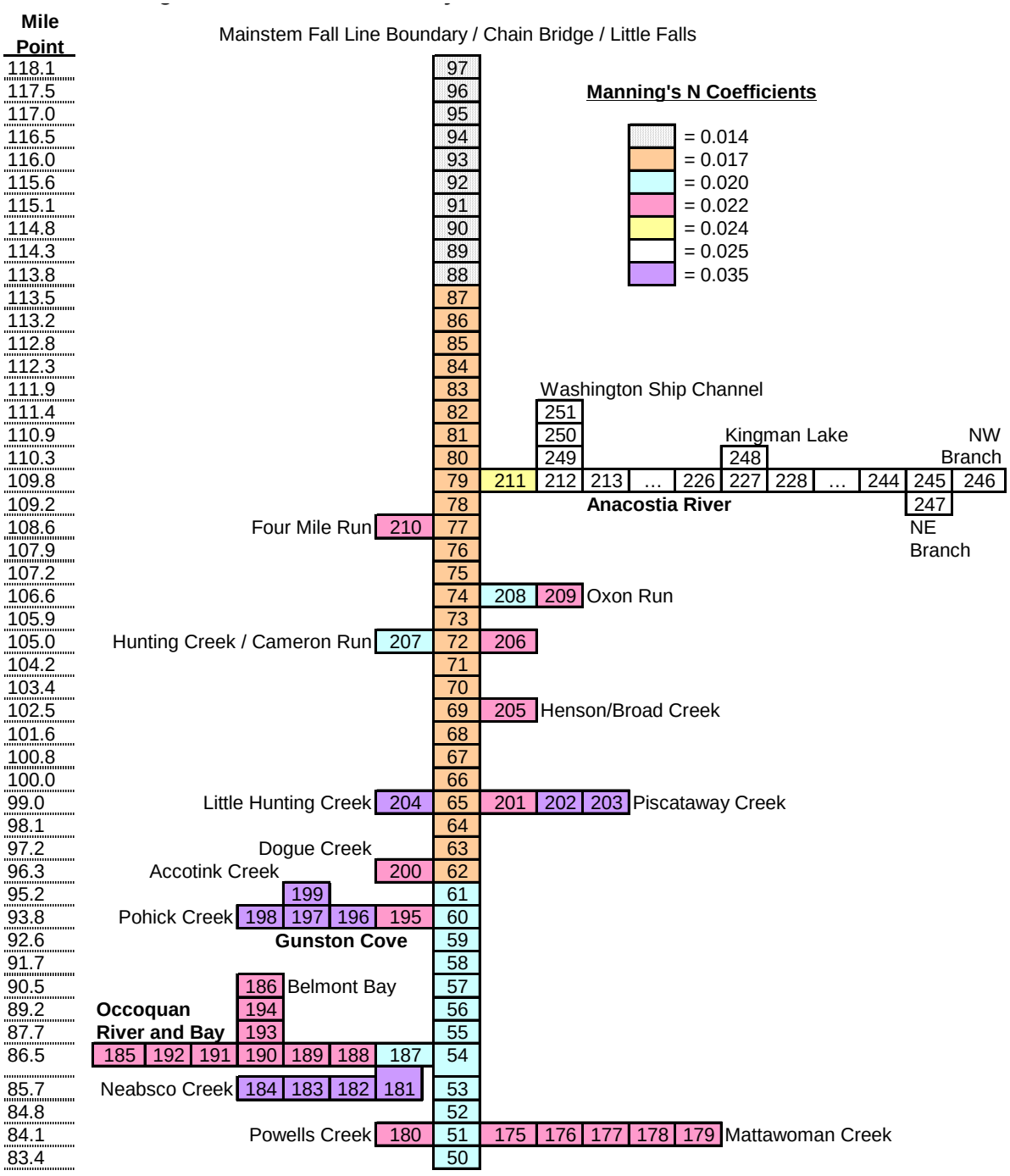

Figure 15. Potomac Estuary DYNHYD5 Manning's N Assignments

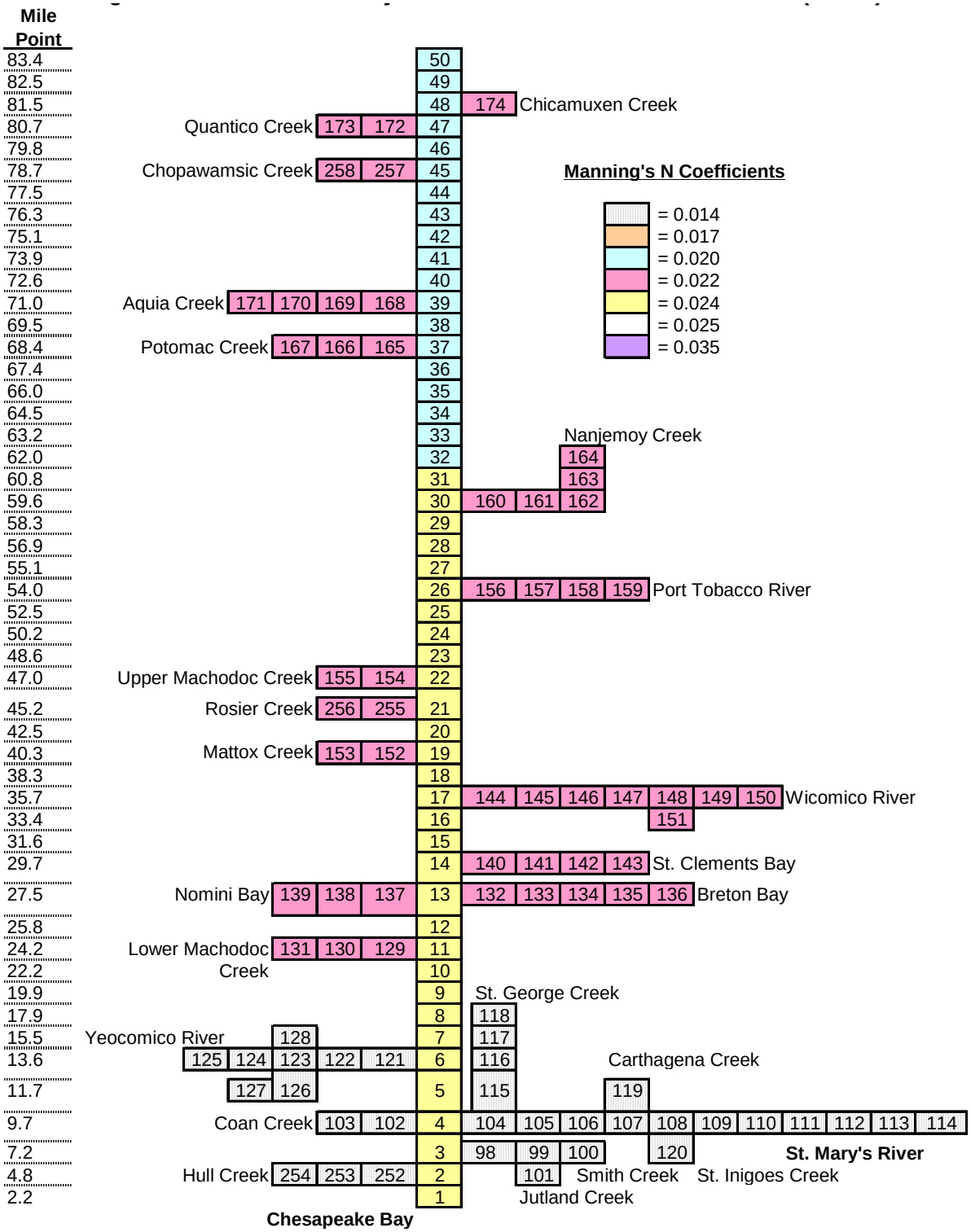

Figure 15. Potomac Estuary DYNHYD5 Manning's N Assignments (continued)

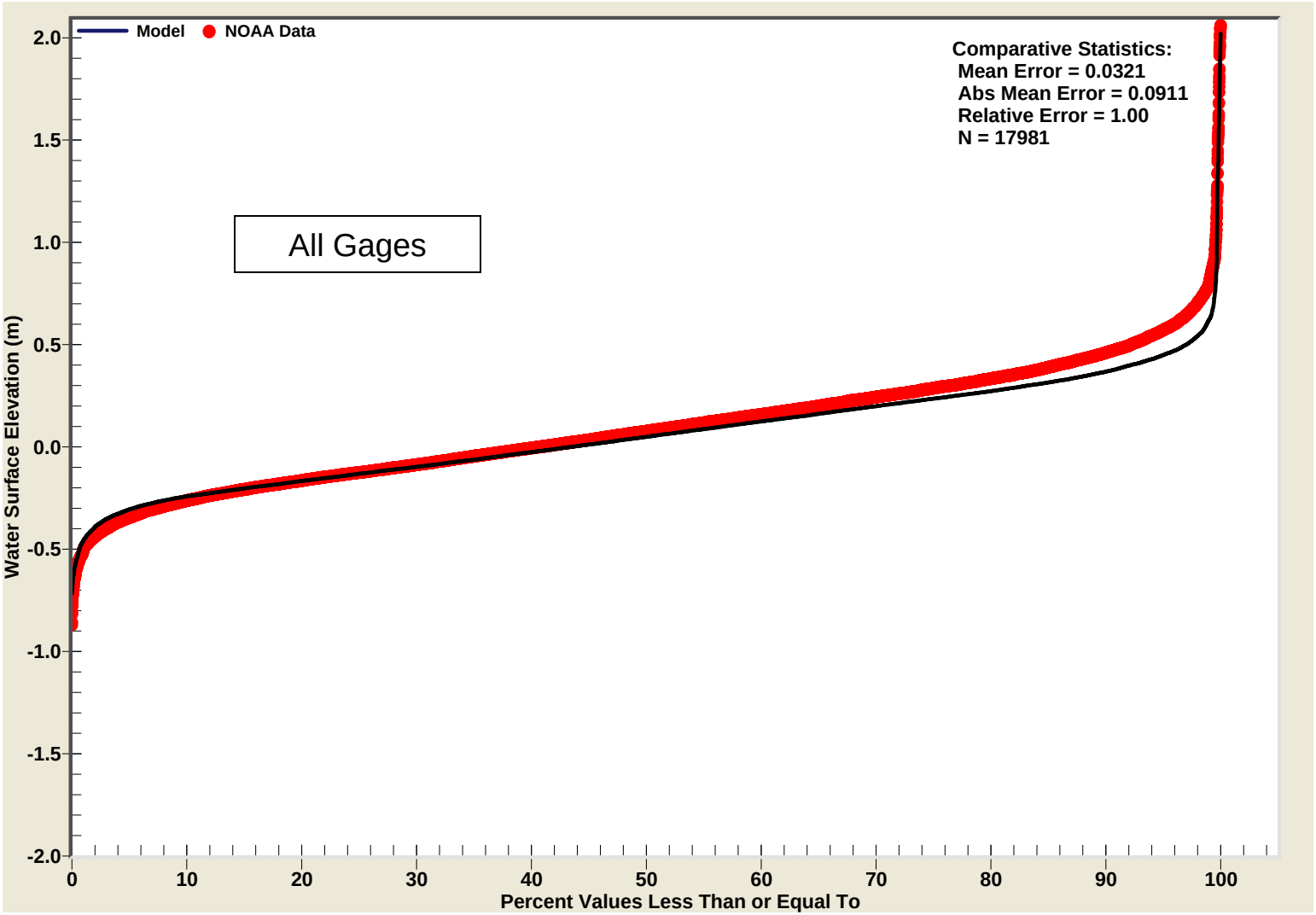

Figure 16. CFD for Computed and Observed Hourly WSE at All Gage Locations (1996-1997)

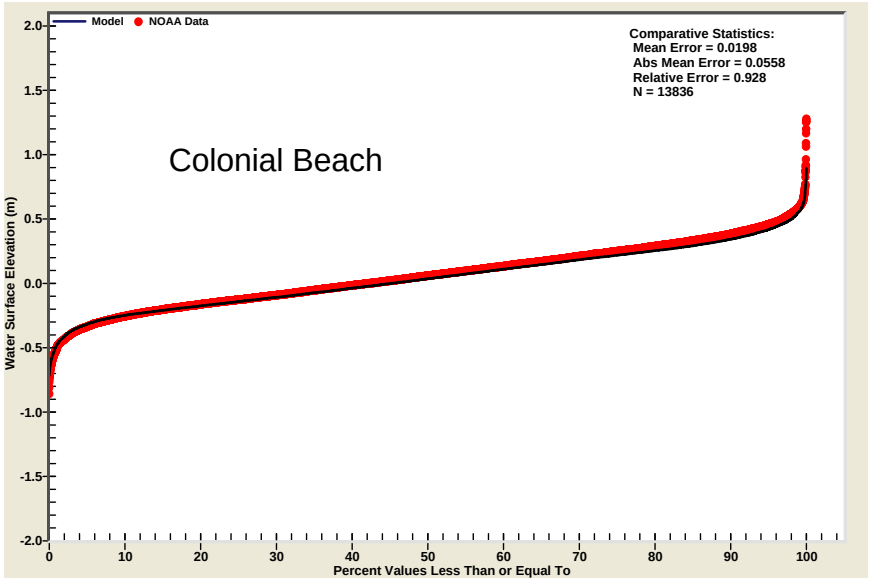

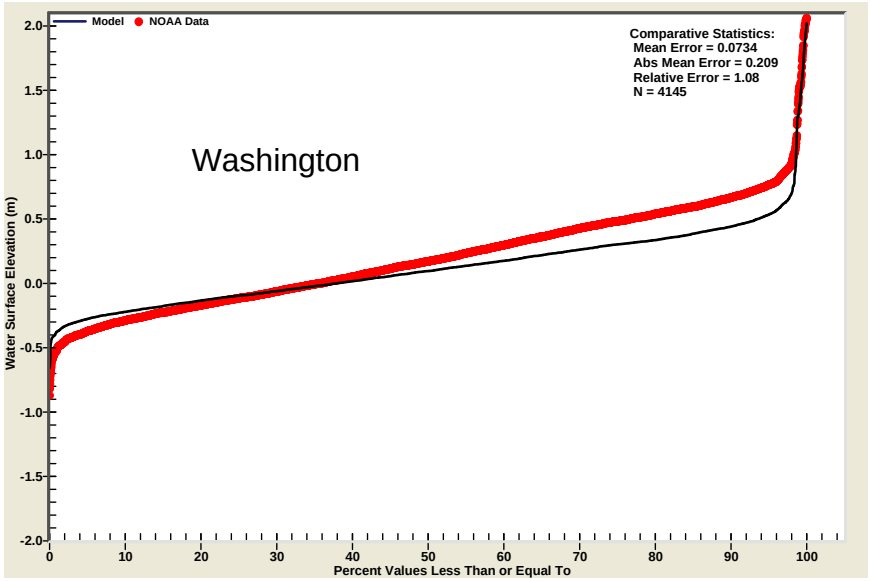

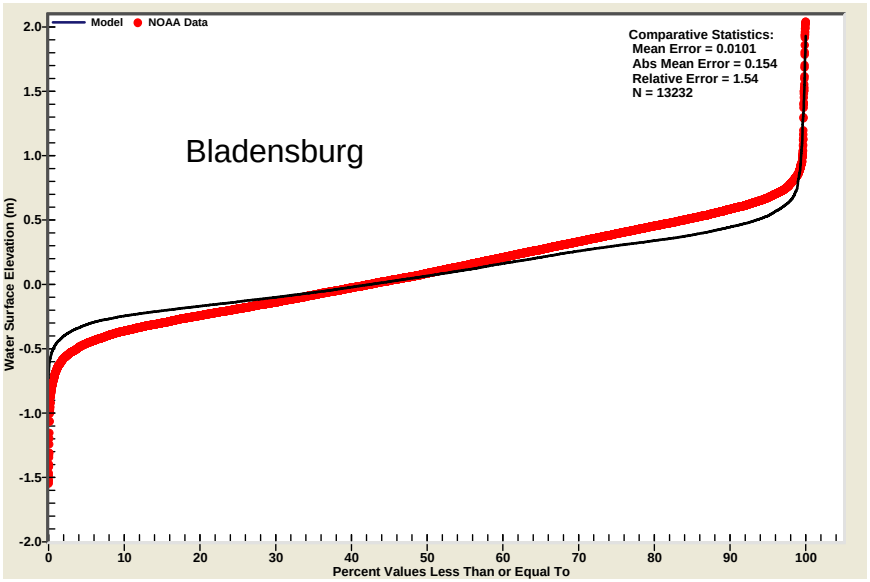

Figure 17. CFDs for Computed and Observed Hourly WSE at Individual Gage Locations (1996-1997)

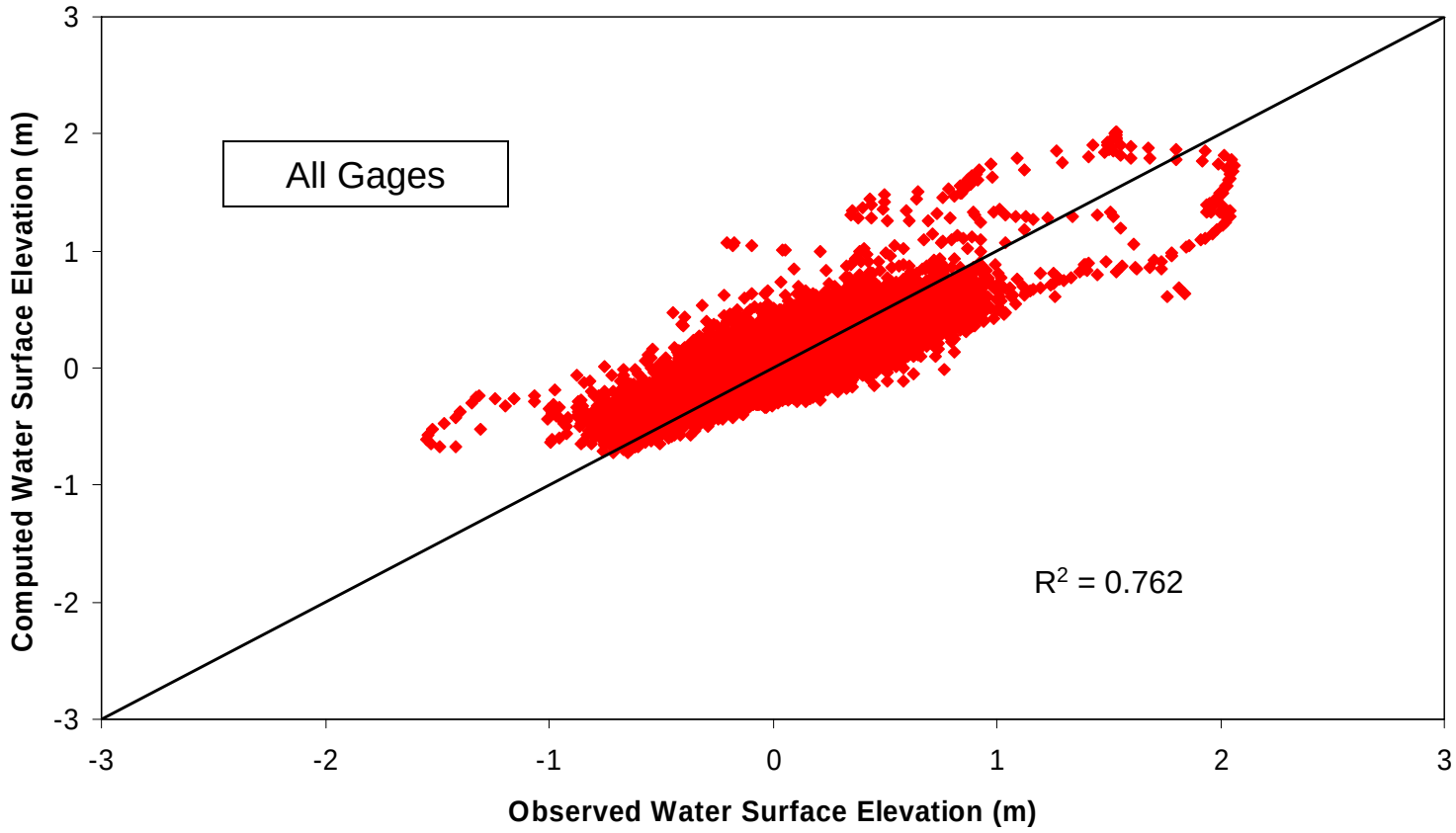

Figure 18. Bivariate Plot and Regression for Computed versus Observed Hourly WSE at All Gage Locations (1996-1997)

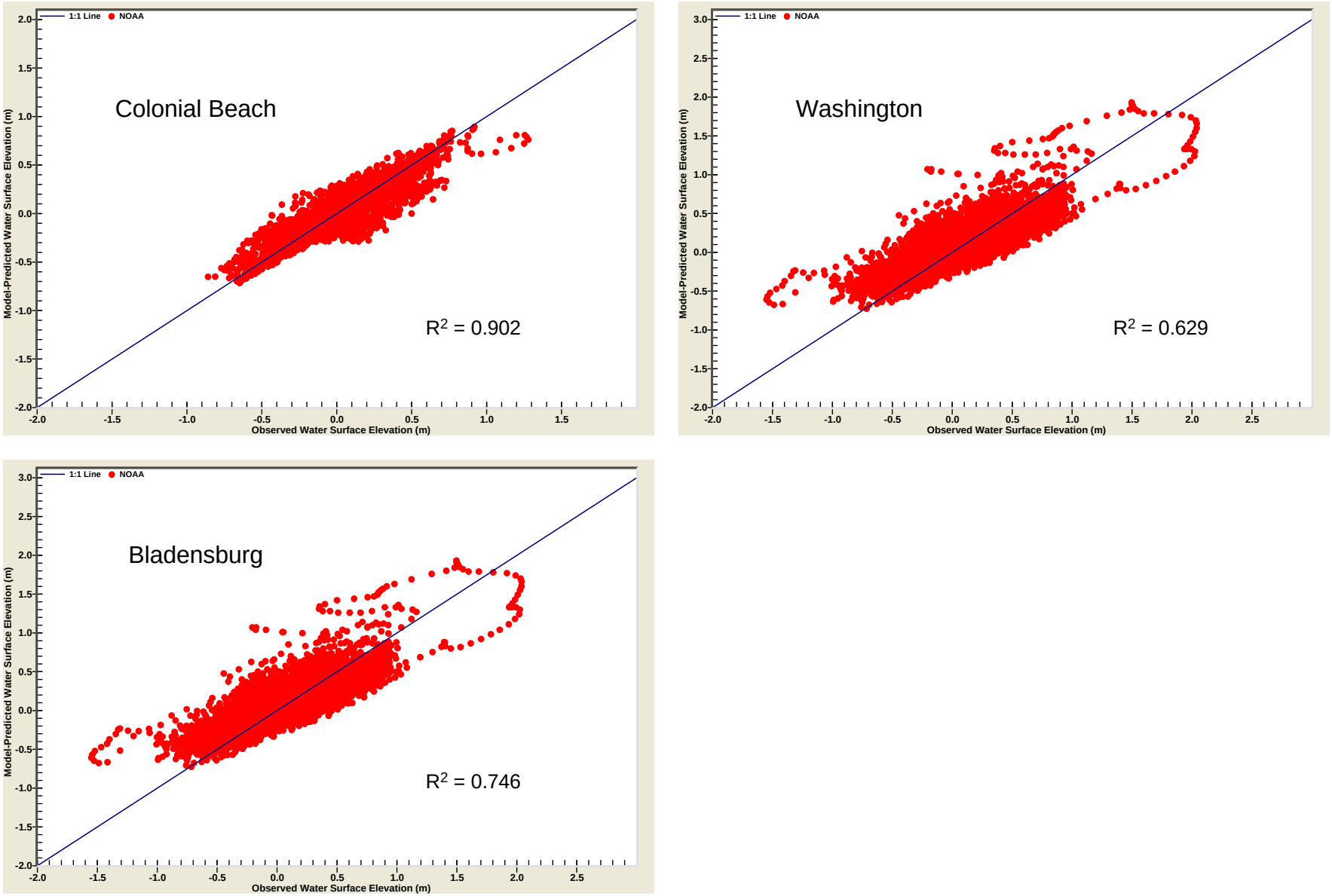

Figure 19. Bivariate Plots and Regressions for Computed versus Observed Hourly WSE at Individual Gage Locations (1996-1997)

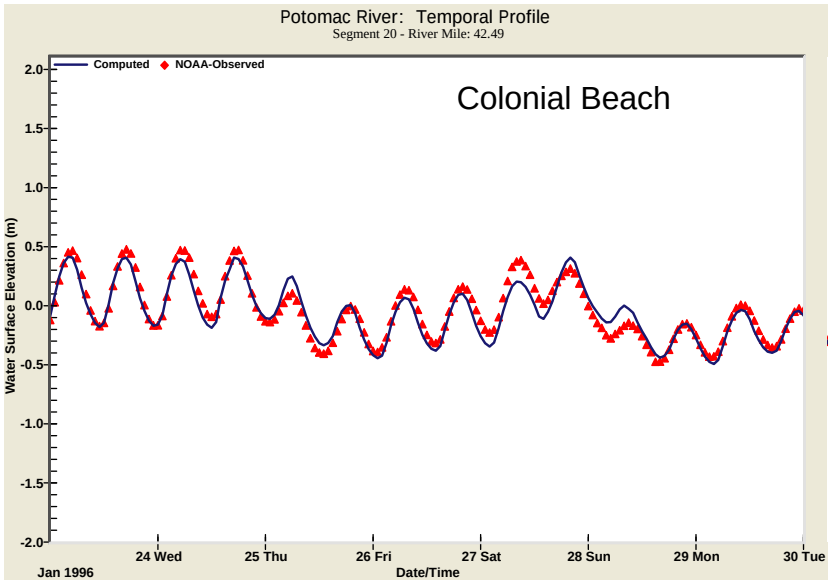

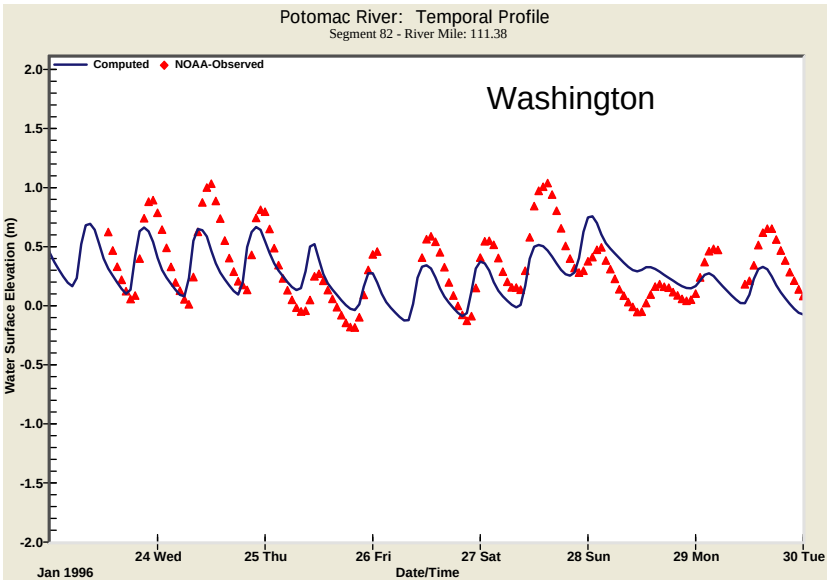

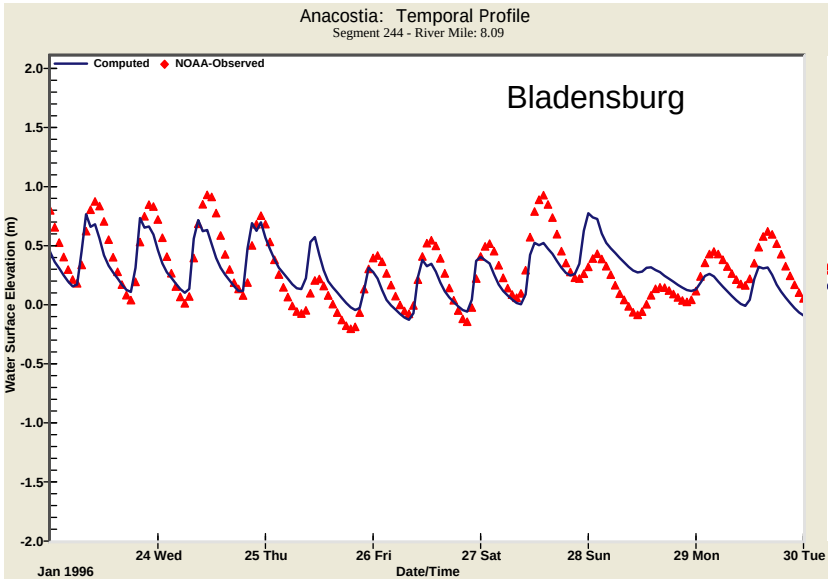

January 24-30, 1996

70,200 cfs at Little Falls

Figure 20. Comparisons Between Computed and Observed Hourly WSE for a High Flow Period (1996-1997)

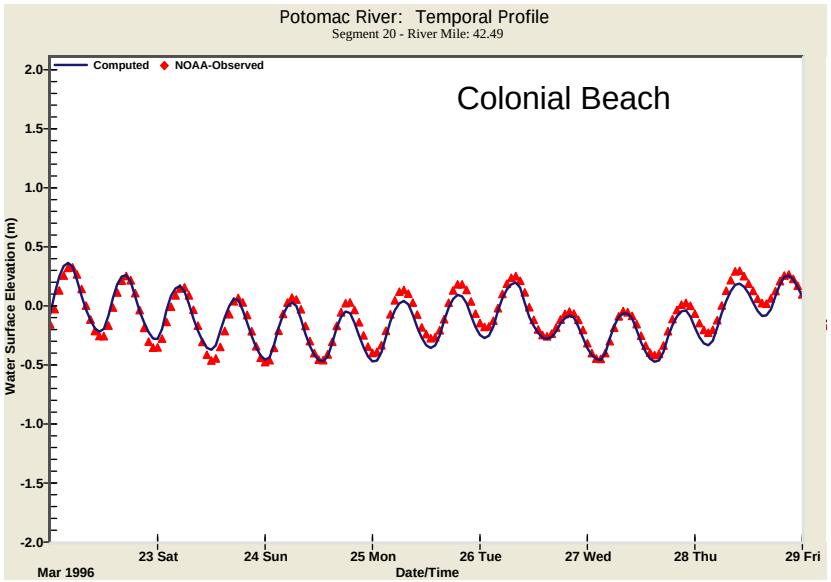

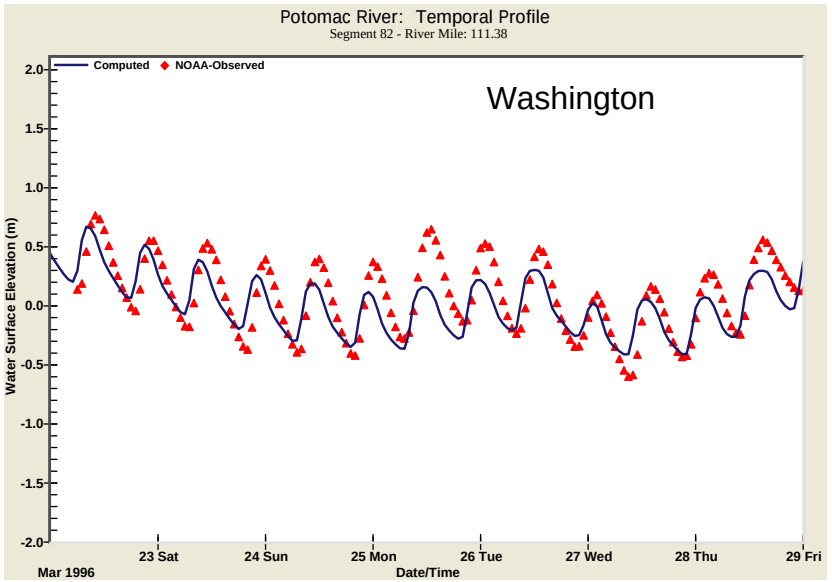

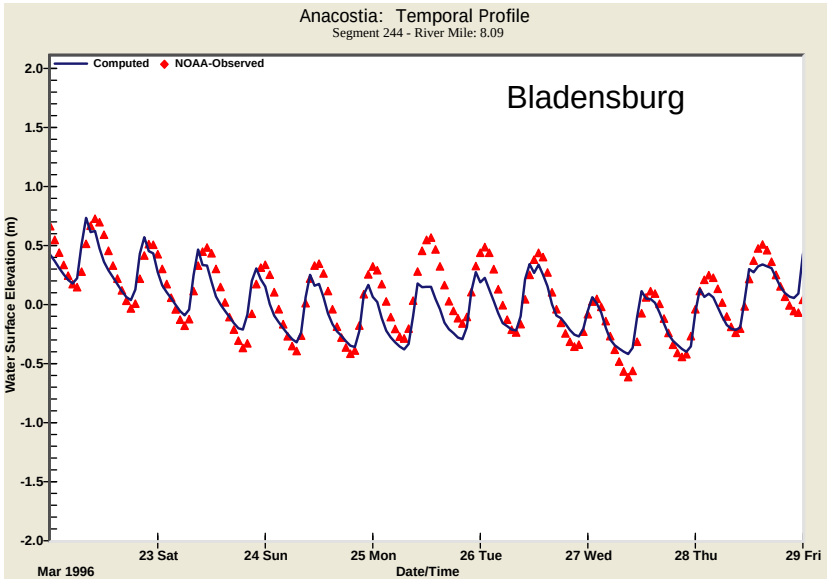

March 23-29, 1996

38,600 cfs at Little Falls

Figure 21. Comparisons Between Computed and Observed Hourly WSE for a Moderate Flow Period (1996-1997)

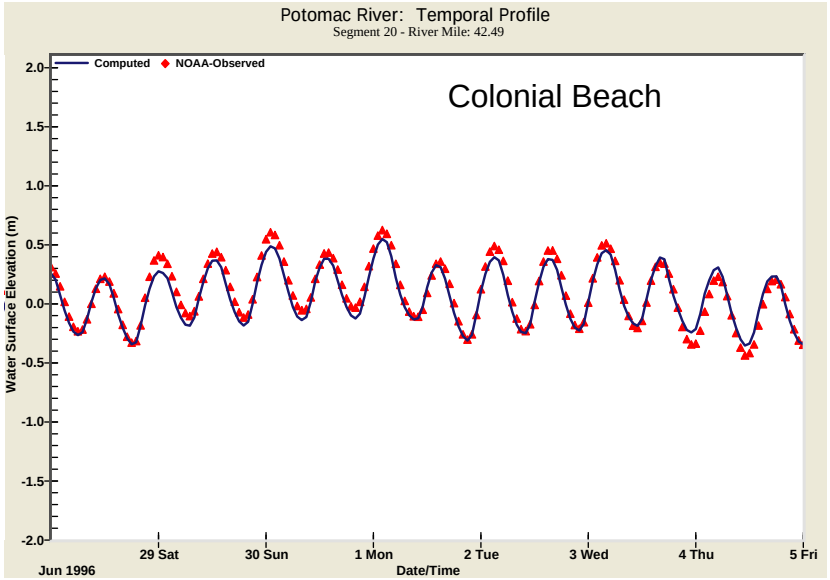

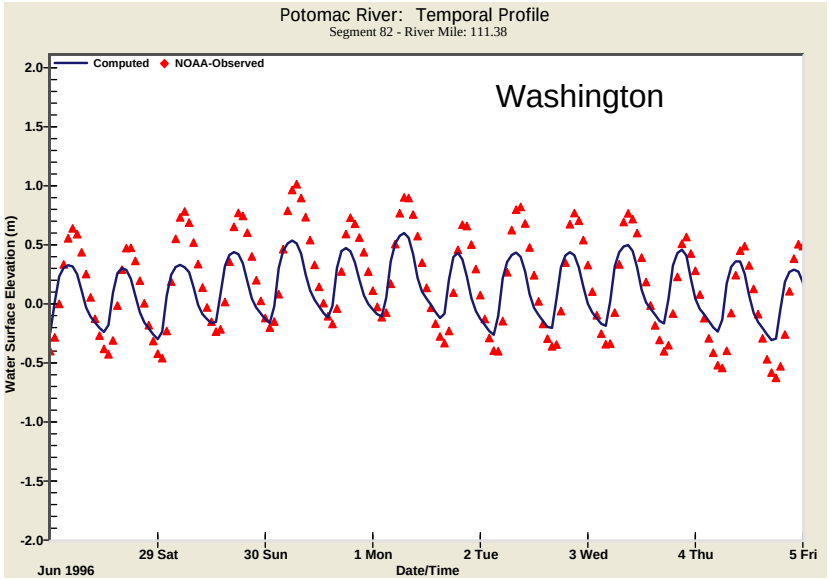

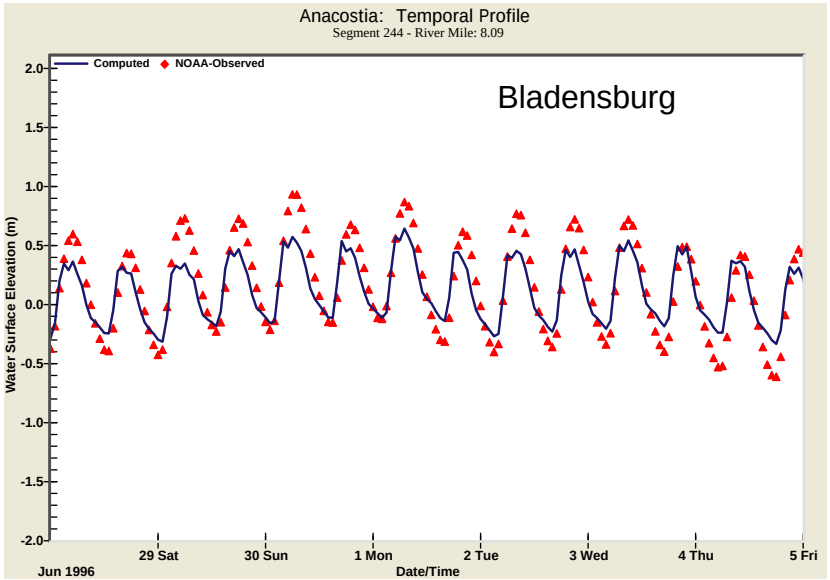

June 29 - July 5, 1996

10,800 cfs at Little Falls

Figure 22. Comparisons Between Computed and Observed Hourly WSE for a Low Flow Period (1996-1997)

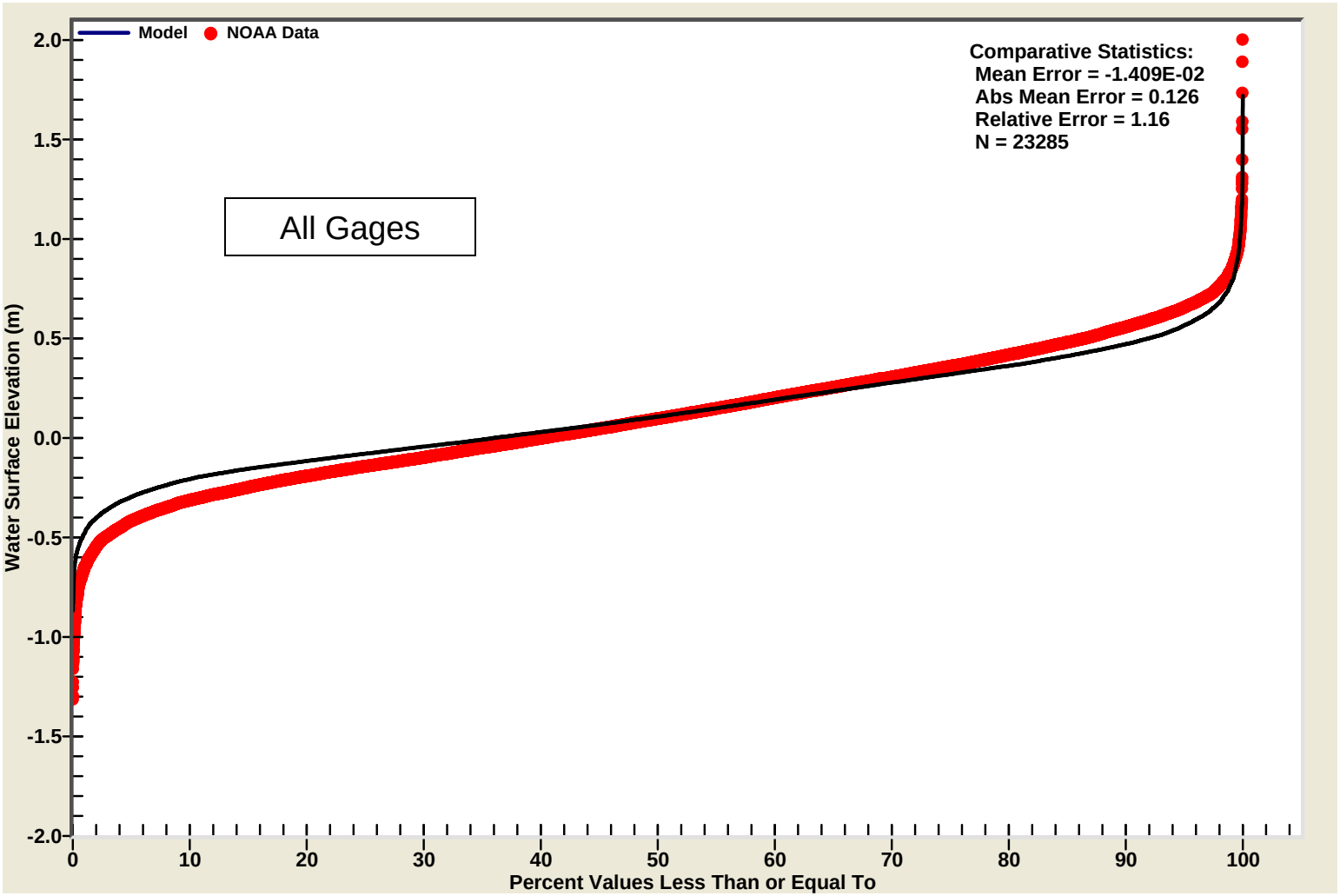

Figure 23. CFD for Computed and Observed Hourly WSE at All Gage Locations (2002-2005)

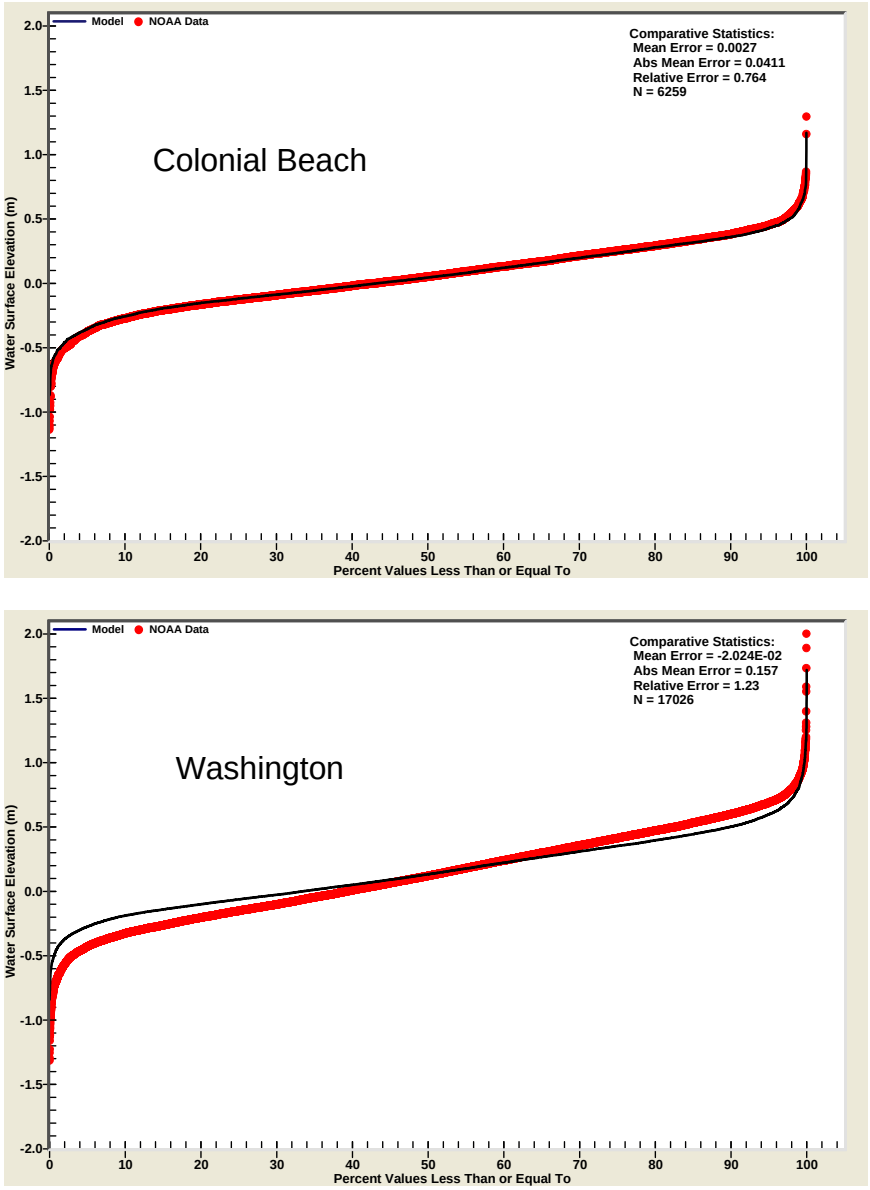

Figure 24. CFDs for Computed and Observed Hourly WSE at Individual Gage Locations (2002-2005)

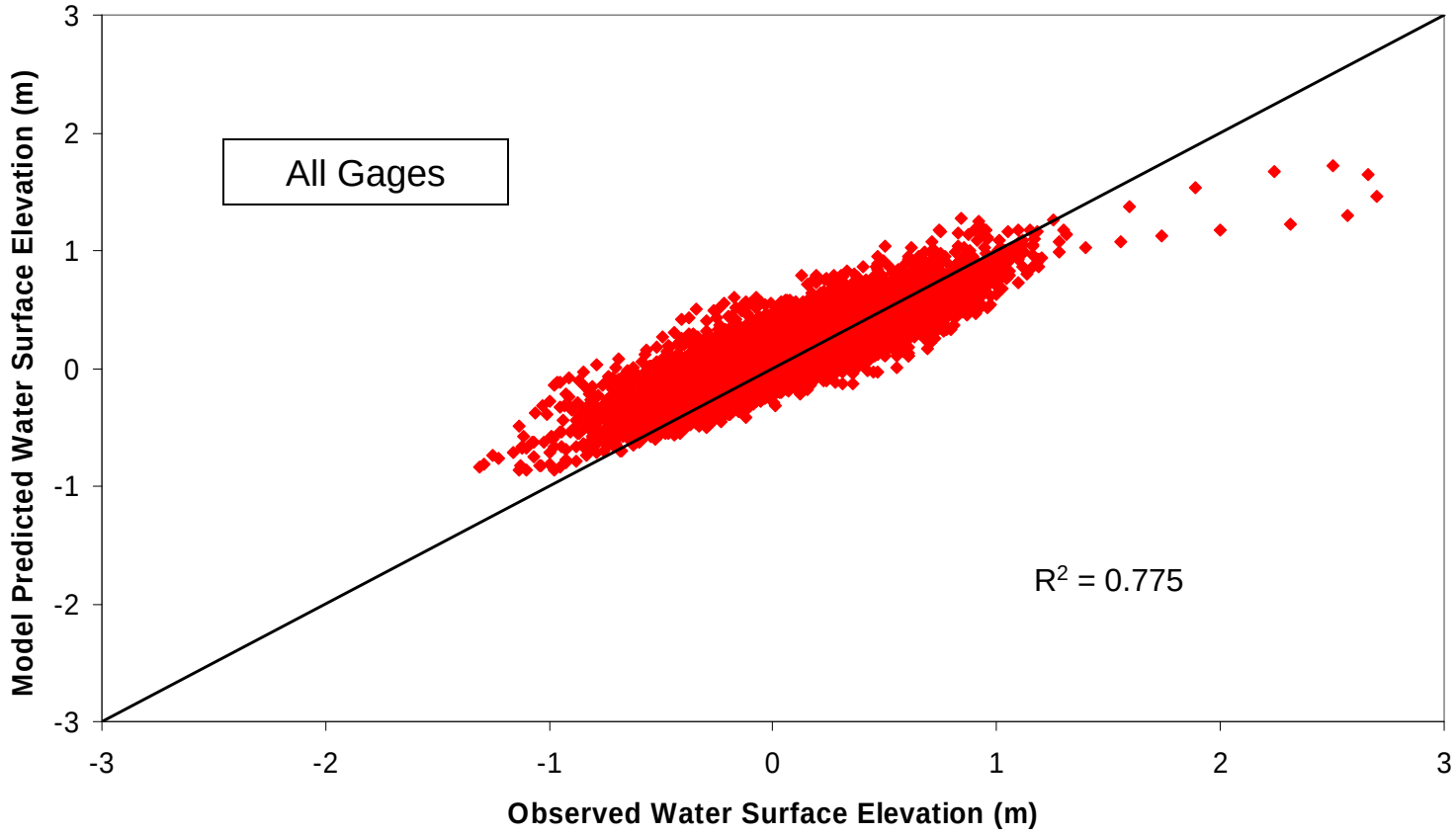

Figure 25. Bivariate Plot and Regression for Computed versus Observed Hourly WSE at Both Gage Locations (2002-2005)

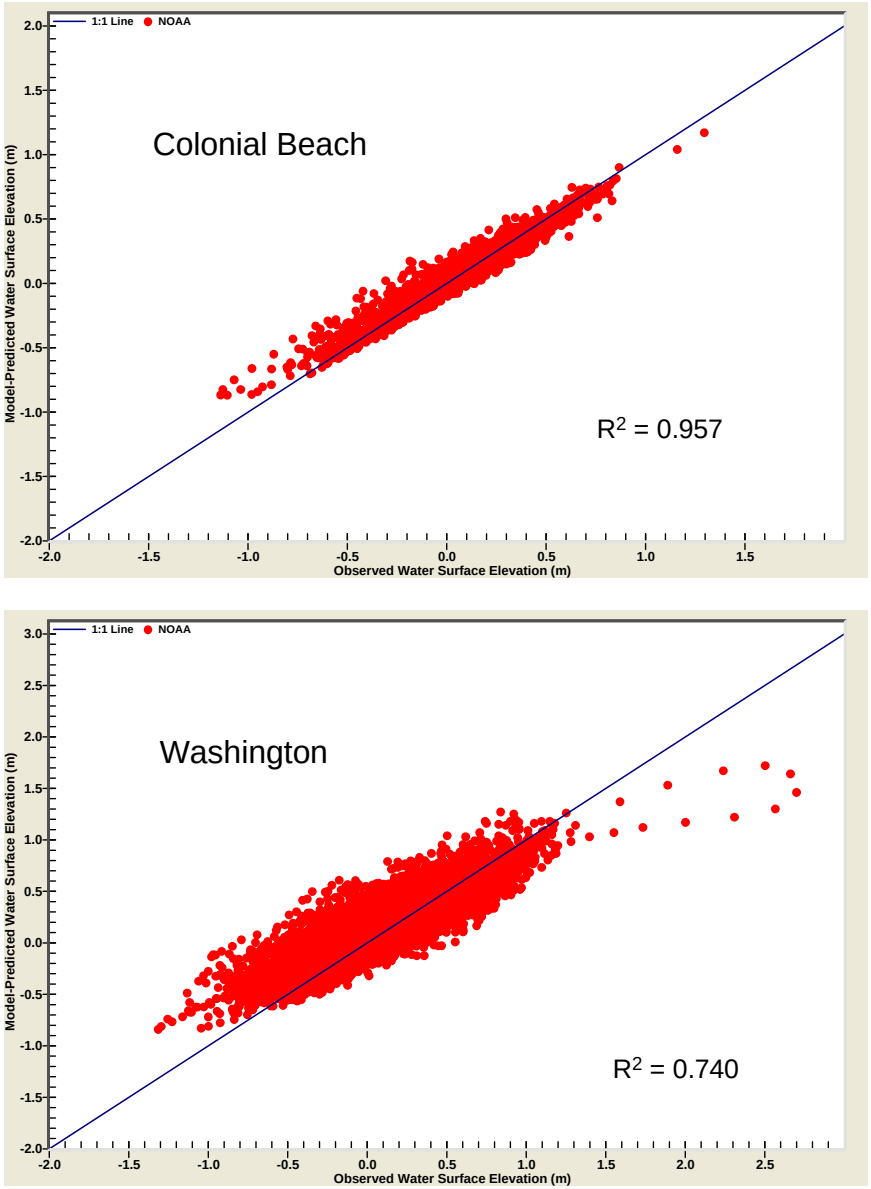

Figure 26. Bivariate Plots for Computed versus Observed Hourly WSE at Individual Gage Locations (2002-2005)

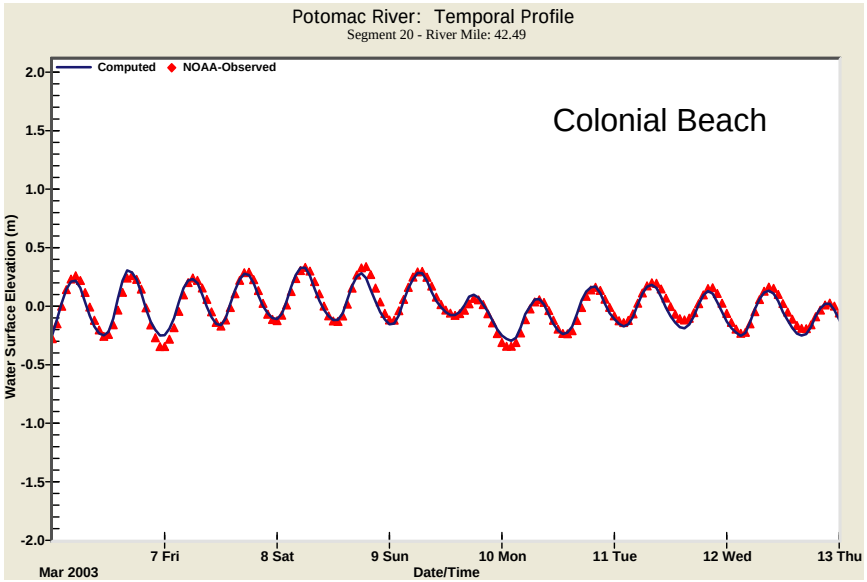

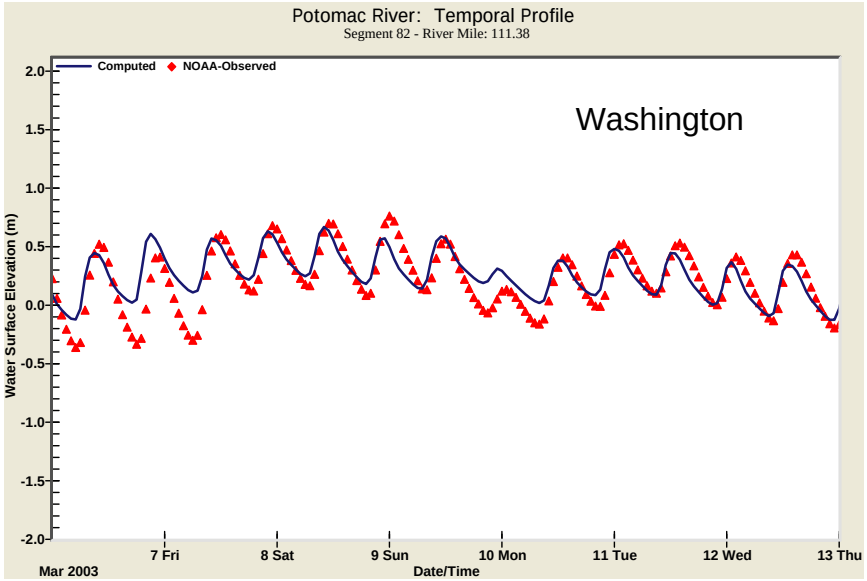

March 7-13, 2003

66,900 cfs at Little Falls

Figure 27. Comparisons Between Computed and Observed Hourly WSE for a High Flow Period (2002-2005)

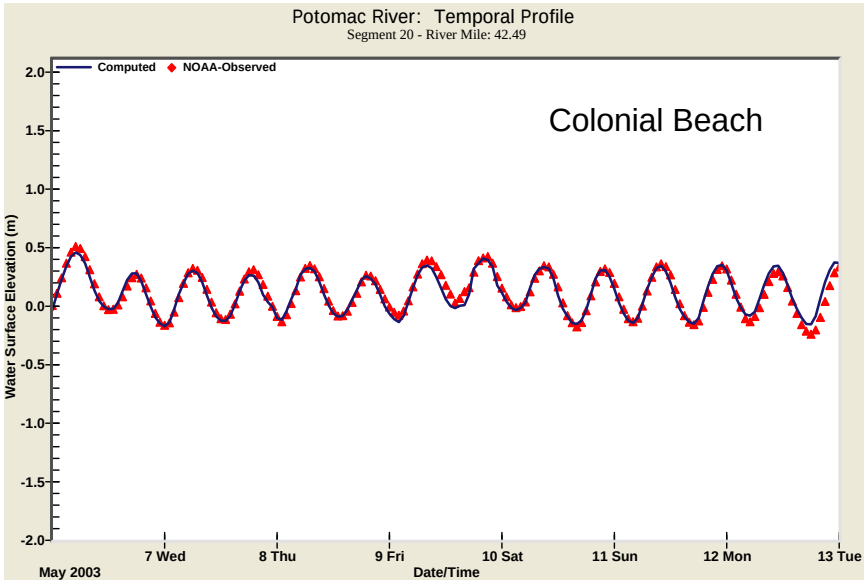

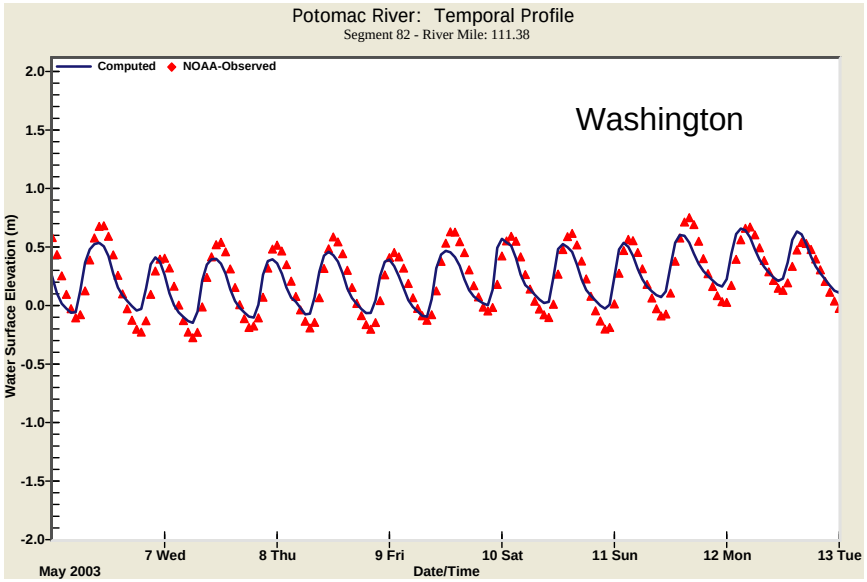

May 7-13, 2003

38,300 cfs at Little Falls

Figure 28. Comparisons Between Computed and Observed Hourly WSE for a Moderate Flow Period (2002-2005)

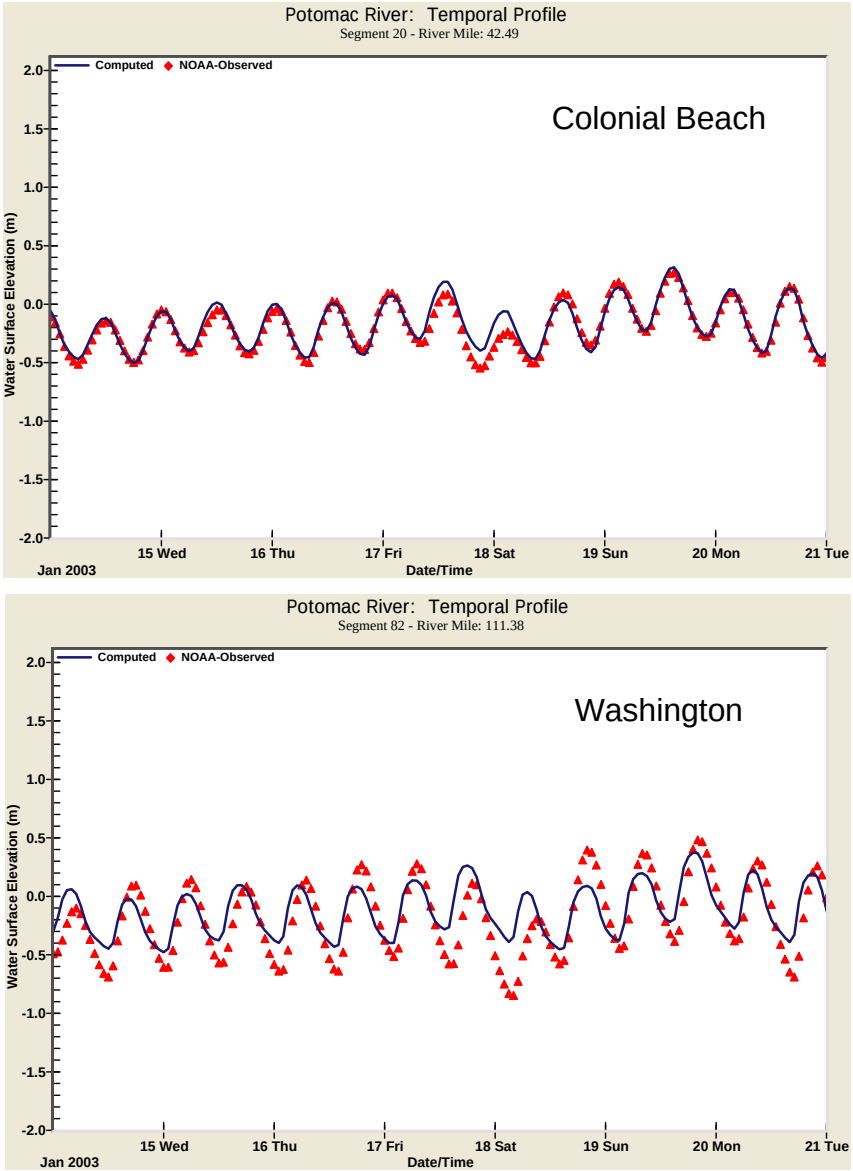

January 15-21, 2003

10,200 cfs at Little Falls

Figure 29. Comparisons Between Computed and Observed Hourly WSE for a Low Flow Period (2002-2005)

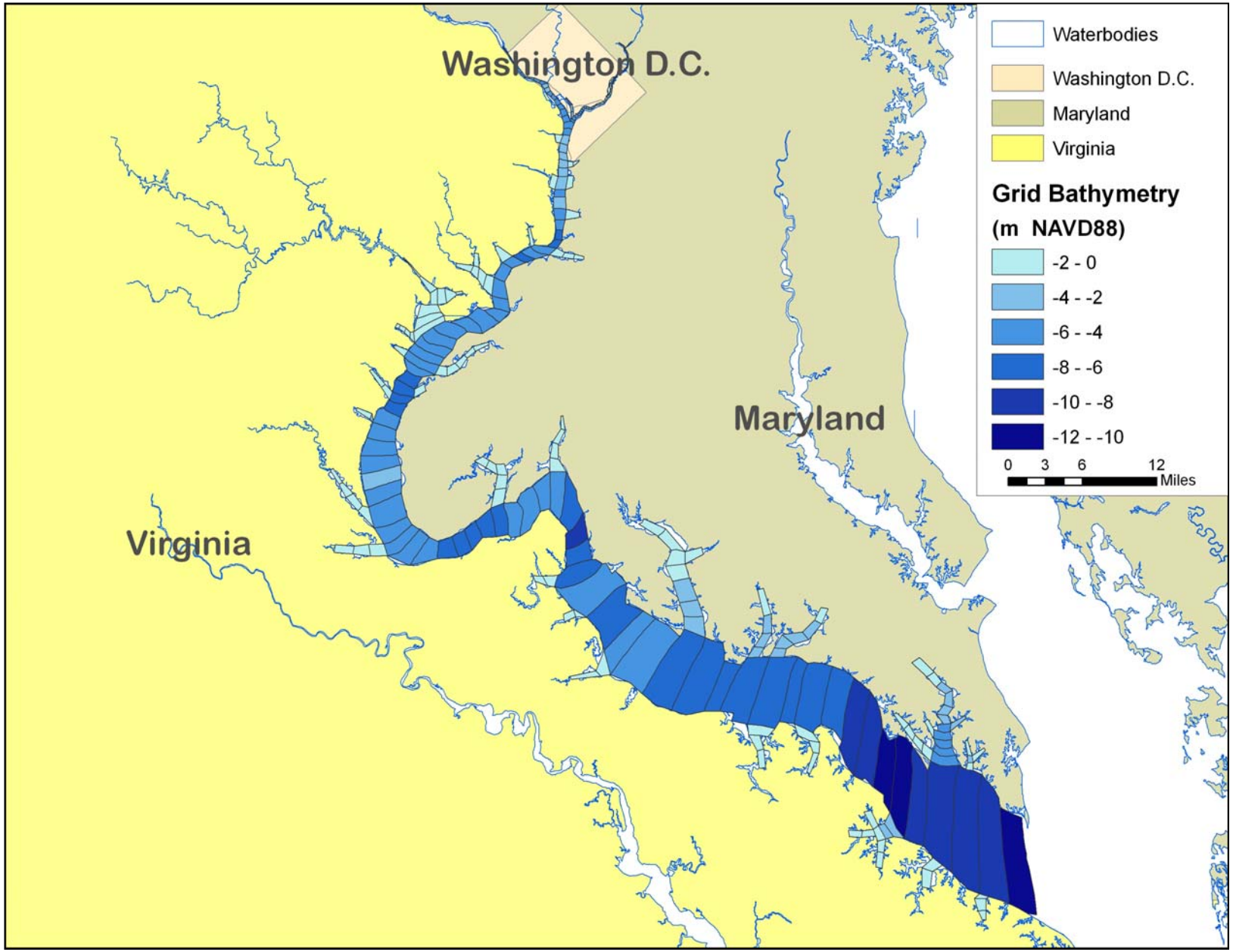

Figure 30. Model Spatial Grid for WASP5/TOXI5 Component of POTPCB

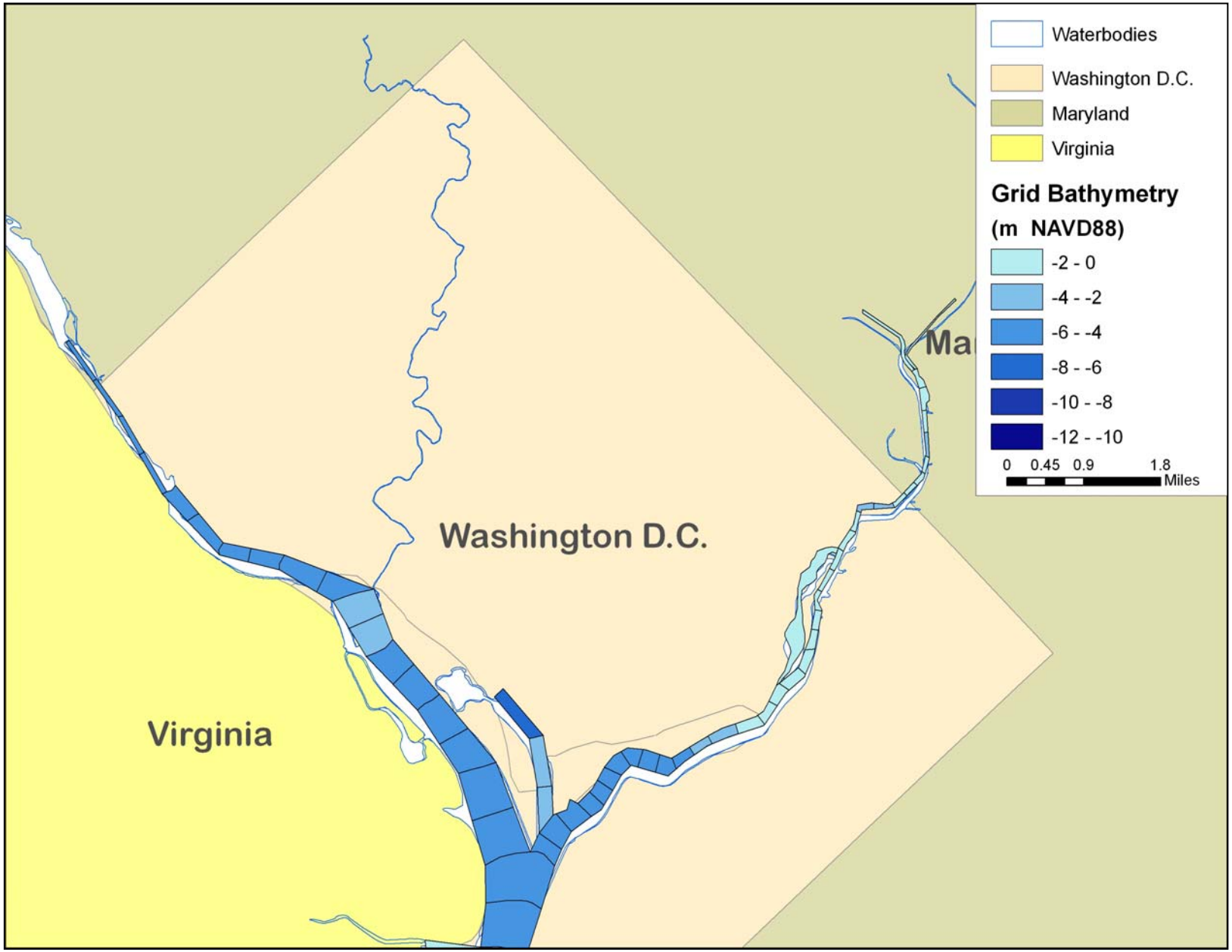

Figure 31. Model Spatial Grid for WASP5/TOXI5 Component of POTPCB (Washington DC)

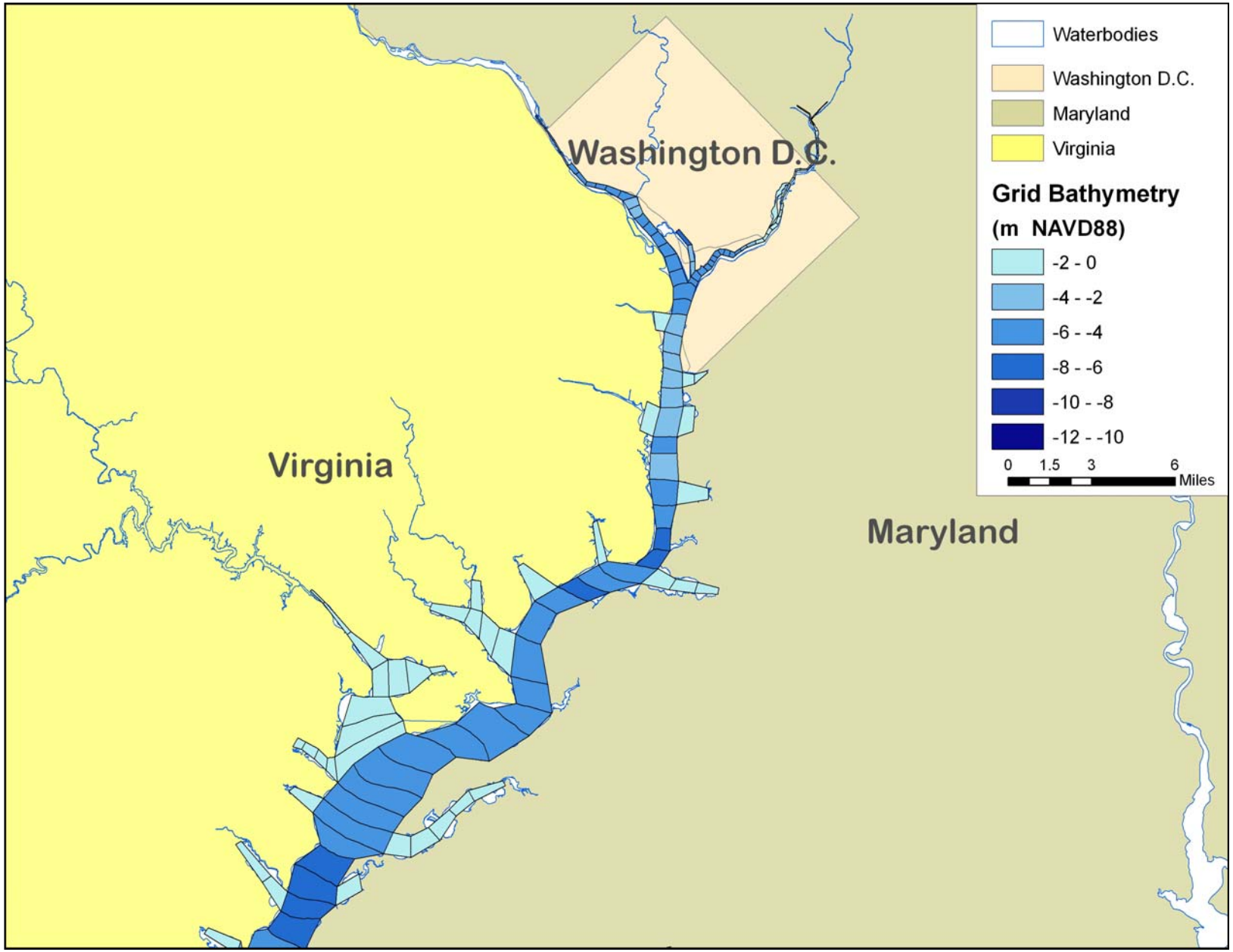

Figure 32. Model Spatial Grid for WASP5/TOXI5 Component of POTPCB (Upper Potomac)

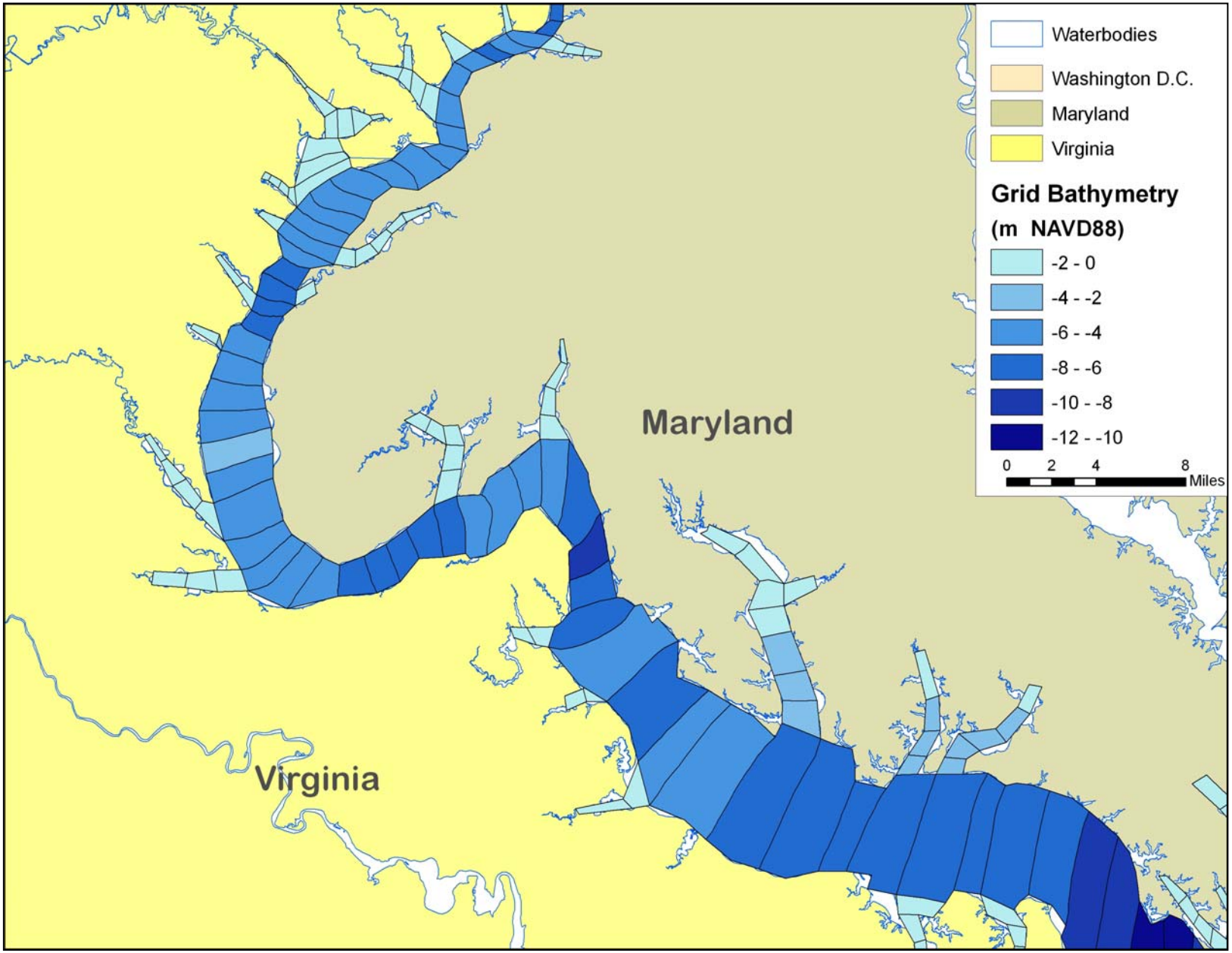

Figure 33. Model Spatial Grid for WASP5/TOXI5 Component of POTPCB (Middle Potomac)

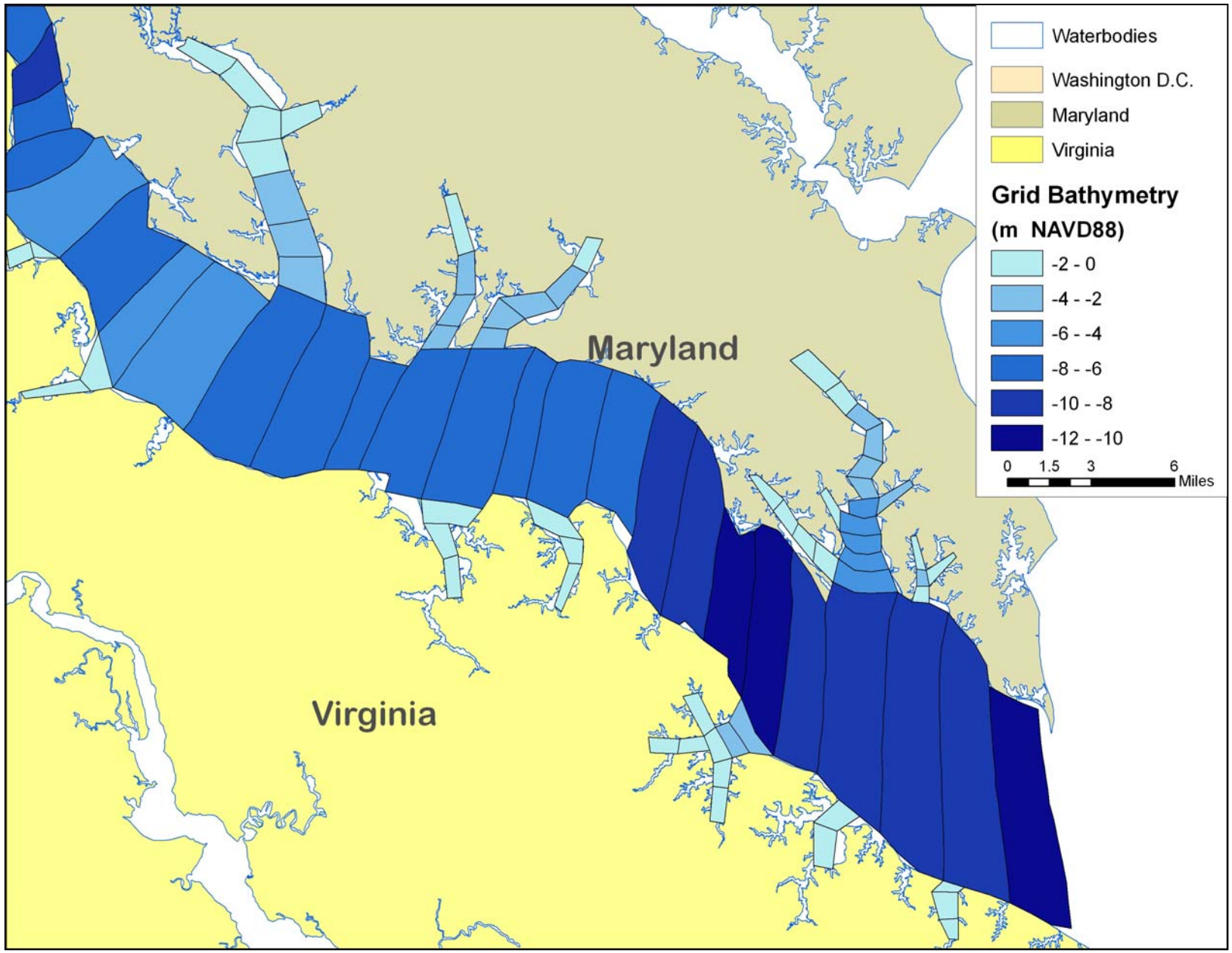

Figure 34. Model Spatial Grid for WASP5/TOXI5 Component of POTPCB (Lower Potomac)

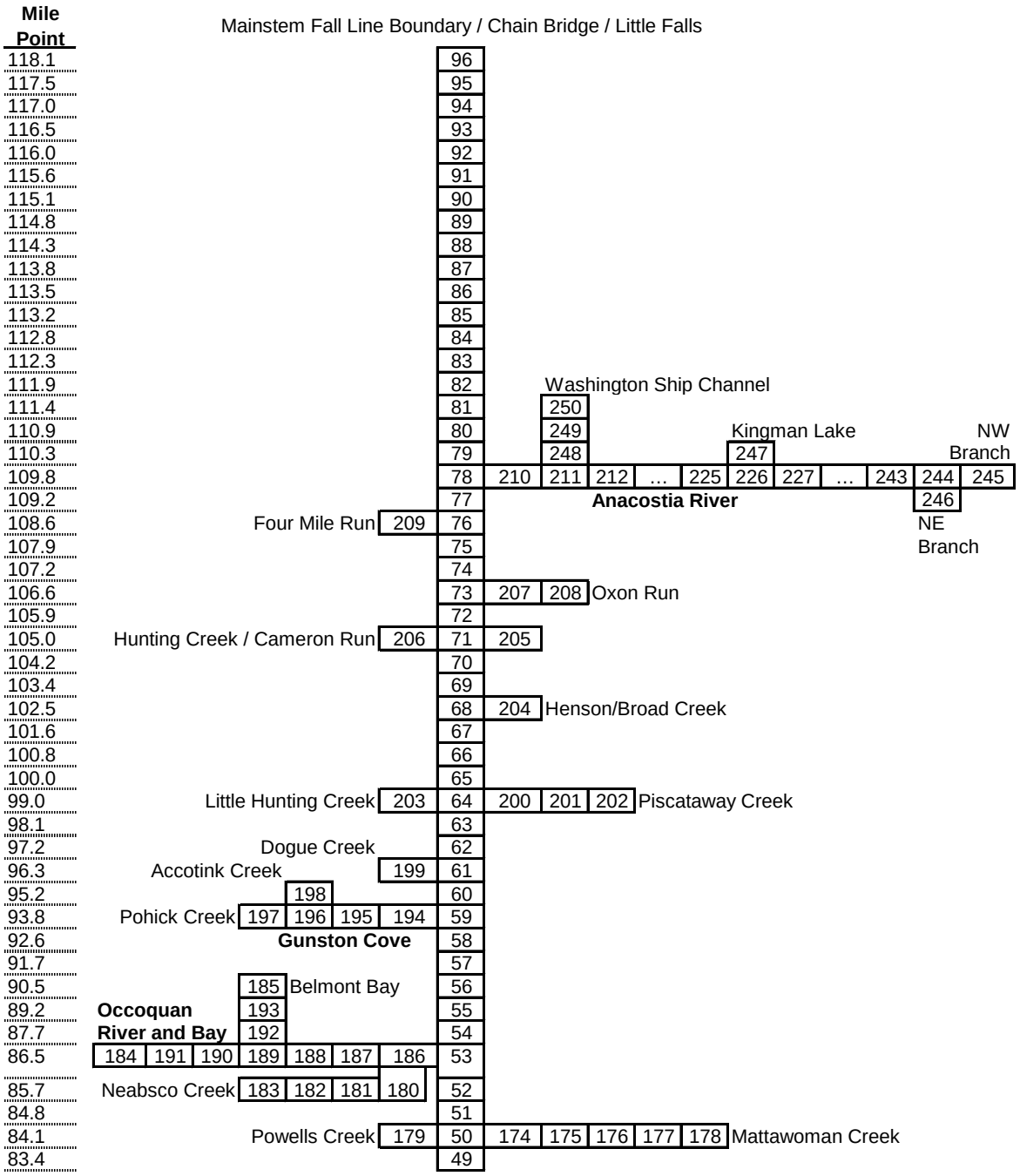

Figure 35. Potomac Estuary POTPCB Salinity Model Segment Schematic

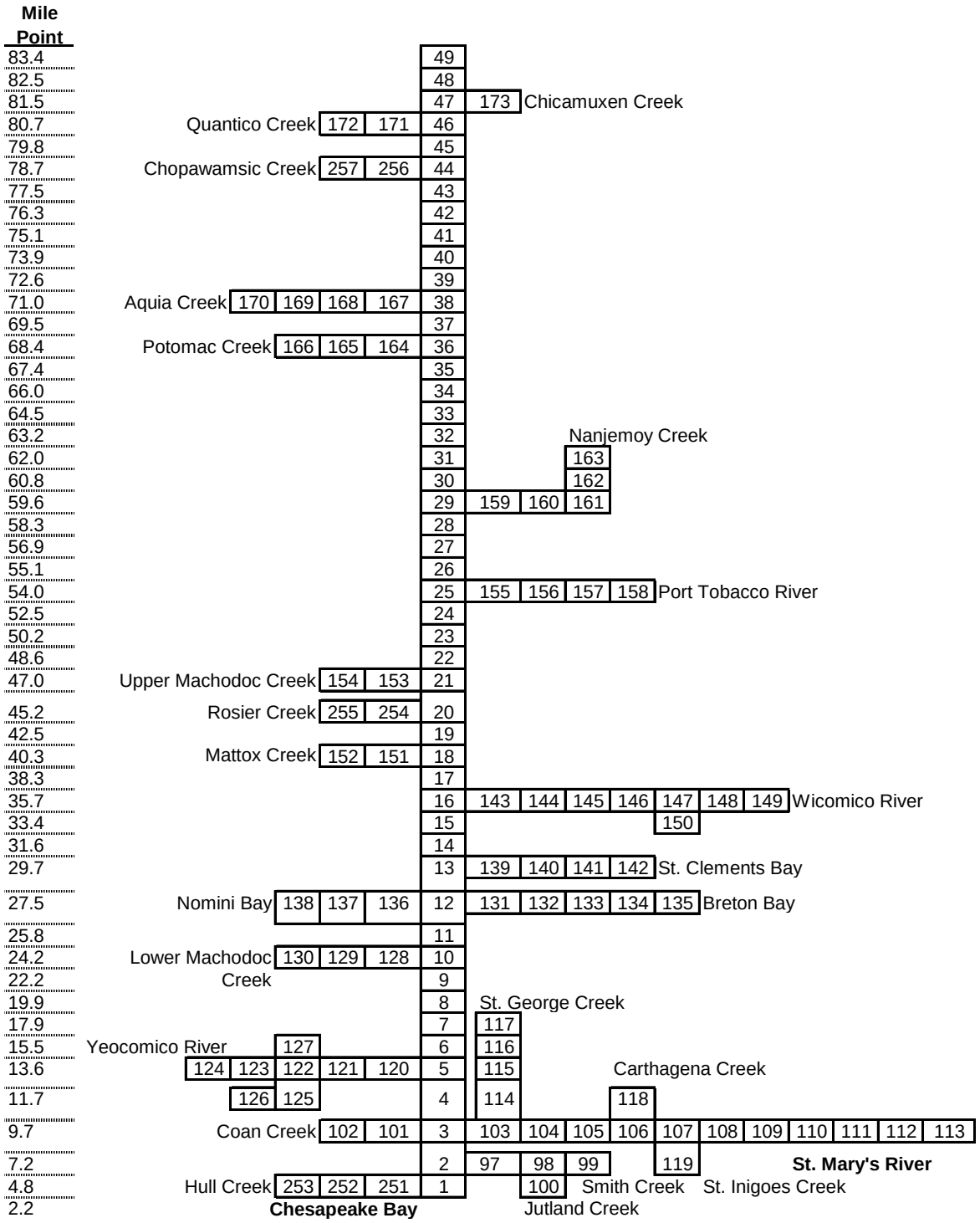

Figure 35. Potomac Estuary POTPCB Salinity Model Segment Schematic (continued)

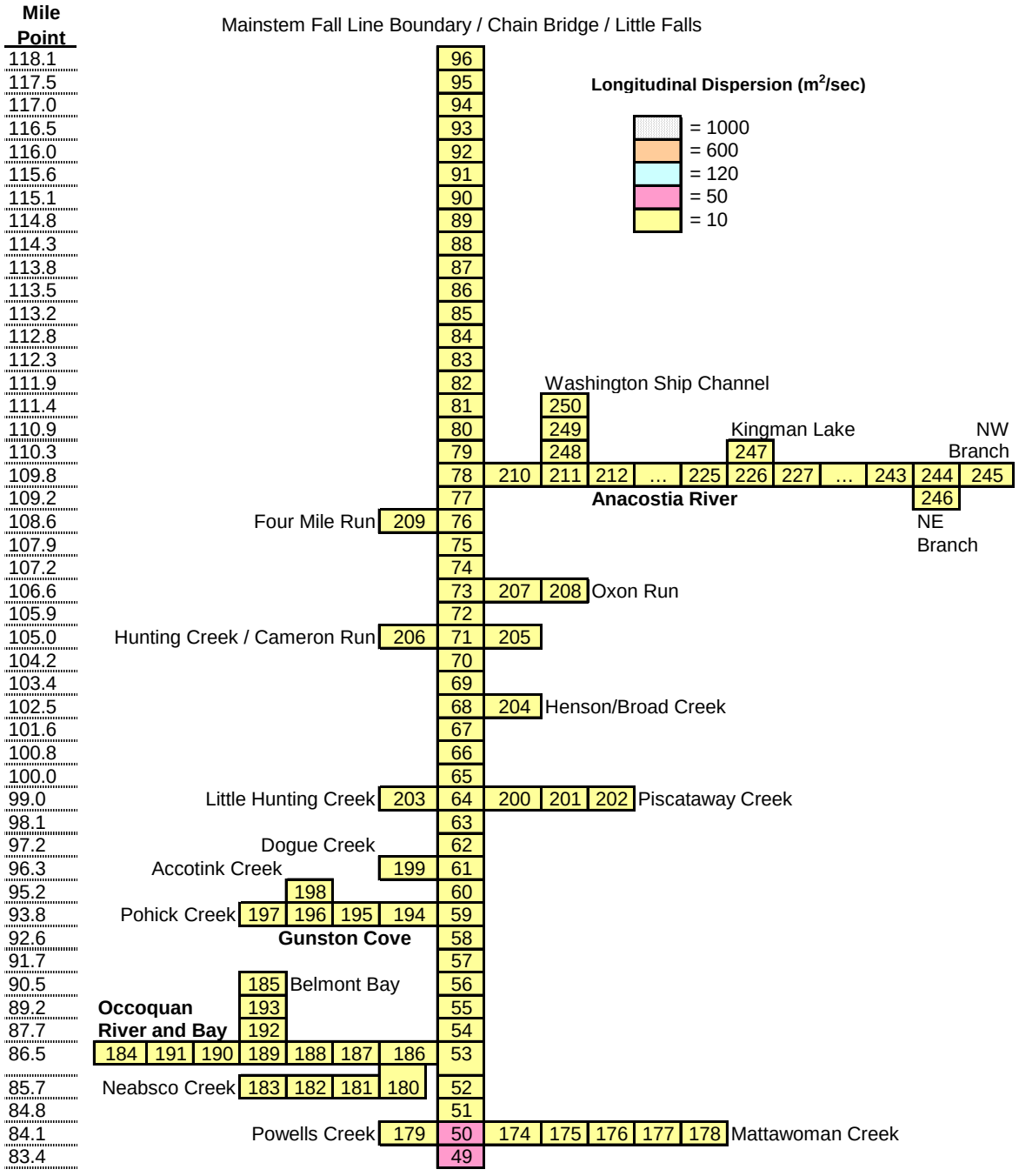

Figure 36. Potomac Estuary POTPCB Salinity Model Dispersion Coefficients

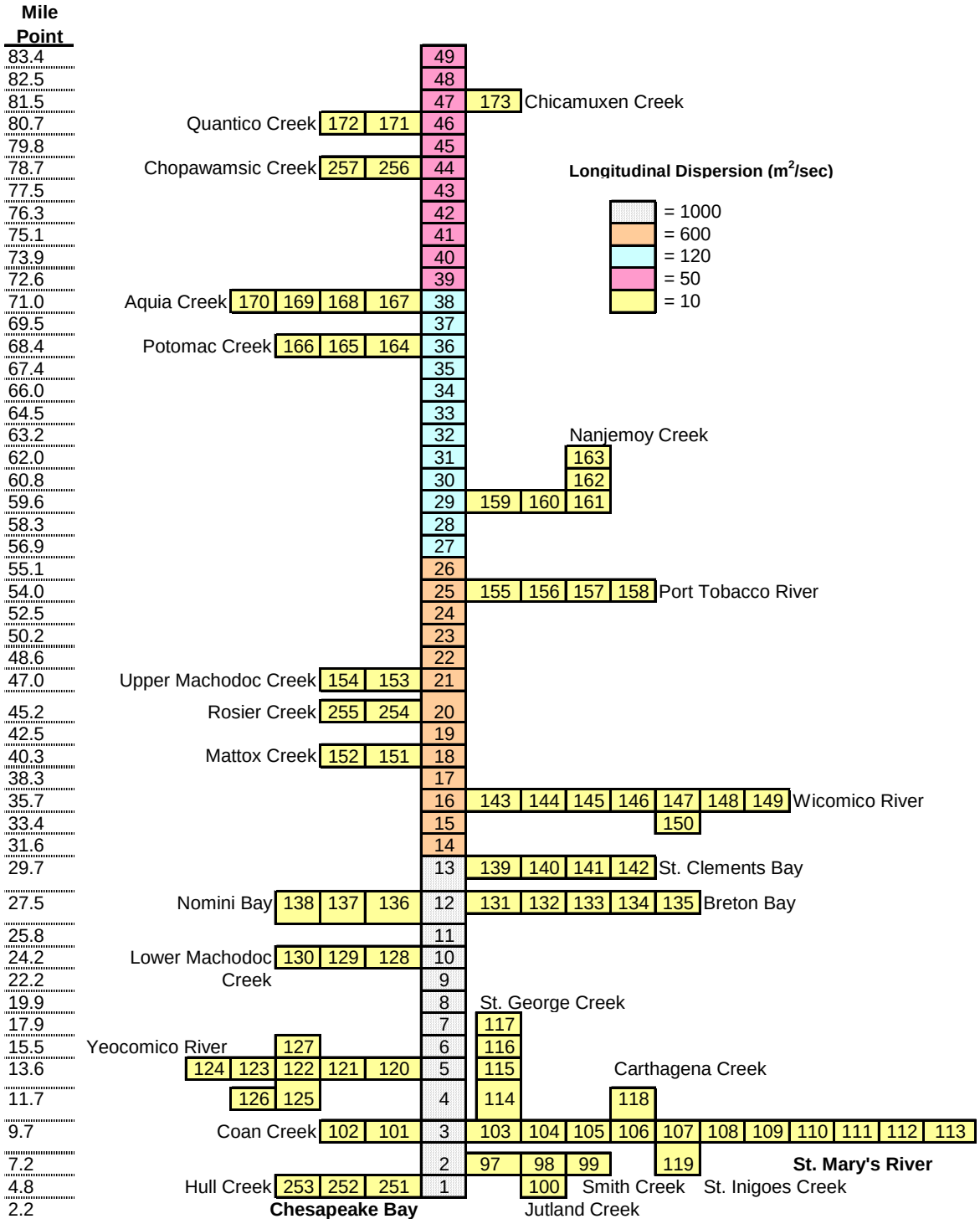

Figure 36. Potomac Estuary POTPCB Salinity Model Dispersion Coefficients (continued)

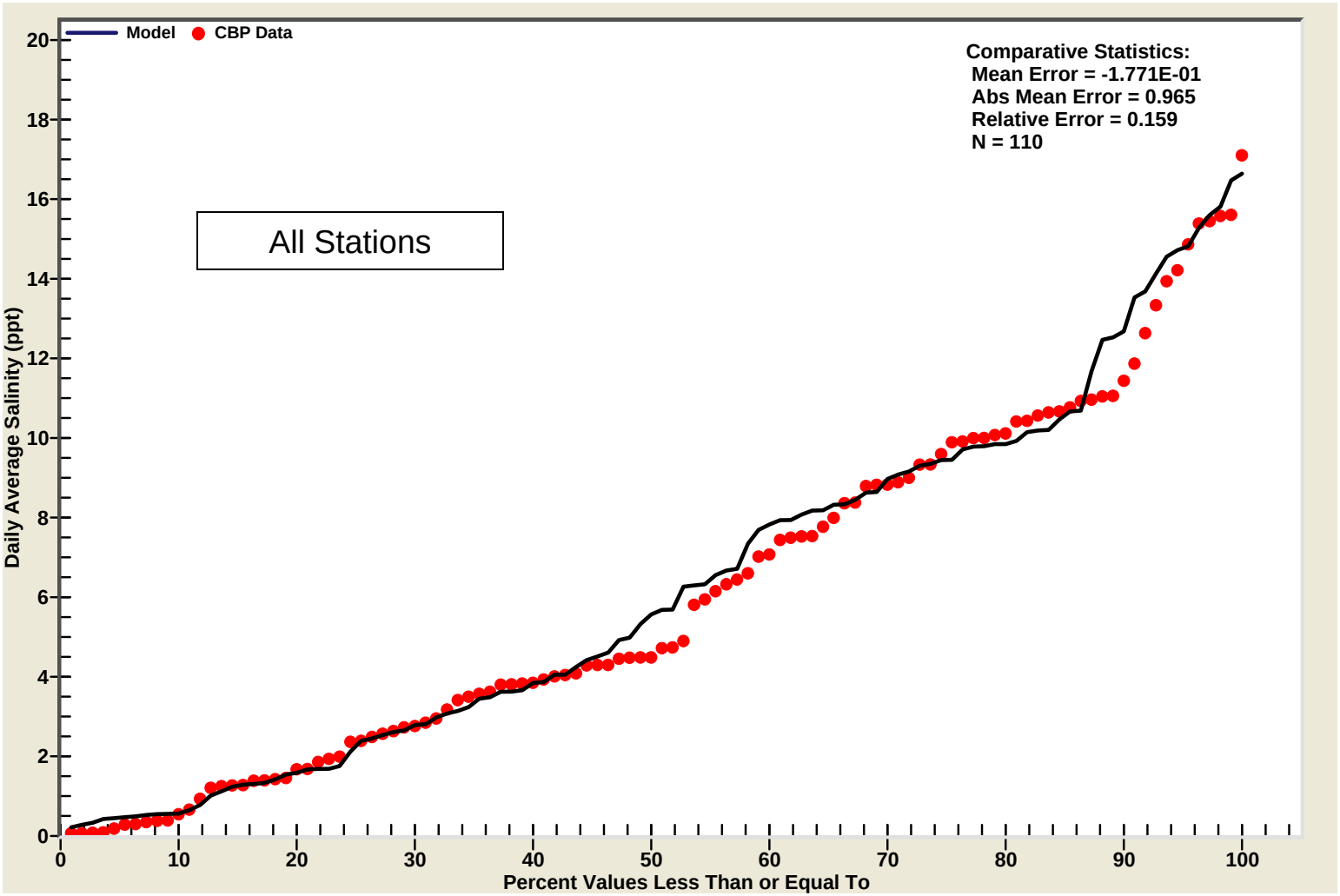

Figure 37. CFD for Computed and Observed Daily Average Salinity at All Stations (1996-1997)

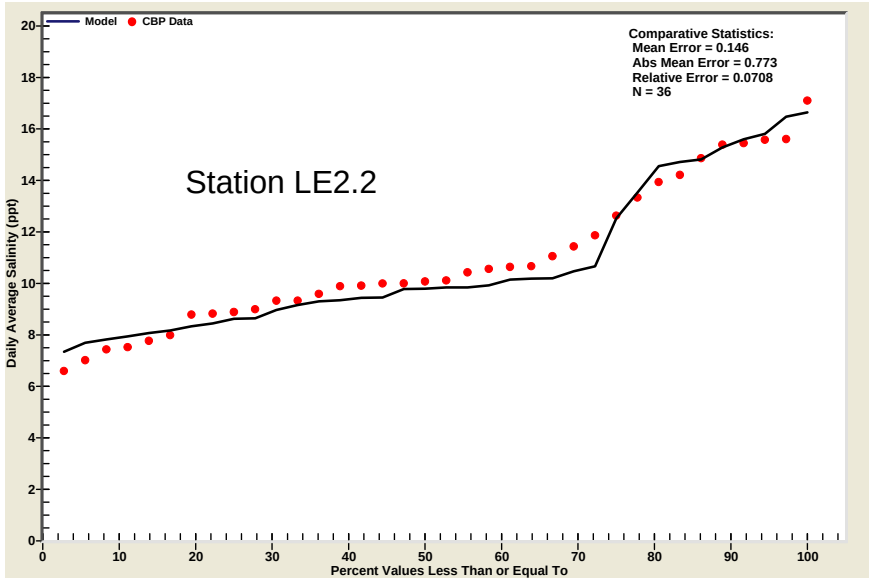

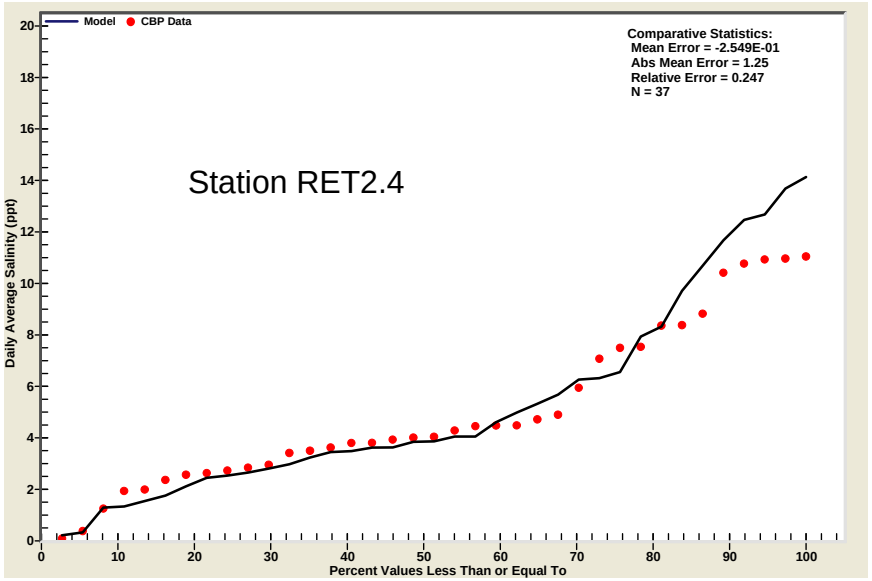

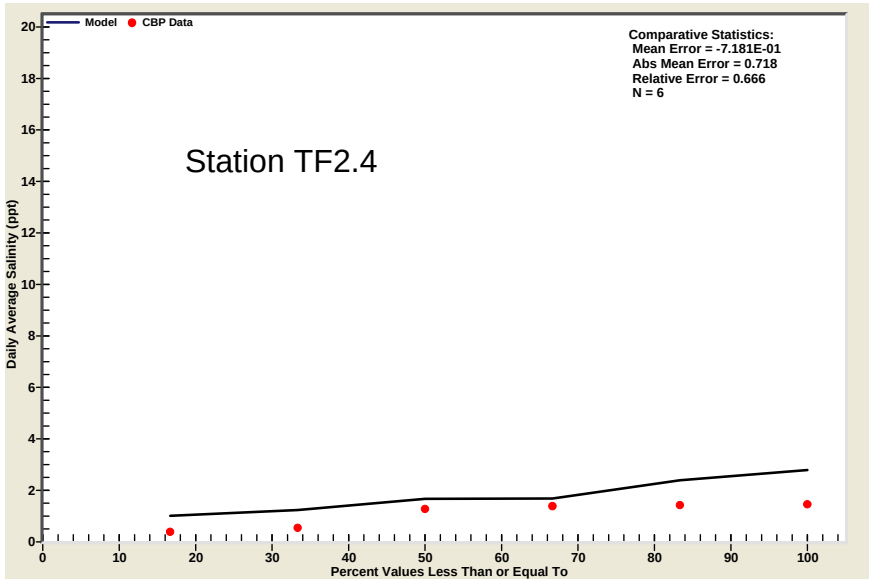

Figure 38. CFDs for Computed and Observed Daily Average Salinity (1996-1997)

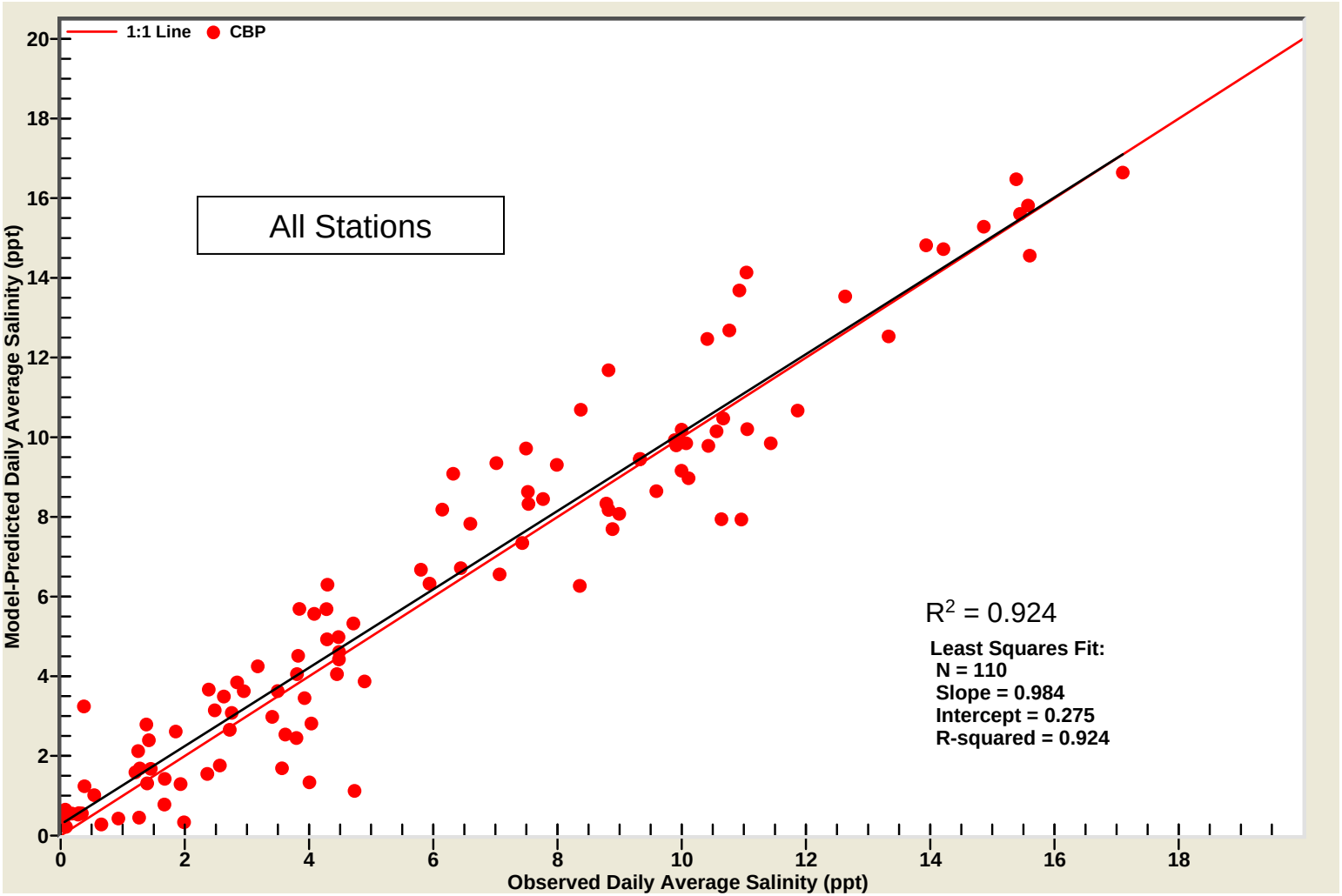

Figure 39. Bivariate Plot and Regression for Computed versus Observed Daily Average Salinity at All Stations (1996-1997)

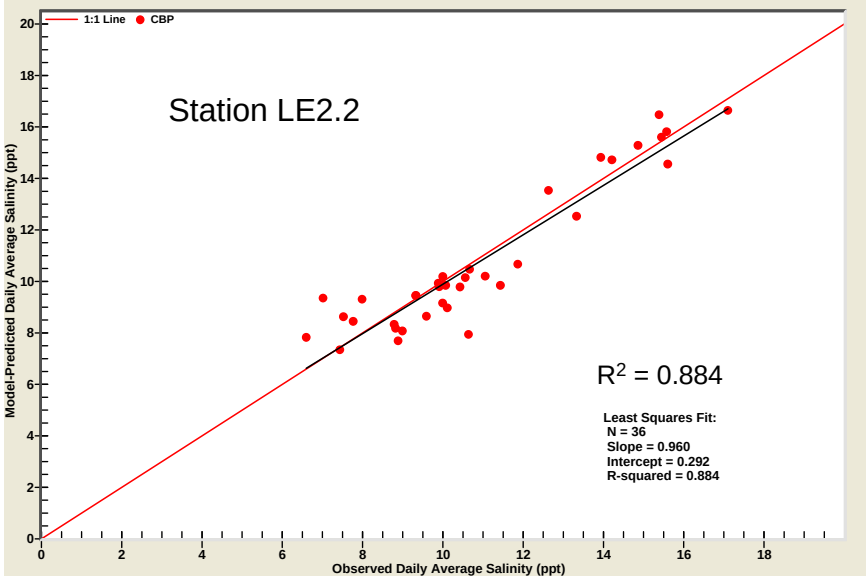

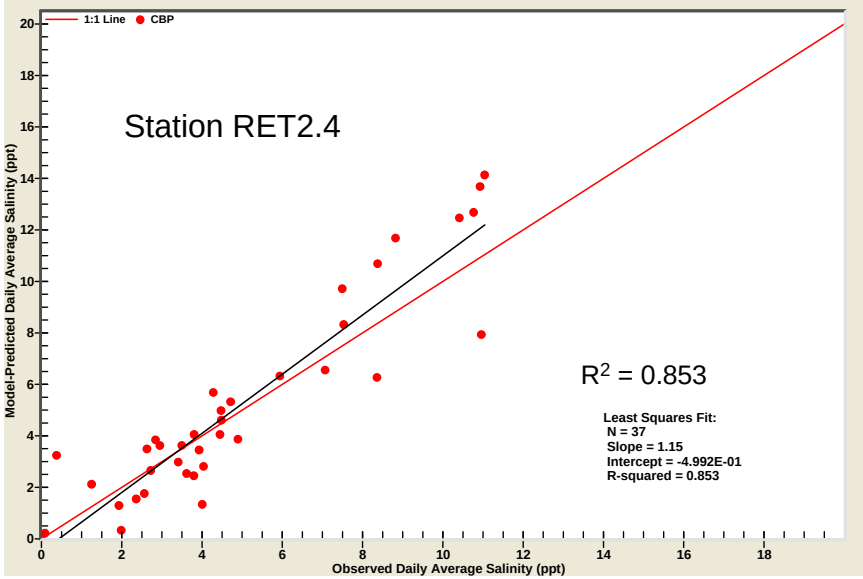

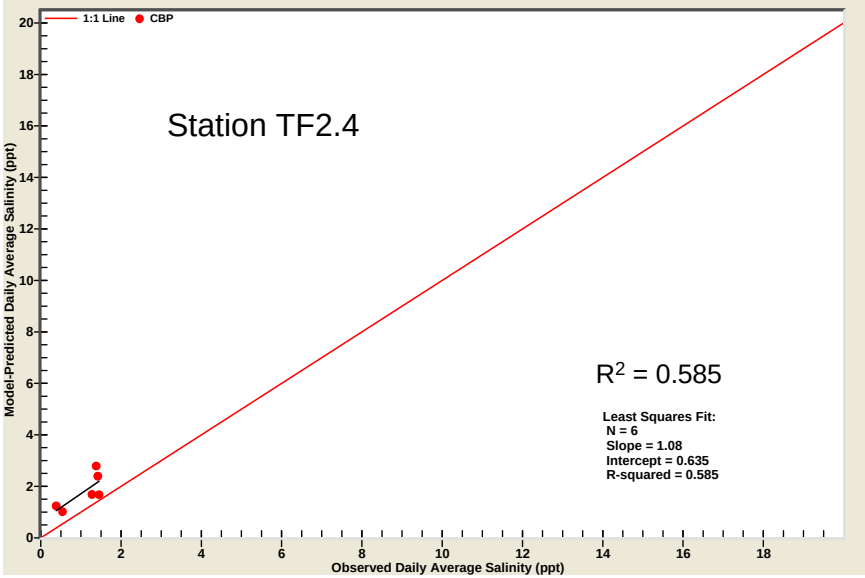

Figure 40. Bivariate Plots and Regressions for Computed versus Observed Daily Average Salinity (1996-1997)

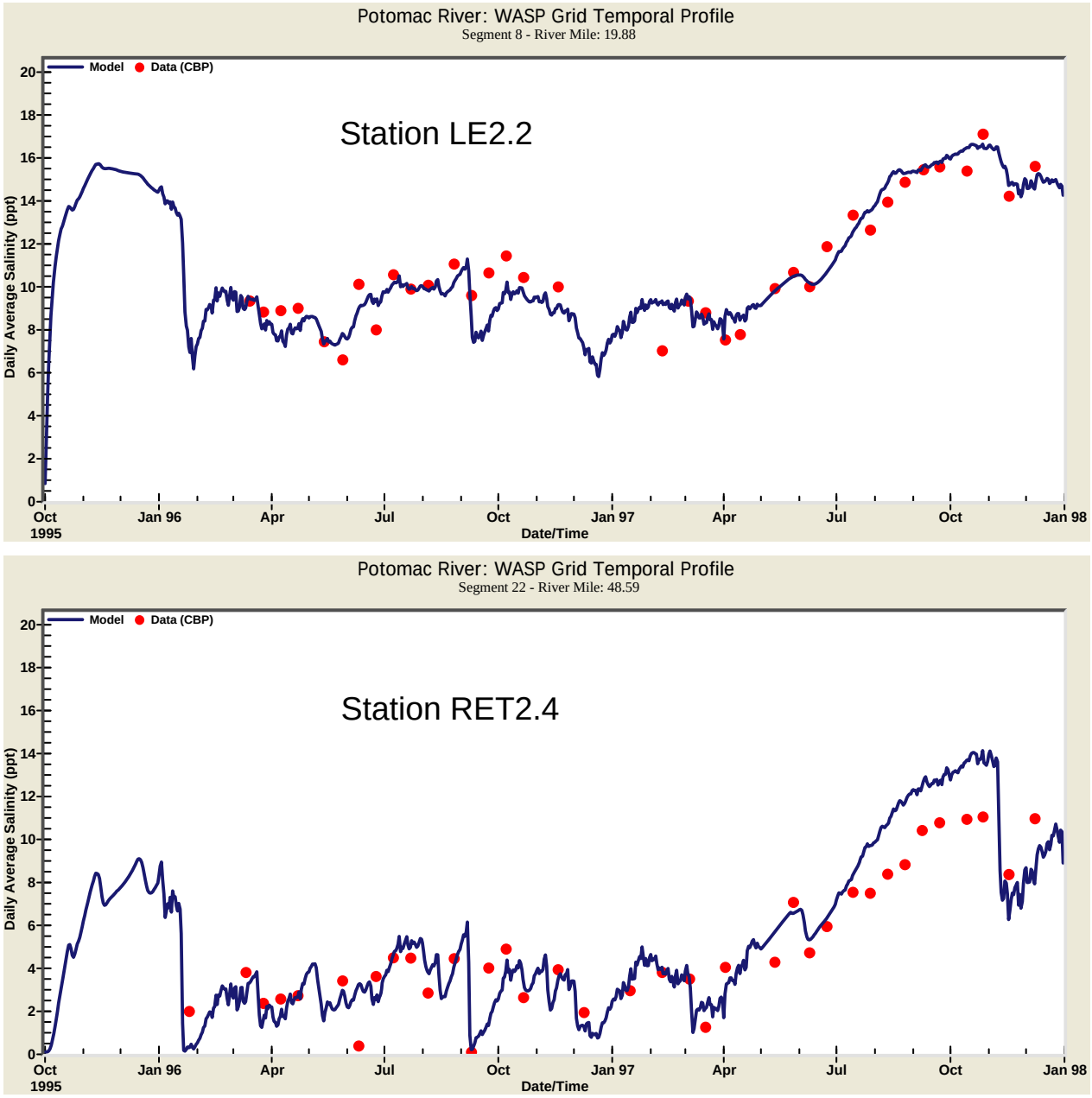

Figure 41. Time Series Plots for Computed and Observed Daily Average Salinity (1996-1997)

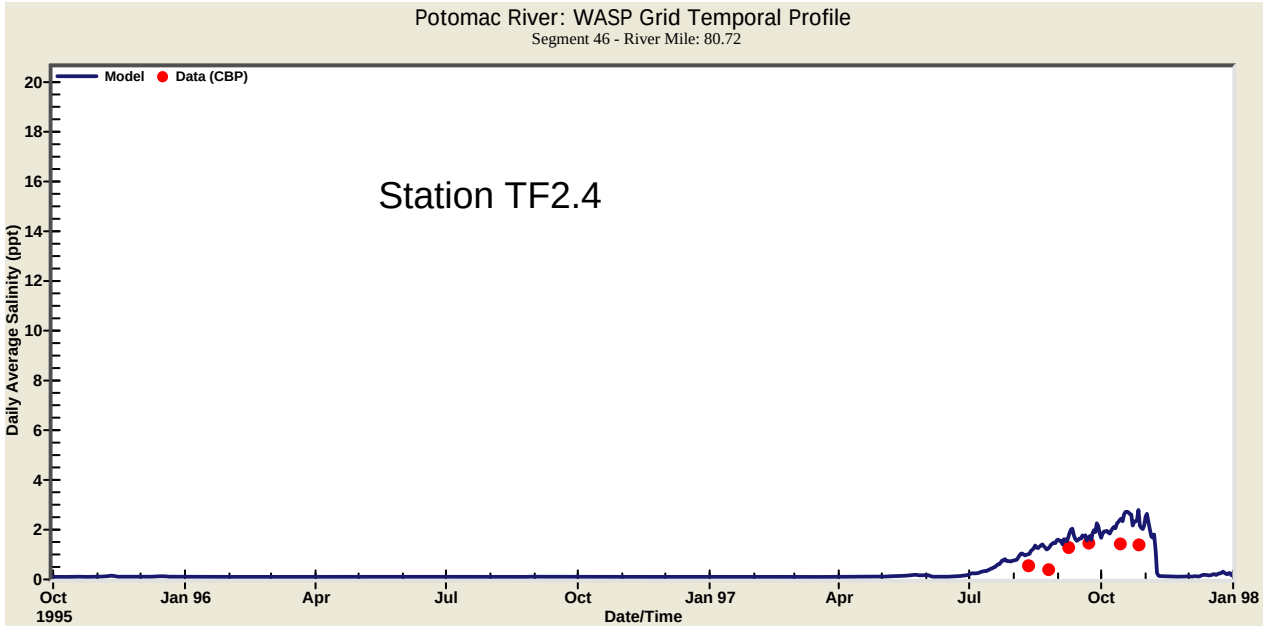

Figure 42. Time Series Plot for Computed and Observed Daily Average Salinity (1996-1997)

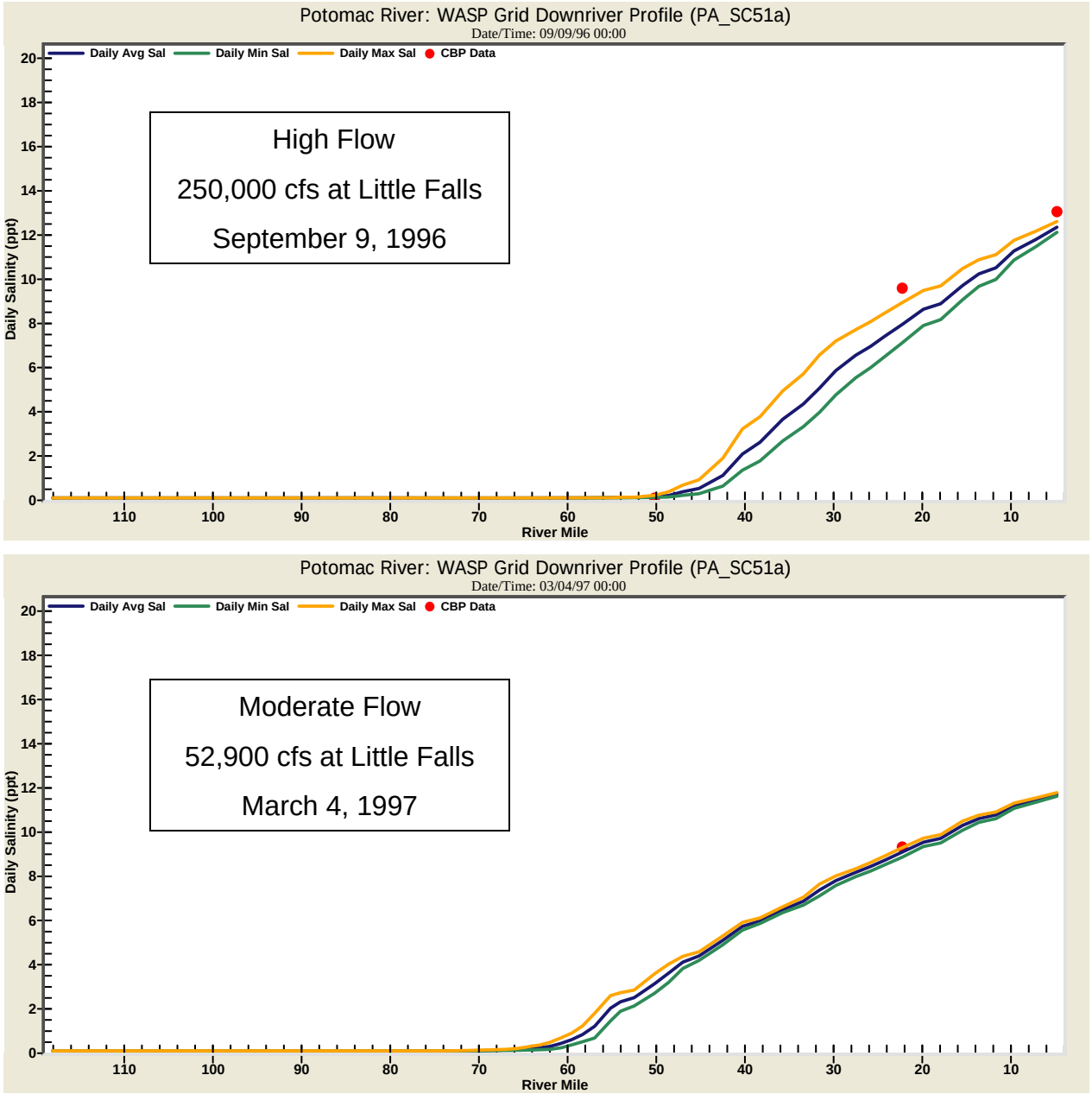

Figure 43. Spatial Profiles of Computed and Observed Daily Average Salinity for High and Moderate Flows (1996-1997)

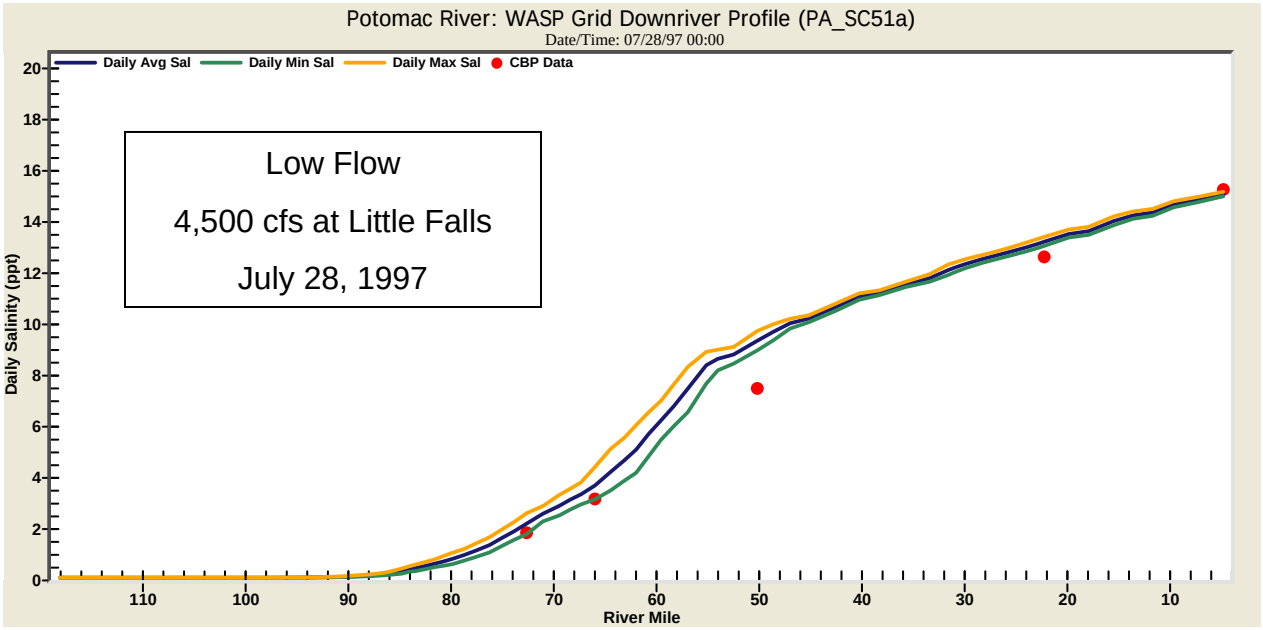

Figure 44. Spatial Profiles of Computed and Observed Daily Average Salinity for Low Flow (1996-1997)

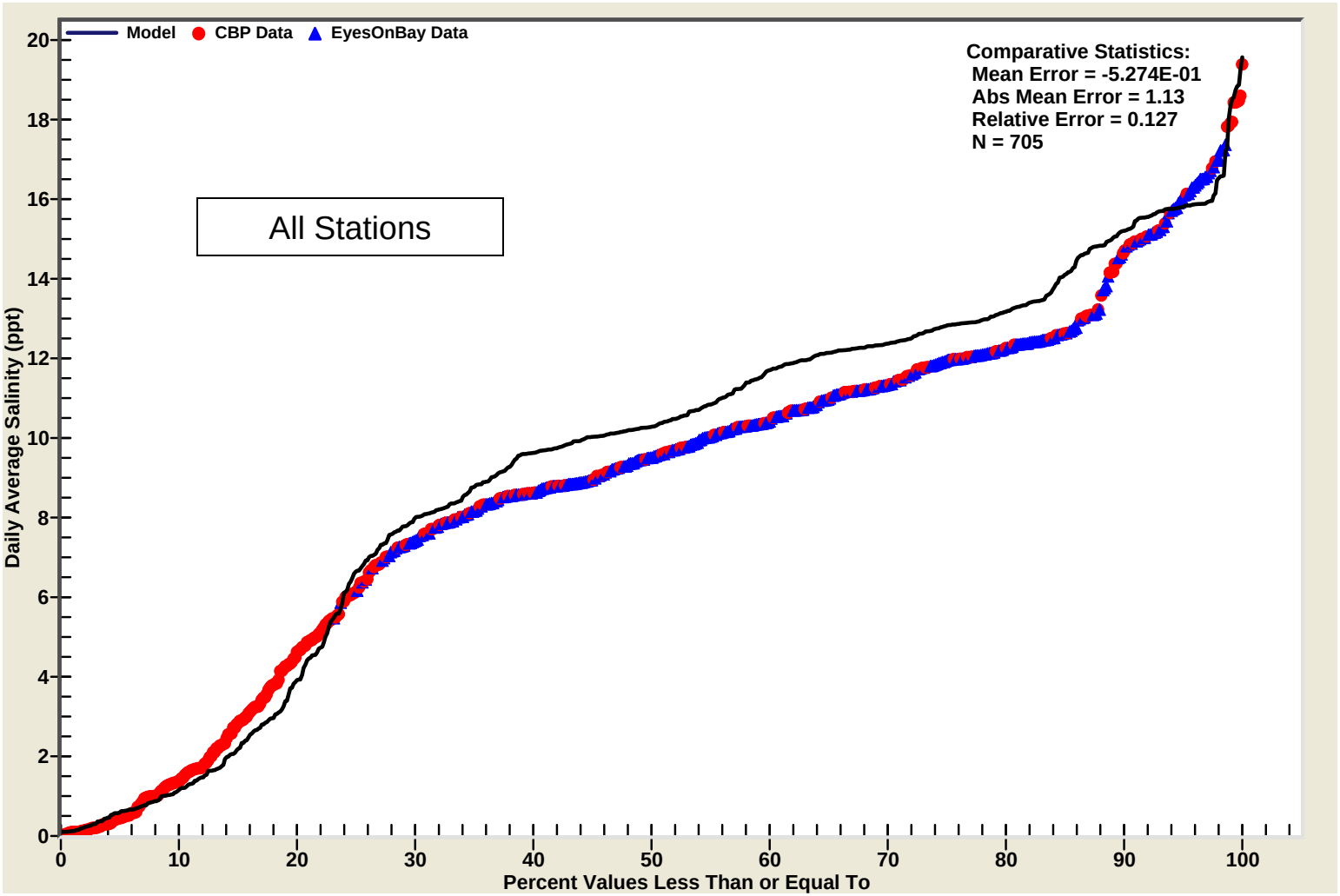

Figure 45. CFD for Computed and Observed Daily Average Salinity at All Stations (2002-2005)

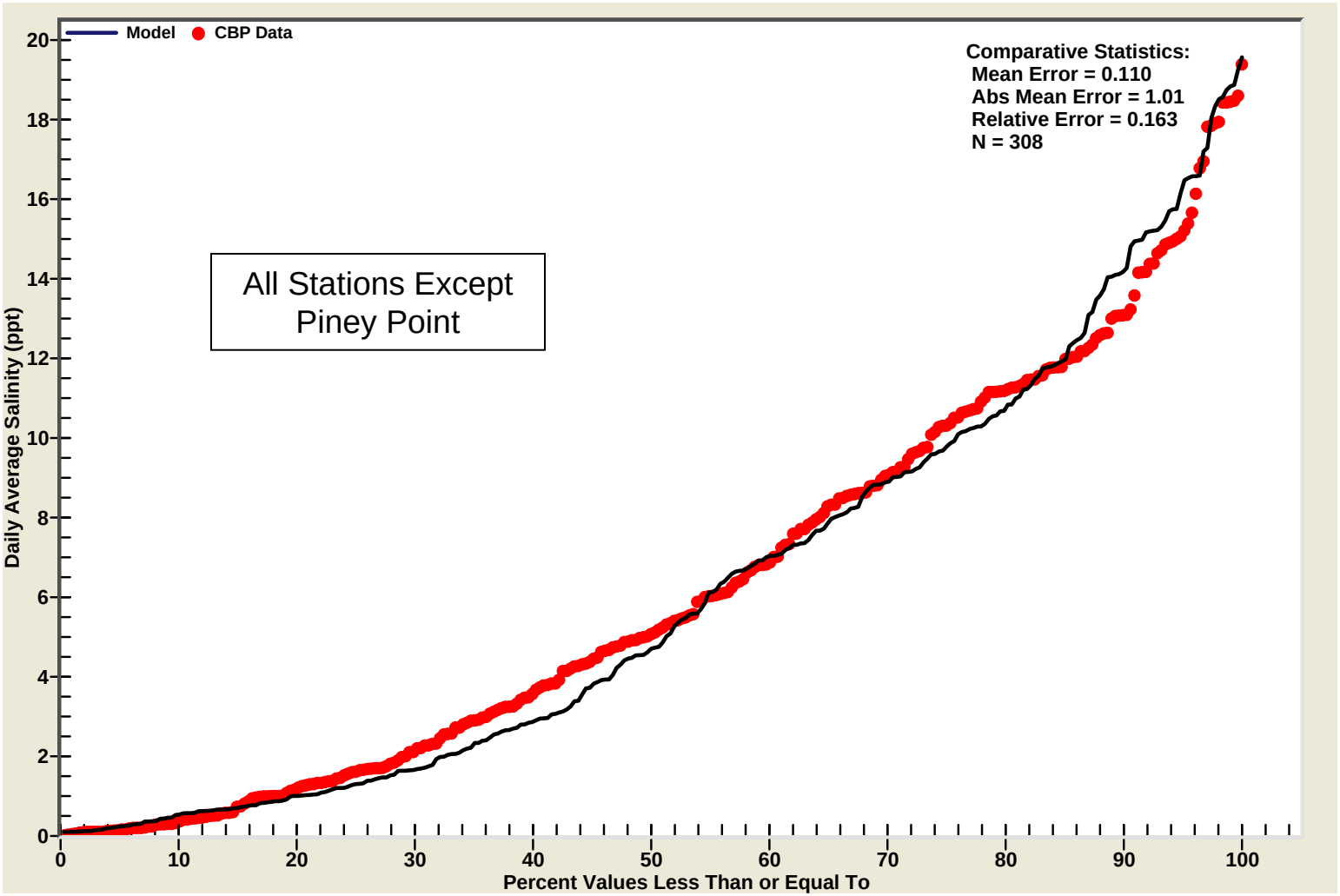

Figure 46. CFD for Computed and Observed Daily Average Salinity at All Stations Except Piney Point (2002-2005)

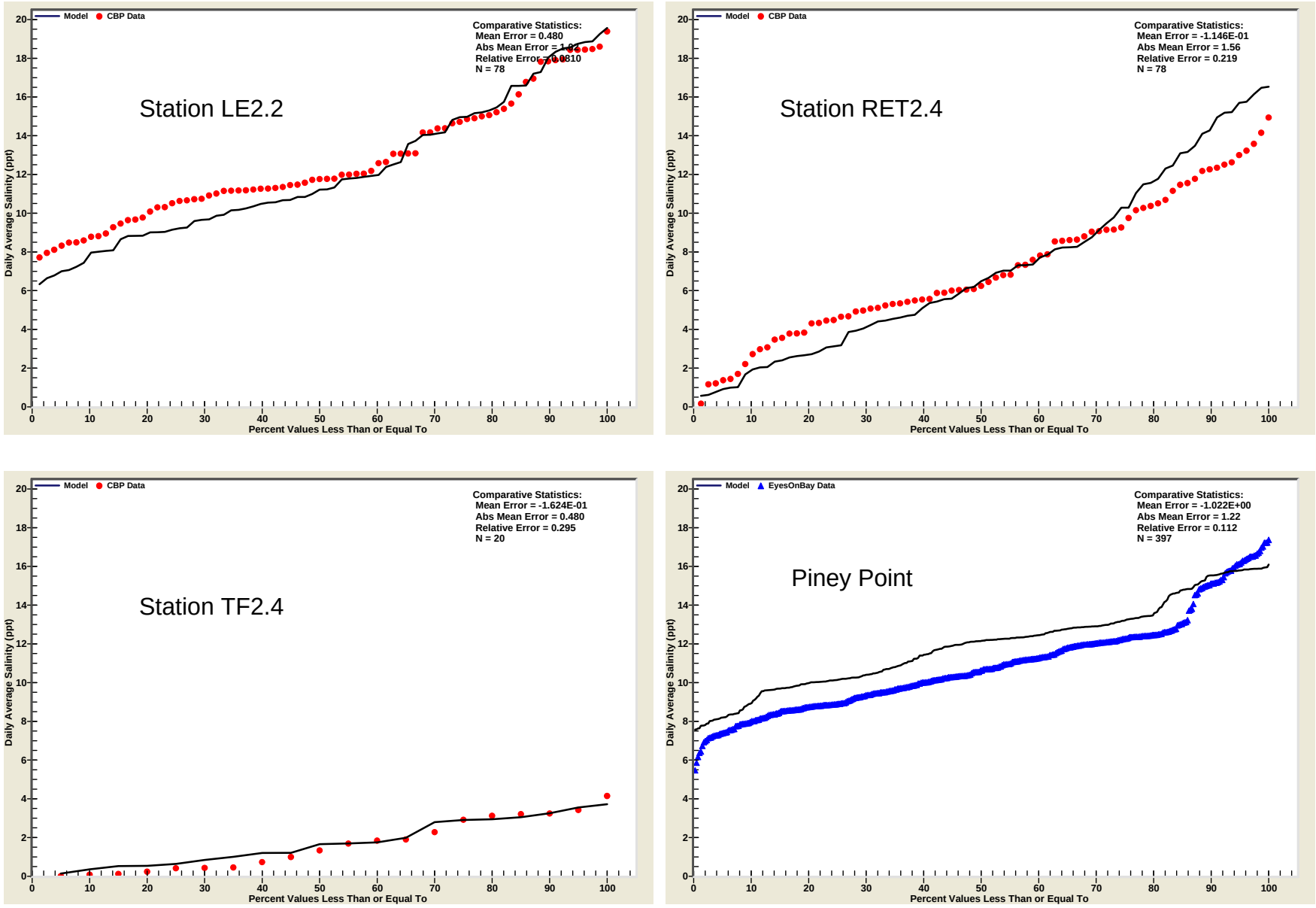

Figure 47. CFDs for Computed and Observed Daily Average Salinity (2002-2005)

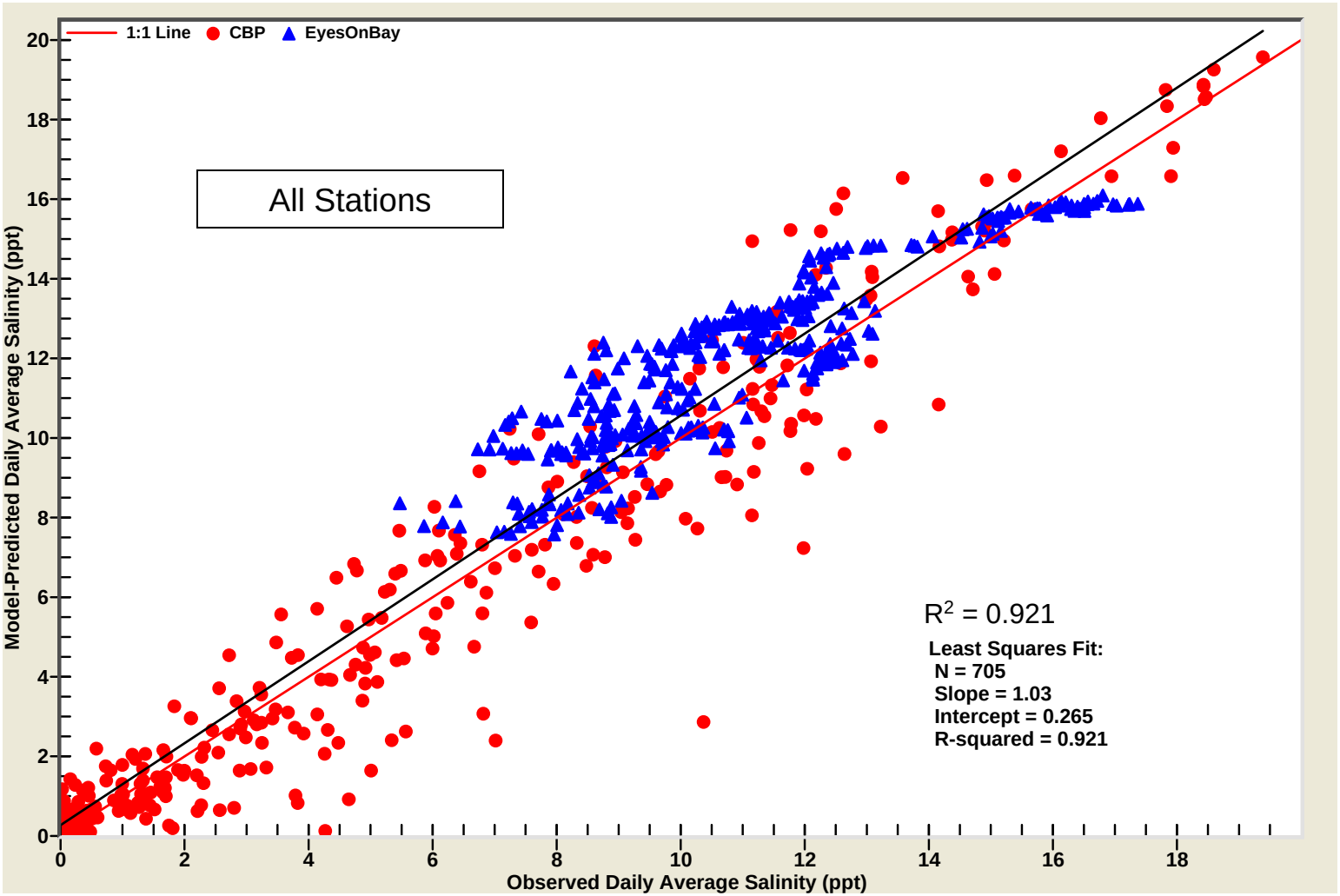

Figure 48. Bivariate Plot and Regression for Computed versus Observed Daily Average Salinity at All Stations (2002-2005)

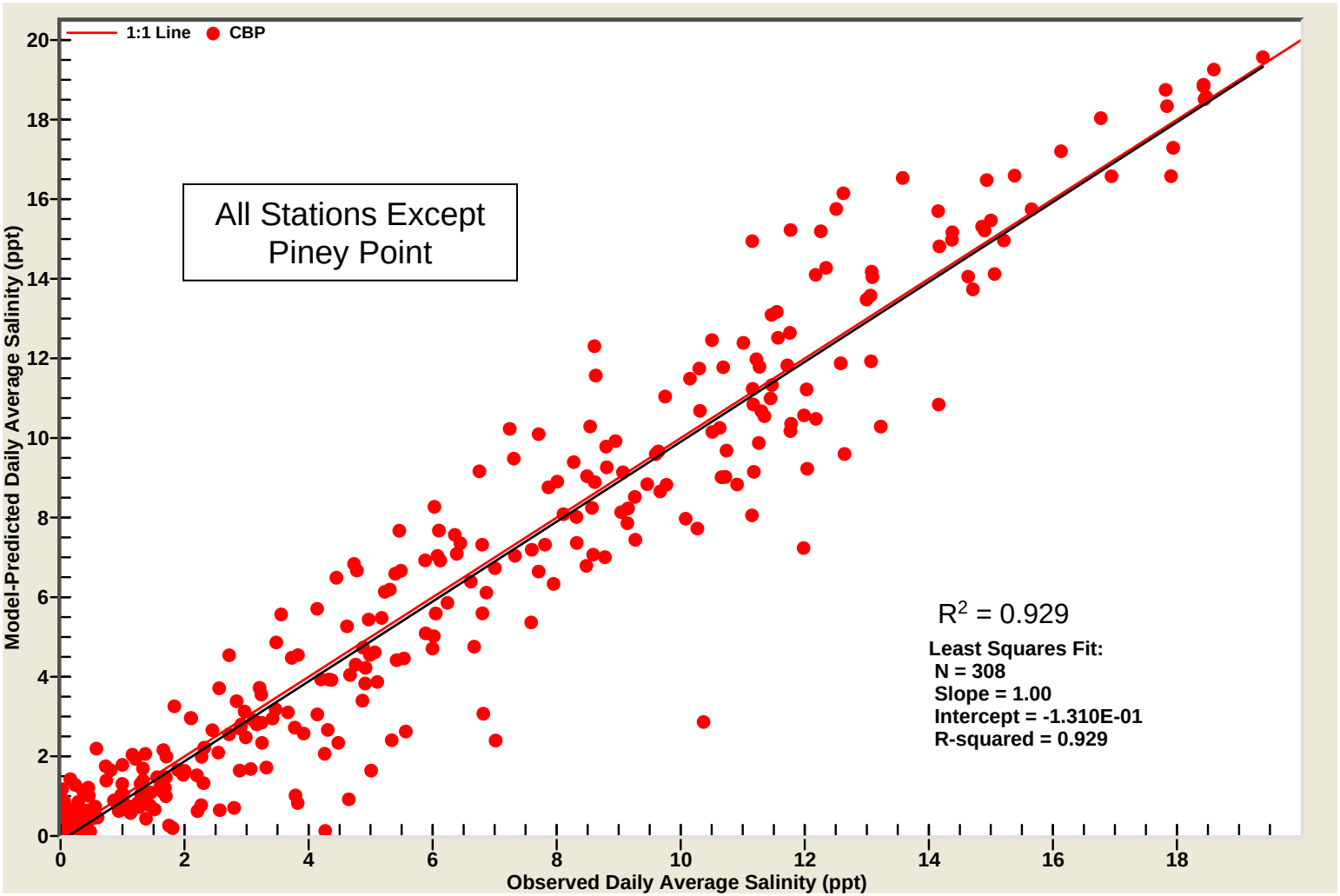

Figure 49. Bivariate Plot for Computed versus Observed Daily Average Salinity at All Stations Piney Point (2002-2005)

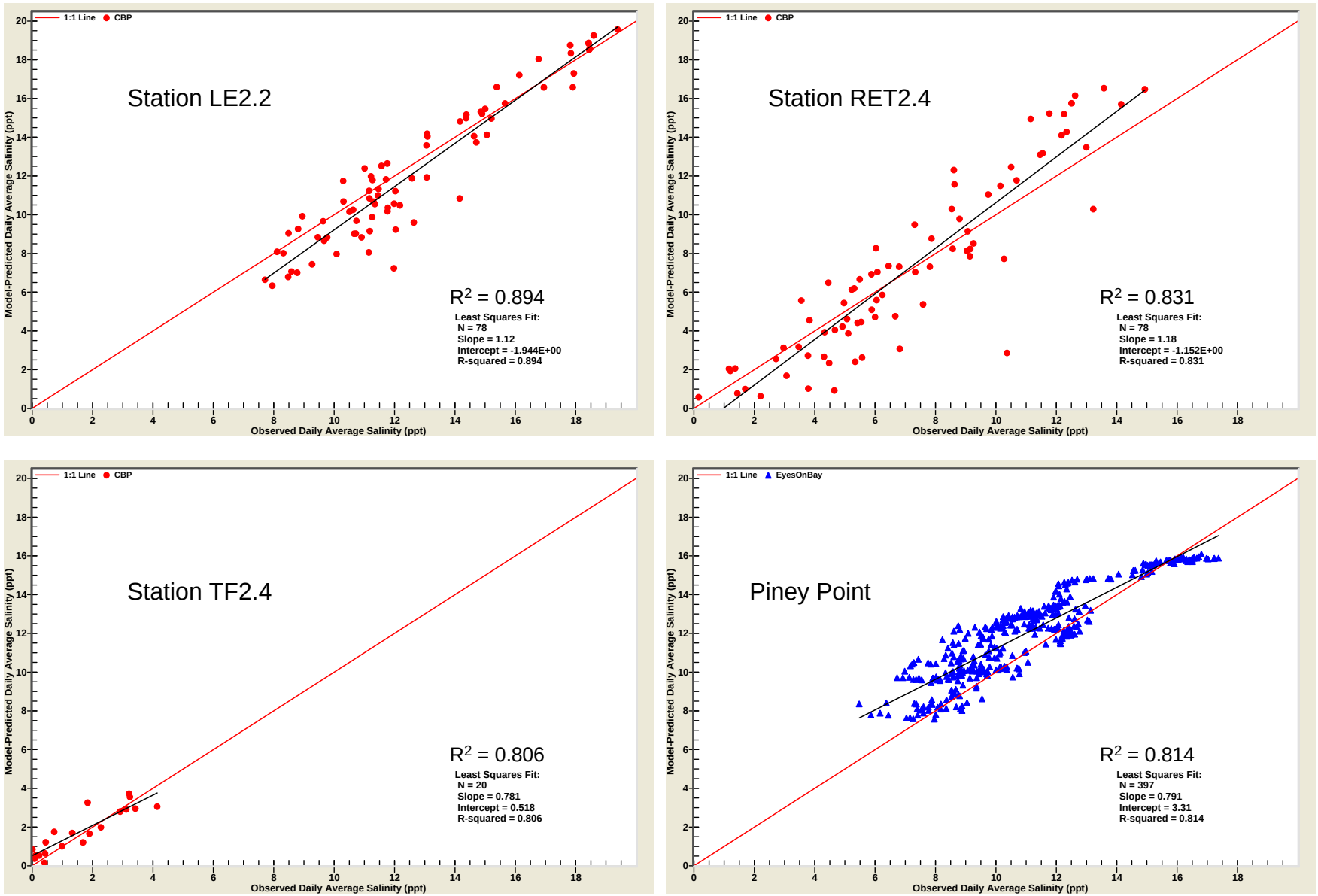

Figure 50. Bivariate Plots and Regressions for Computed versus Observed Daily Average Salinity (2002-2005)

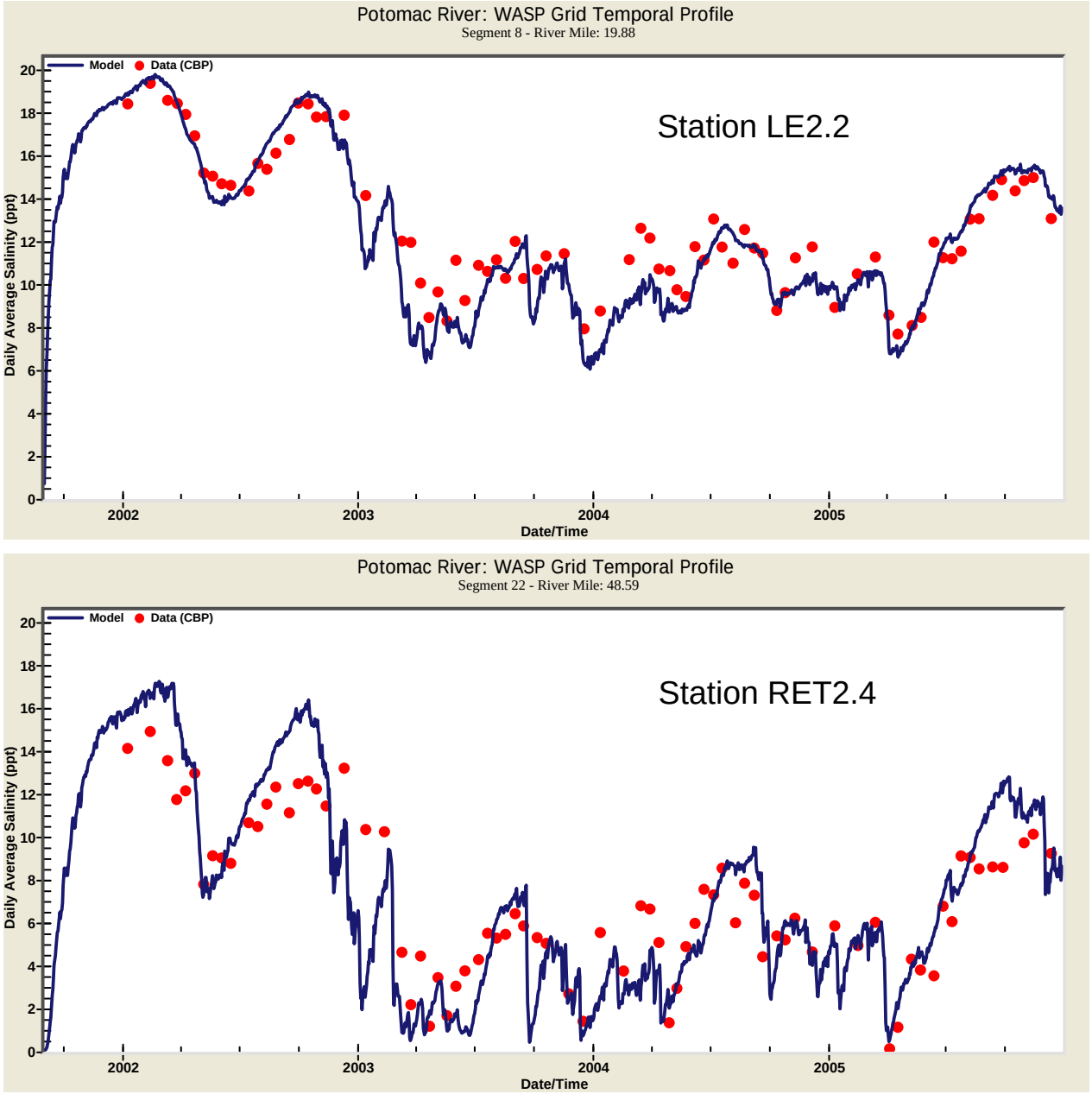

Figure 51. Time Series Plots for Computed and Observed Daily Average Salinity (2002-2005)

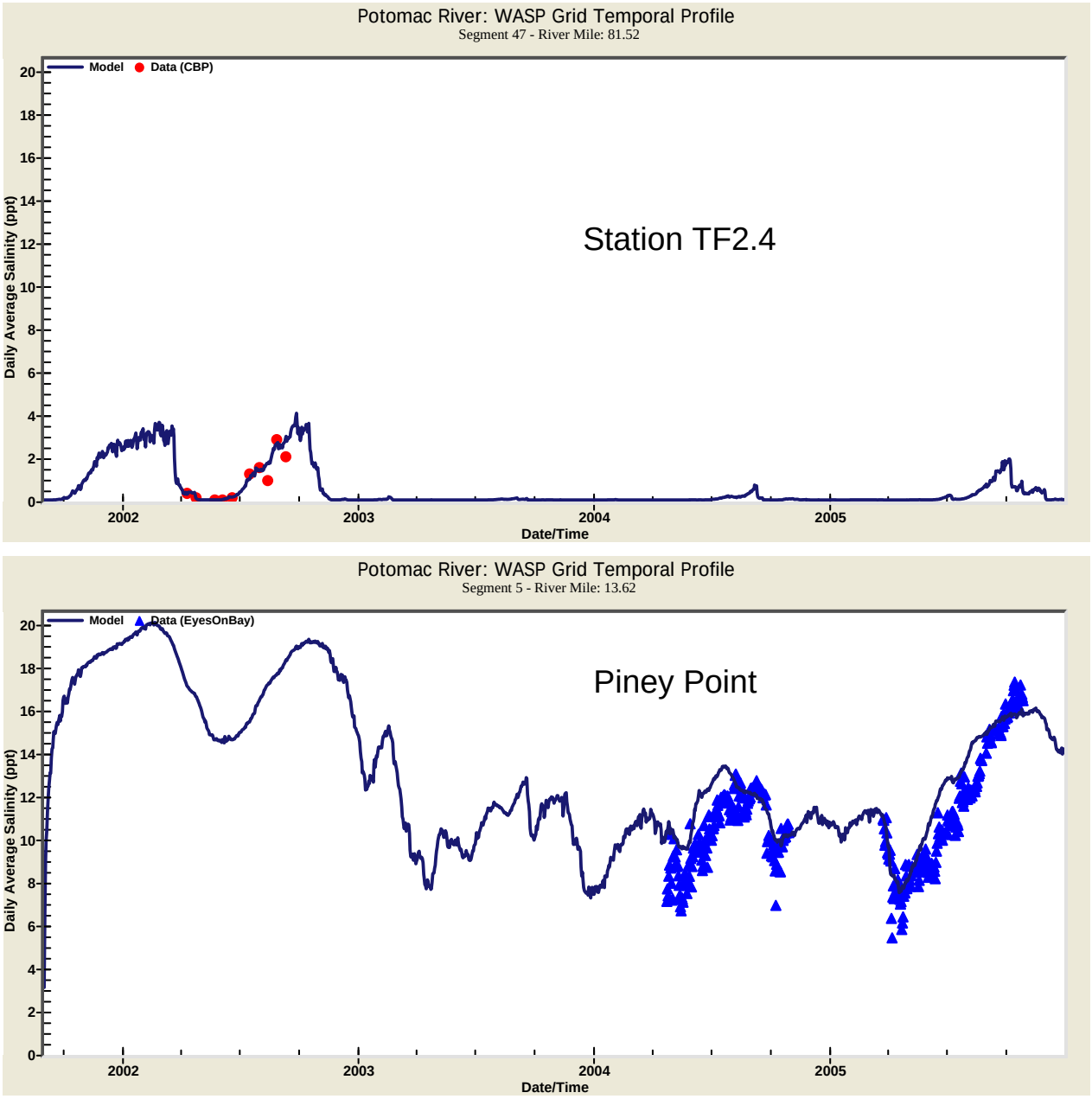

Figure 52. Time Series Plots for Computed and Observed Daily Average Salinity (2002-2005)

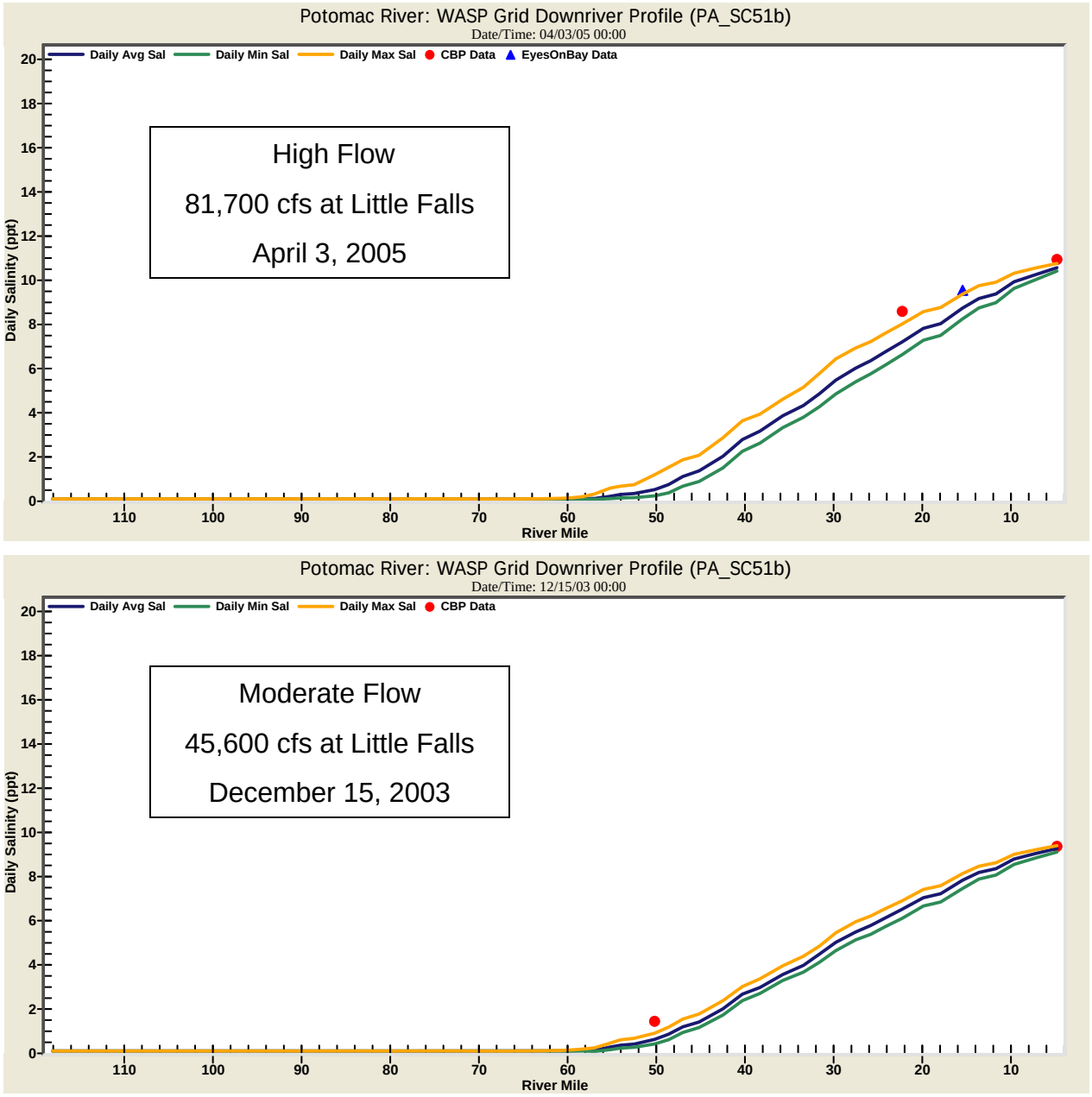

Figure 53. Spatial Profiles of Computed and Observed Daily Average Salinity for High and Moderate Flows (2002-2005)

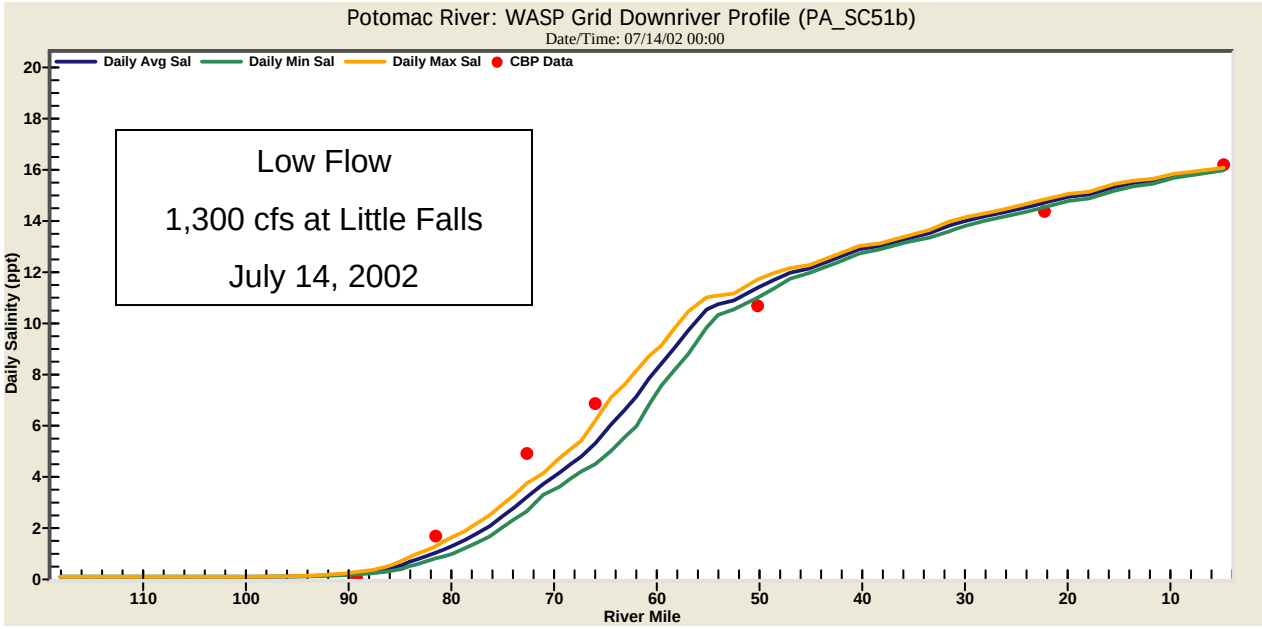

Figure 54. Spatial Profiles of Computed and Observed Daily Average Salinity for Low Flow (2002-2005)

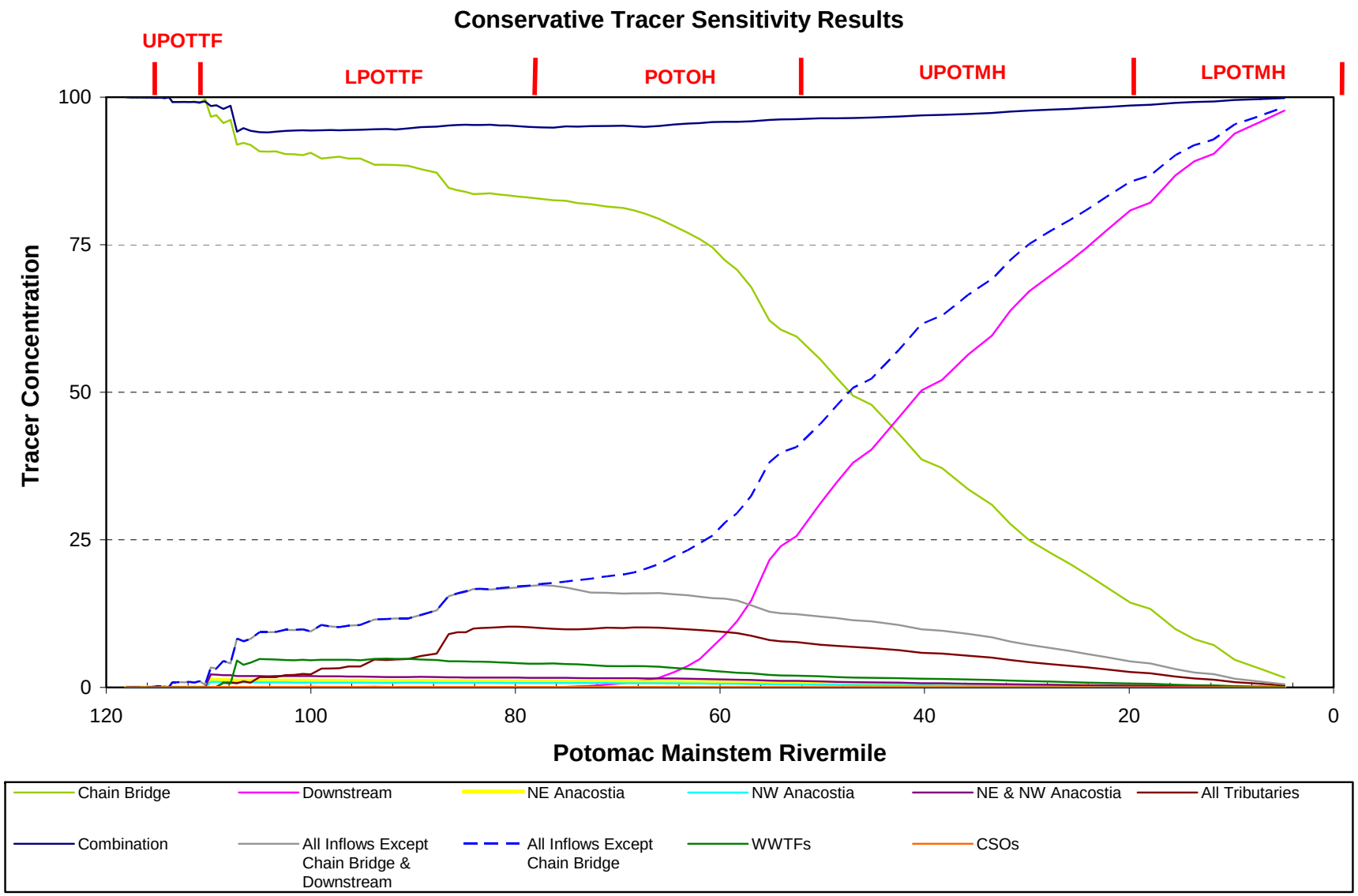

Figure 55. Relative Impacts of External Boundaries on the Potomac Mainstem For a Conservative Tracer

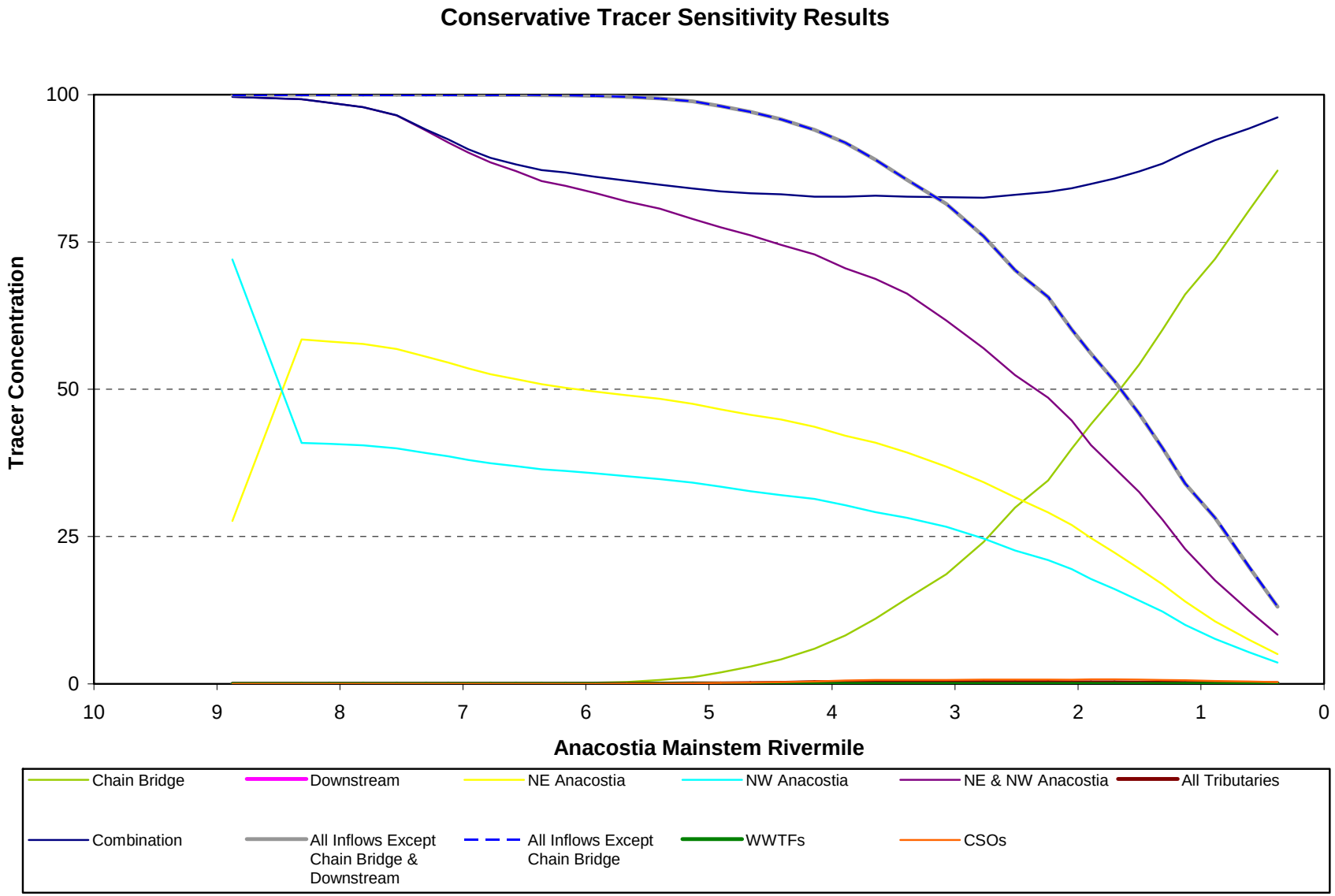

Figure 56. Relative Impacts of External Boundaries on the Anacostia Mainstem For a Conservative Tracer

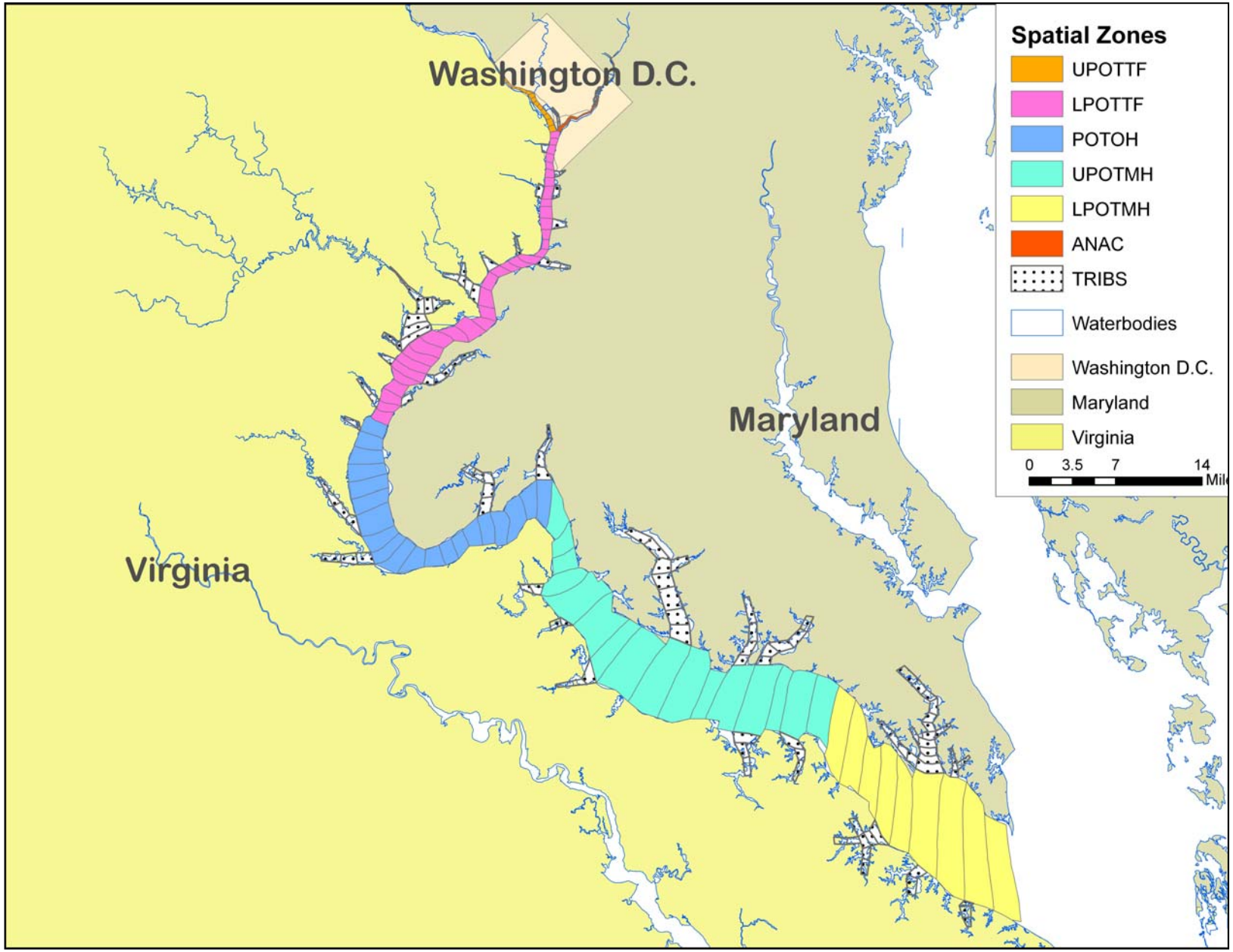

Figure 57. Model Spatial Zones

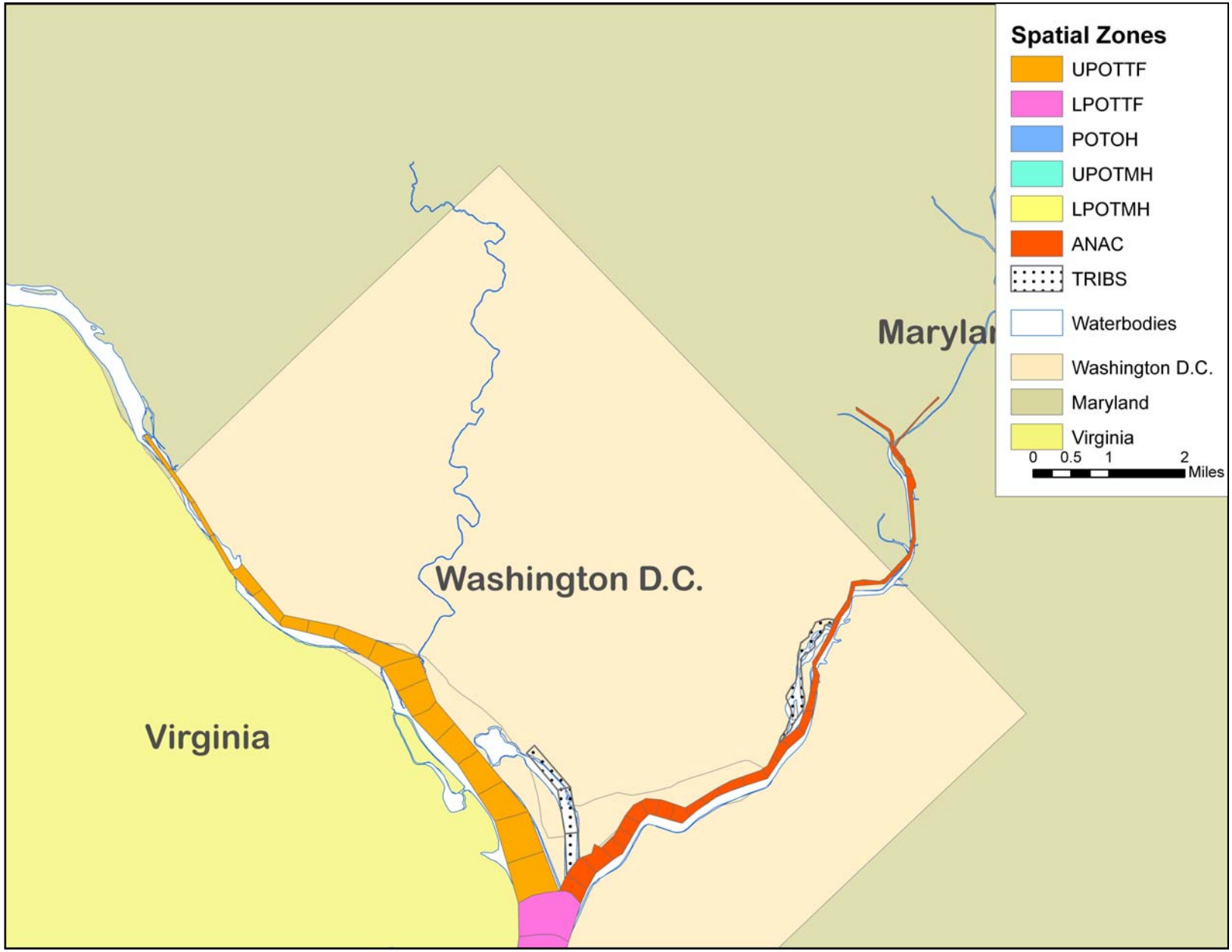

Figure 58. Model Spatial Zones (Washington DC)

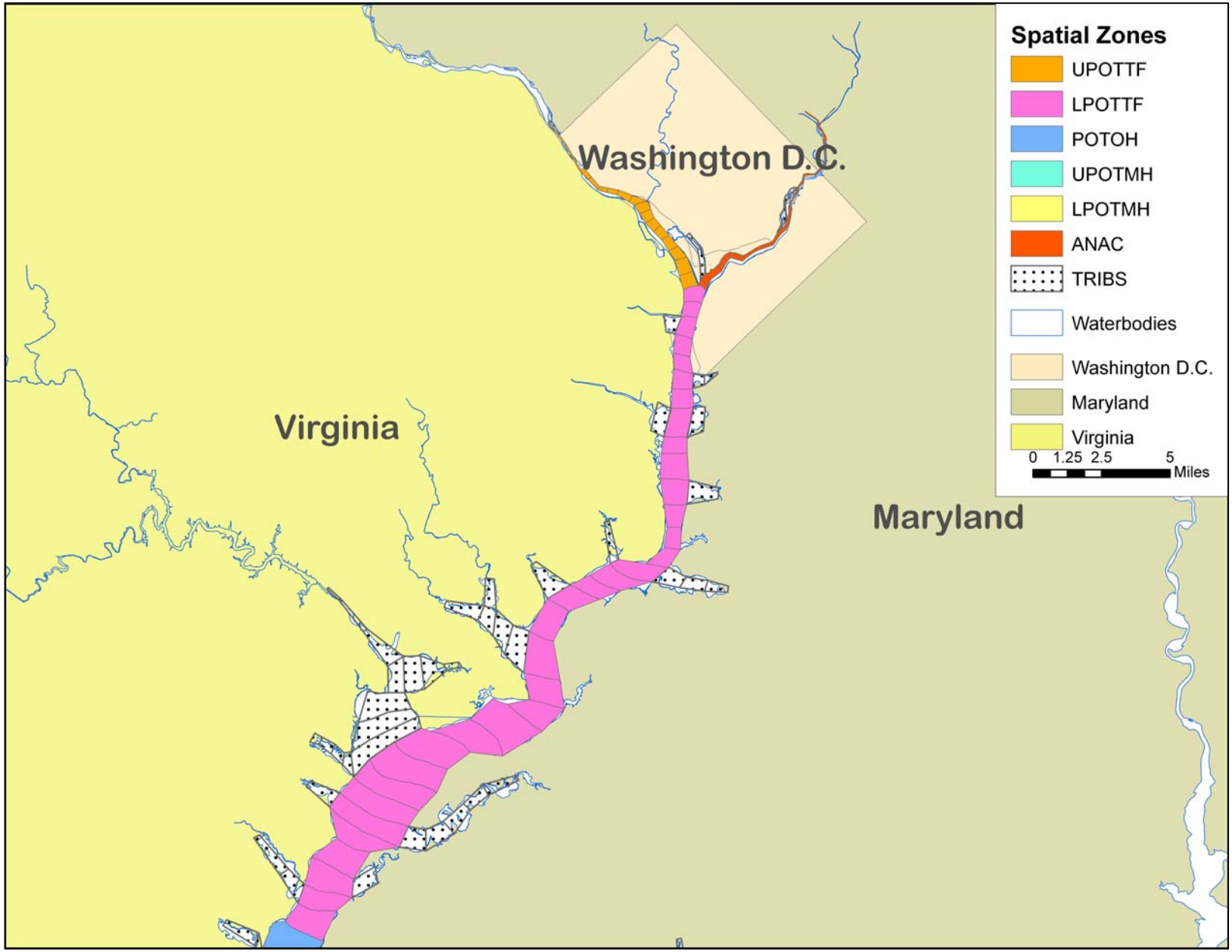

Figure 59. Model Spatial Zones (Upper Potomac)

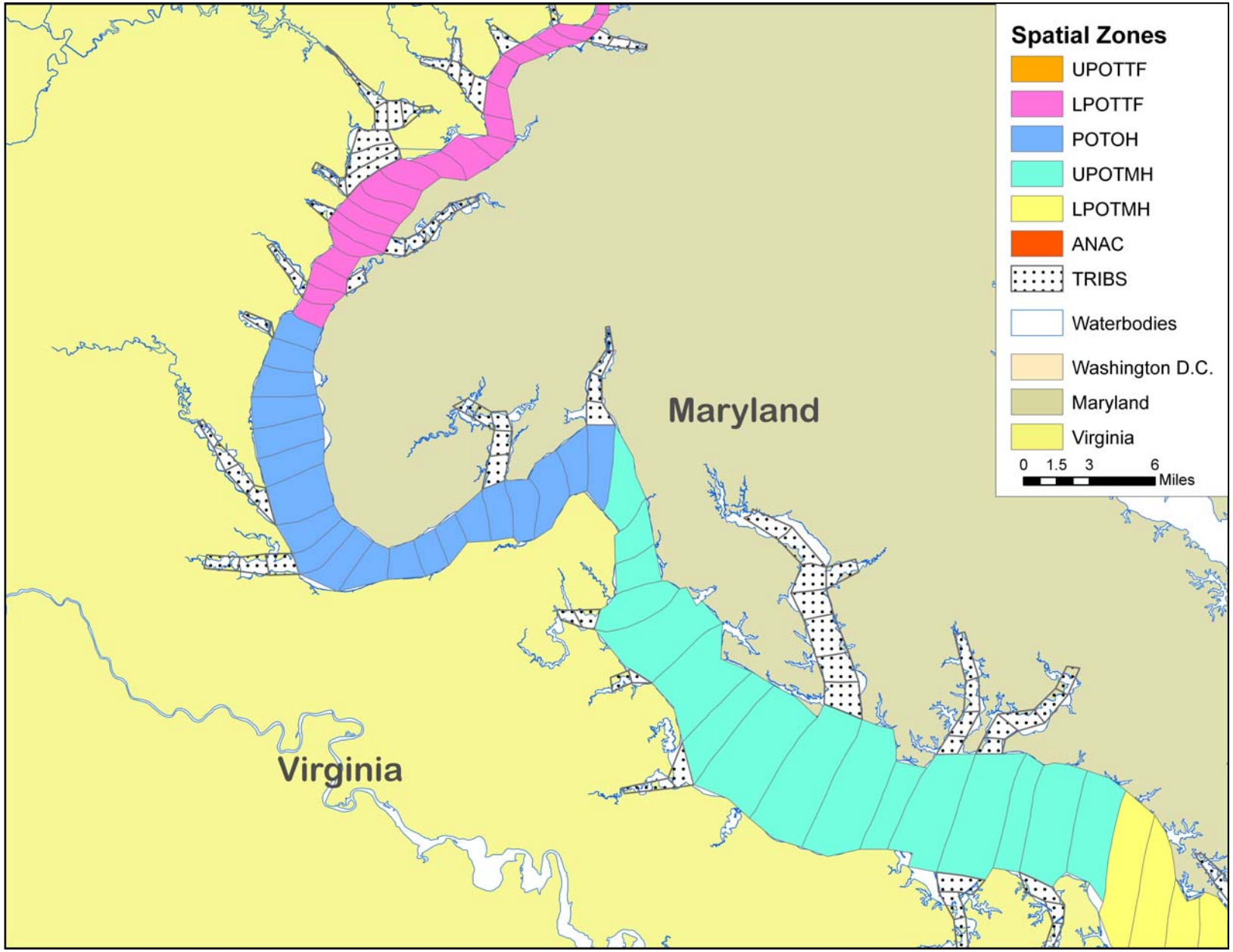

Figure 60. Model Spatial Zones (Middle Potomac)

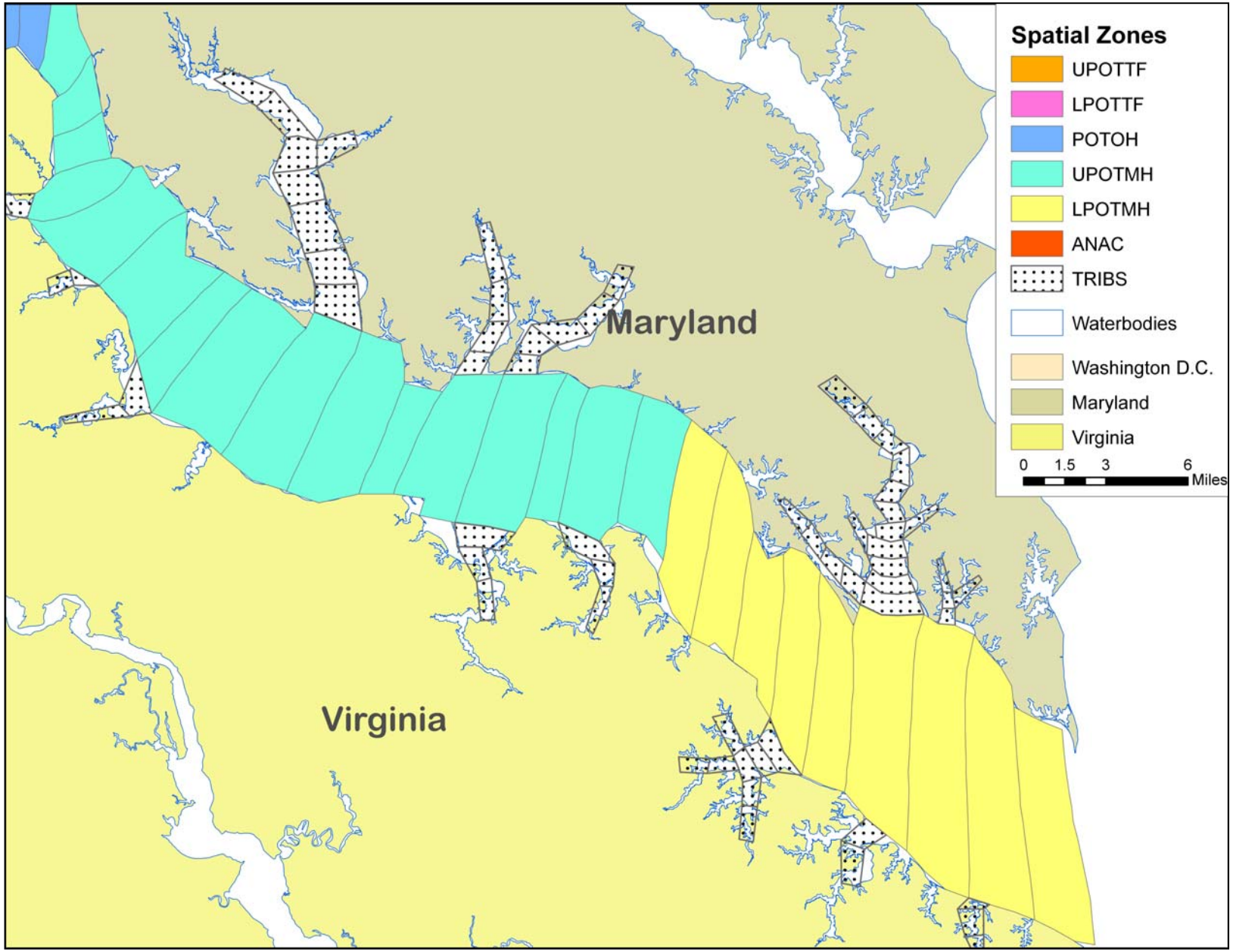

Figure 61. Model Spatial Zones (Lower Potomac)

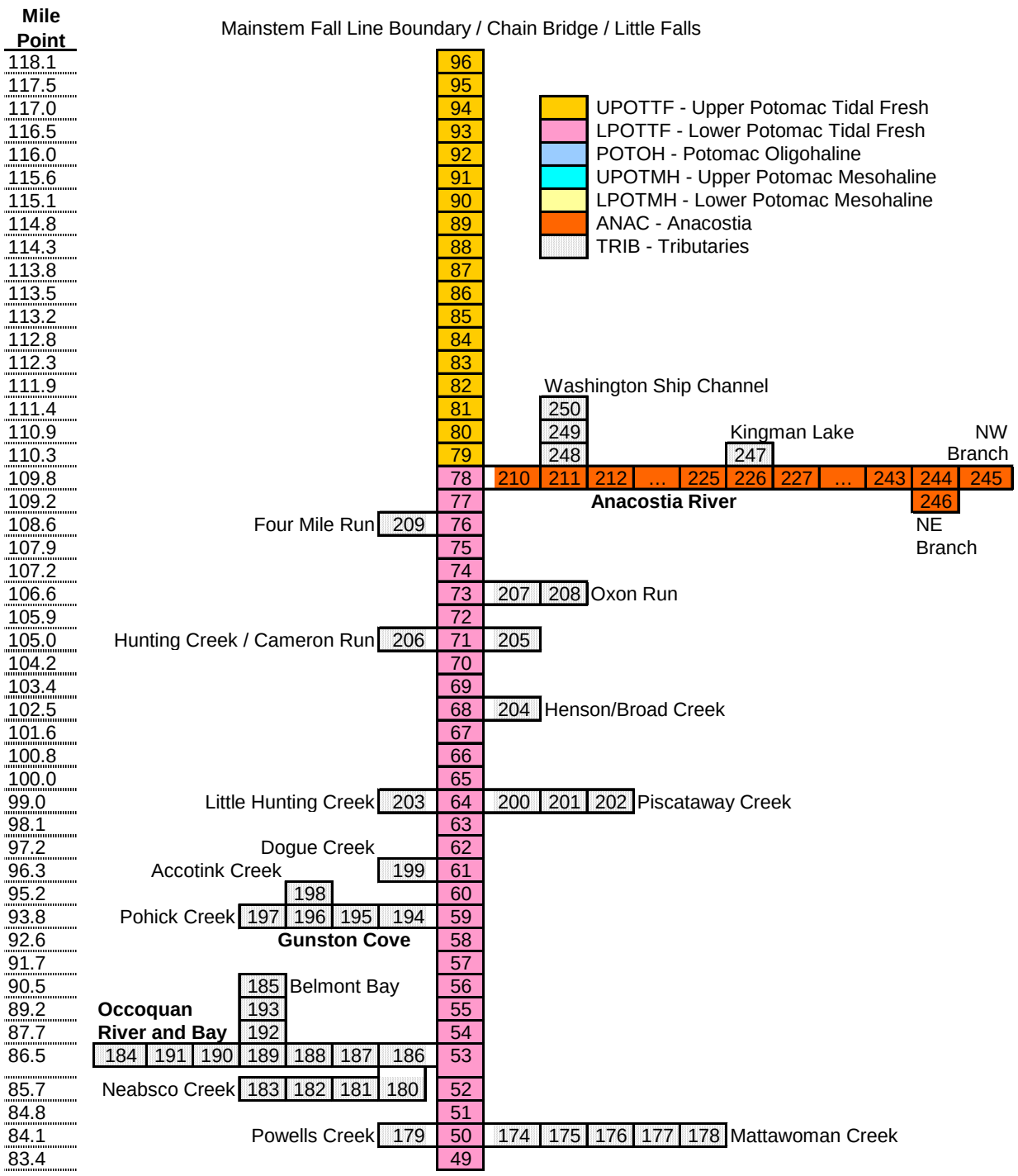

Figure 62. Potomac Estuary POTPCB Spatial Zone Assignments

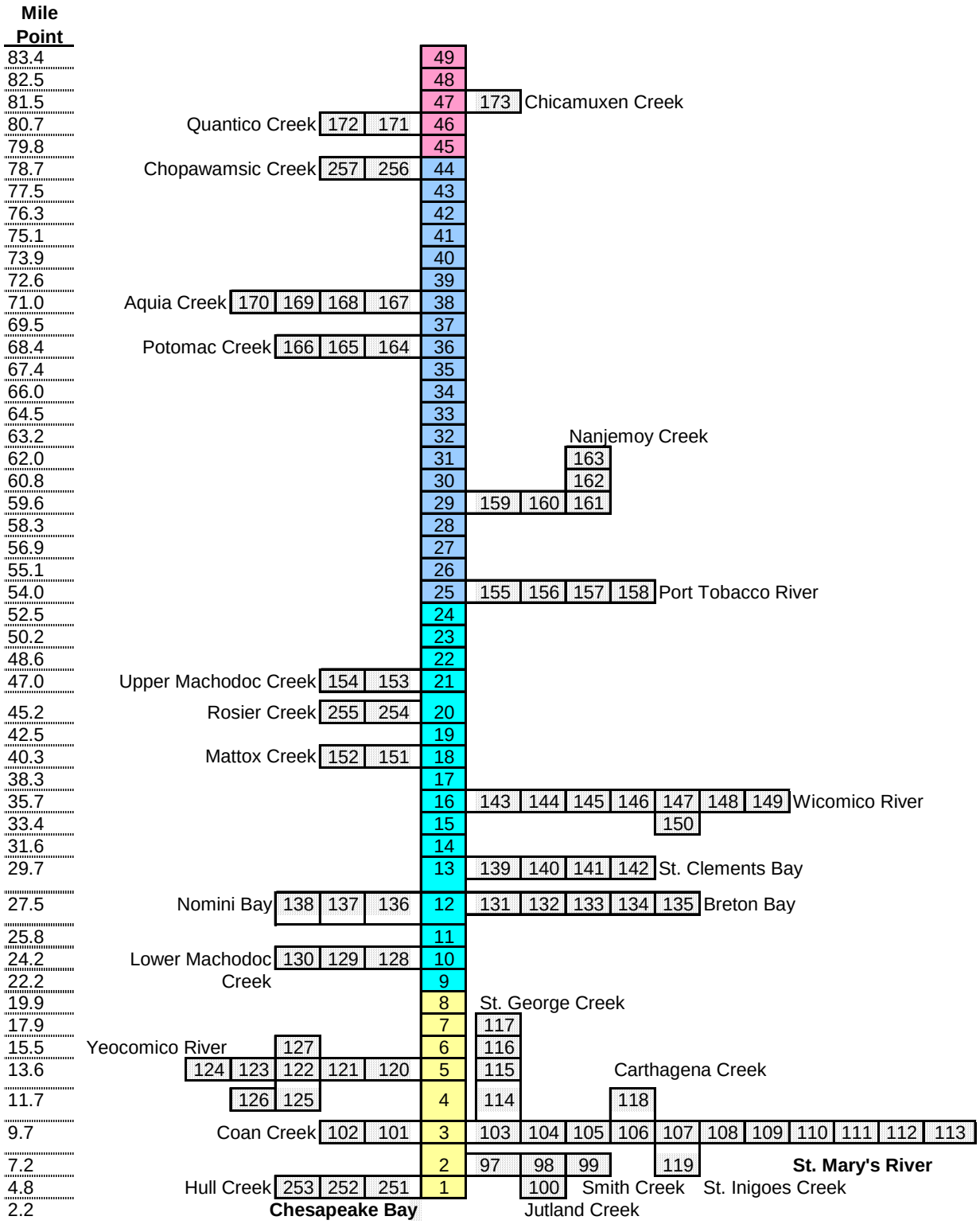

Figure 62. Potomac Estuary POTPCB Spatial Zone Assignments (continued)

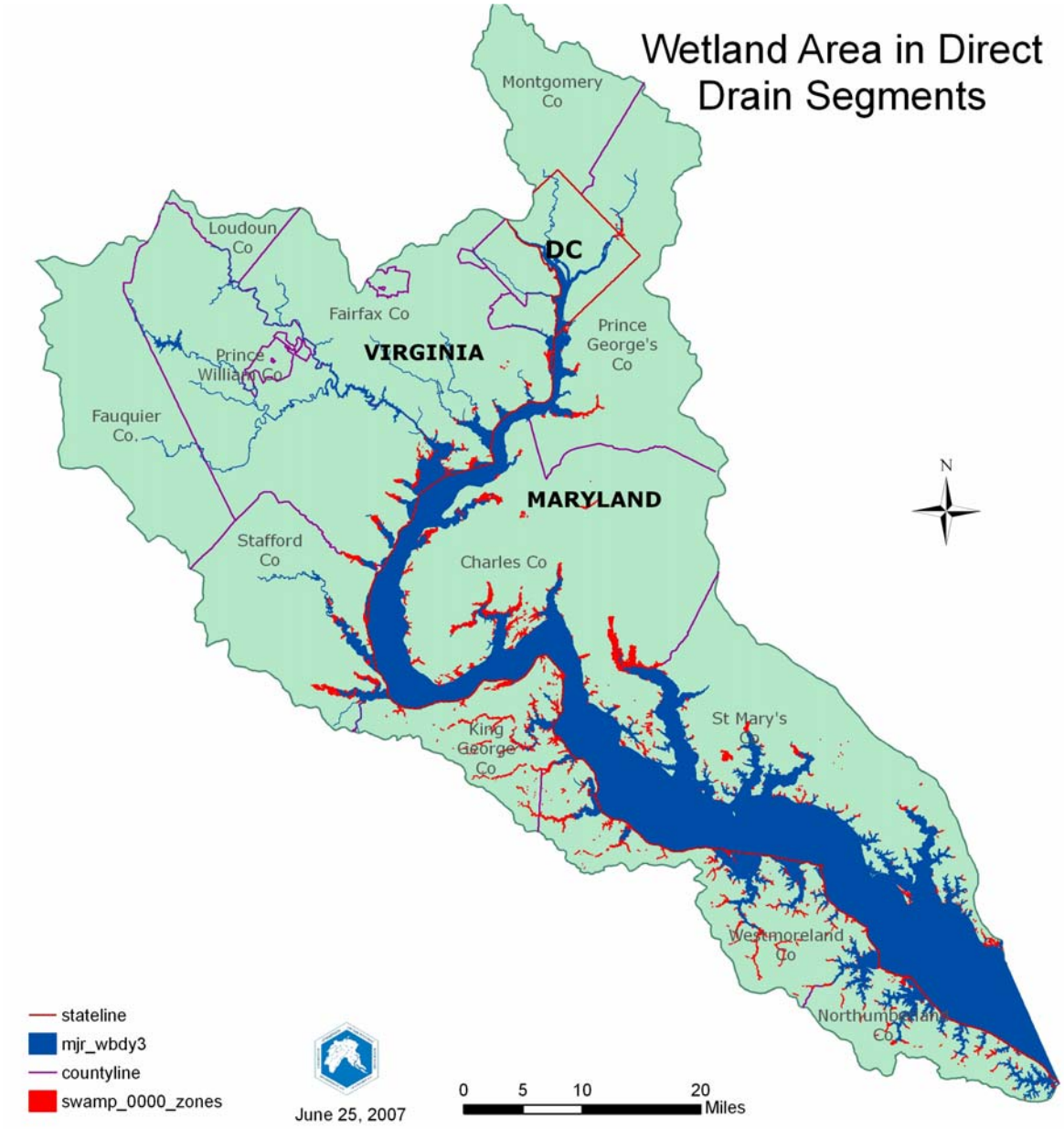

Figure 63. Wetland Areas in Direct Drainage Model Segments

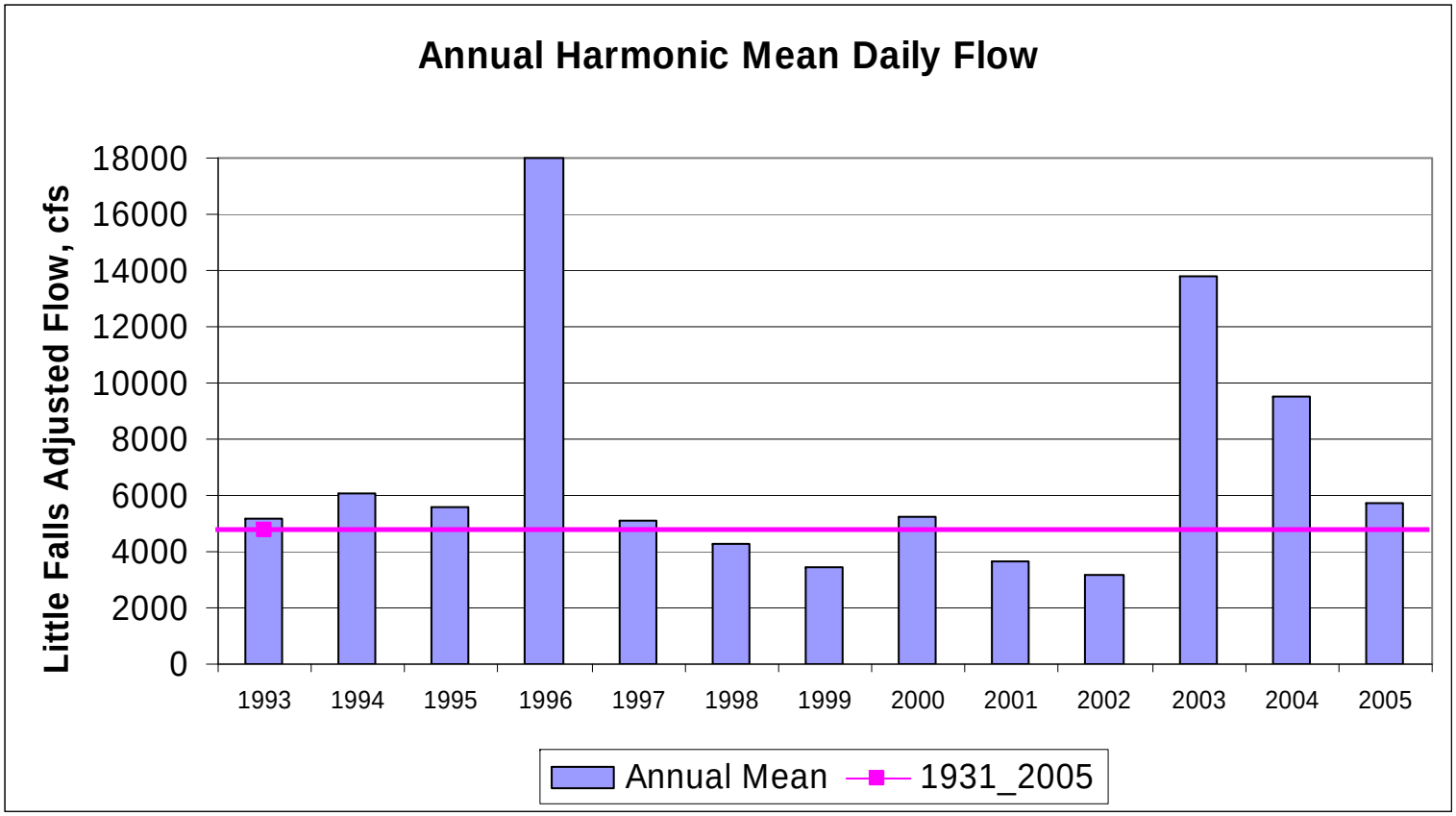

Figure 64. Recent and Historical Annual Mean Flows at Little Falls, VA

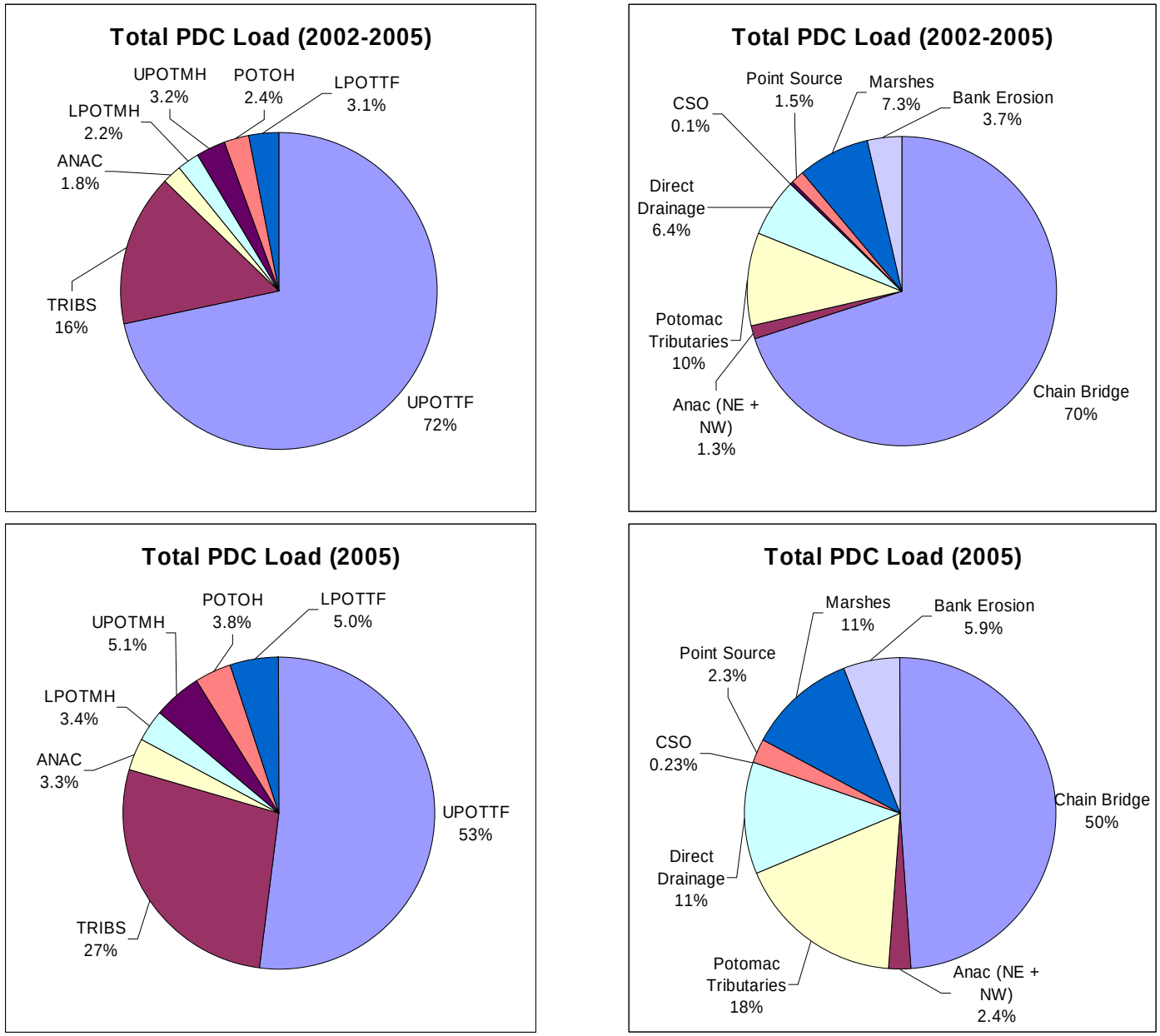

Figure 65. Total PDC Mass Load by Time Period, Spatial Zone and Source Category

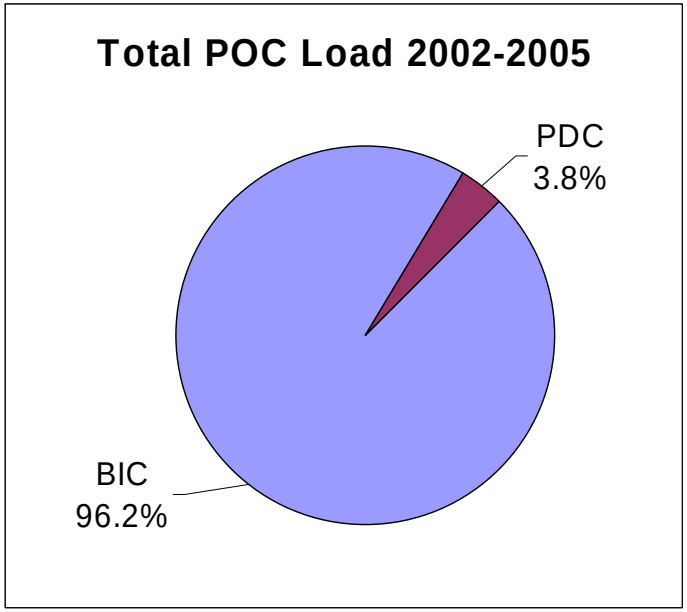

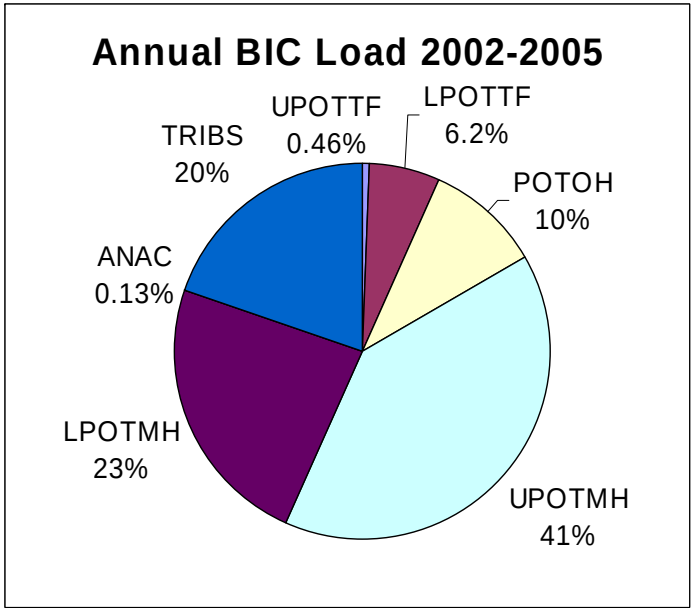

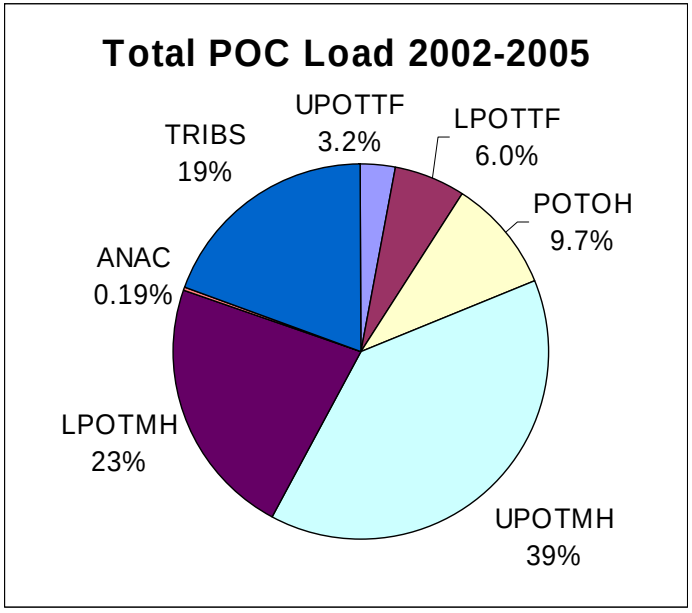

Figure 66. Total POC Mass Load with BIC, PDC and Spatial Zone Components

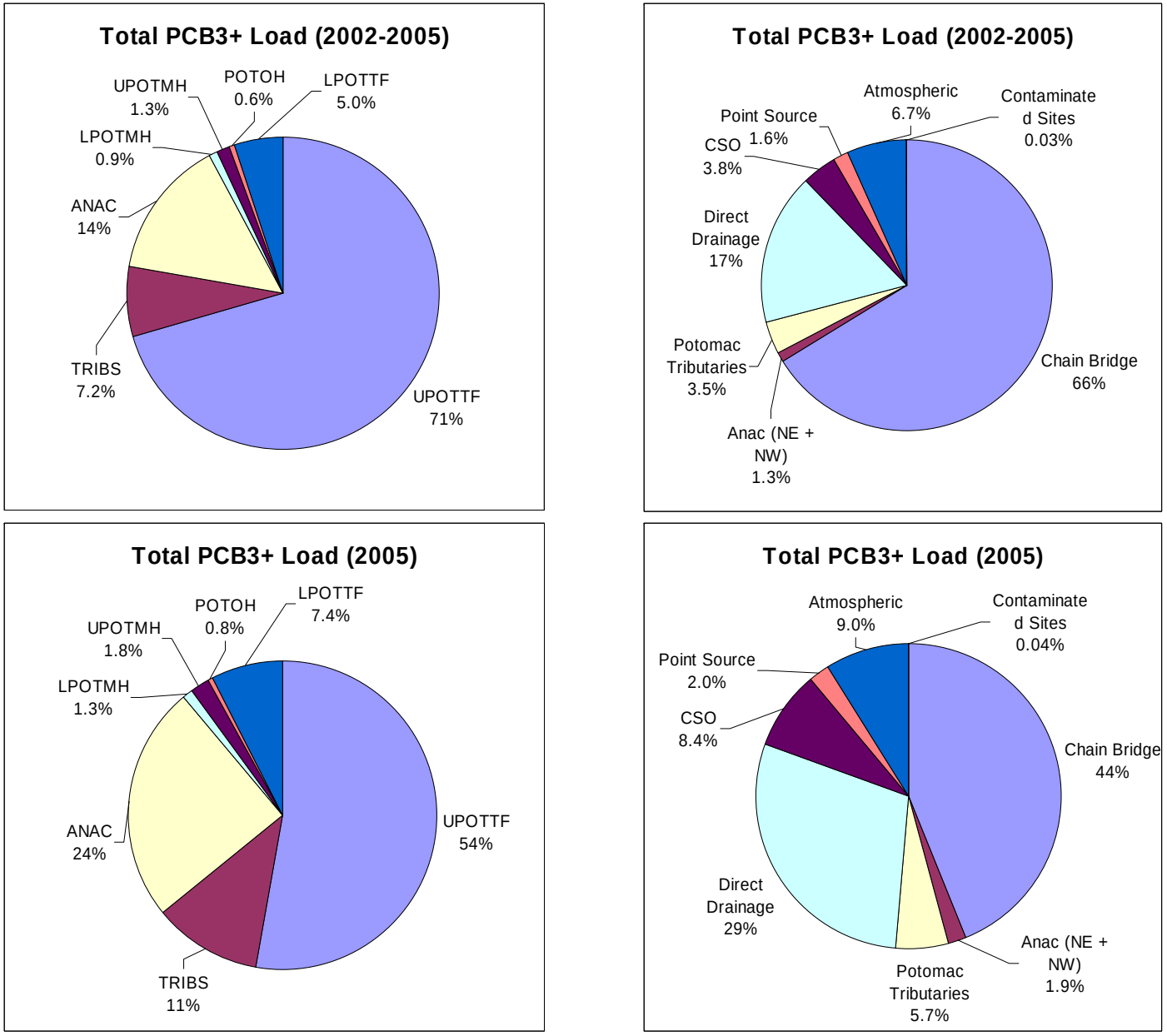

Figure 67. Total PCB3+ Mass Load by Time Period, Spatial Zone and Source Category

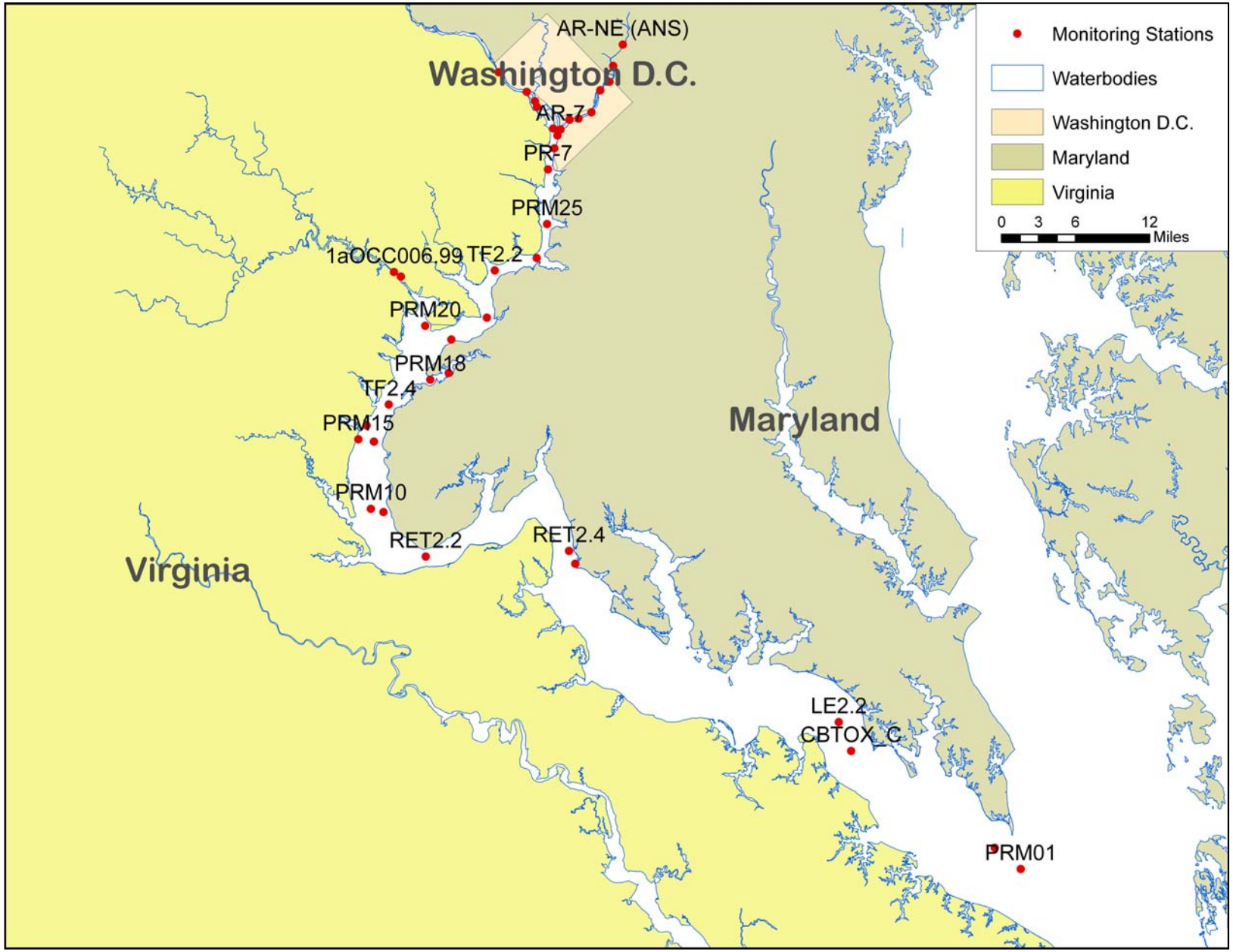

Figure 68. Locations of Water Column Monitoring Stations for Sorbents and PCB3+

Figure 69. Locations of Water Column Monitoring Stations for Sorbents and PCB3+ (Washington DC)

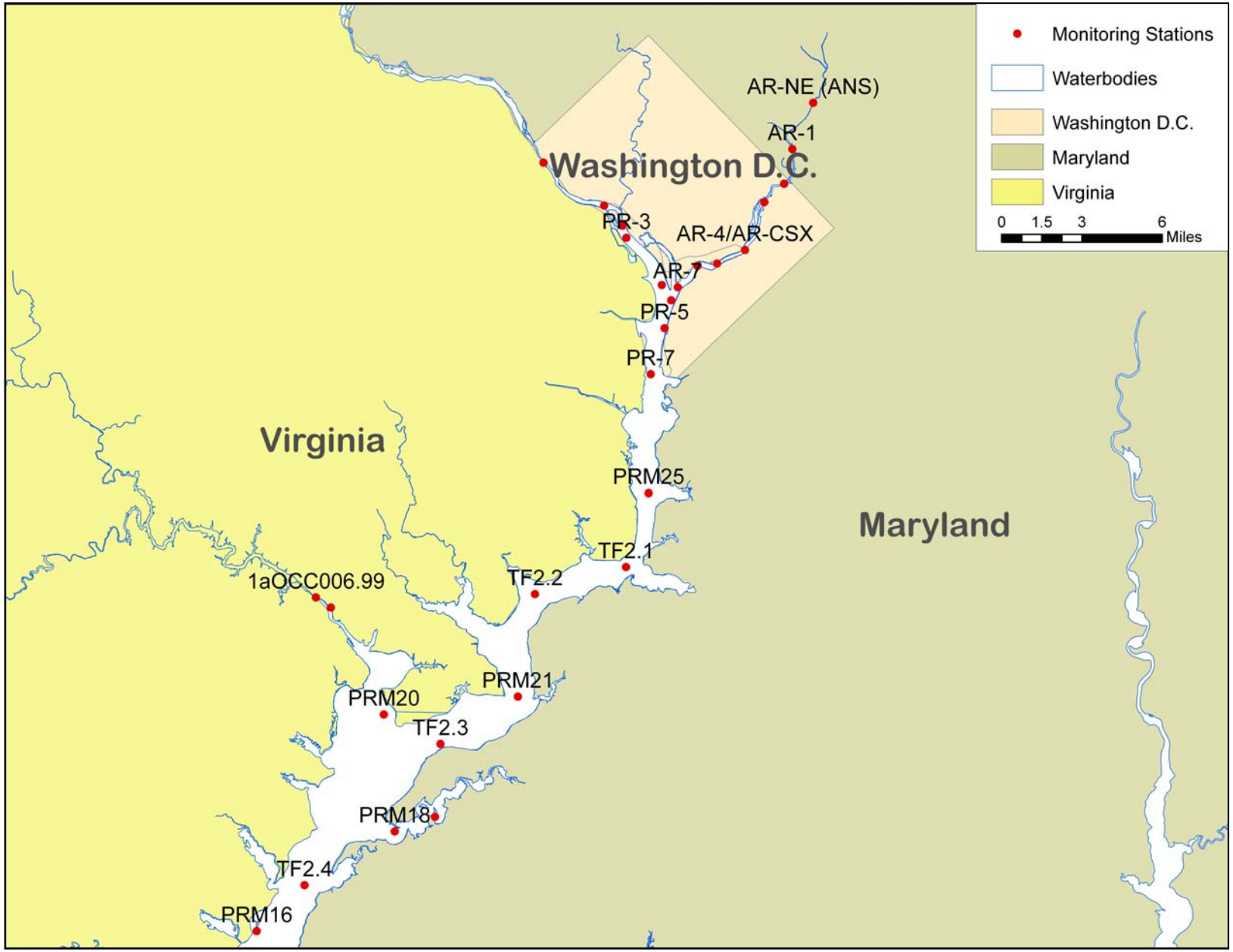

Figure 70. Locations of Water Column Monitoring Stations for Sorbents and PCB3+ (Upper Potomac)

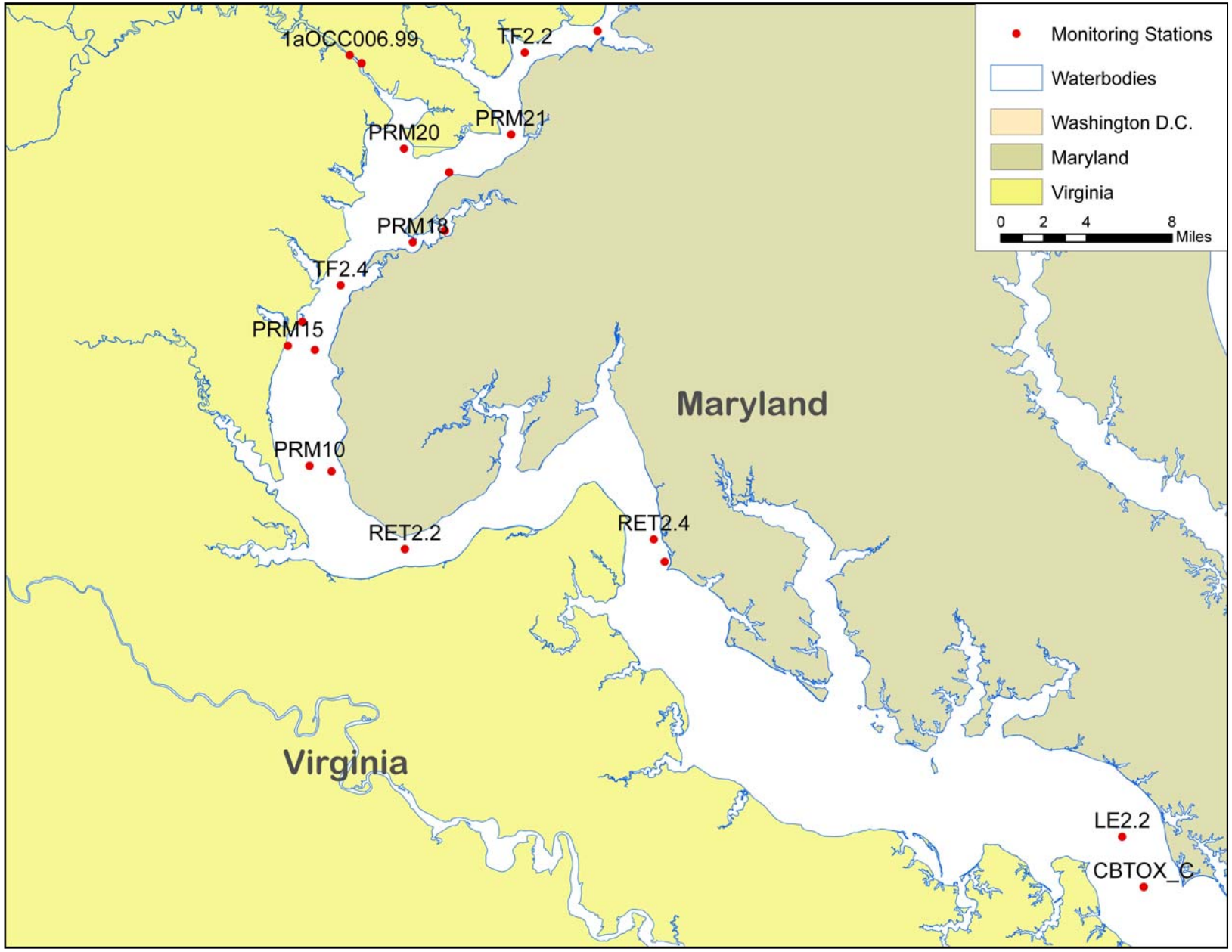

Figure 71. Locations of Water Column Monitoring Stations for Sorbents and PCB3+ (Middle Potomac)

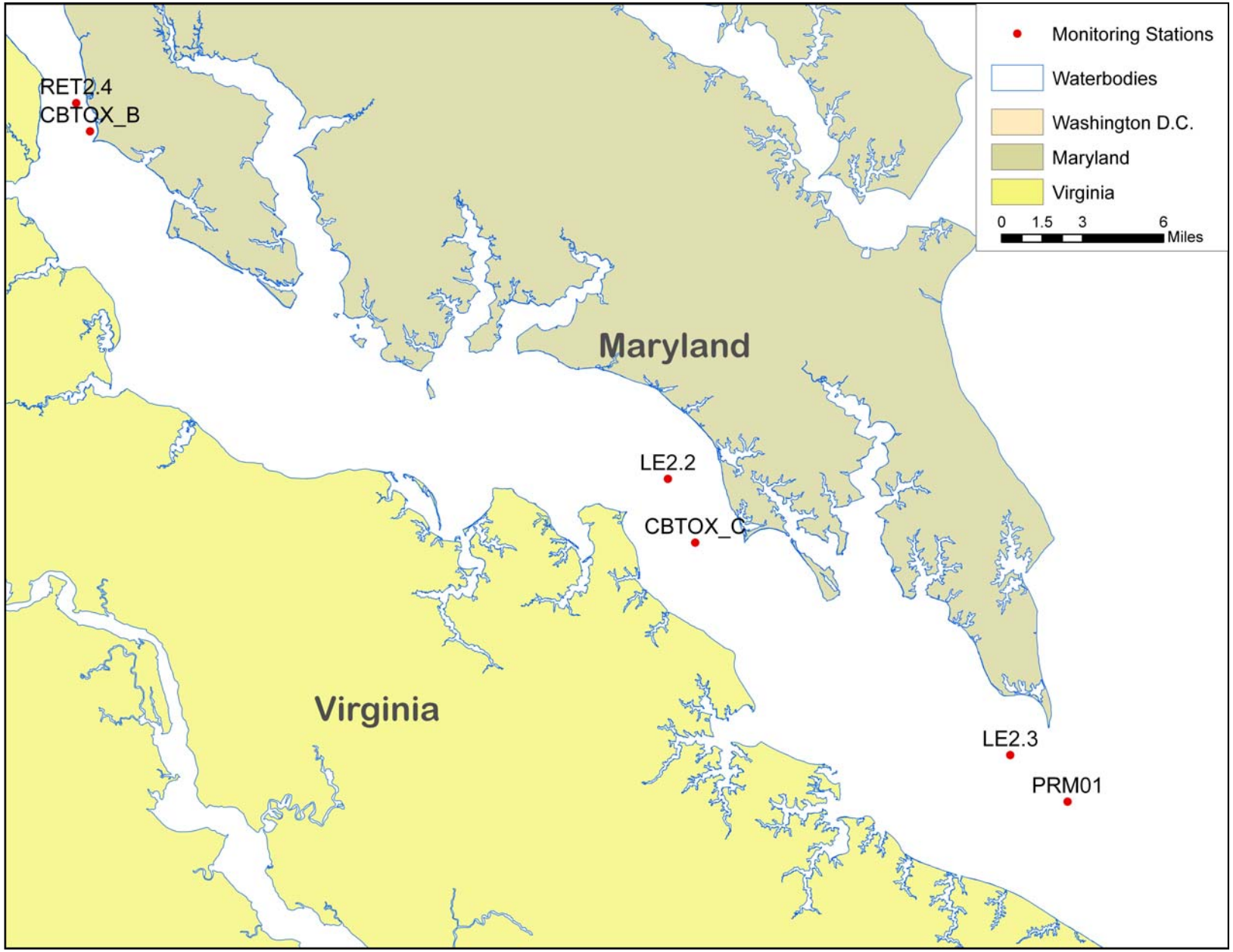

Figure 72. Locations of Water Column Monitoring Stations for Sorbents and PCB3+ (Lower Potomac)

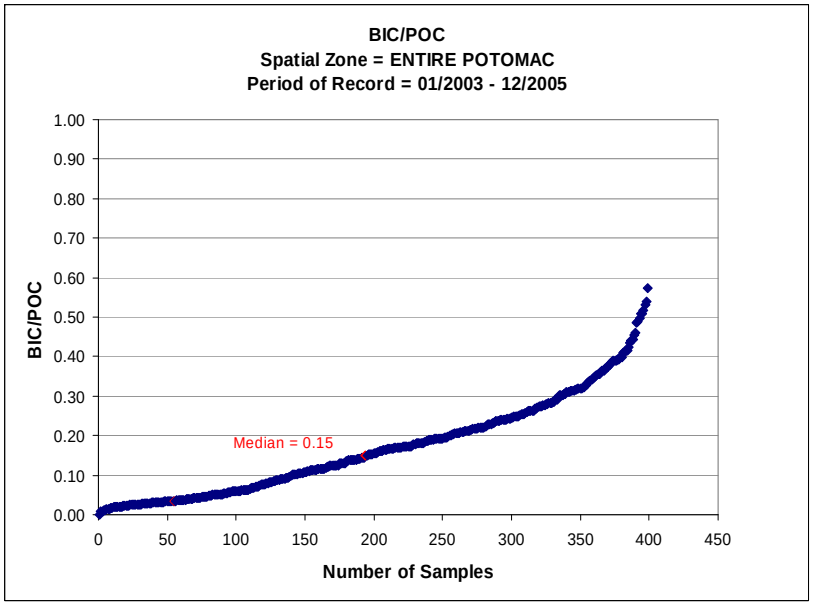

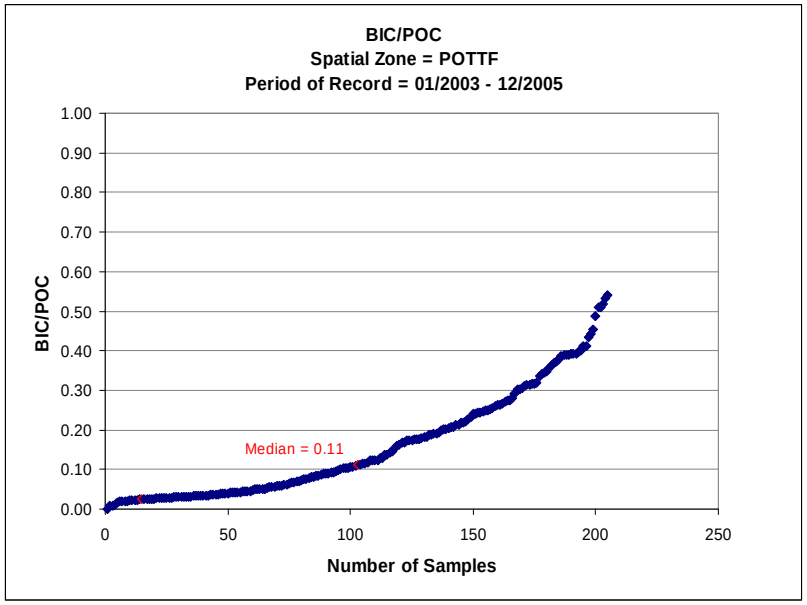

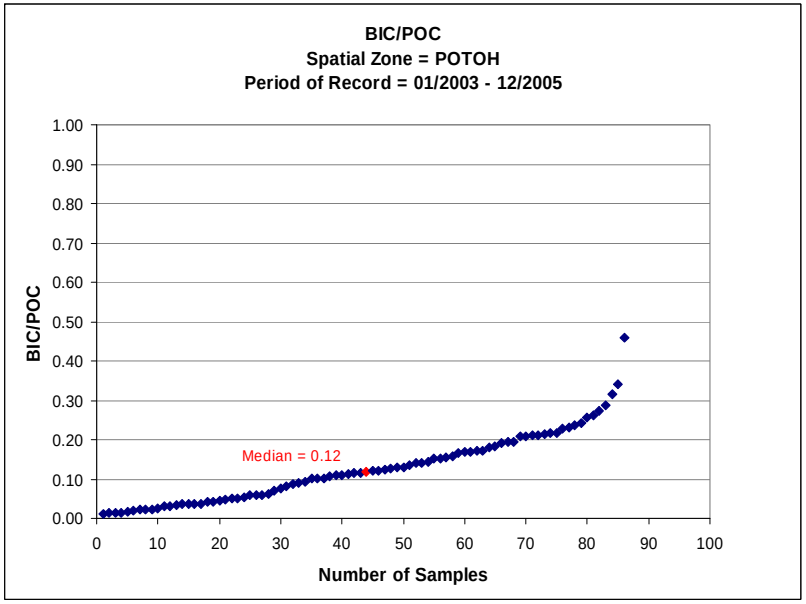

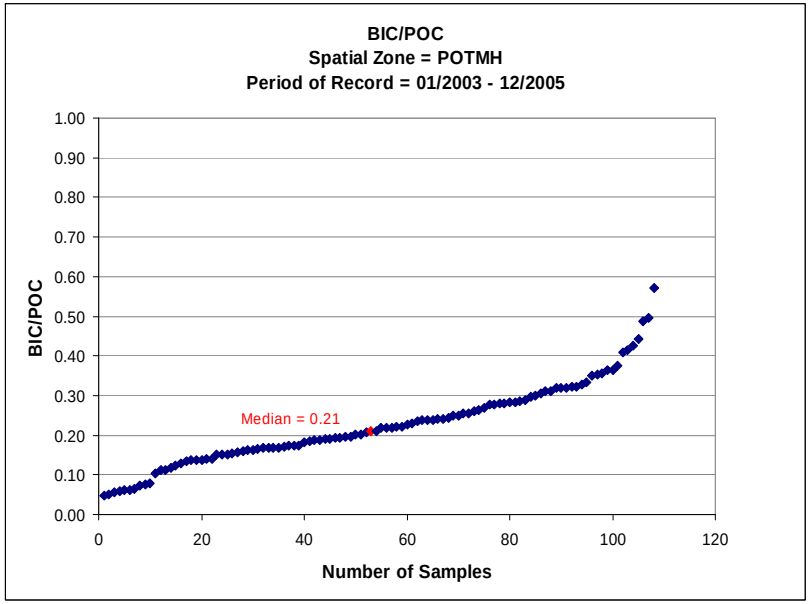

Figure 73. Derived BIC Calibration Targets as Fractions of POC in the Potomac

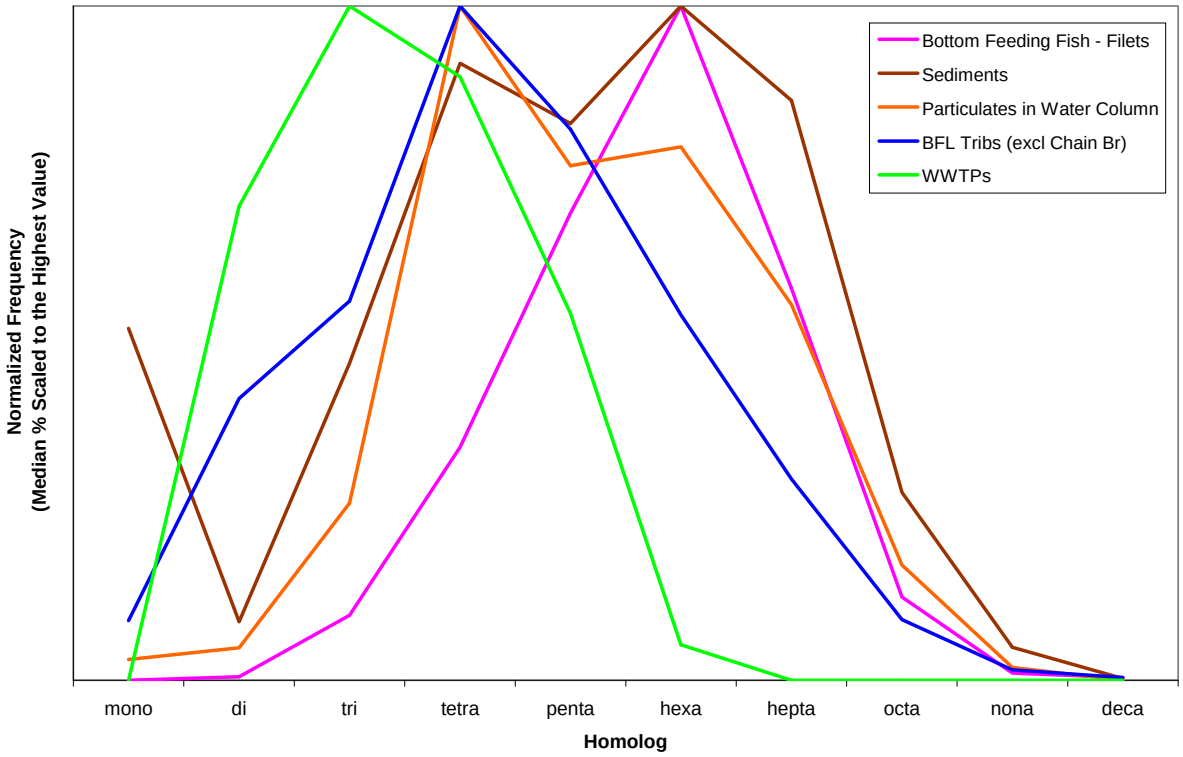

Figure 74. Normalized Frequency Distributions for Homologs in Different Media in the Potomac and Anacostia (Data from ICPRB)

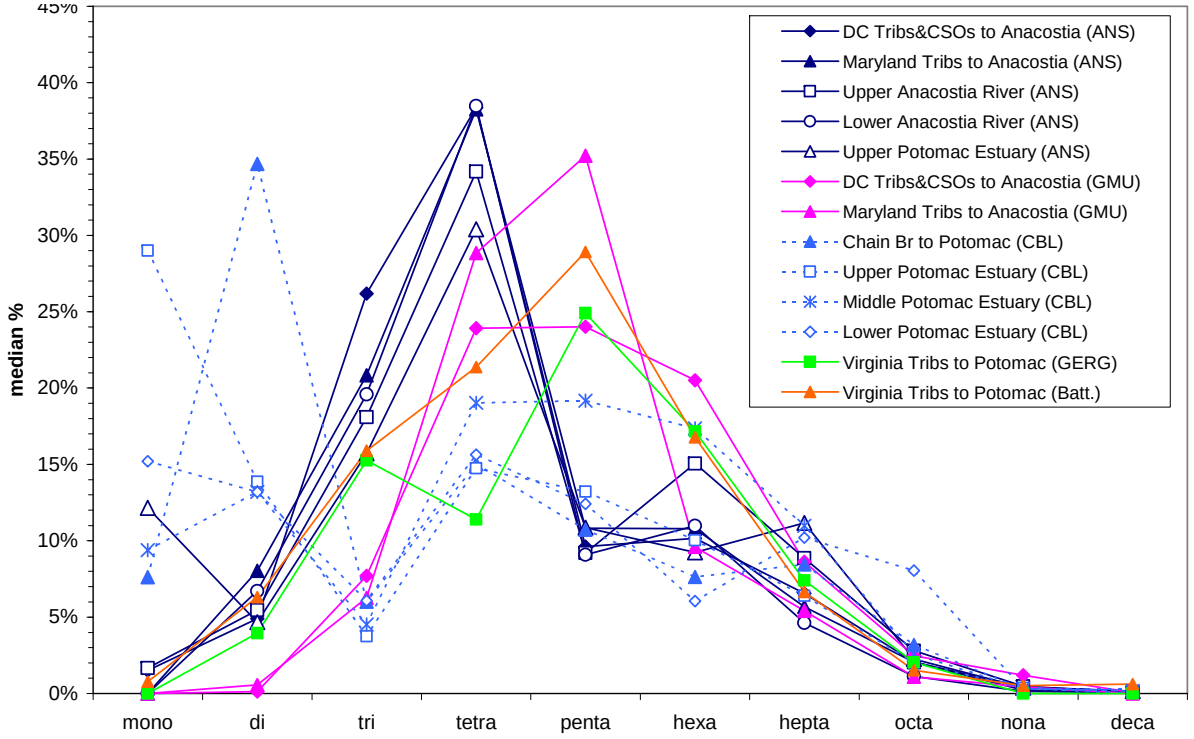

Figure 75. Median Distributions of Homologs in Total PCBs in the Potomac and Anacostia (Data from ICPRB)

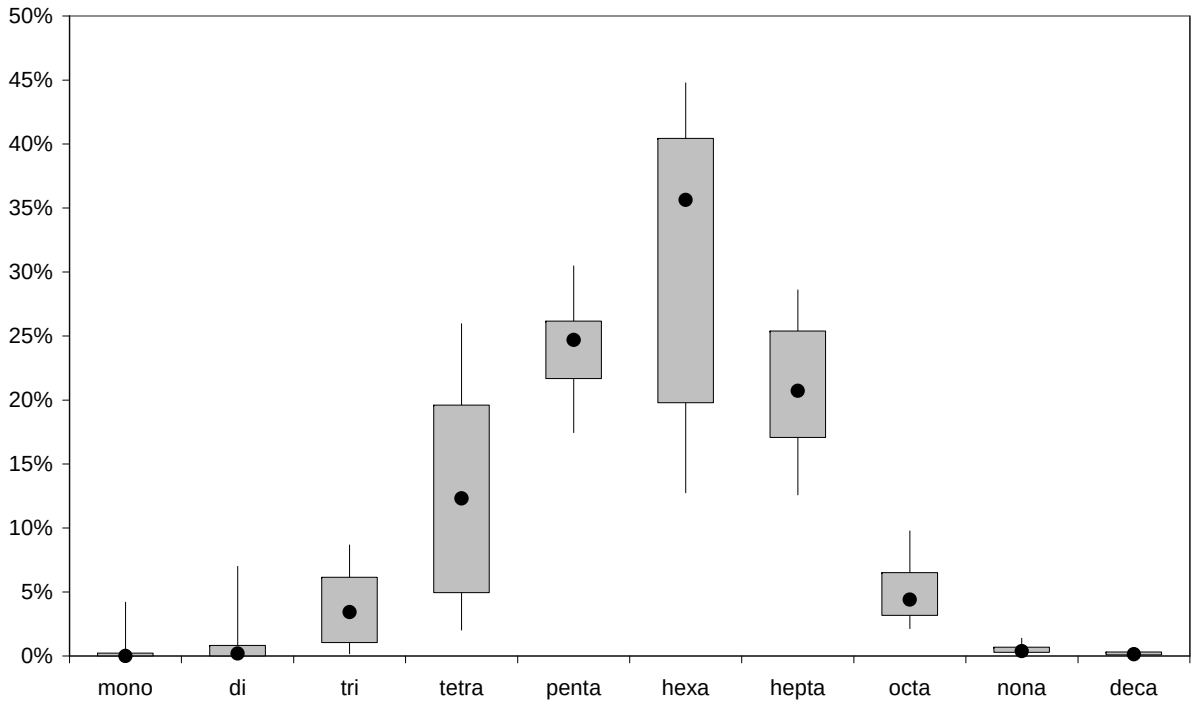

Figure 76. Median Distributions of Homologs in Total PCBs in Fish Filets of Bottom Feeders in the Potomac and Anacostia (Data from ICPRB)

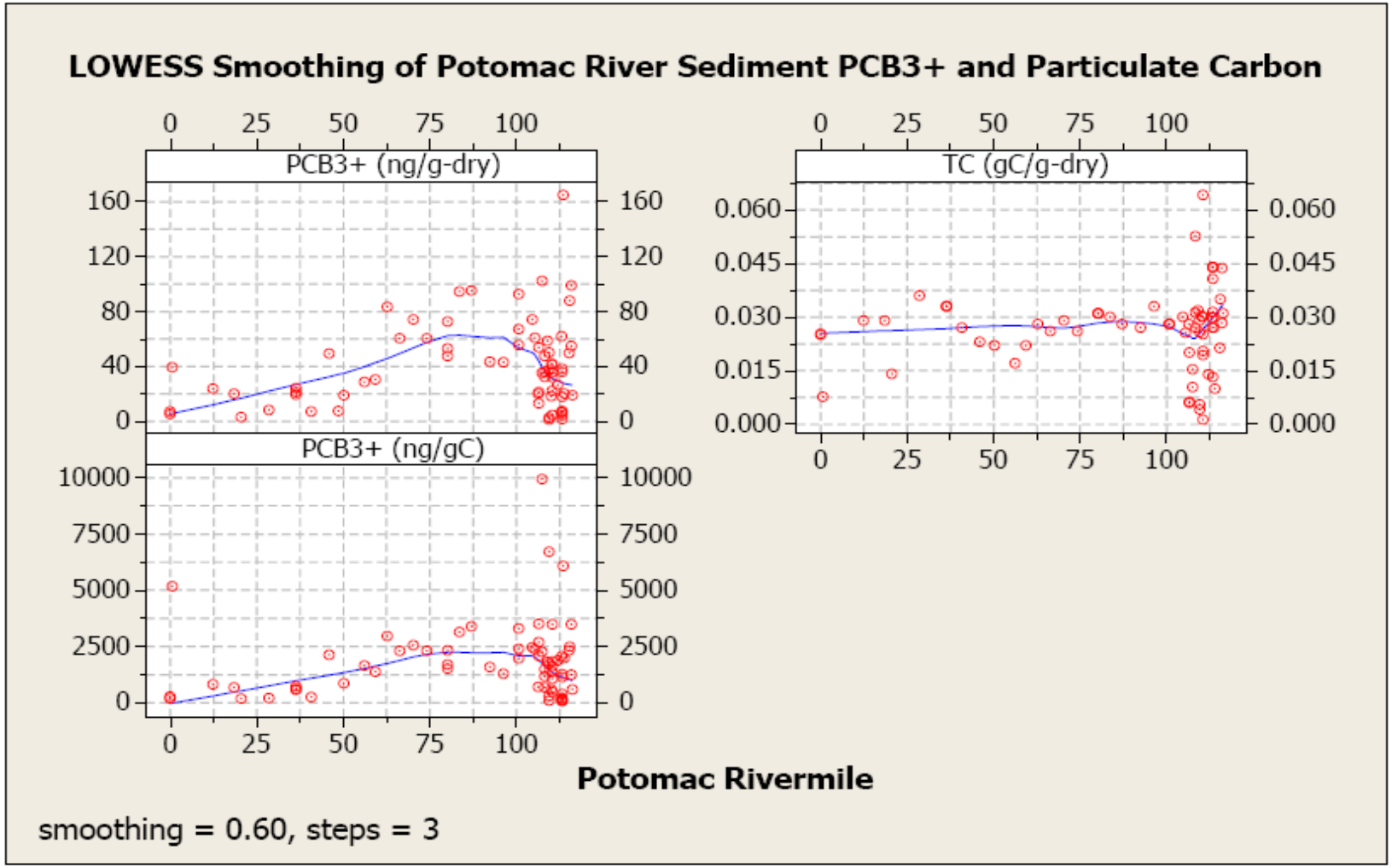

Figure 77. Sediment Data and Spatially-Smoothed LOWESS Results for Sediment Initial Conditions in the Potomac

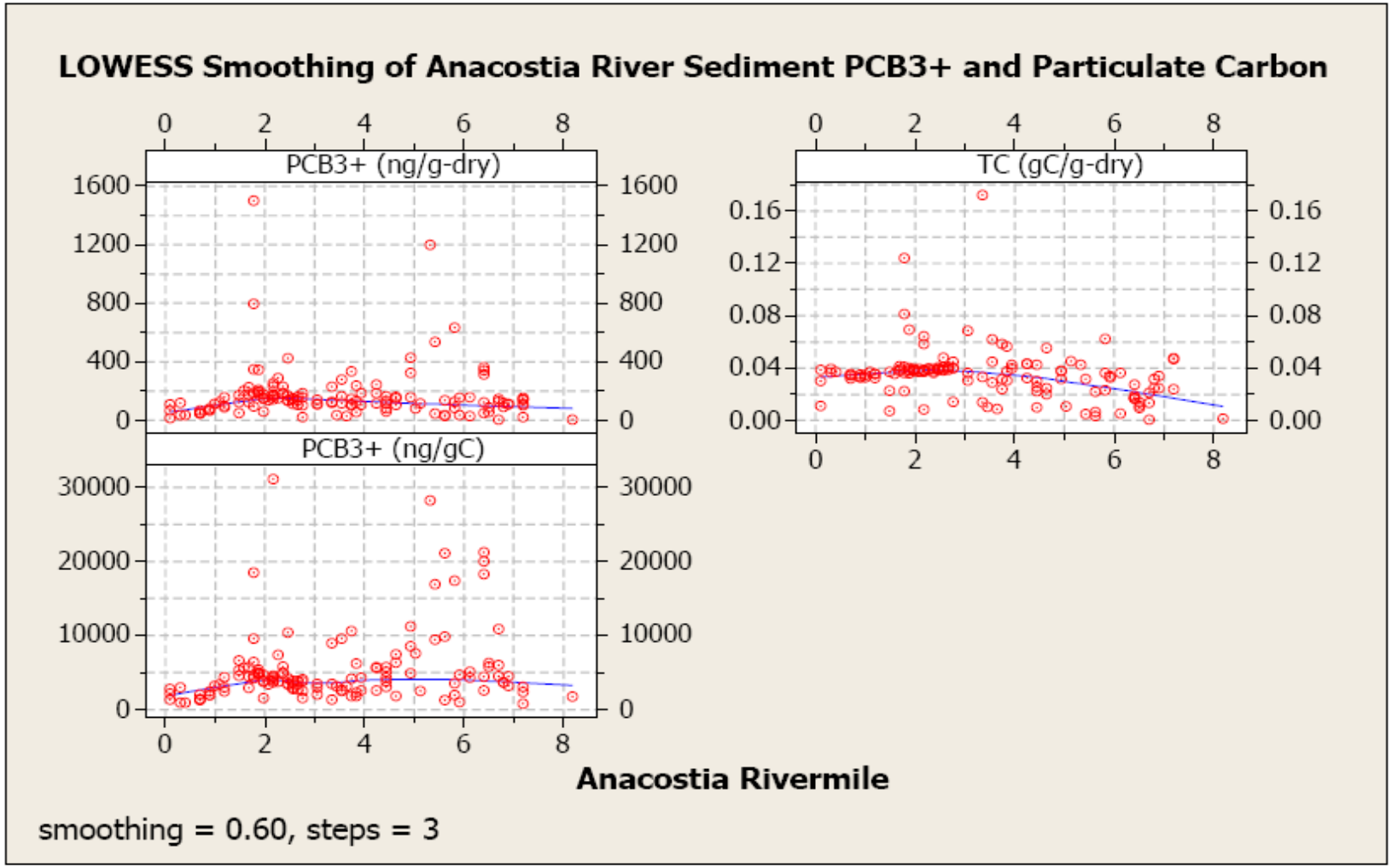

Figure 78. Sediment Data and Spatially-Smoothed LOWESS Results for Sediment Initial Conditions in the Anacostia

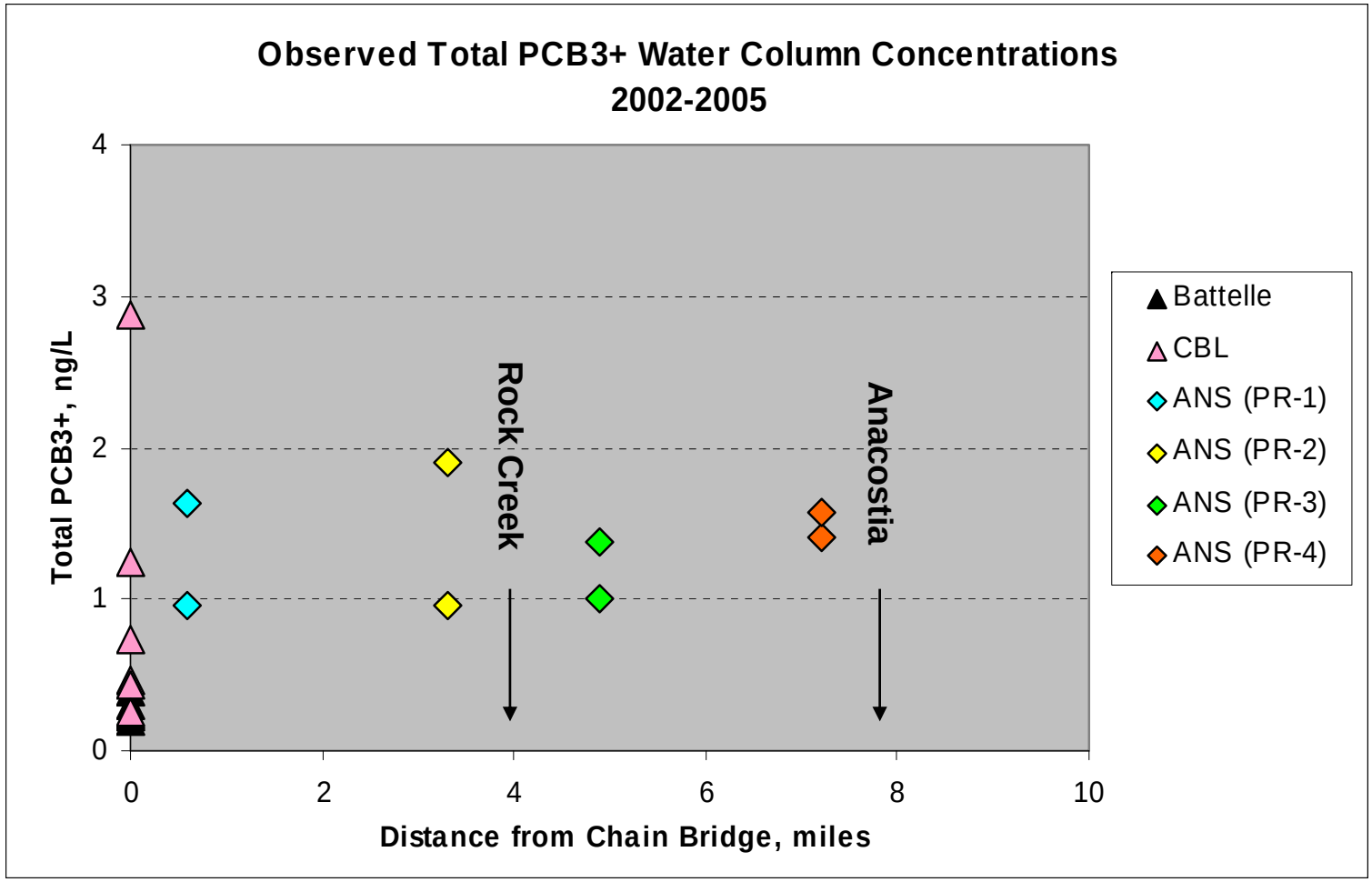

Figure 79. Reported Observations for Total PCB3+ in the Vicinity of Chain Bridge

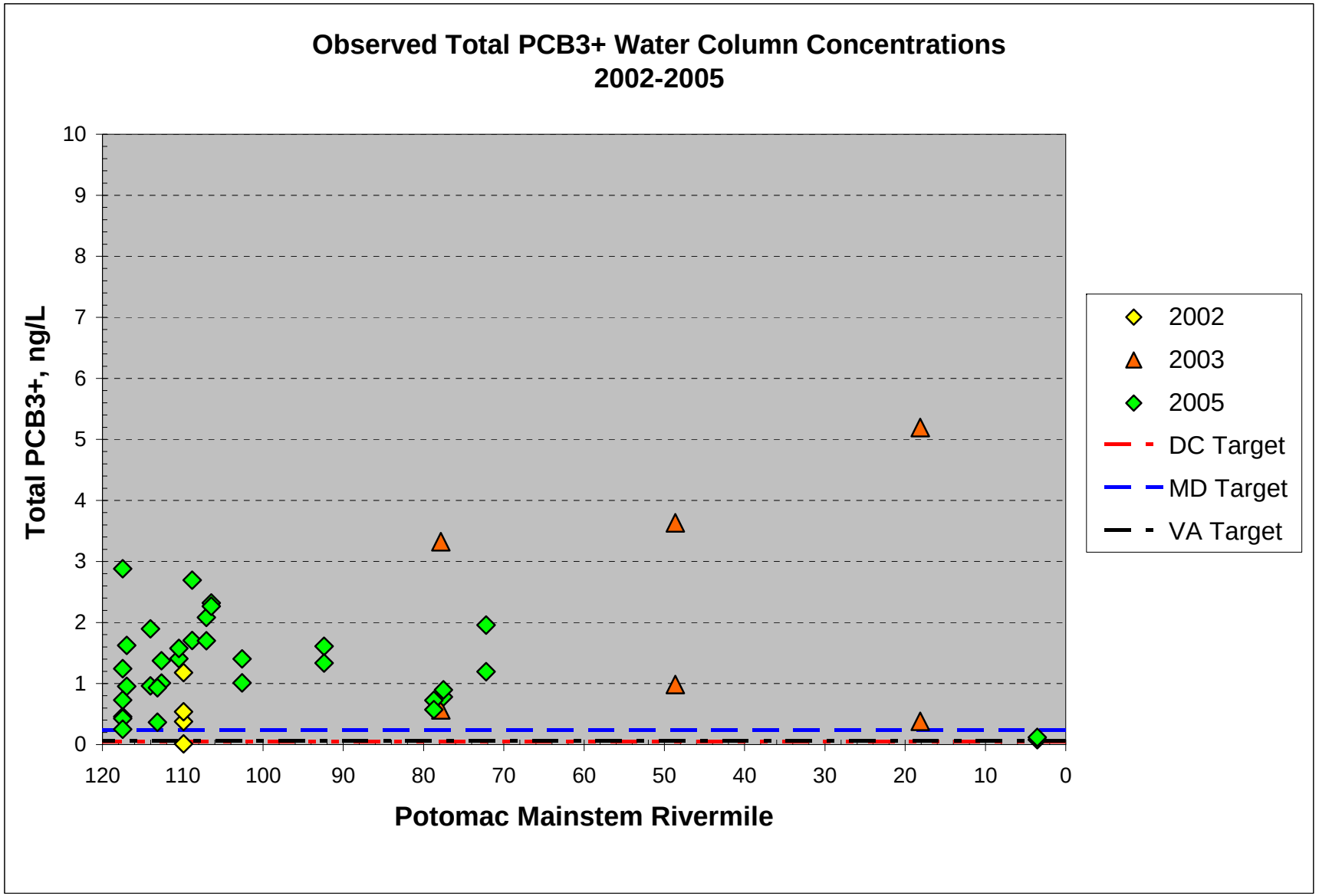

Figure 80. Reported Observations for Total PCB3+ in the Mainstem Potomac

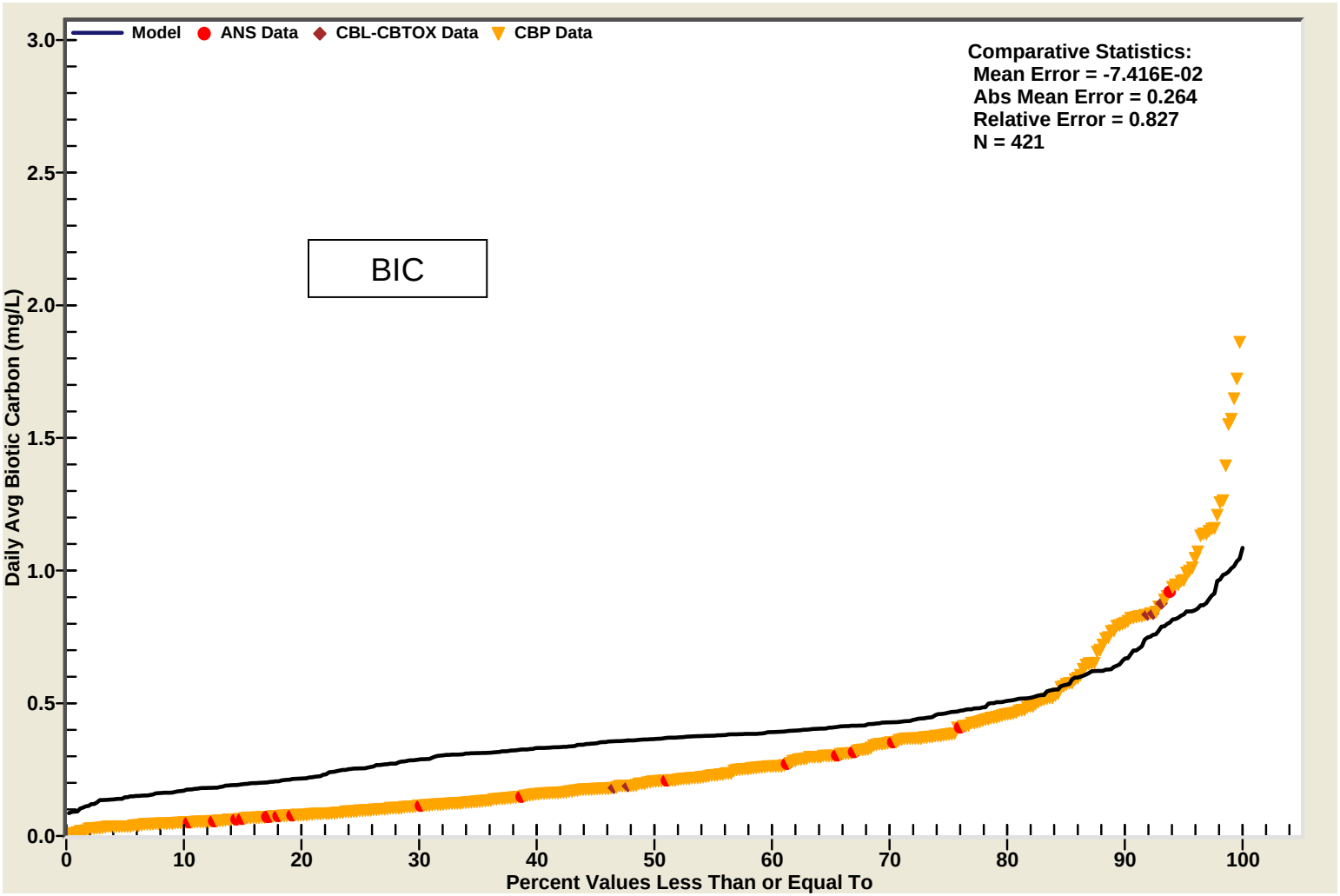

Figure 81. CFD for Computed and Observed Daily Average BIC (Whole Potomac)

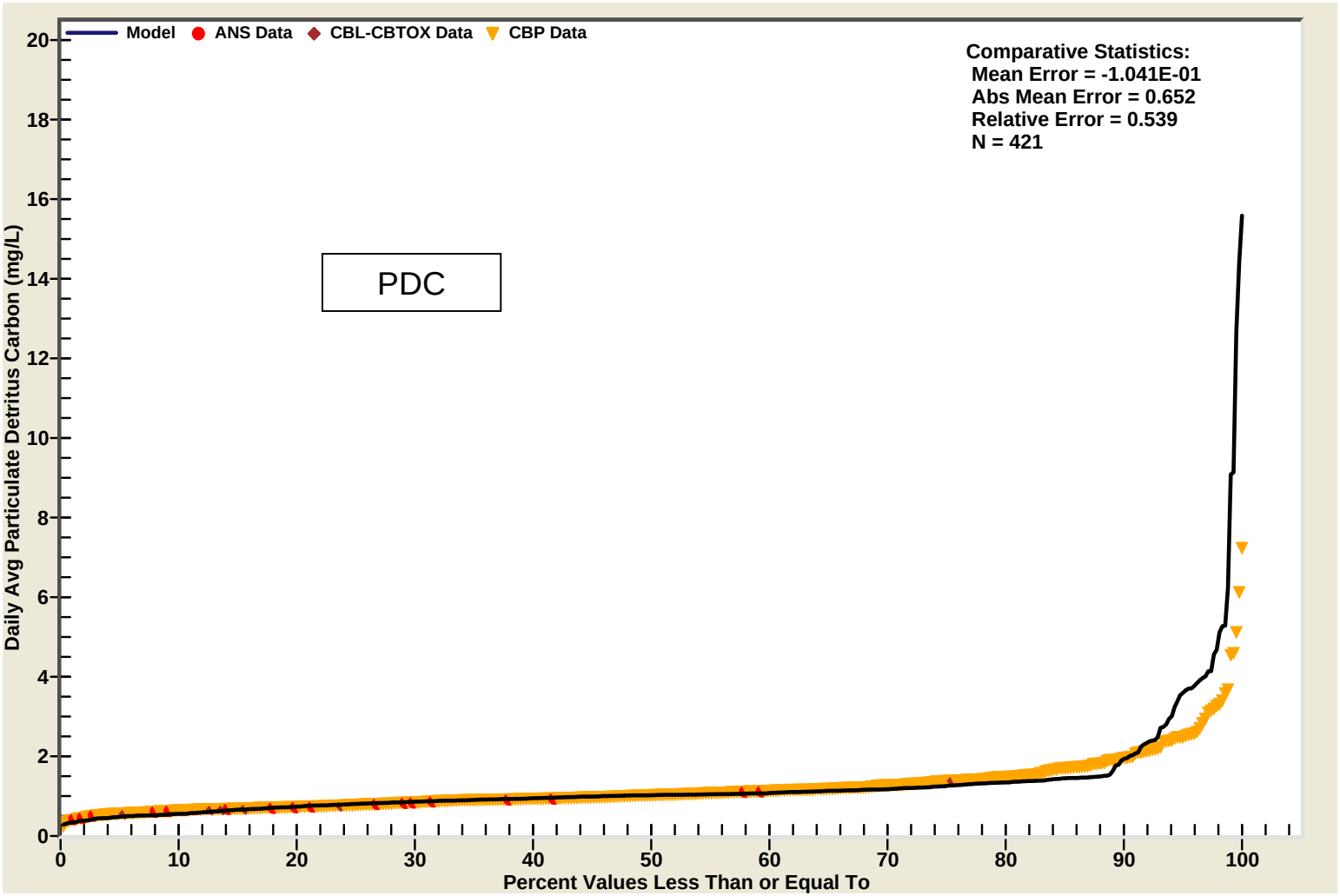

Figure 82. CFD for Computed and Observed Daily Average PDC (Whole Potomac)

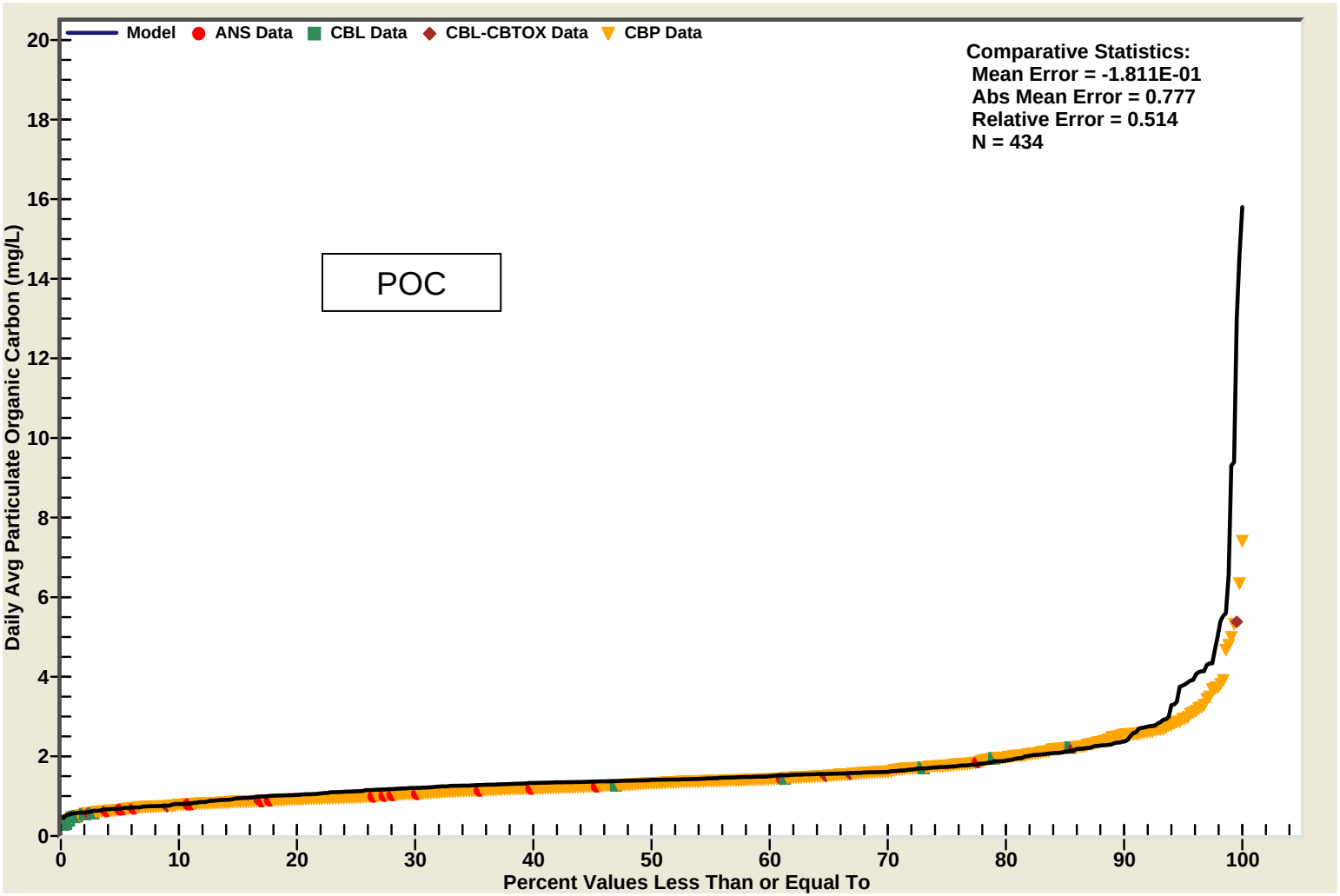

Figure 83. CFD for Computed and Observed Daily Average Derived POC (Whole Potomac)

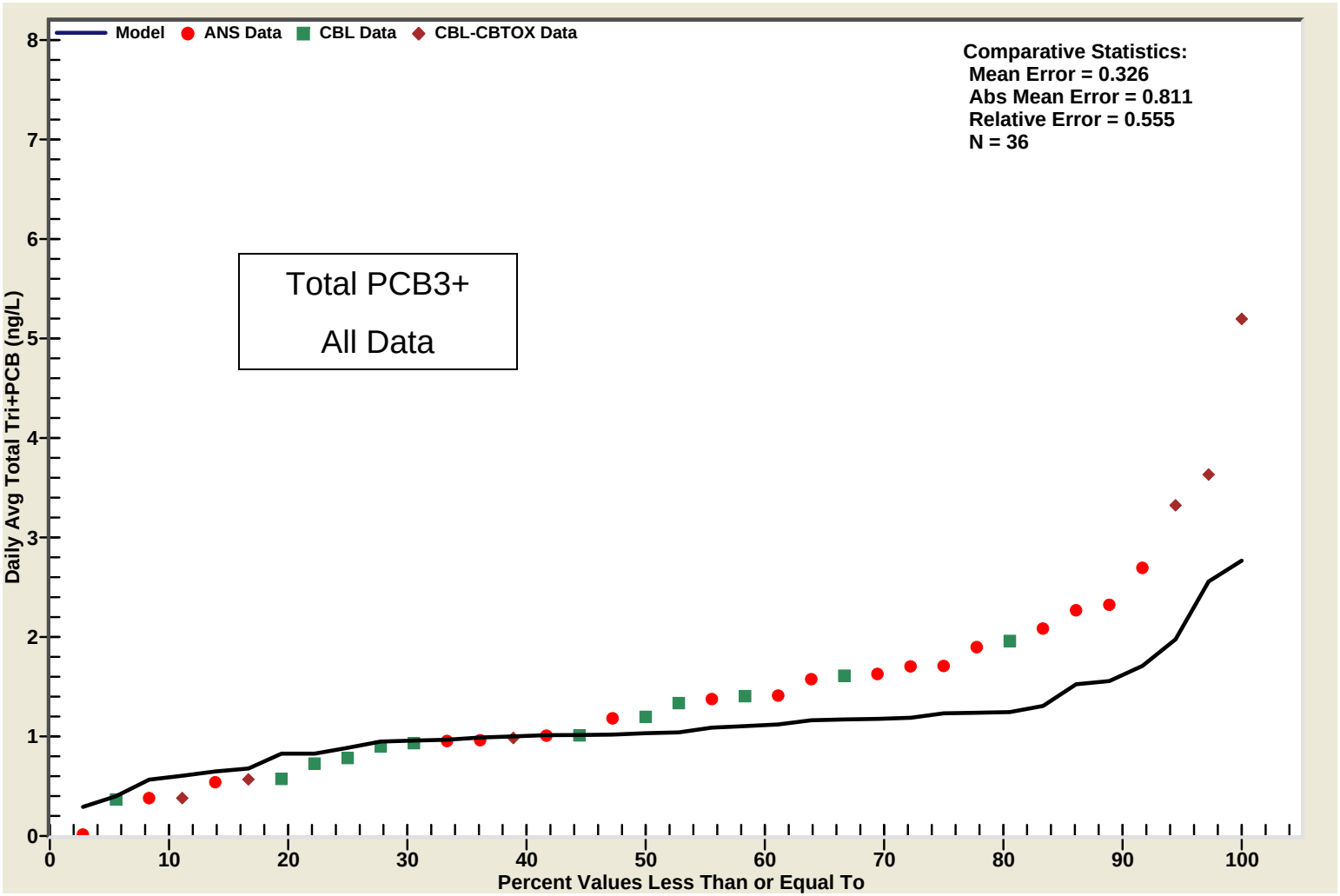

Figure 84. CFD for Computed and Observed Daily Average Total PCB3+ (Whole Potomac – All Data)

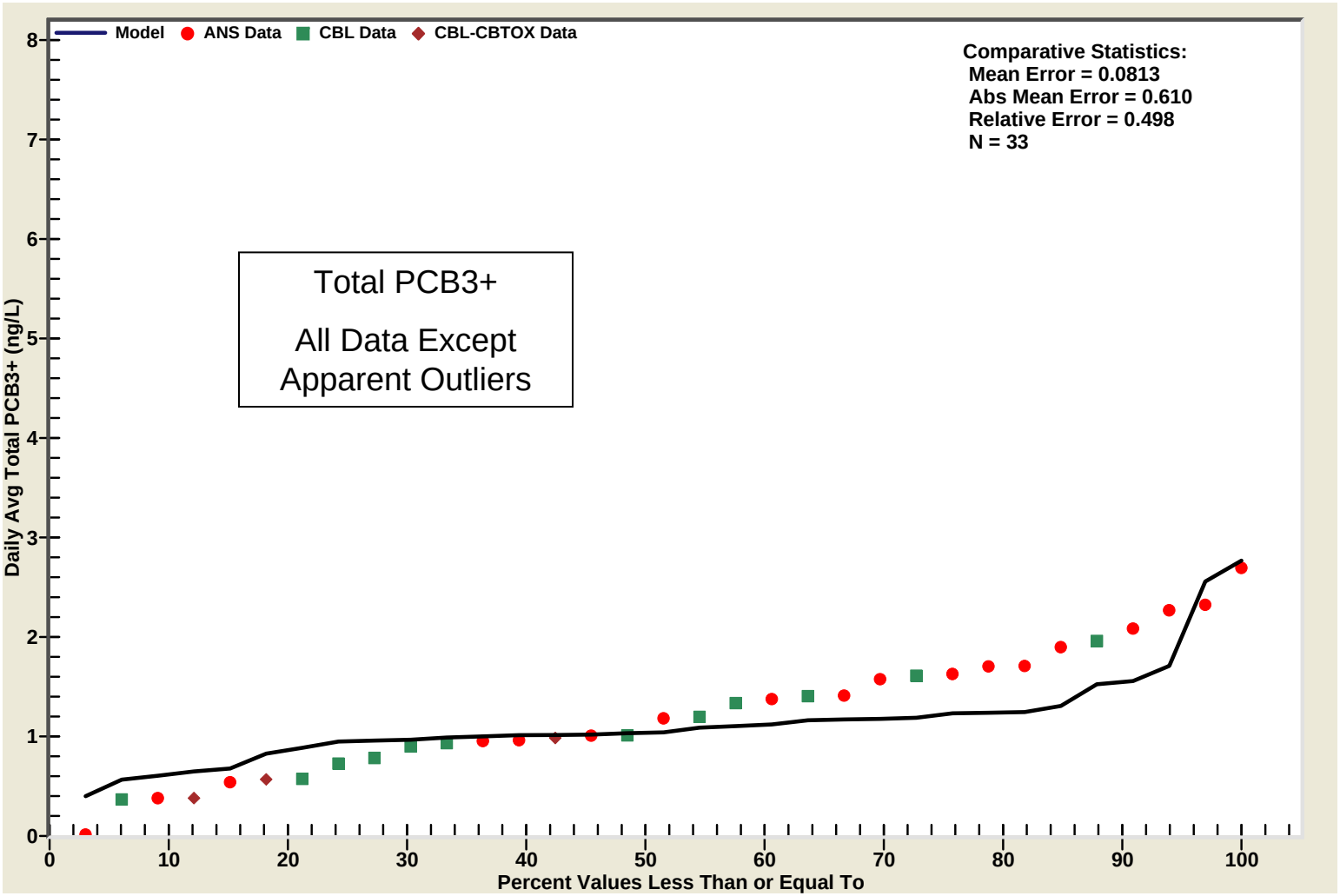

Figure 85. CFD for Computed and Observed Daily Average Total PCB3+ (Whole Potomac – Excluding Apparent Outliers)

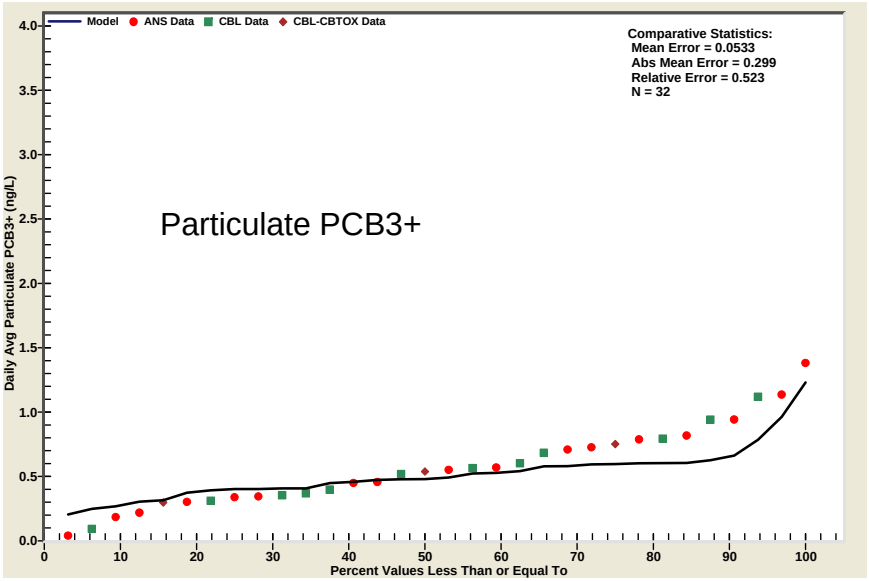

Figure 86. CFDs for Computed and Observed Daily Average Particulate and Dissolved PCB3+ (Whole Potomac)

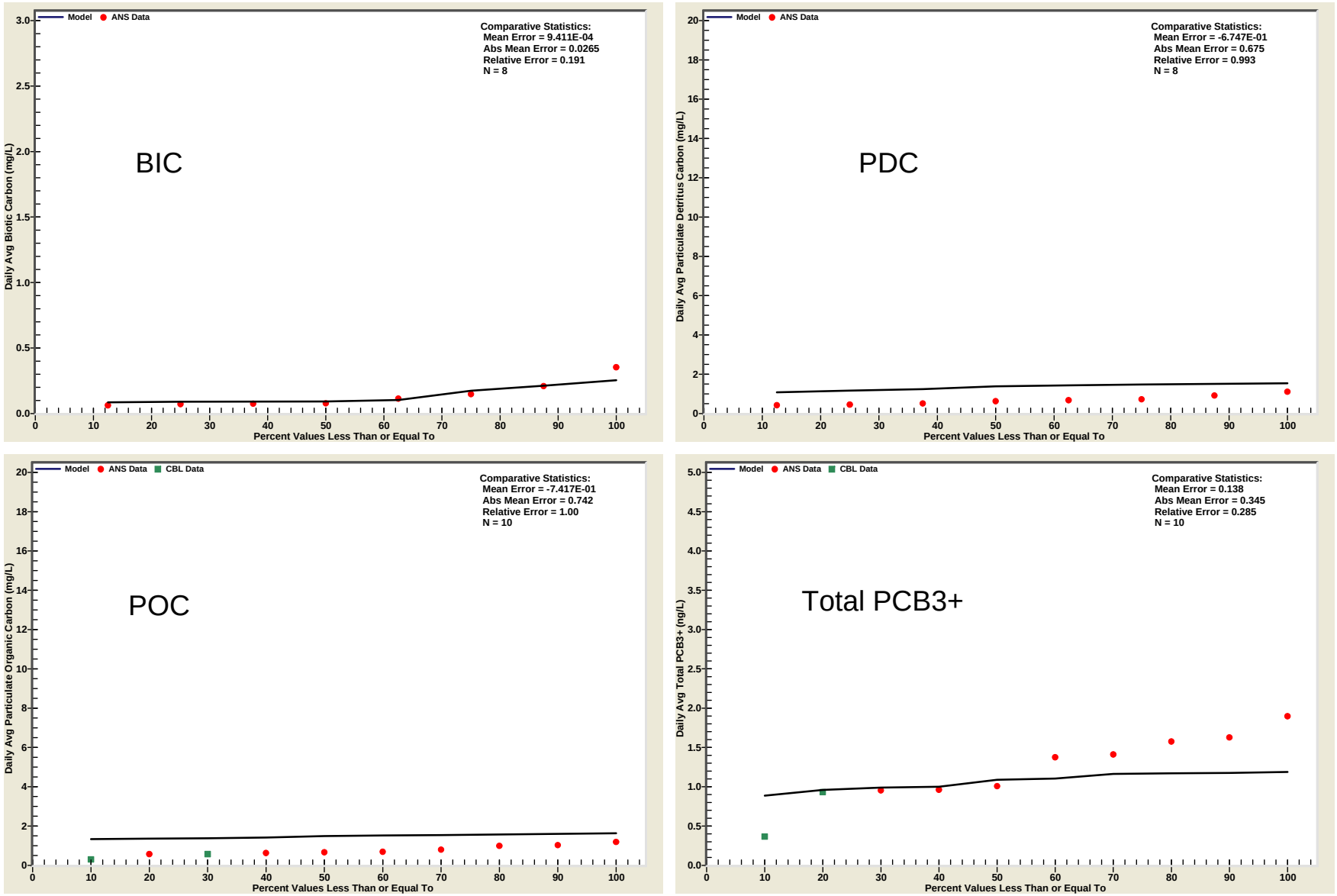

Figure 87. CFDs for Computed and Observed Daily Average Sorbents and PCB3+ (UPOTTF)

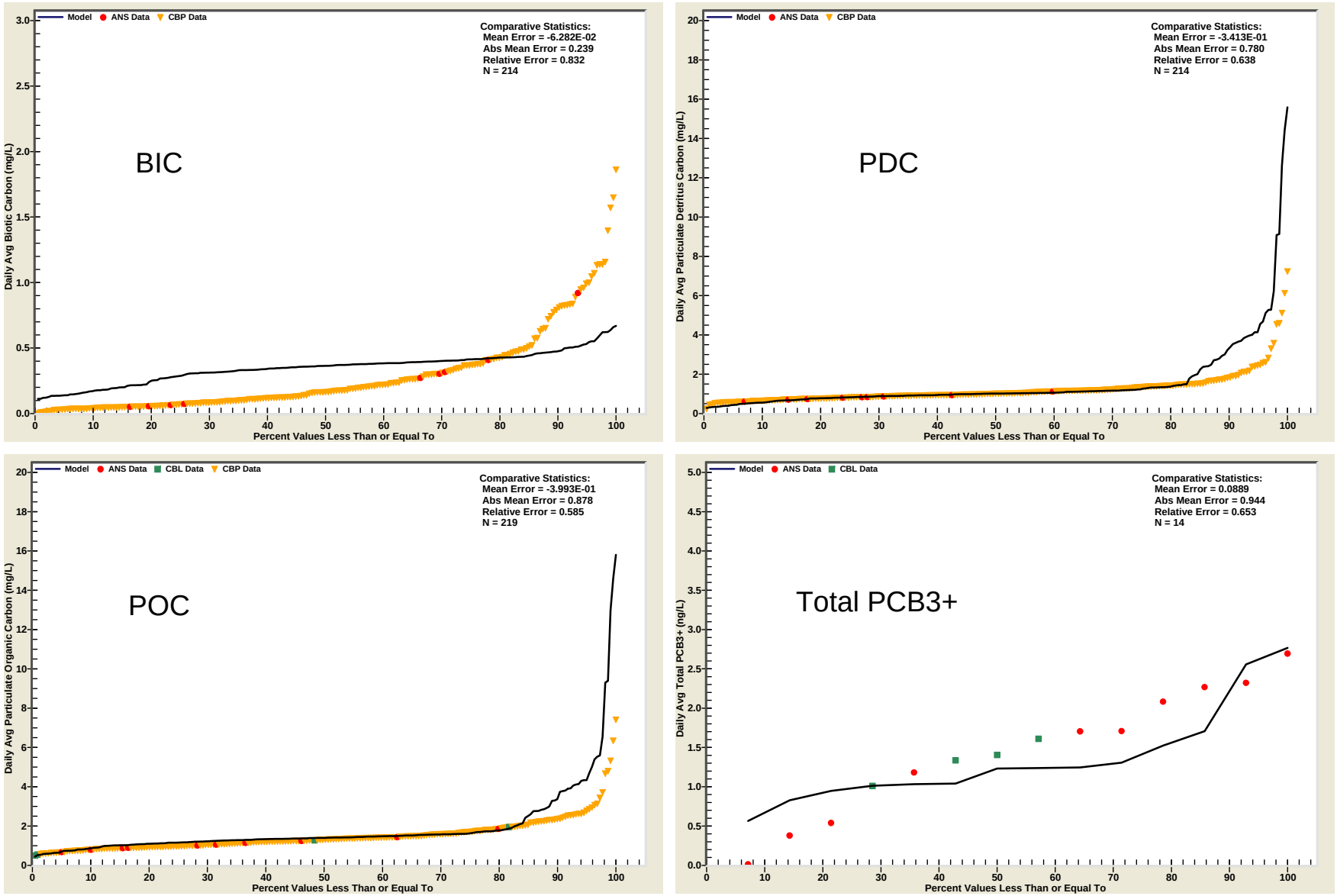

Figure 88. CFDs for Computed and Observed Daily Average Sorbents and PCB3+ (LPOTTF)

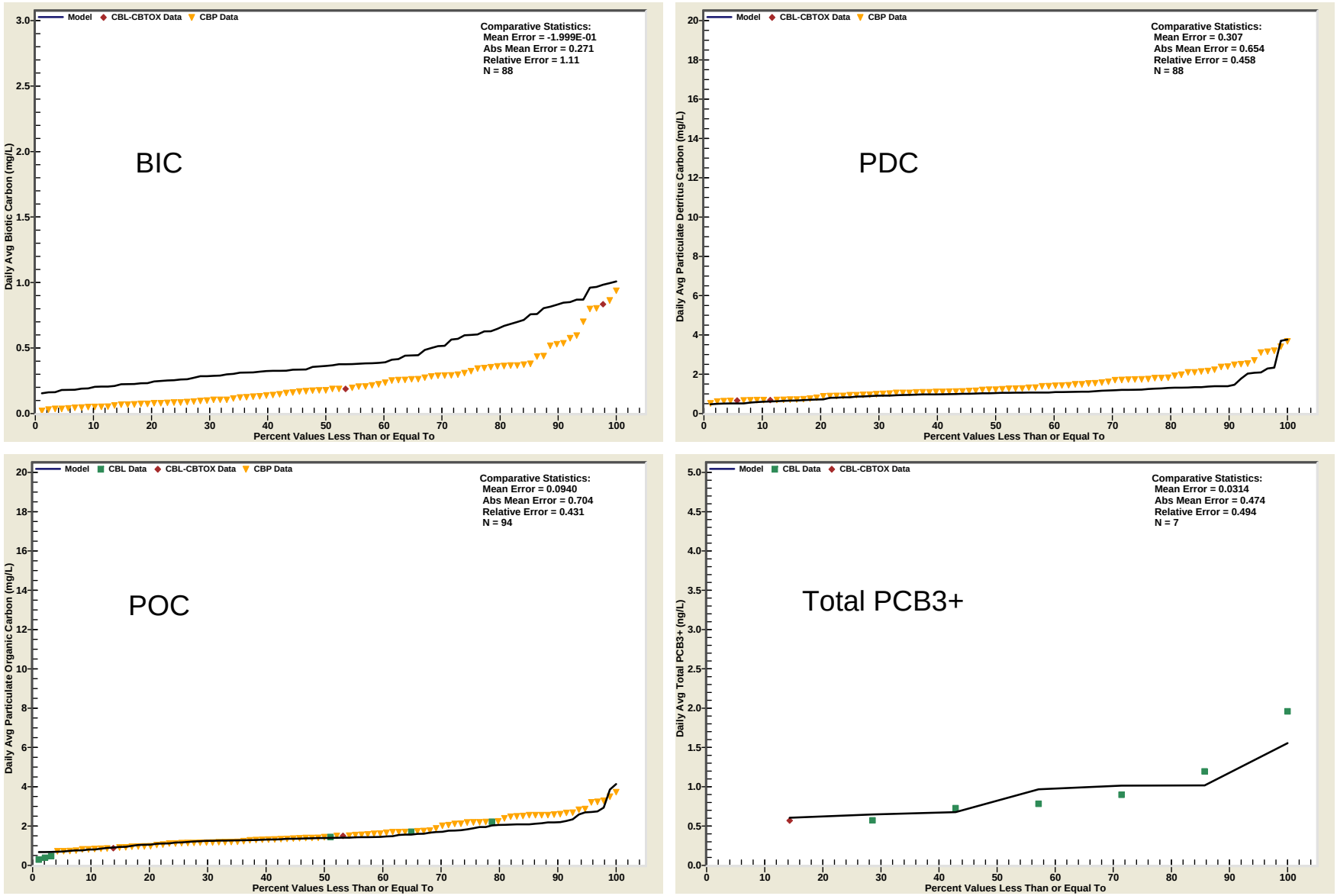

Figure 89. CFDs for Computed and Observed Daily Average Sorbents and PCB3+ (POTOH)

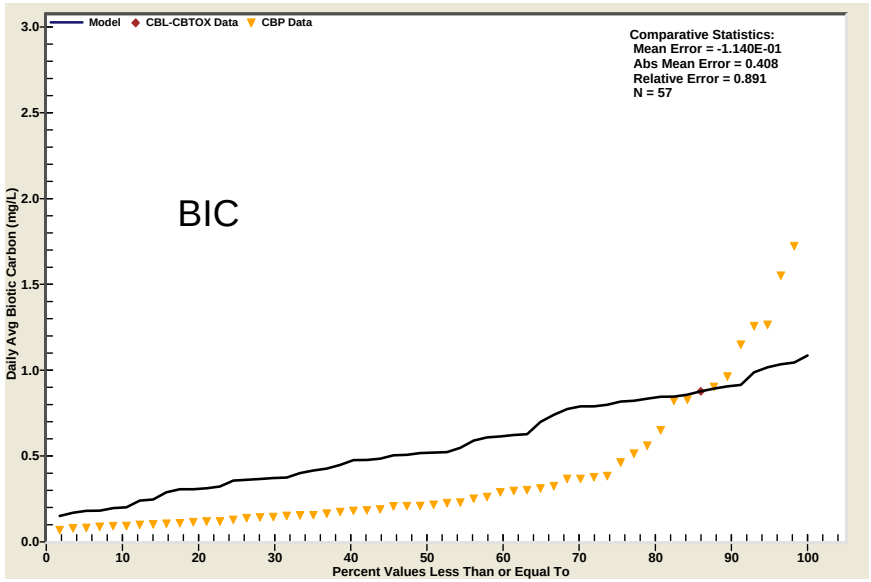

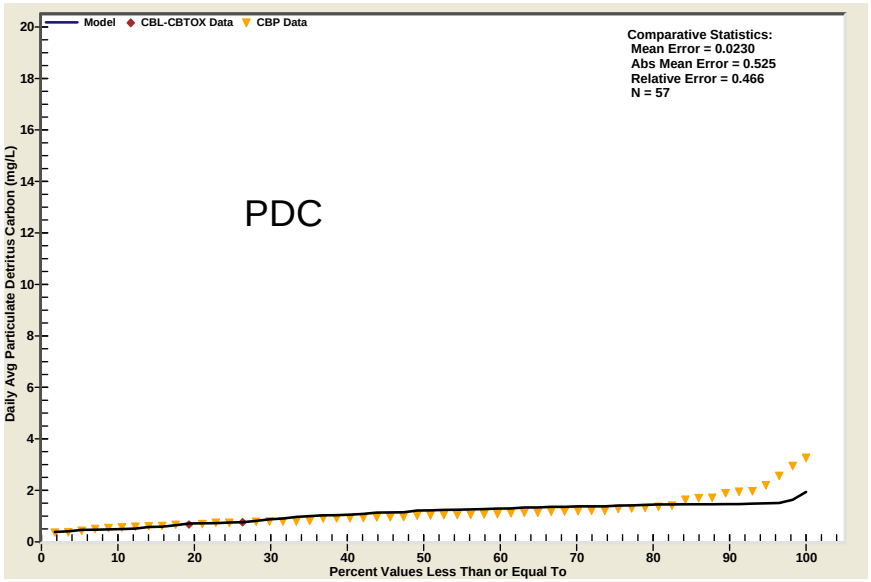

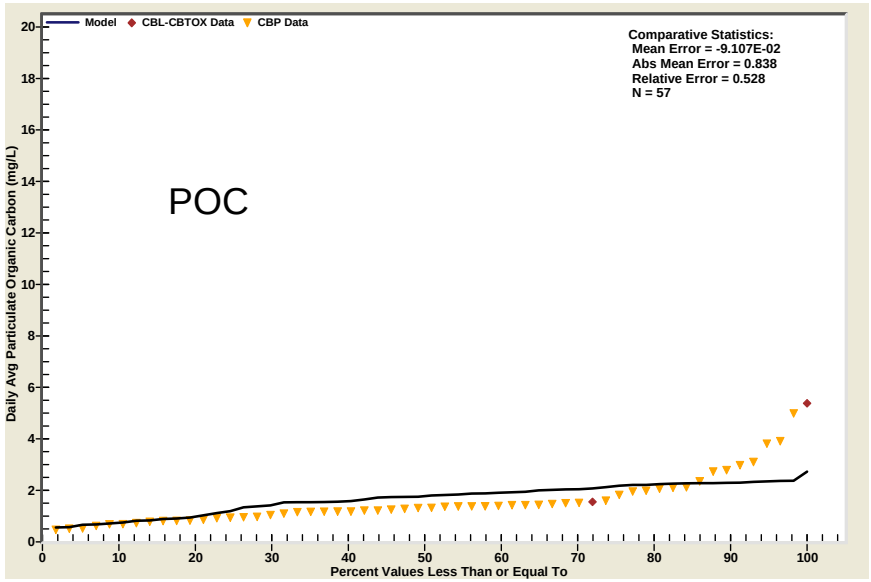

Figure 90. CFDs for Computed and Observed Daily Average Sorbents (UPOTMH)

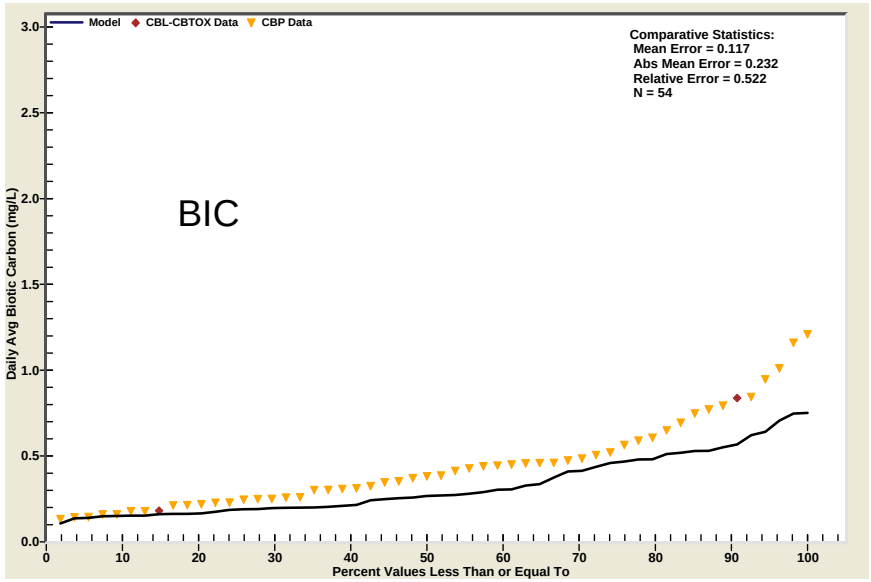

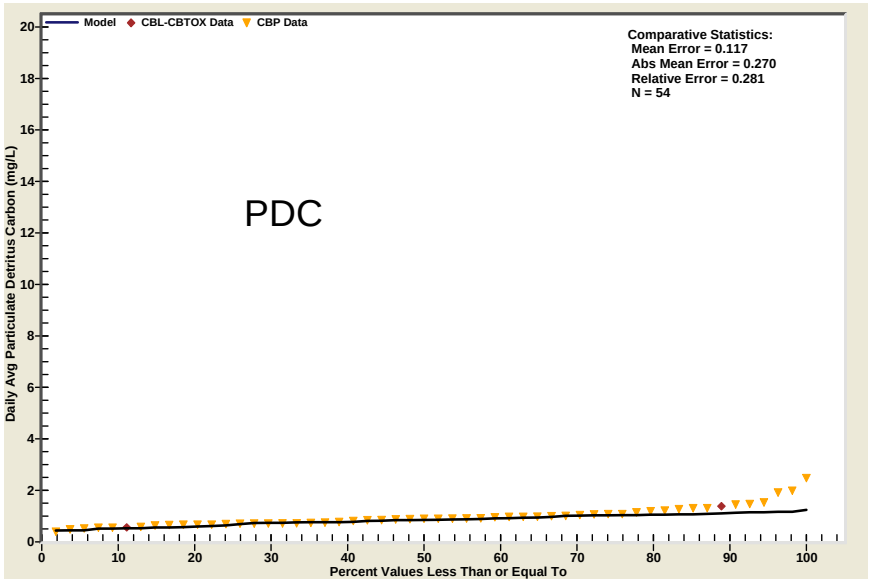

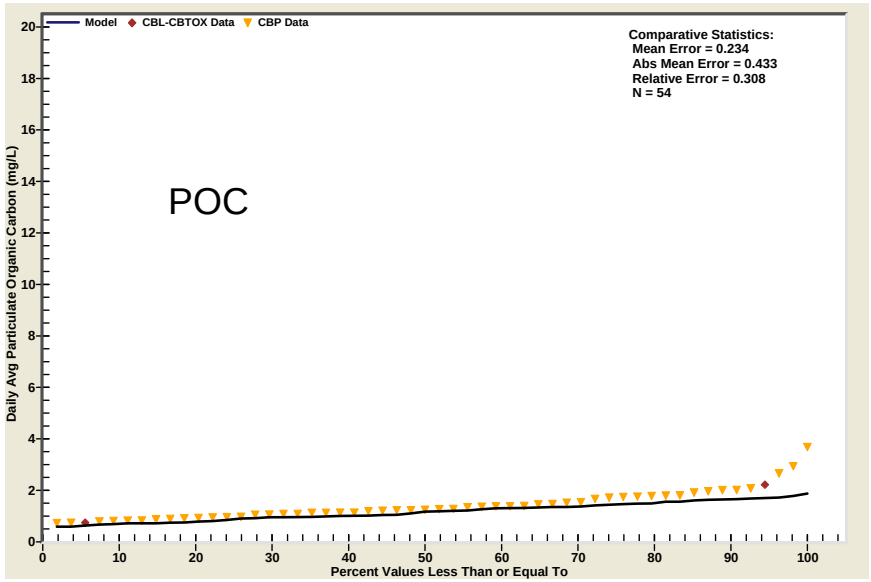

Figure 91. CFDs for Computed and Observed Daily Average Sorbents (LPOTMH)

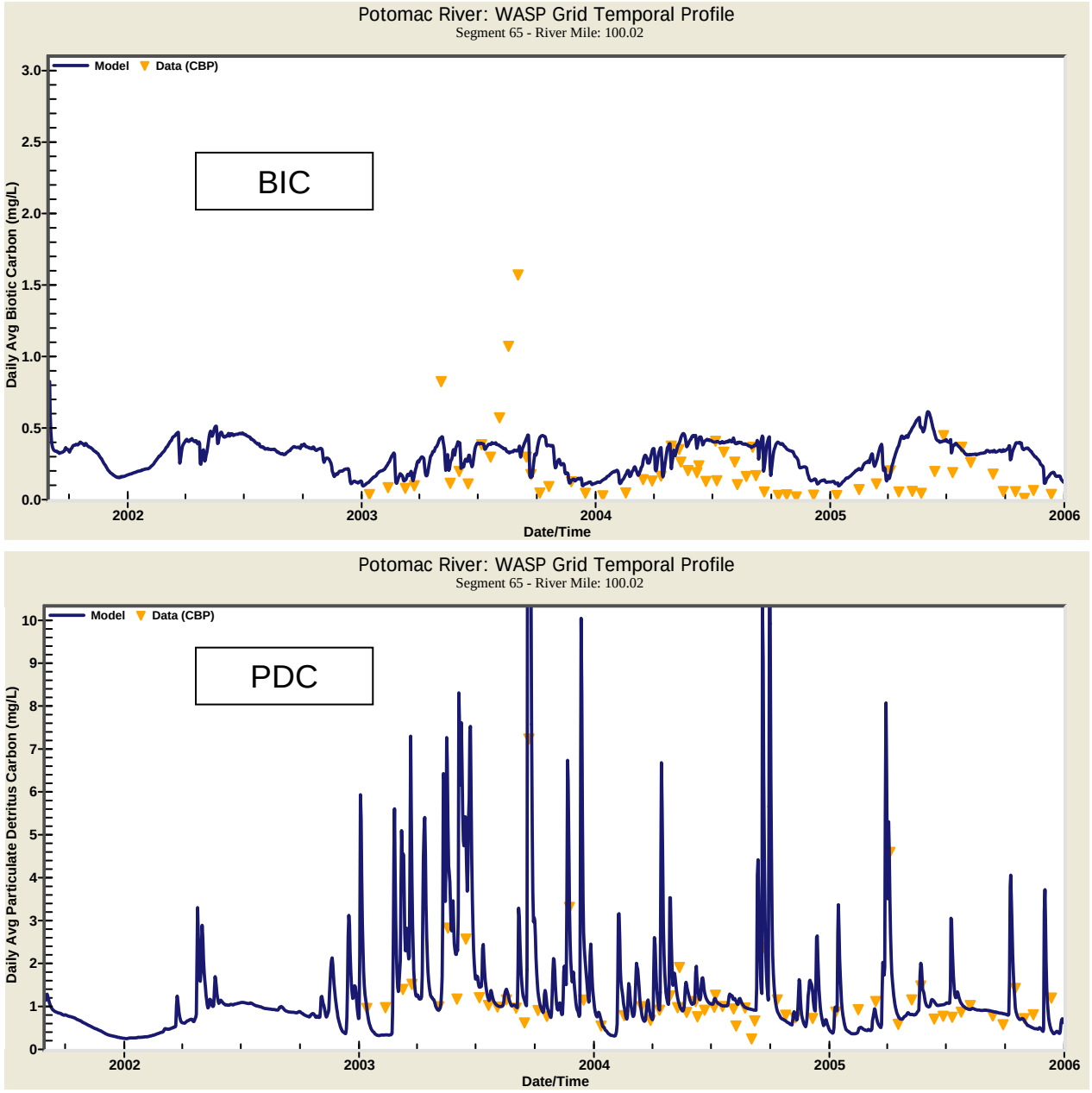

Figure 92. Time Series Plots for Computed and Observed Daily Average BIC and PDC at Potomac River Mile 100.02 (LPOTTF)

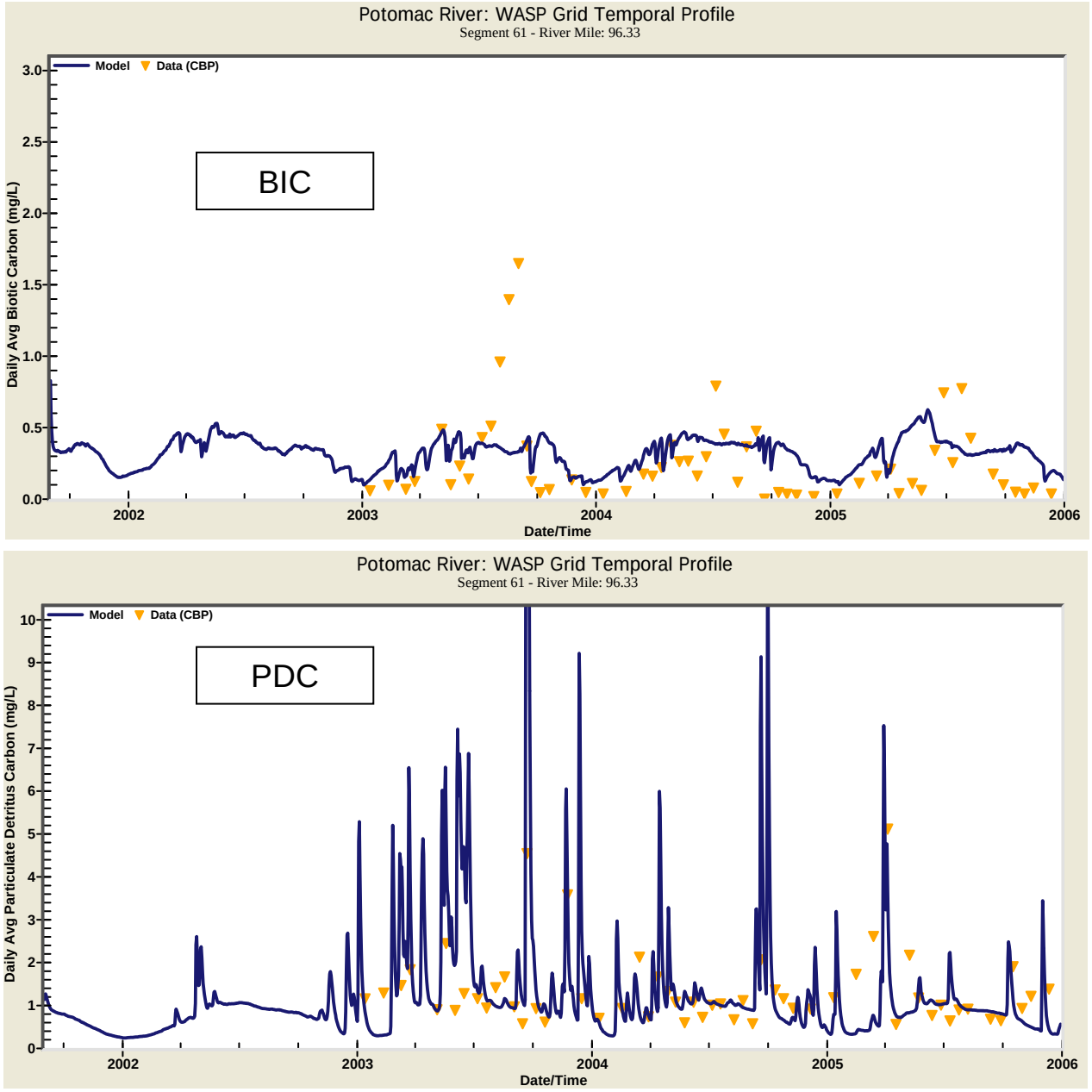

Figure 93. Time Series Plots for Computed and Observed Daily Average BIC and PDC at Potomac River Mile 96.33 (LPOTTF)

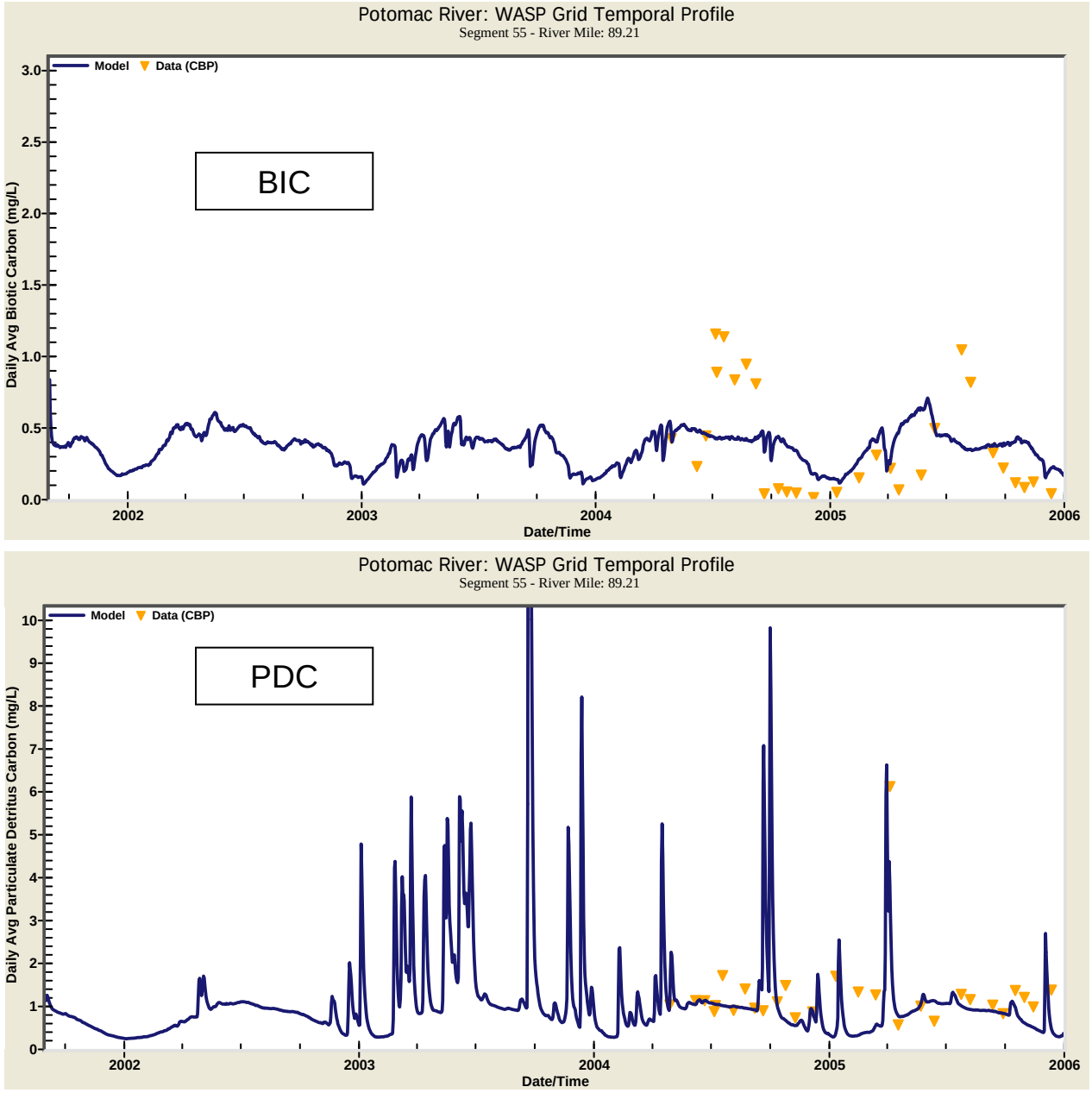

Figure 94. Time Series Plots for Computed and Observed Daily Average BIC and PDC at Potomac River Mile 89.21 (LPOTTF)

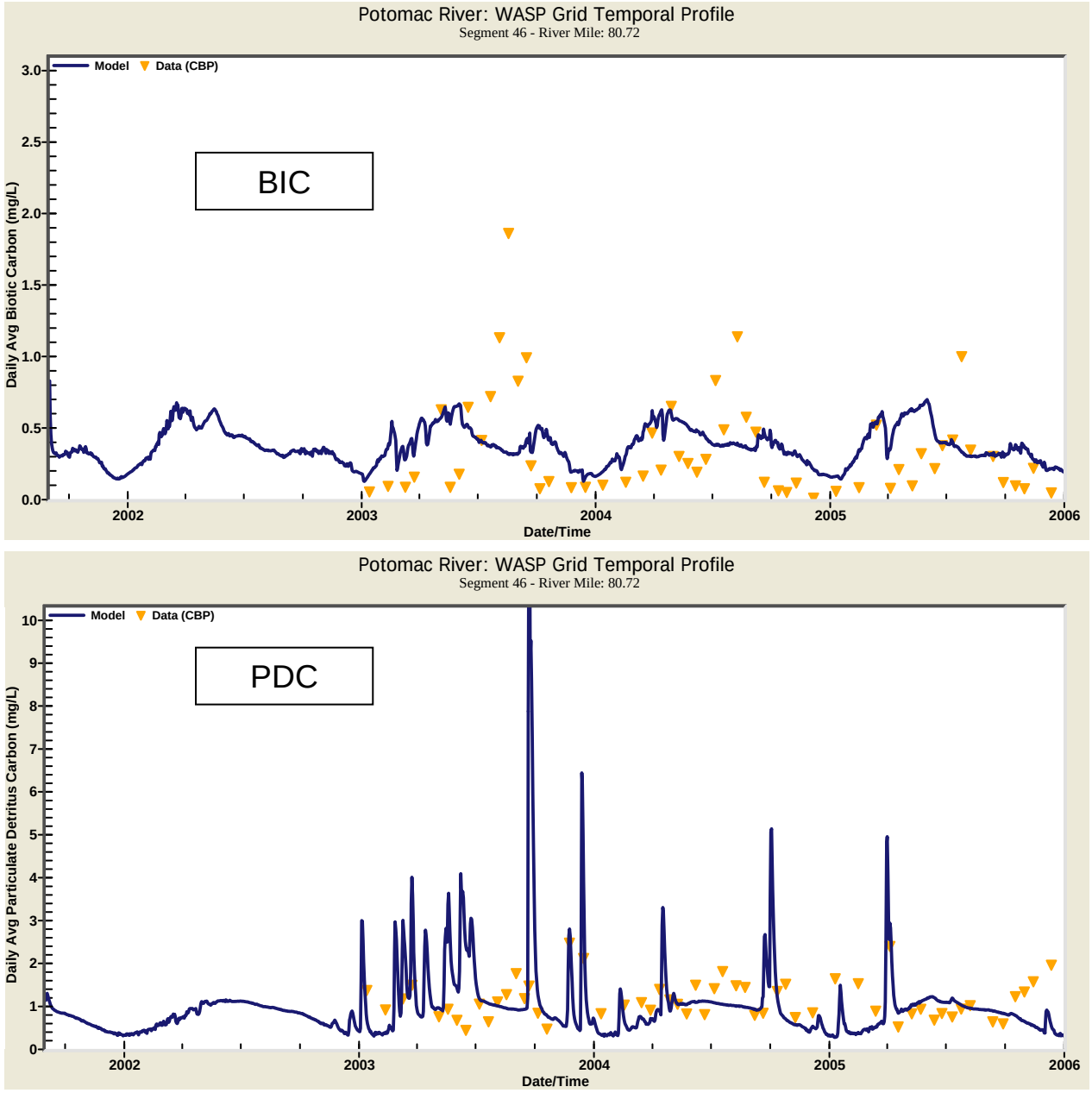

Figure 95. Time Series Plots for Computed and Observed Daily Average BIC and PDC at Potomac River Mile 80.72 (LPOTTF)

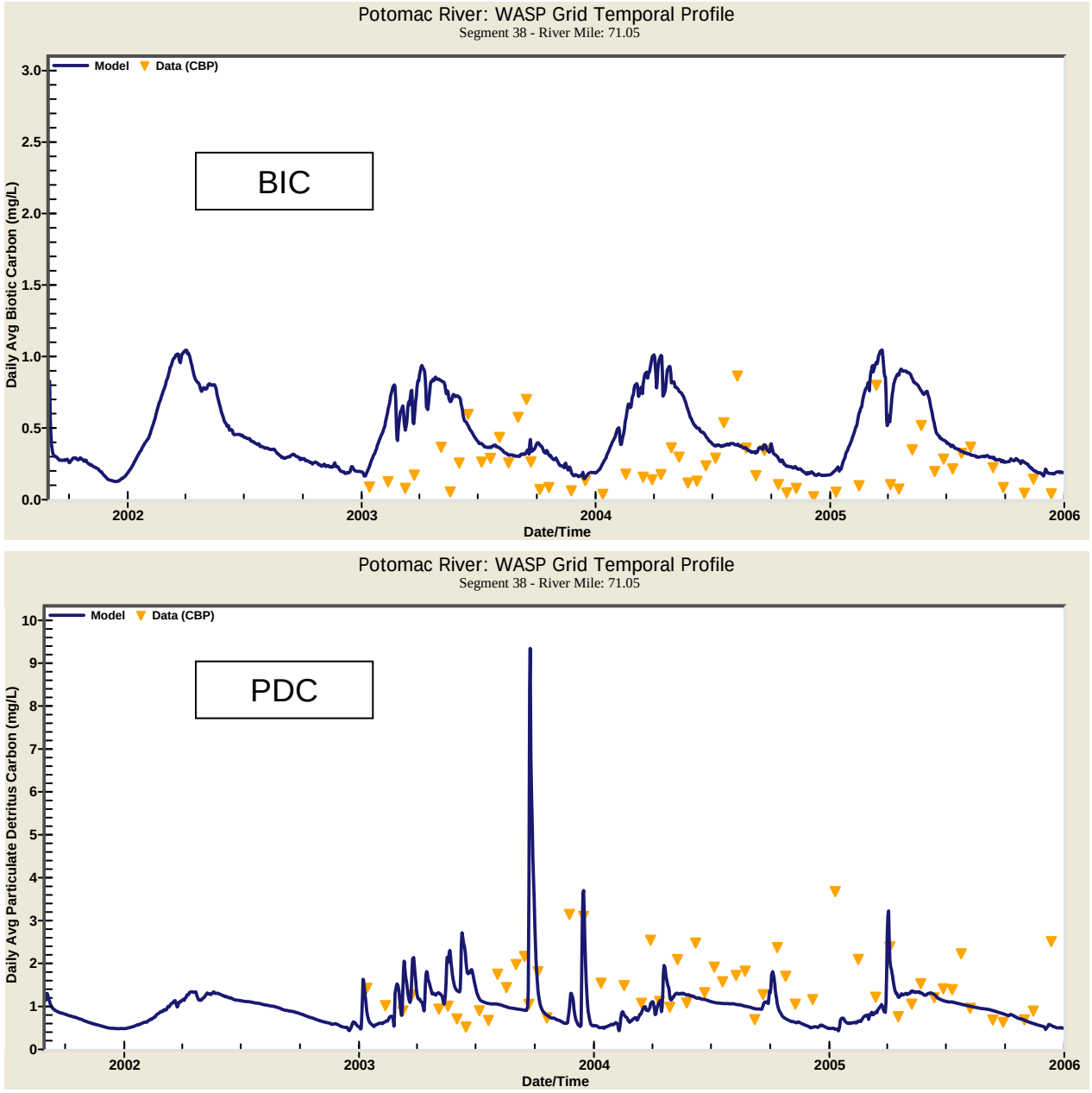

Figure 96. Time Series Plots for Computed and Observed Daily Average BIC and PDC at Potomac River Mile 71.05 (POTOH)

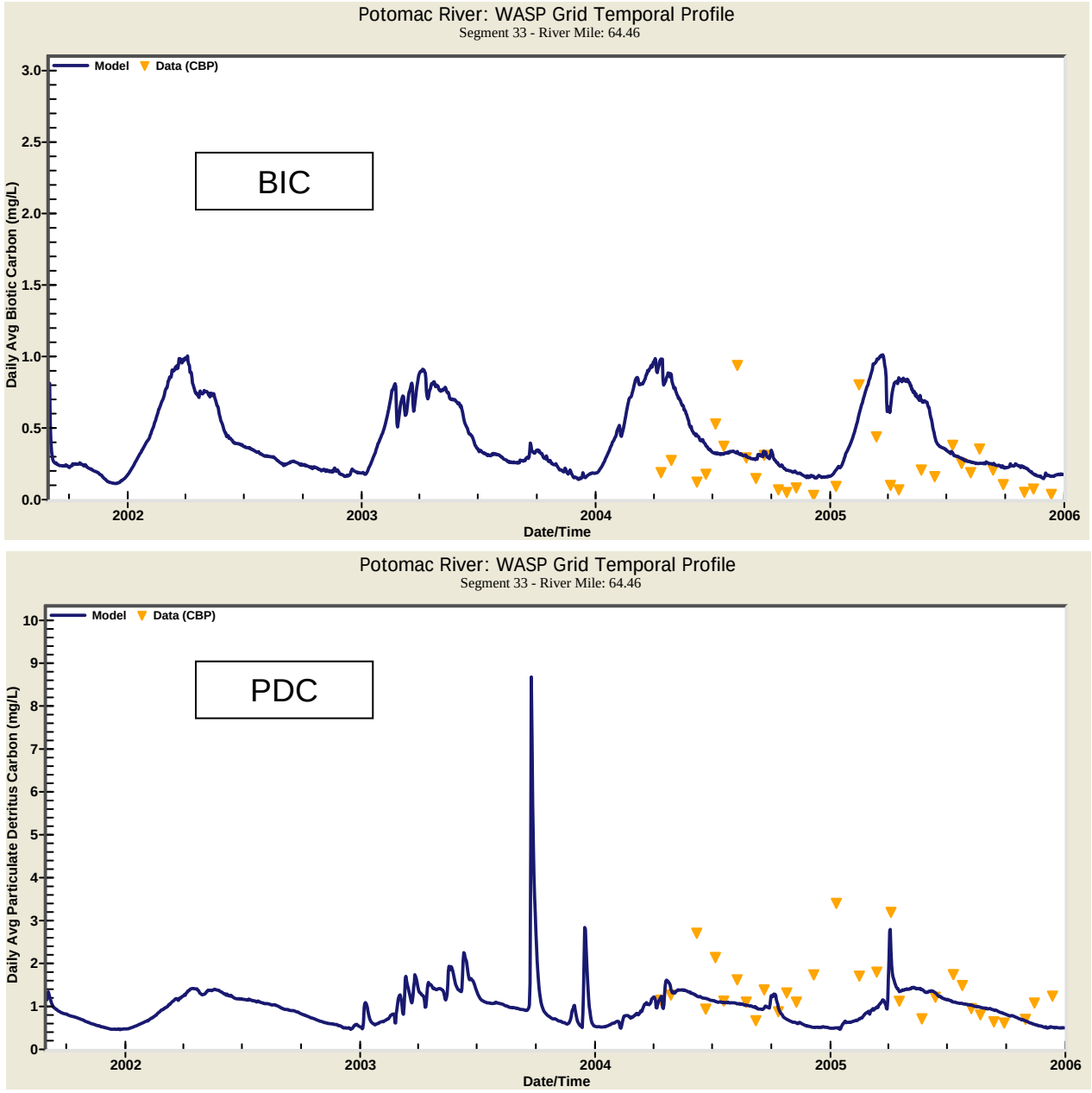

Figure 97. Time Series Plots for Computed and Observed Daily Average BIC and PDC at Potomac River Mile 64.46 (POTOH)

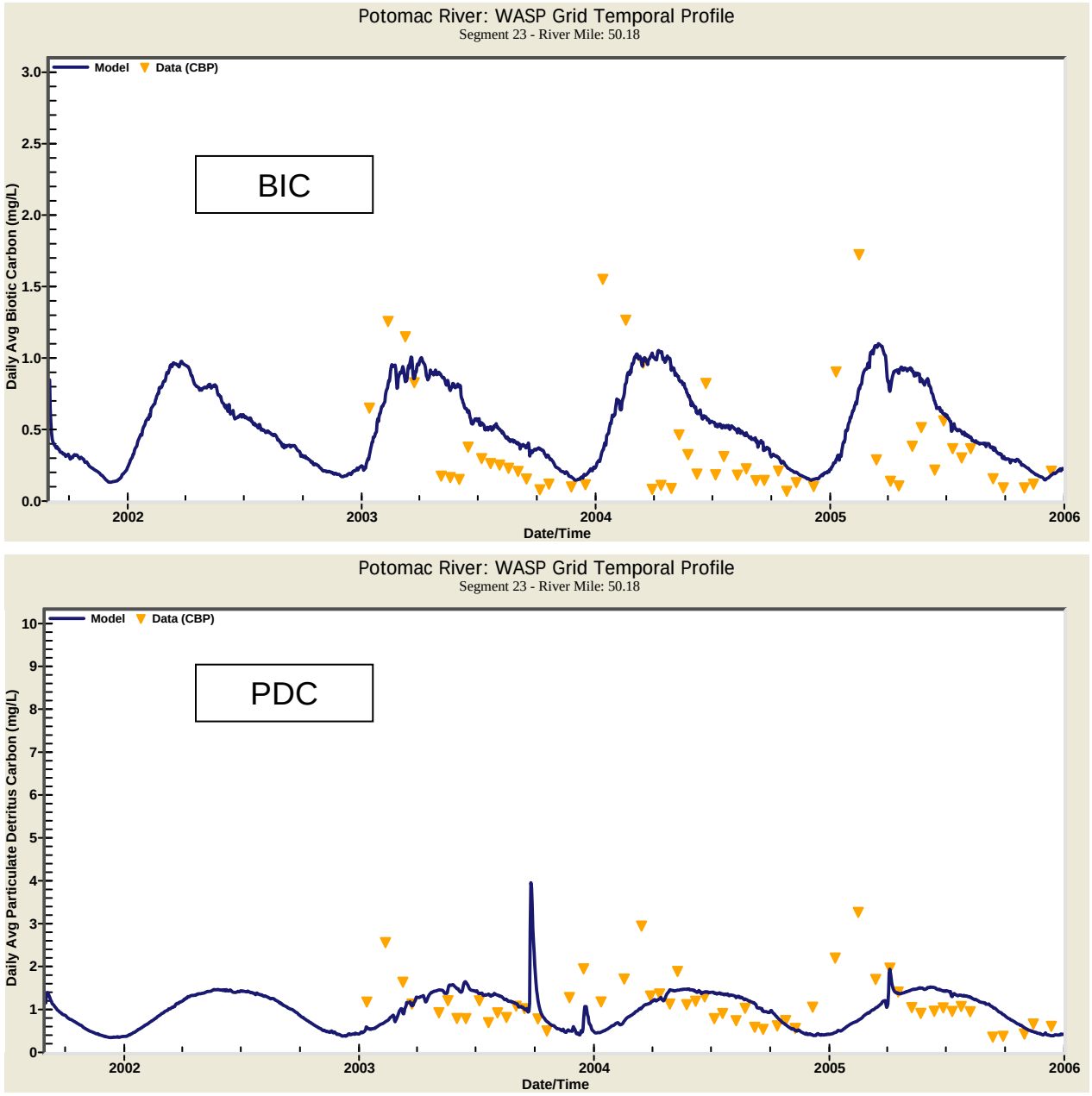

Figure 98. Time Series Plots for Computed and Observed Daily Average BIC and PDC at Potomac River Mile 50.18 (UPOTMH)

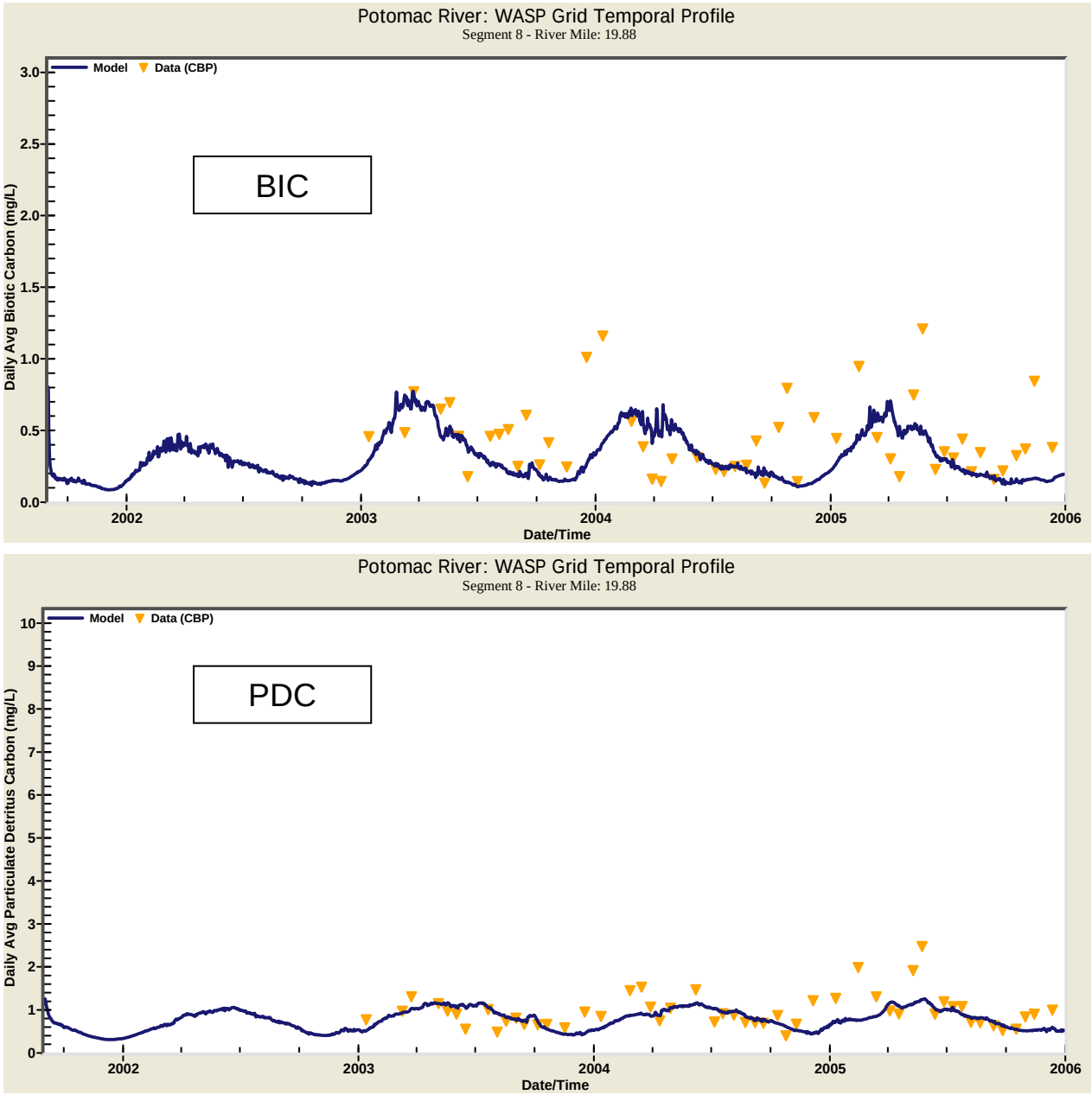

Figure 99. Time Series Plots for Computed and Observed Daily Average BIC and PDC at Potomac River Mile 19.88 (LPOTMH)

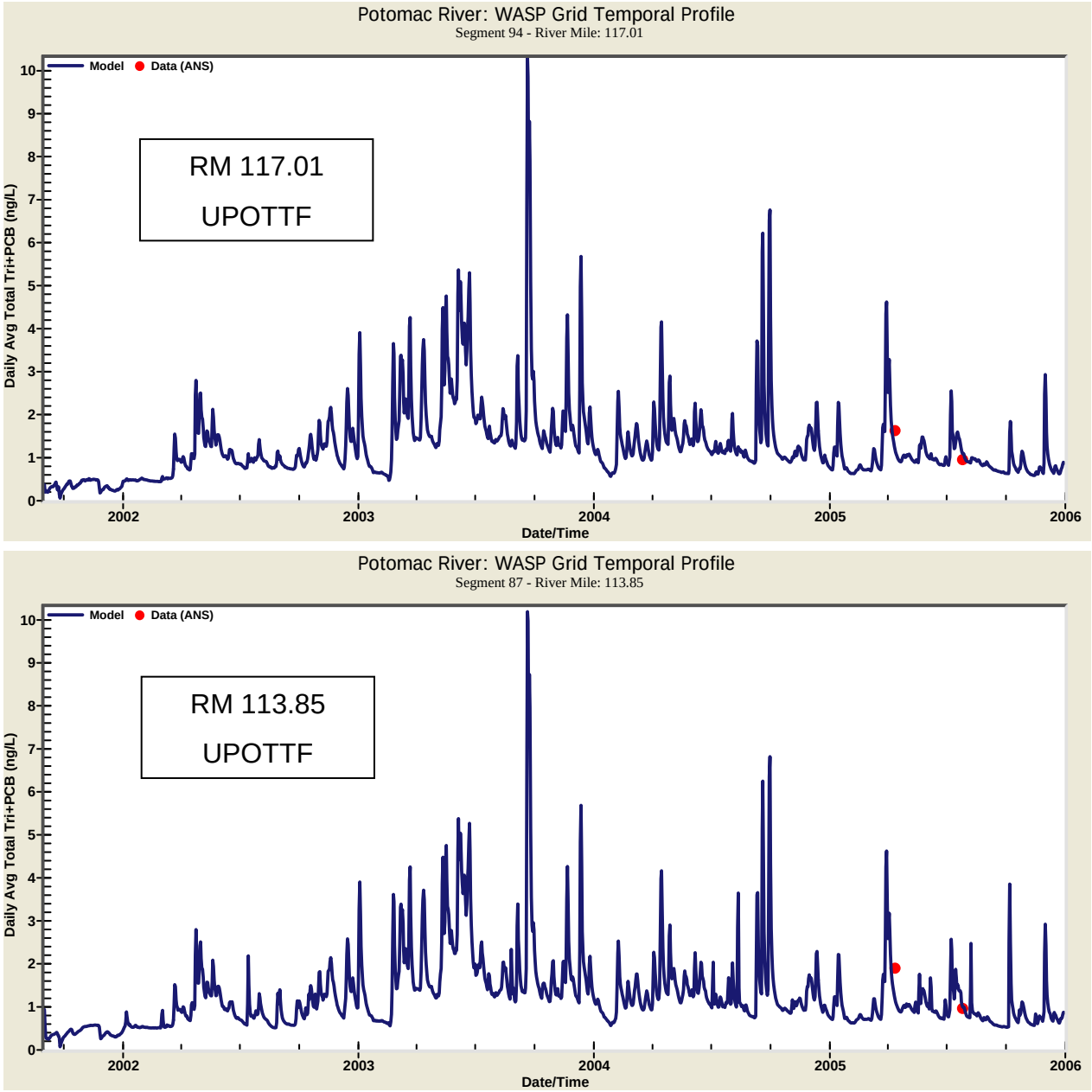

Figure 100. Time Series Plots for Computed and Observed Daily Average PCB3+ at Potomac River Miles 117.01 and 113.85

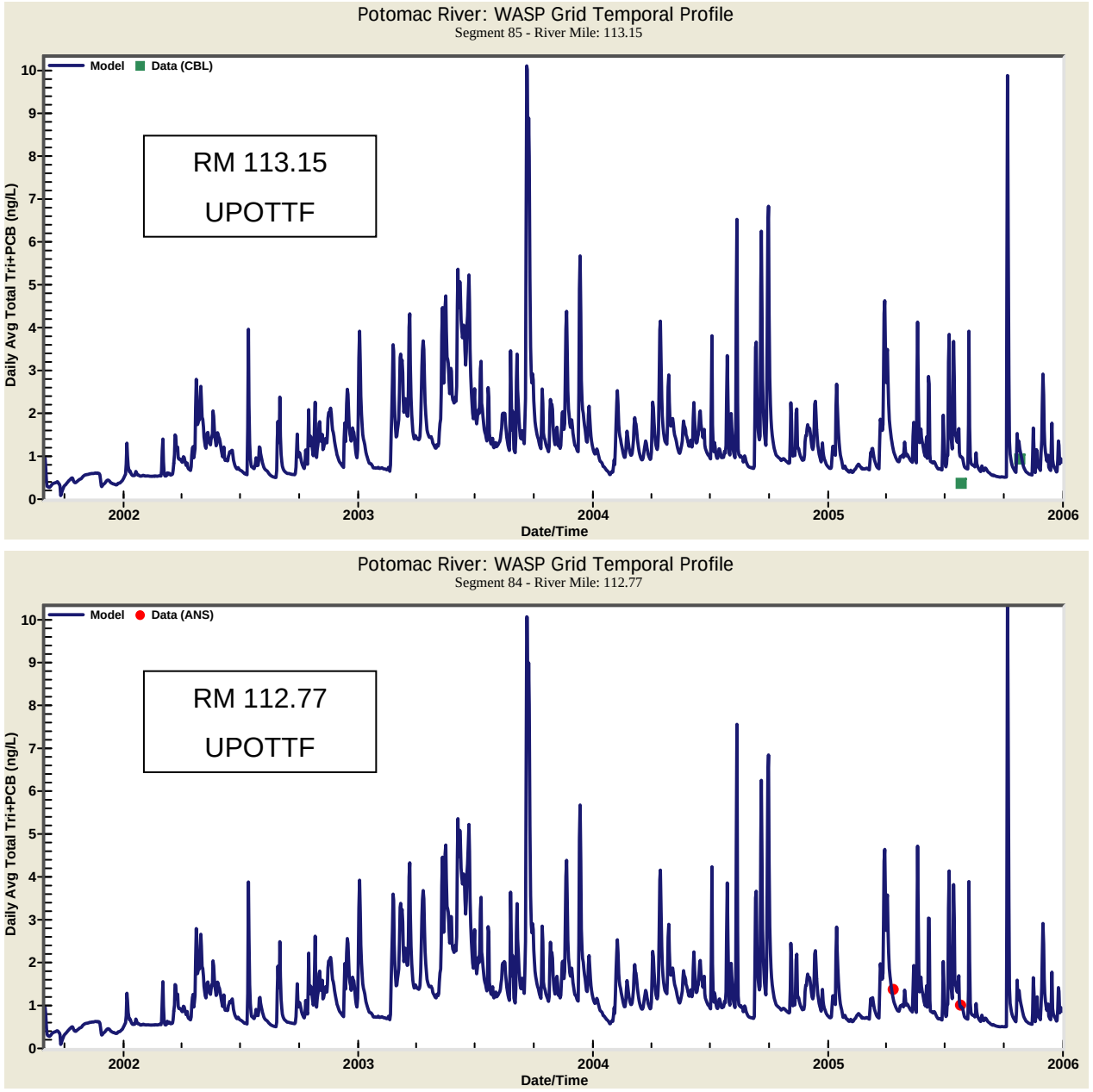

Figure 101. Time Series Plots for Computed and Observed Daily Average PCB3+ at Potomac River Miles 113.15 and 112.77

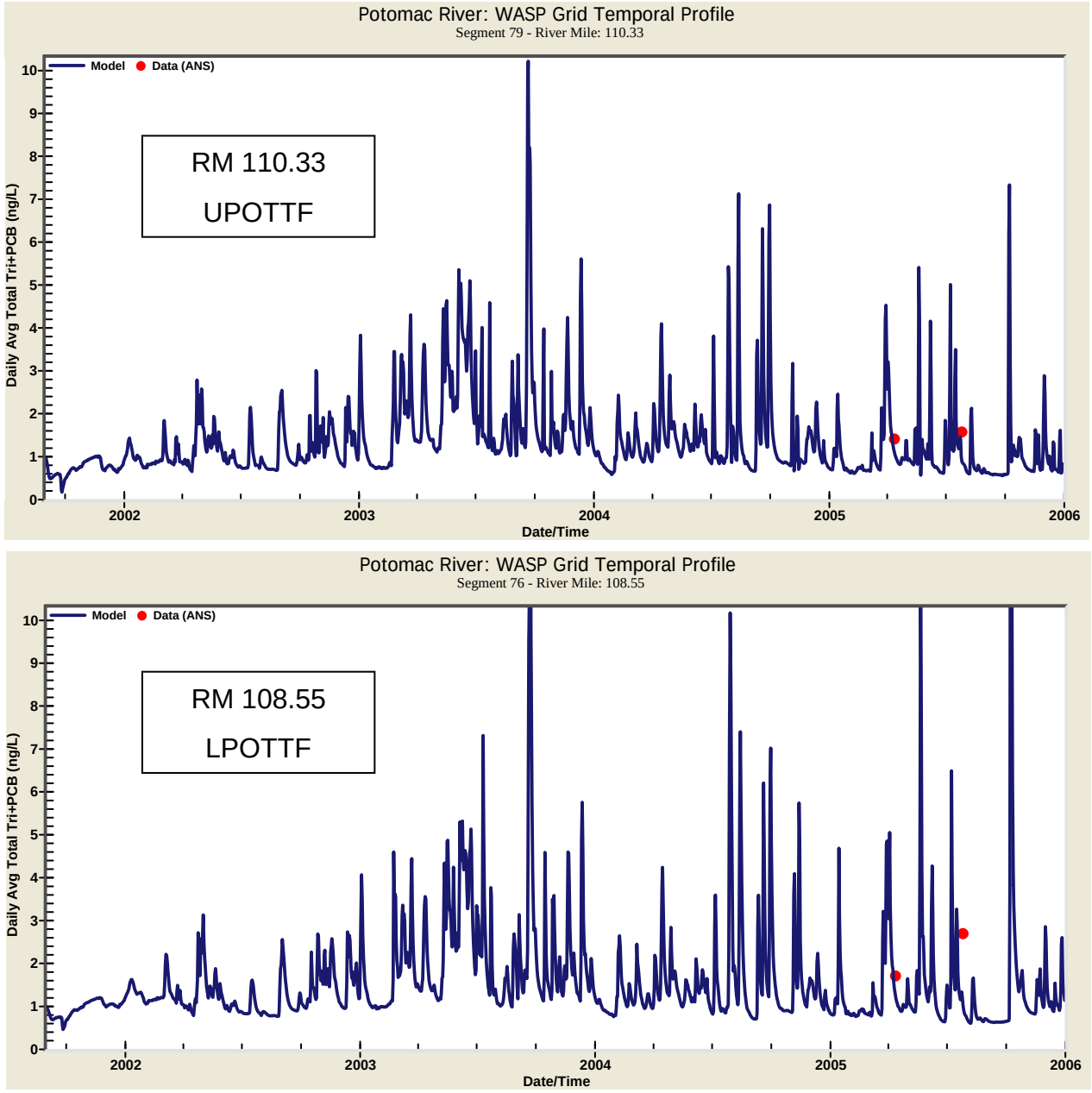

Figure 102. Time Series Plots for Computed and Observed Daily Average PCB3+ at Potomac River Miles 110.33 and 108.55

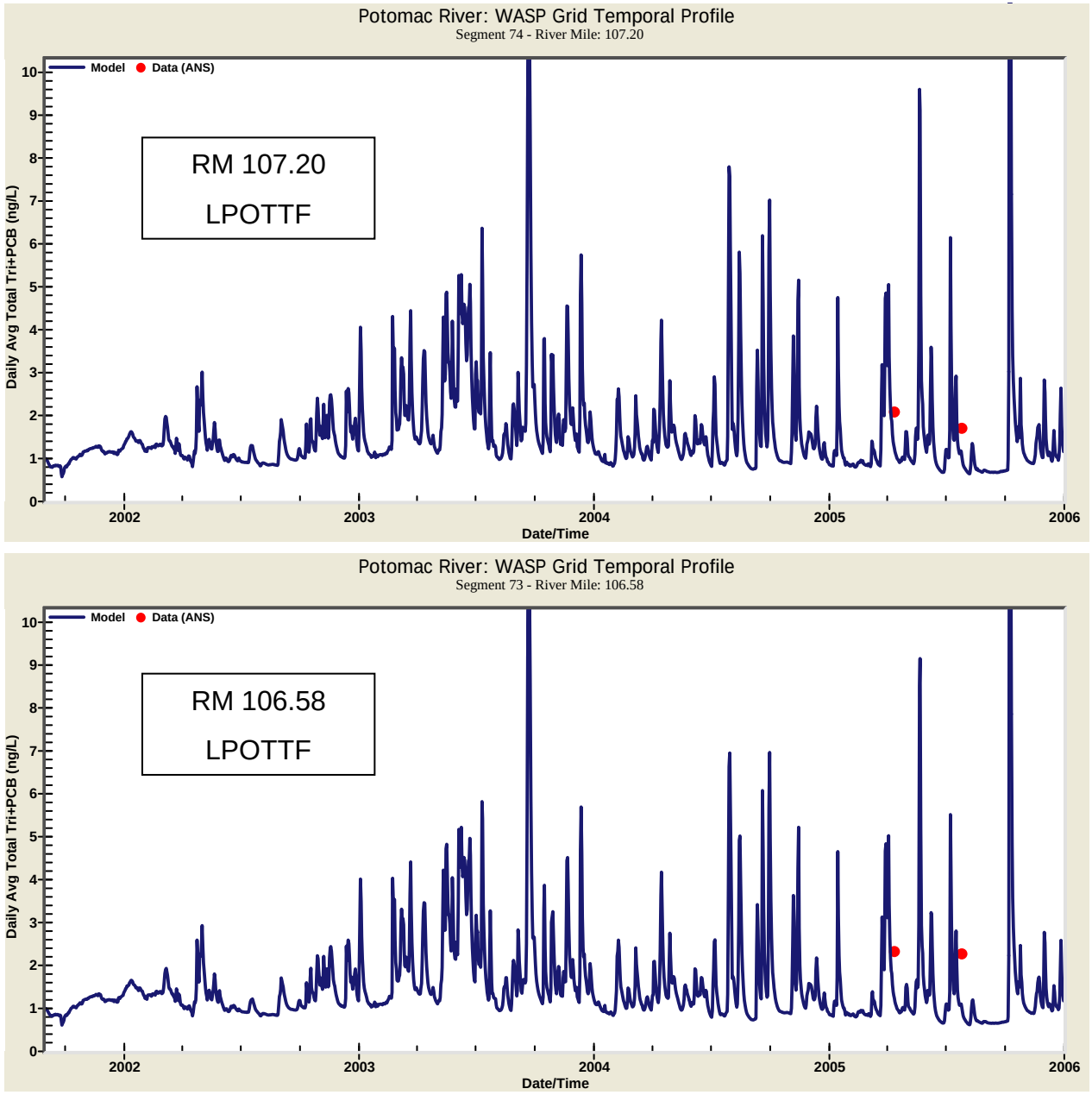

Figure 103. Time Series Plots for Computed and Observed Daily Average PCB3+ at Potomac River Miles 107.20 and 106.58

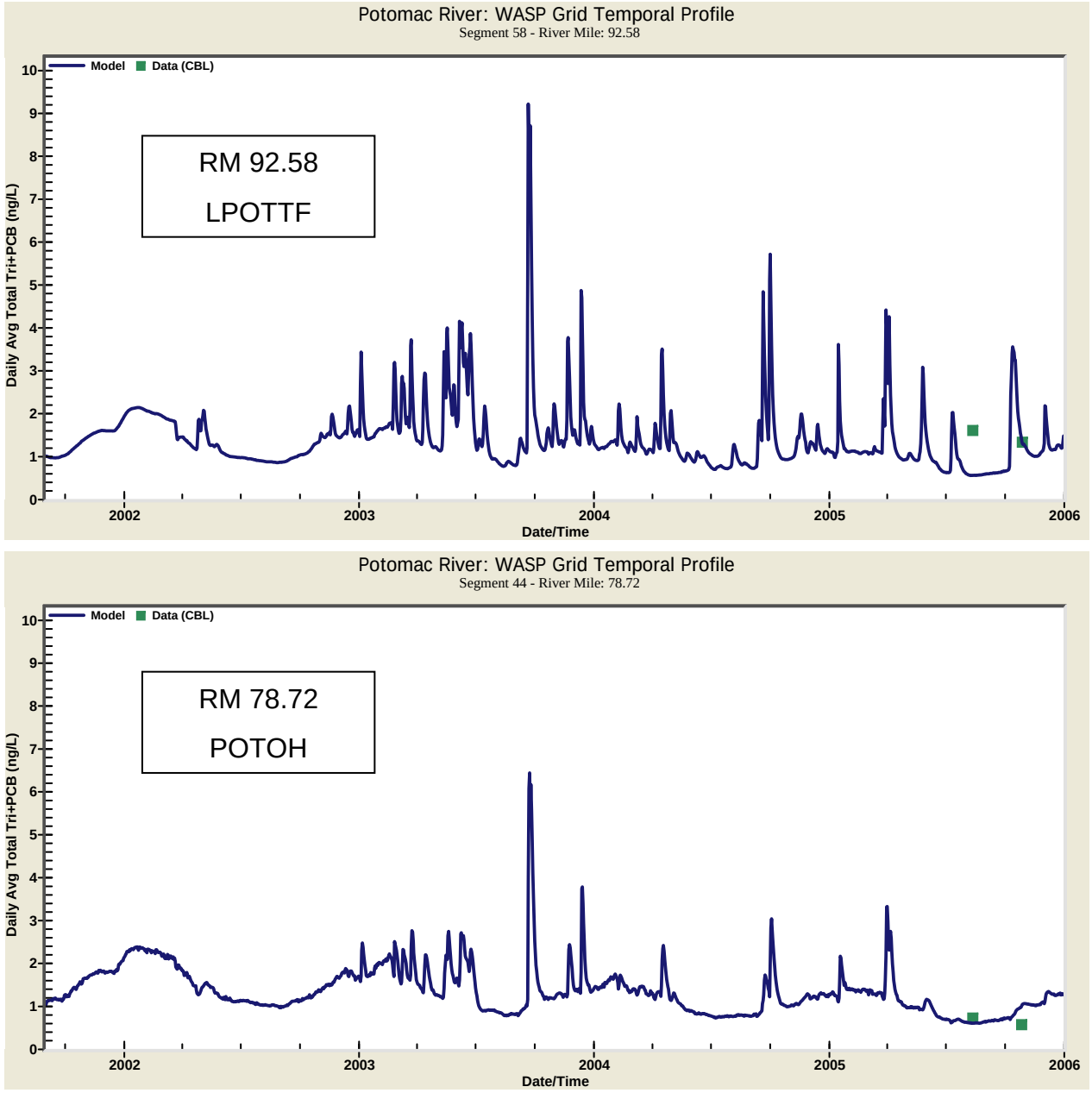

Figure 104. Time Series Plots for Computed and Observed Daily Average PCB3+ at Potomac River Miles 92.58 and 78.72

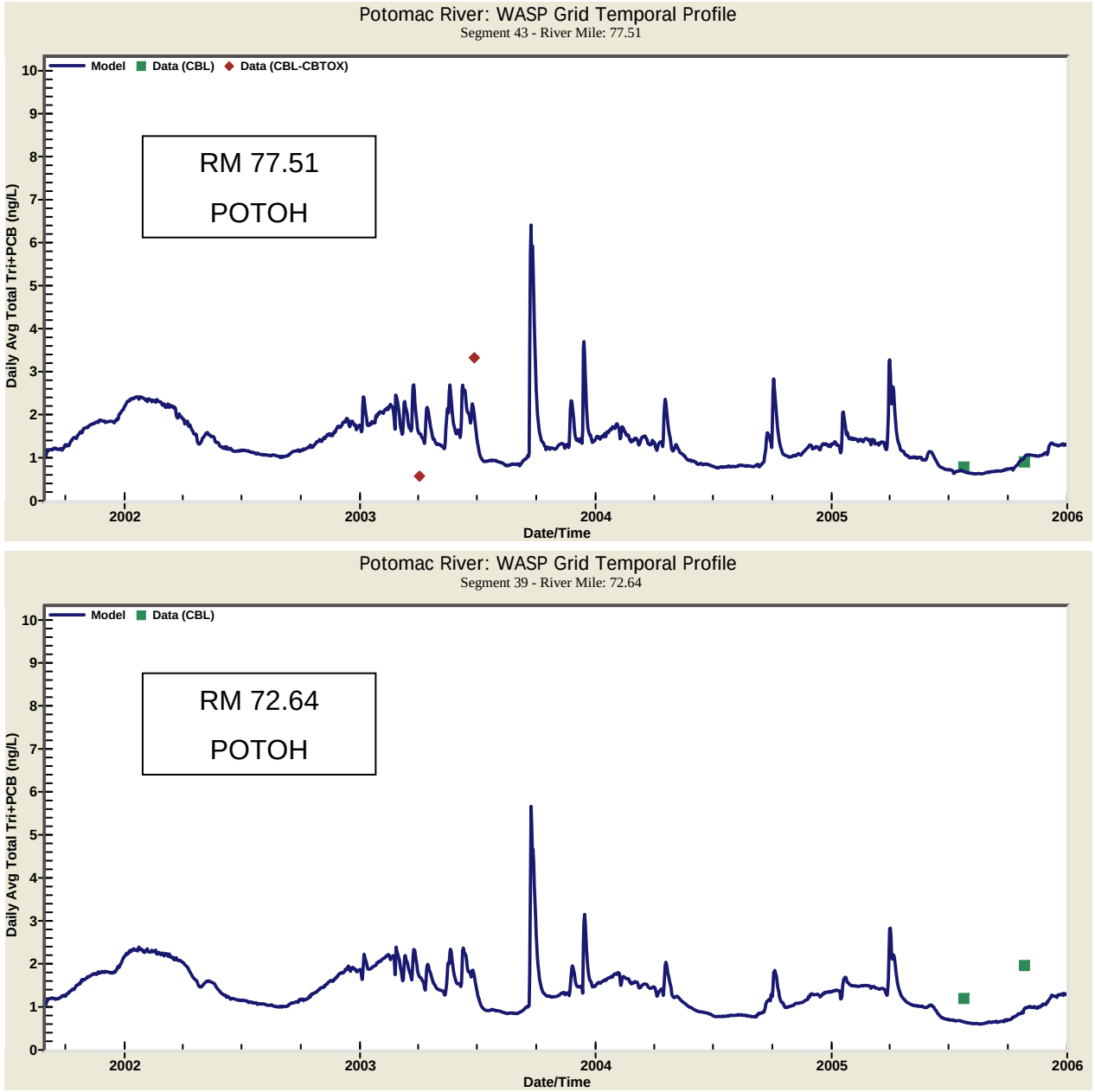

Figure 105. Time Series Plots for Computed and Observed Daily Average PCB3+ at Potomac River Miles 77.51 and 72.64

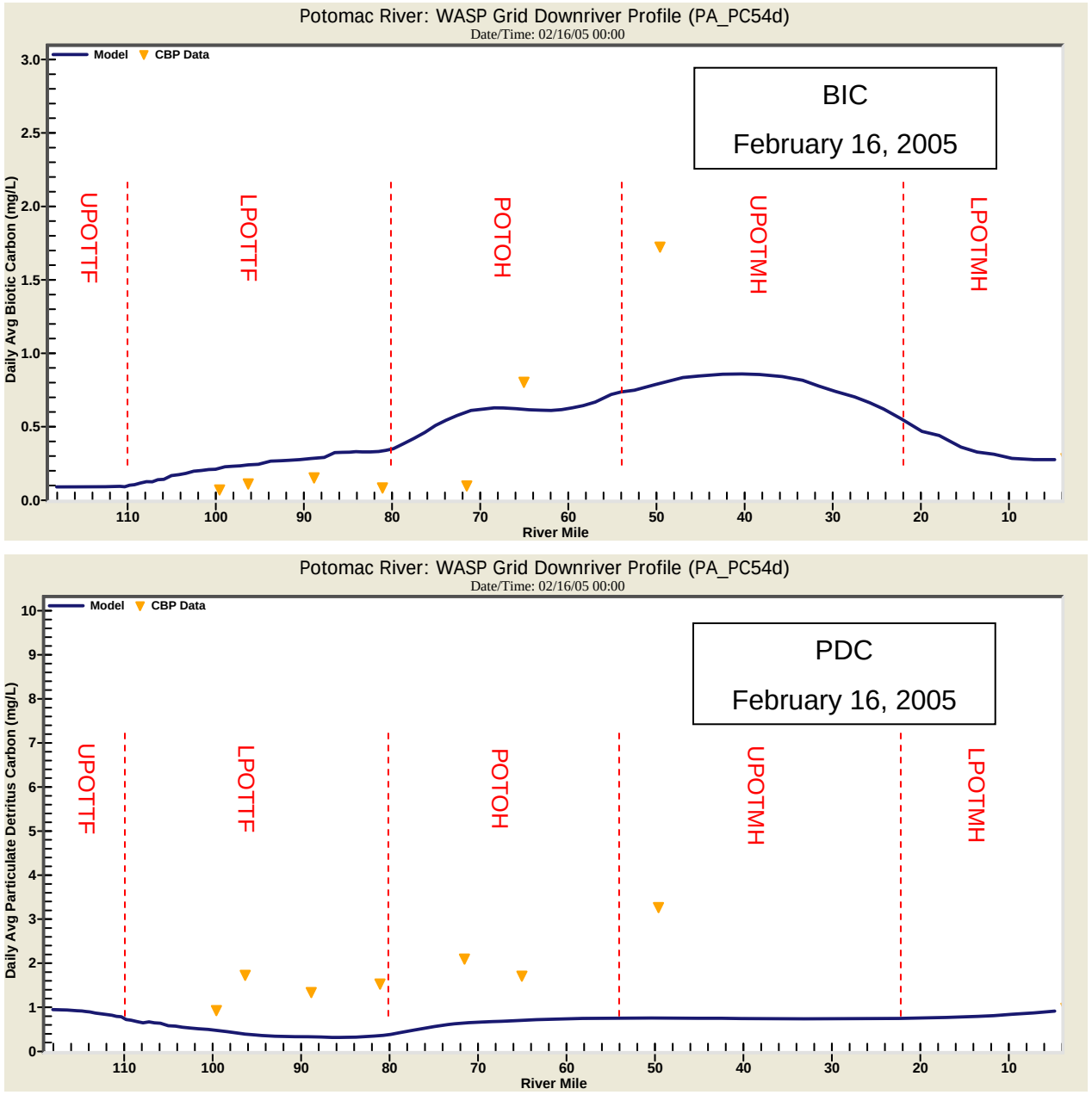

Figure 106. Spatial Profiles of Computed and Observed Daily Average BIC and PDC in Potomac (Winter)

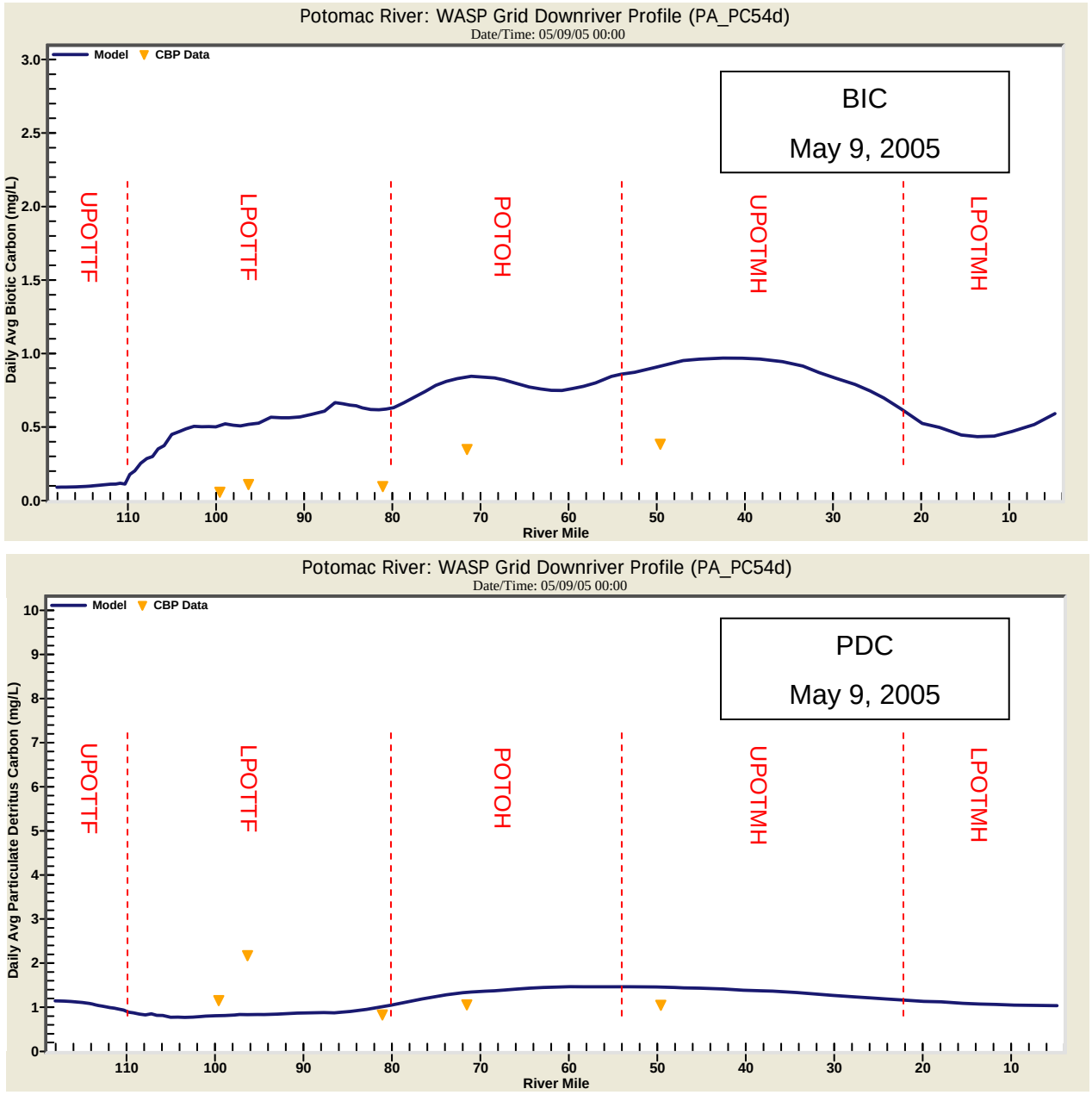

Figure 107. Spatial Profiles of Computed and Observed Daily Average BIC and PDC in Potomac (Spring)

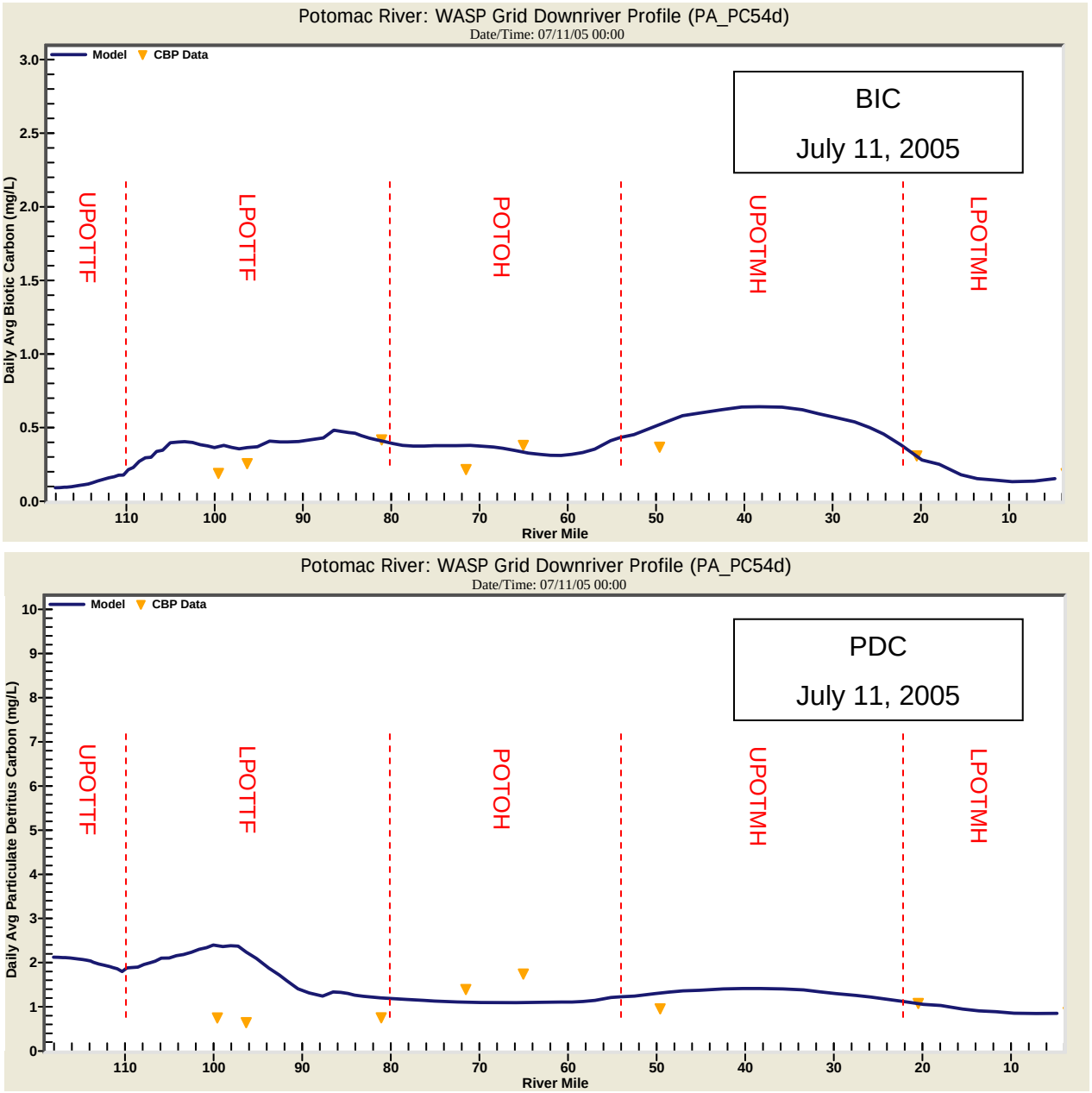

Figure 108. Spatial Profiles of Computed and Observed Daily Average BIC and PDC in Potomac (Summer)

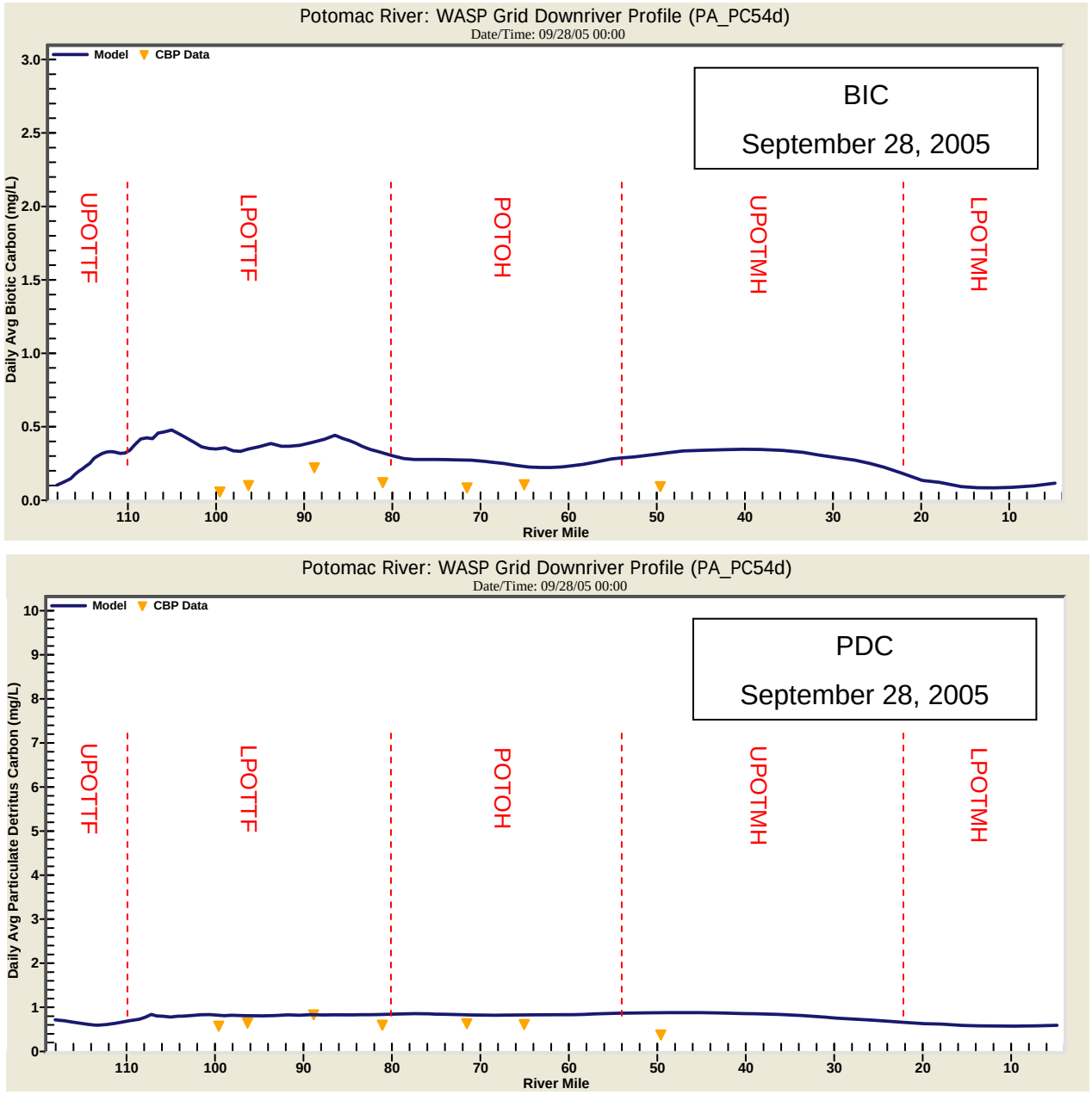

Figure 109. Spatial Profiles of Computed and Observed Daily Average BIC and PDC in Potomac (Fall)

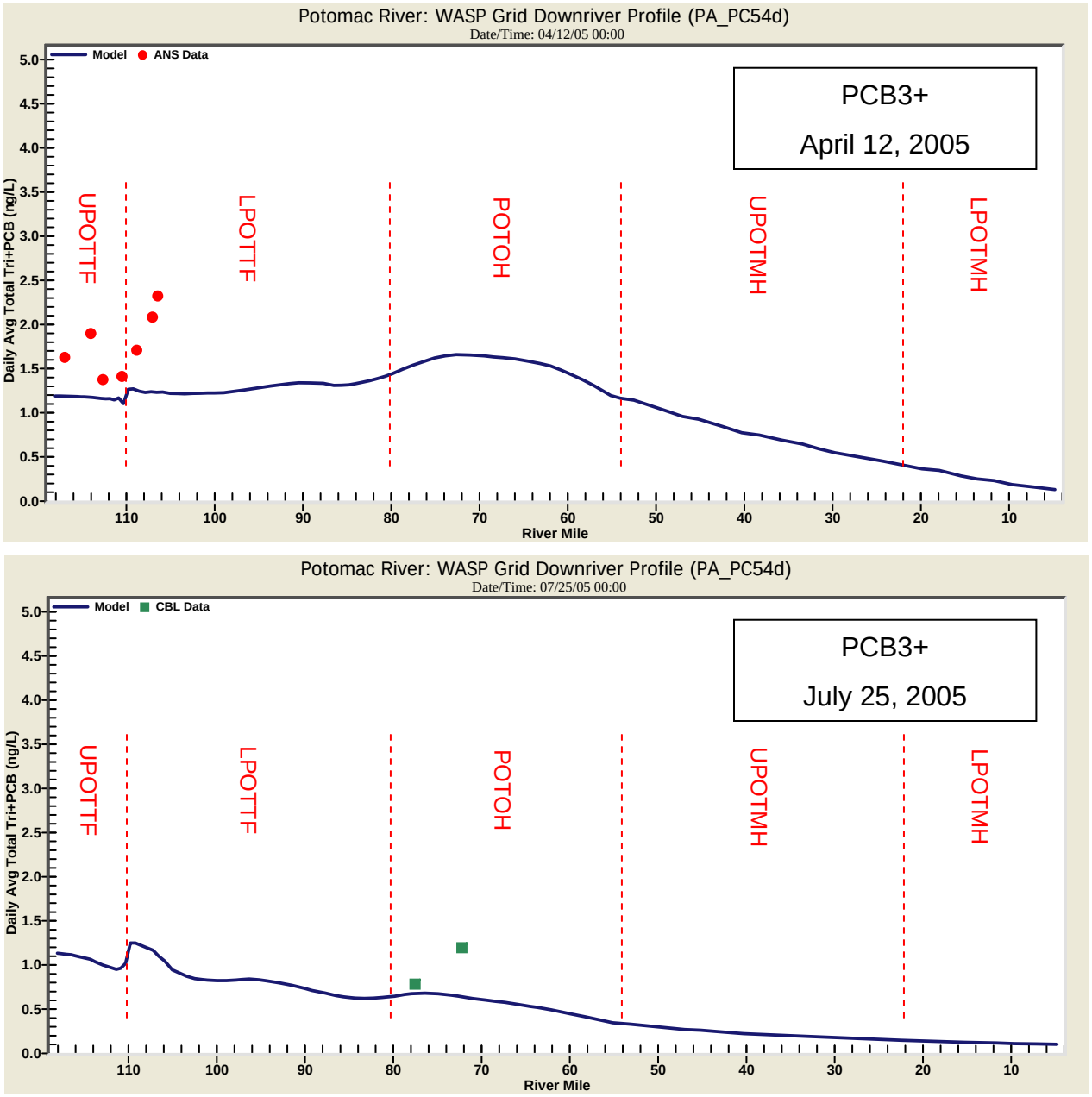

Figure 110. Spatial Profiles of Computed and Observed Daily Average PCB3+ in Potomac on April 12 and July 25, 2005

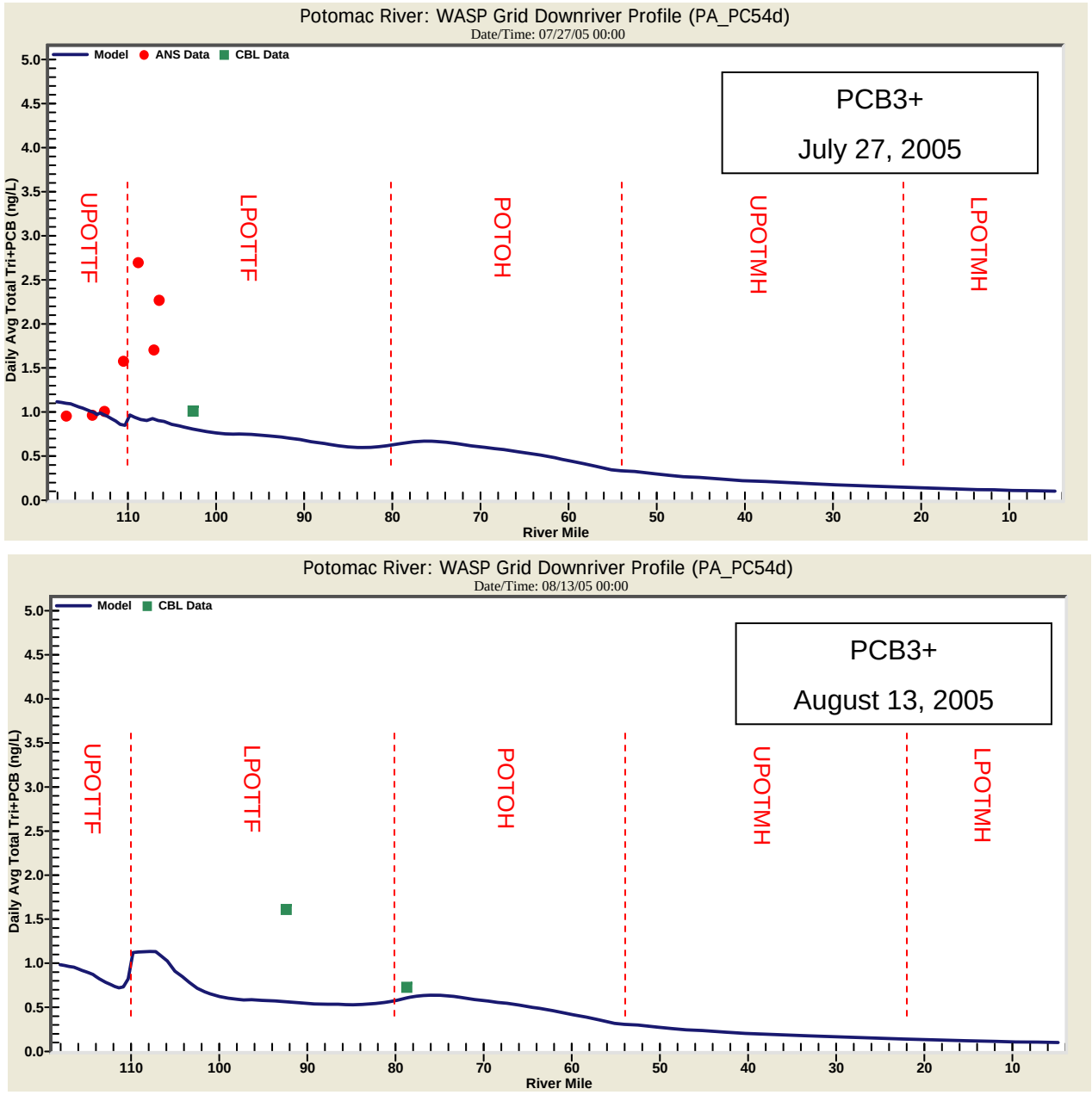

Figure 111. Spatial Profiles of Computed and Observed Daily Average PCB3+ in Potomac on July 27 and August 13, 2005

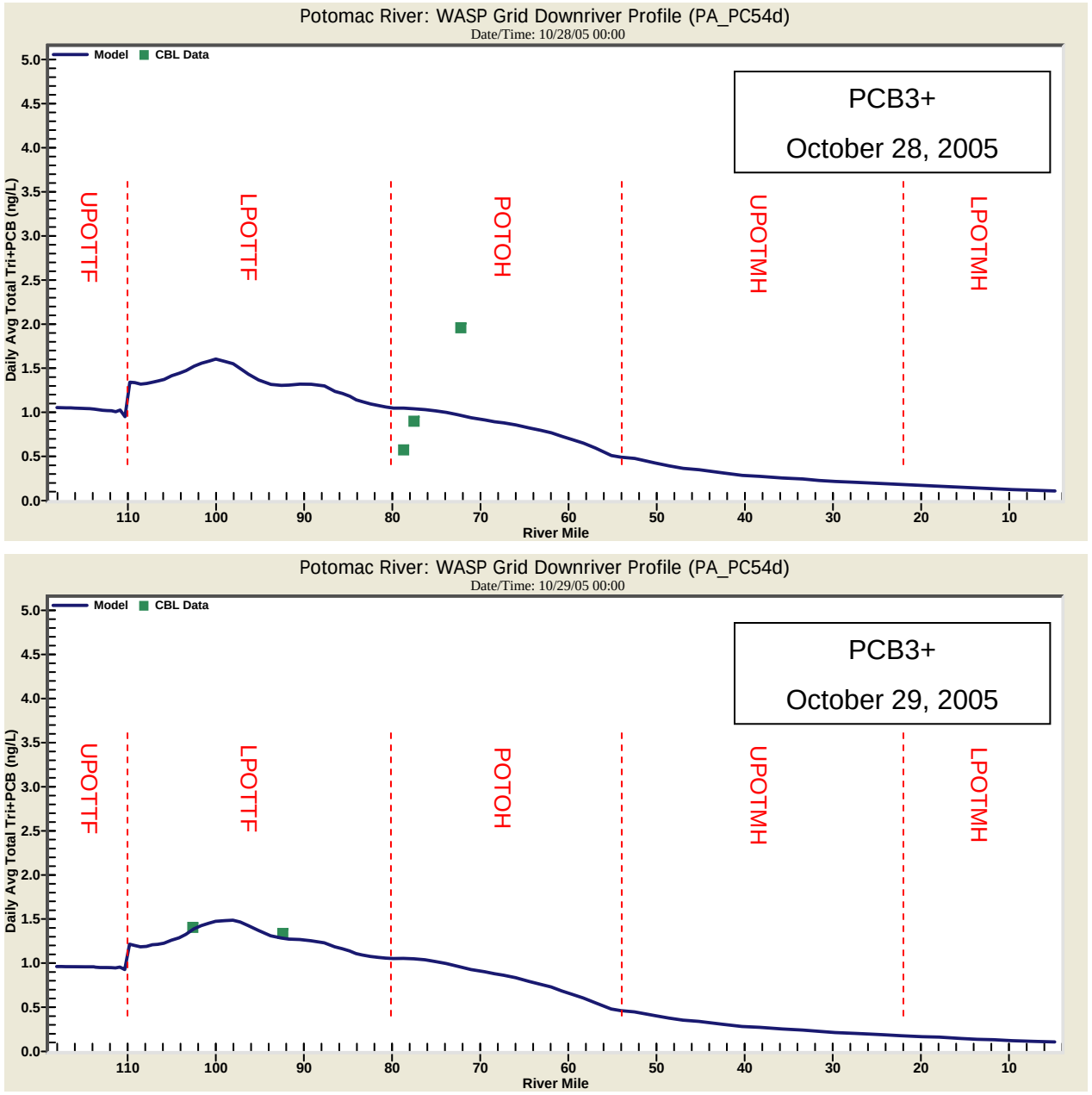

Figure 112. Spatial Profiles of Computed and Observed Daily Average PCB3+ in Potomac on October 28 and 29, 2005

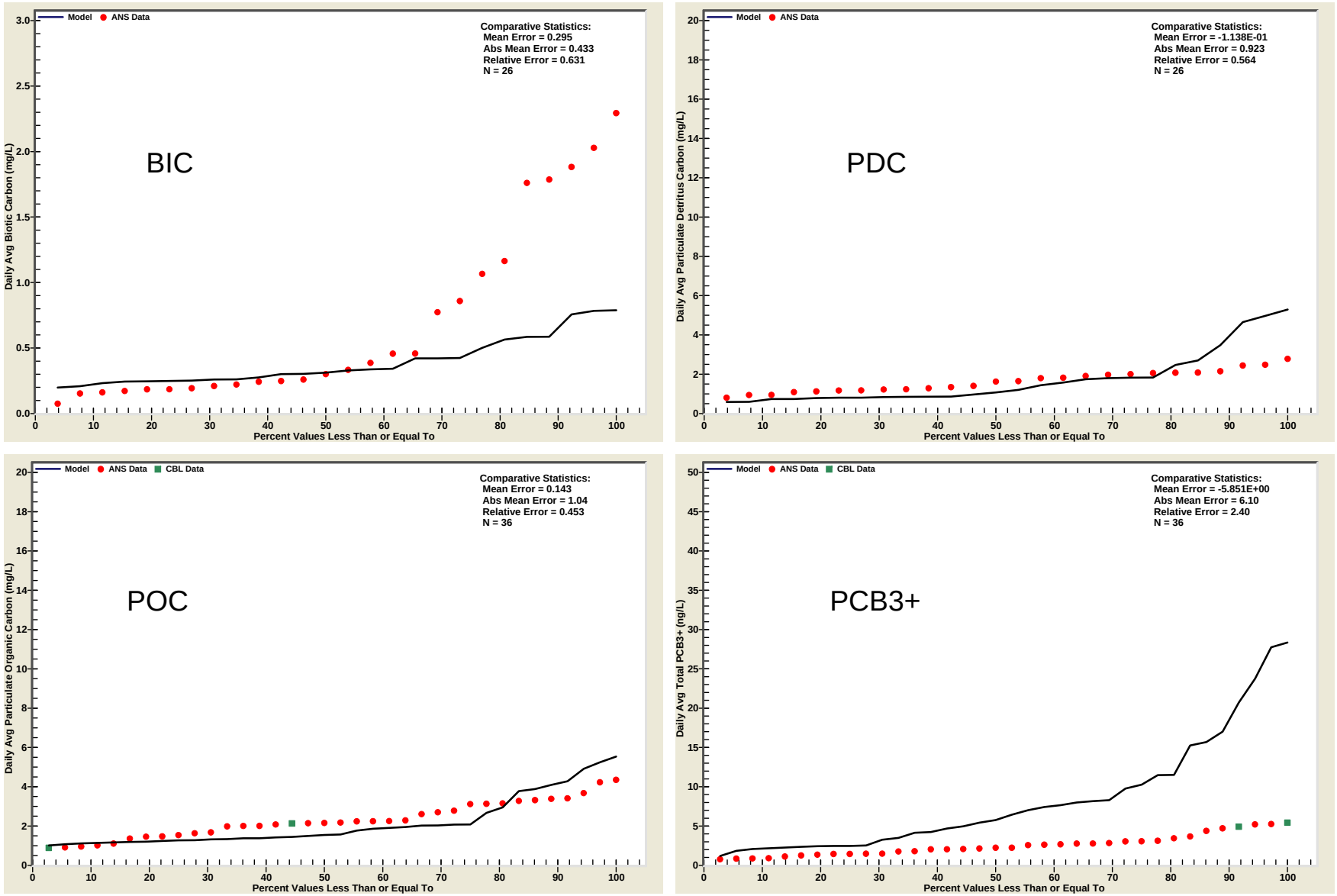

Figure 113. CFDs for Computed and Observed Daily Average Sorbents and PCB3+ in Anacostia

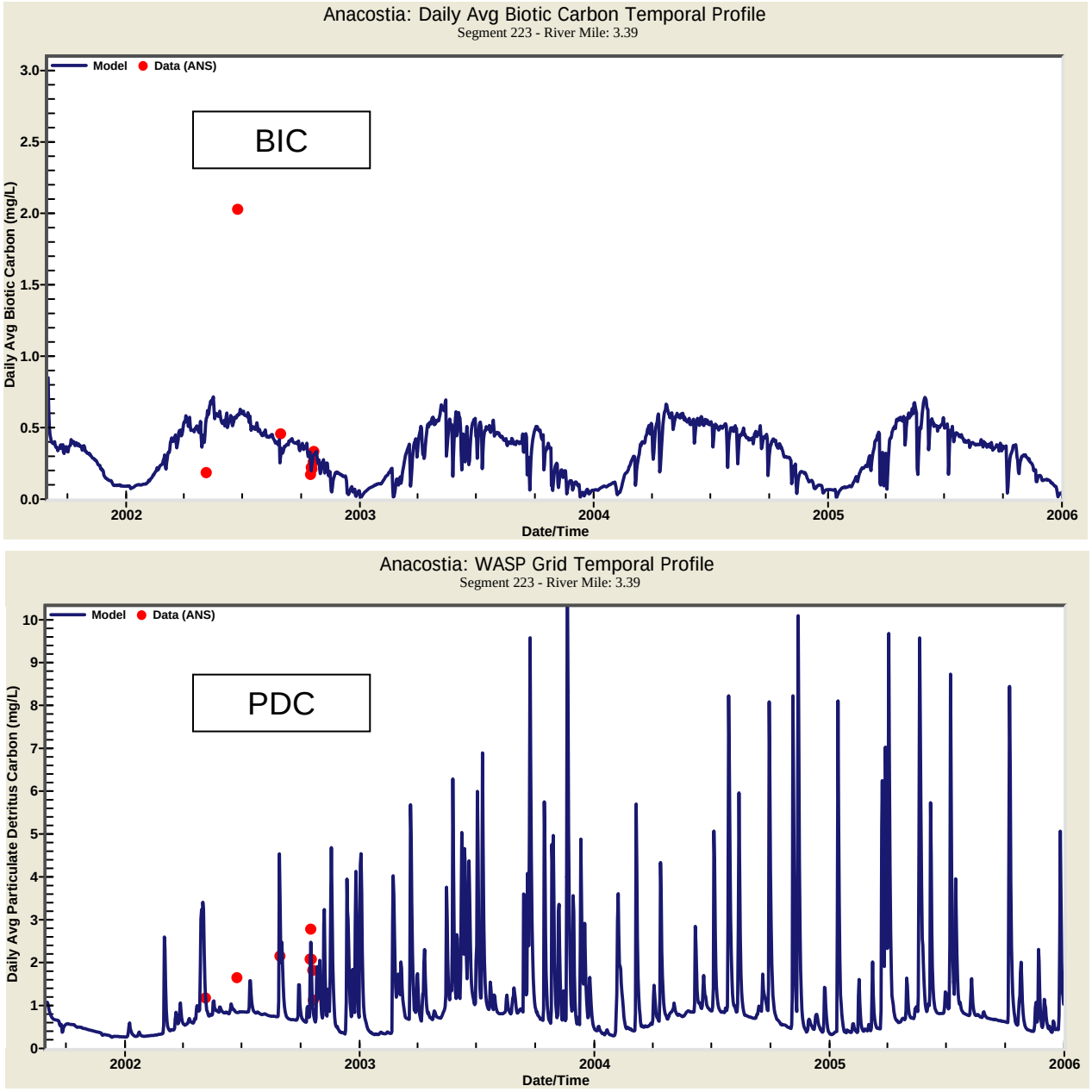

Figure 114. Time Series Plots for Computed and Observed Daily Average BIC and PDC at Anacostia River Mile 3.39

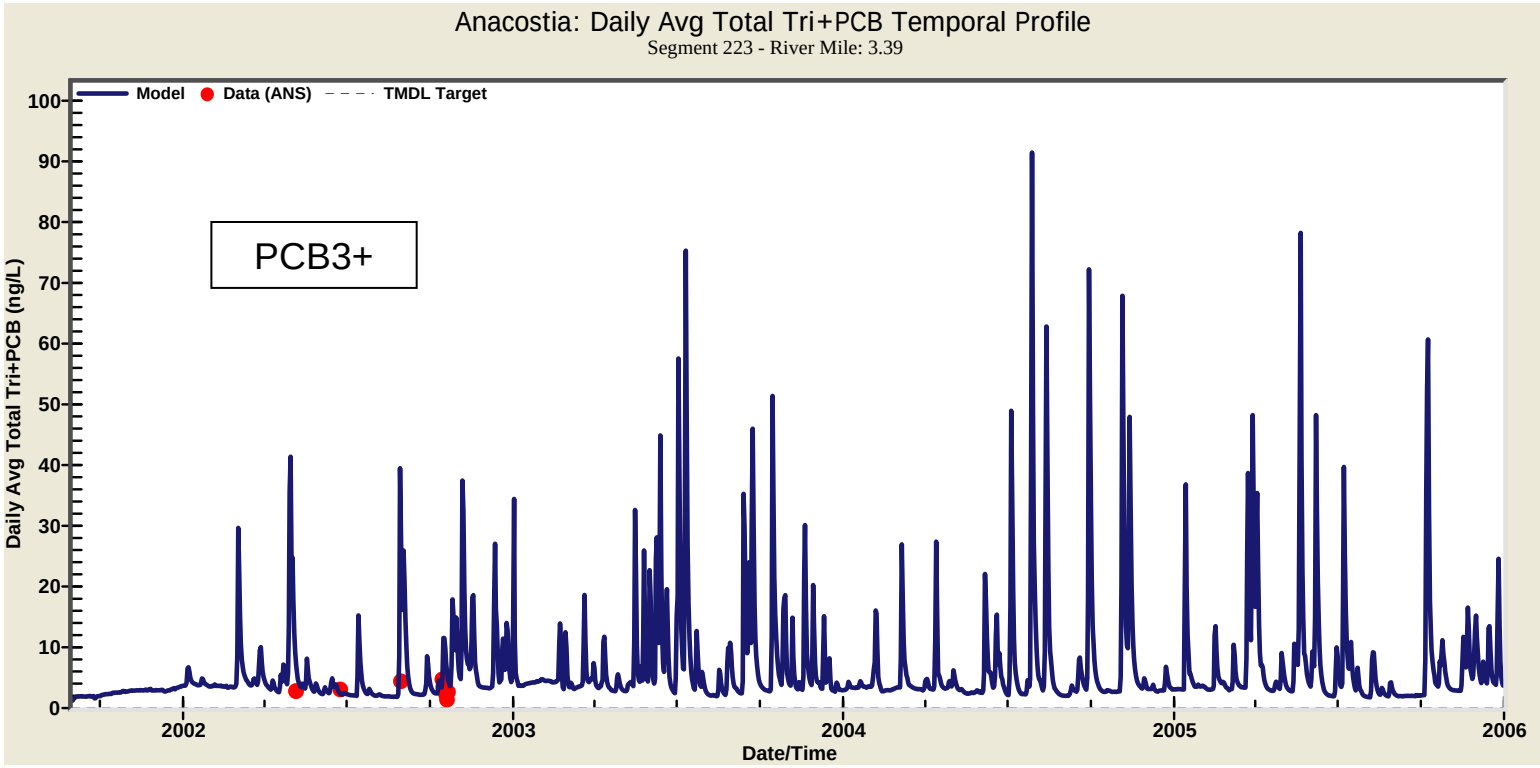

Figure 115. Time Series Plots for Computed and Observed Daily Average PCB3+ at Anacostia River Mile 3.39

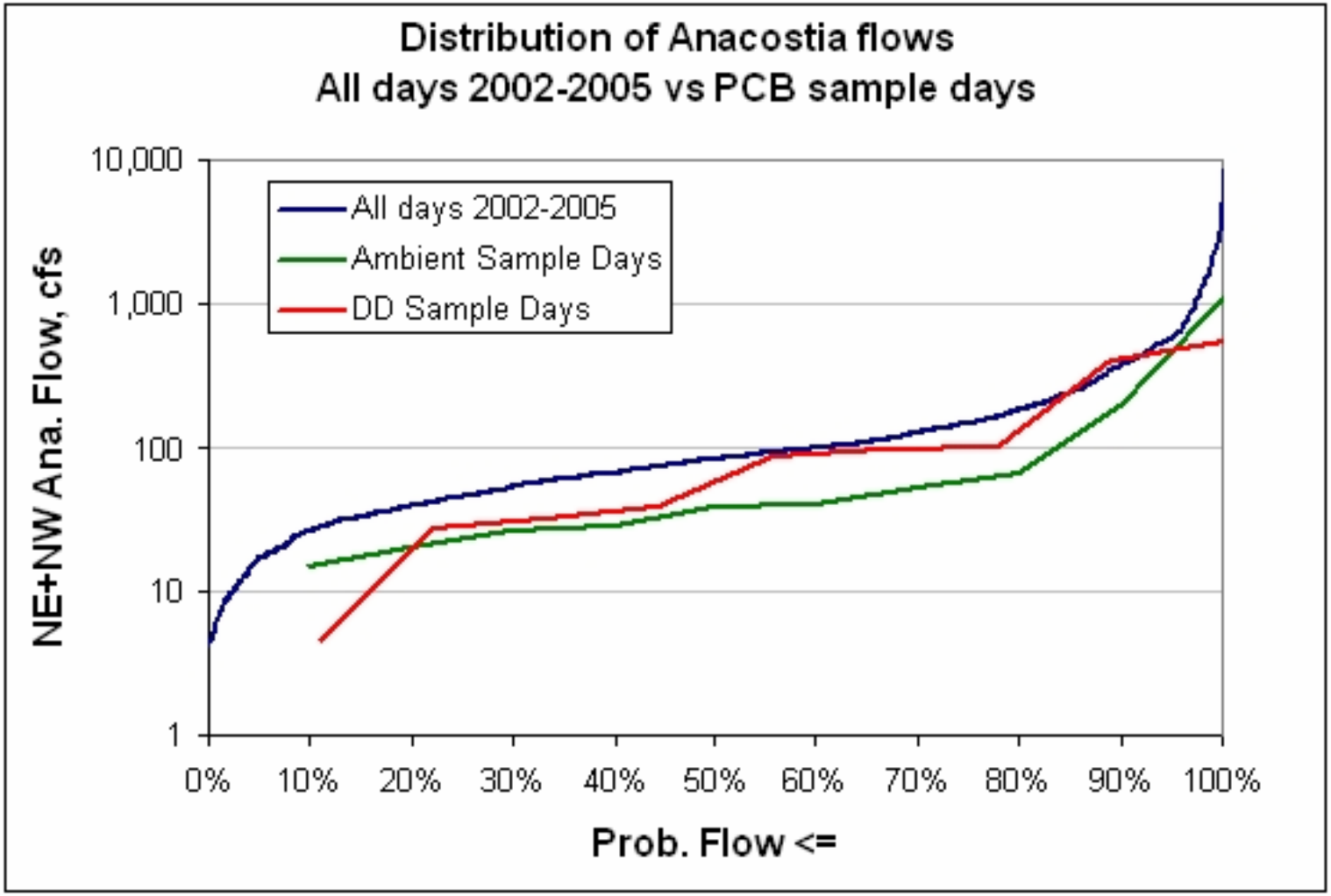

Figure 116. CFDs for Daily Average Flow and Sampling Days for Ambient Conditions and Direct Drainage in the Anacostia

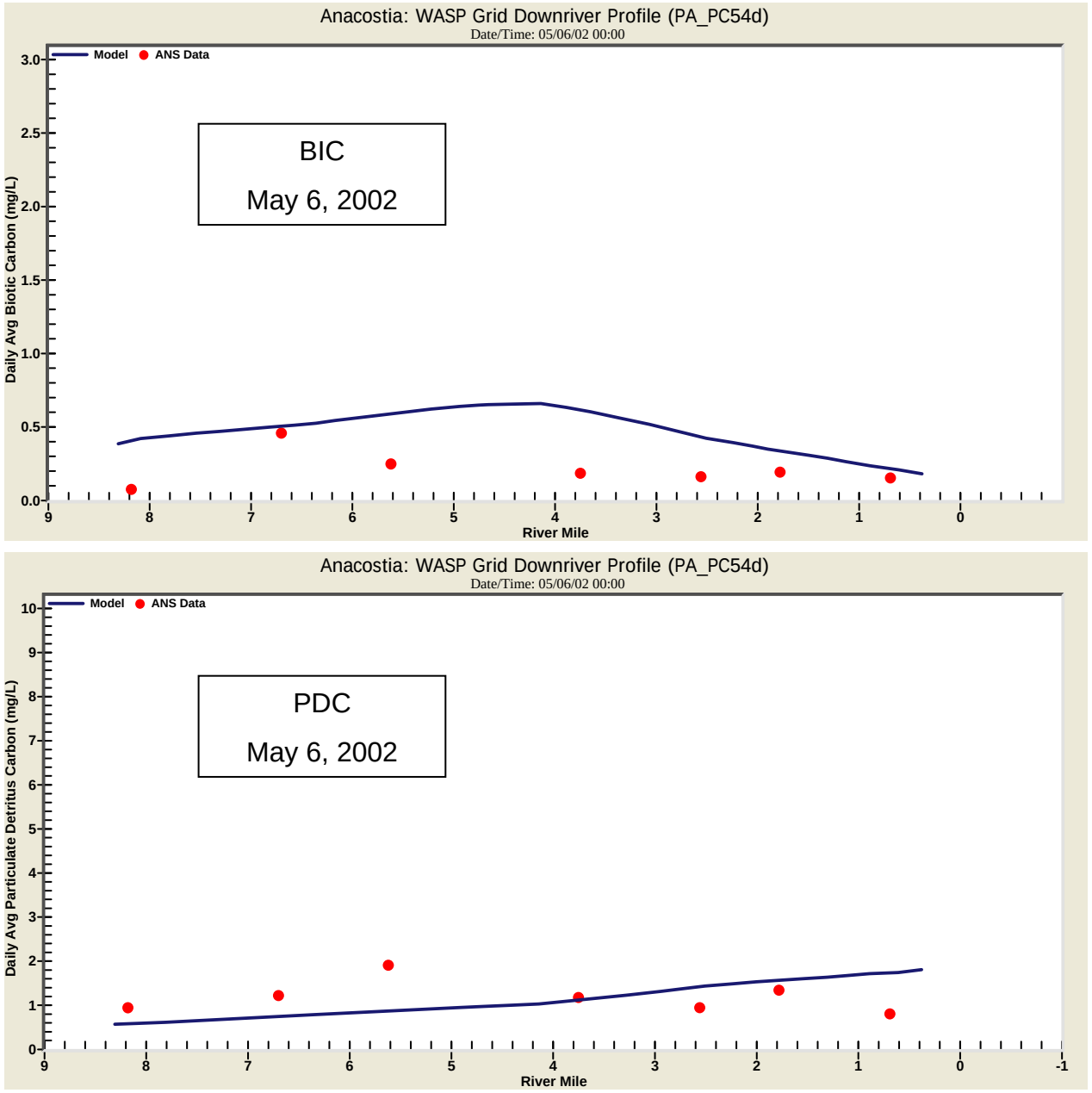

Figure 117. Spatial Profiles of Computed and Observed Daily Average BIC and PDC in Anacostia on May 6, 2002

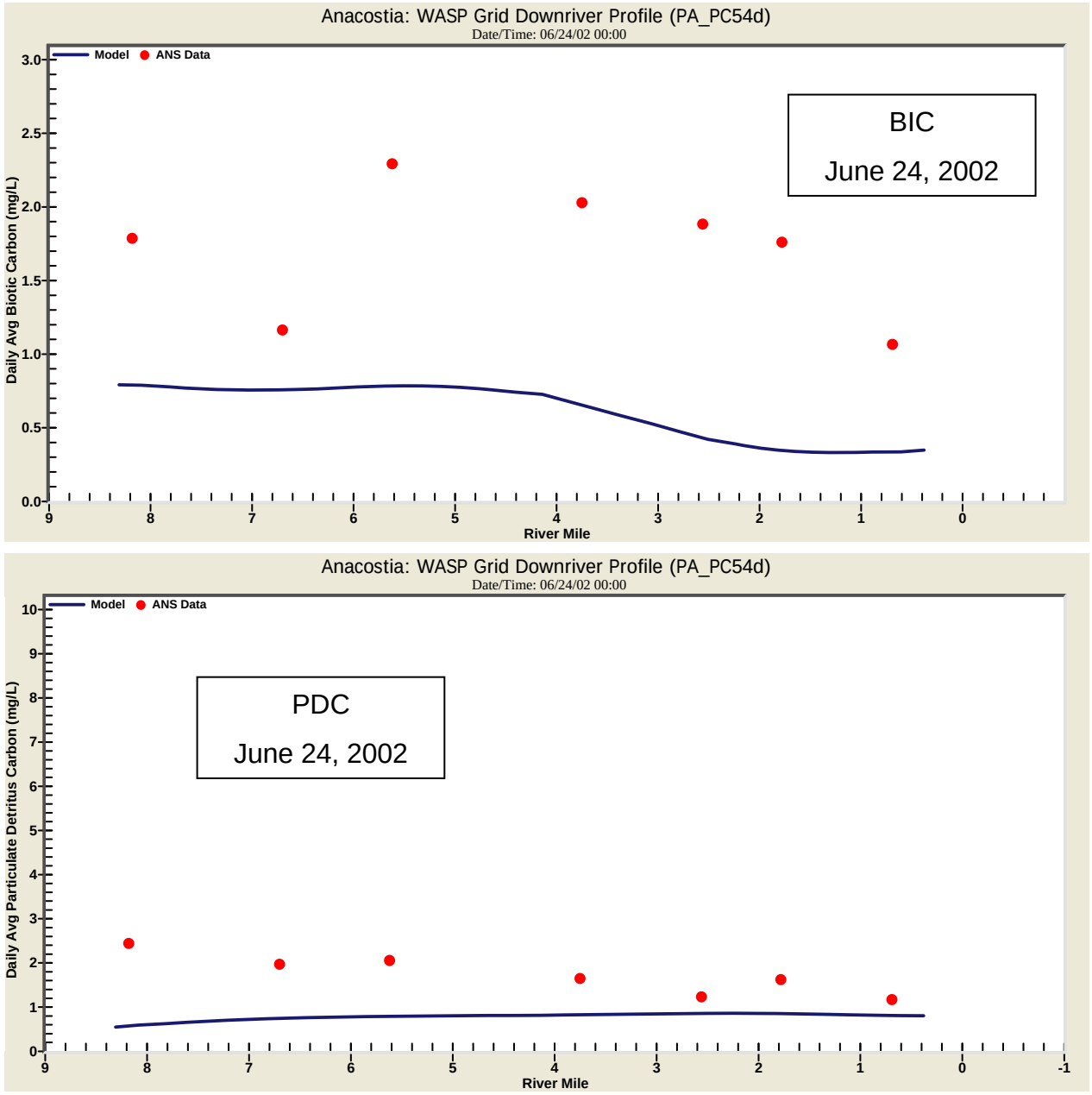

Figure 118. Spatial Profiles of Computed and Observed Daily Average BIC and PDC in Anacostia on June 24, 2002

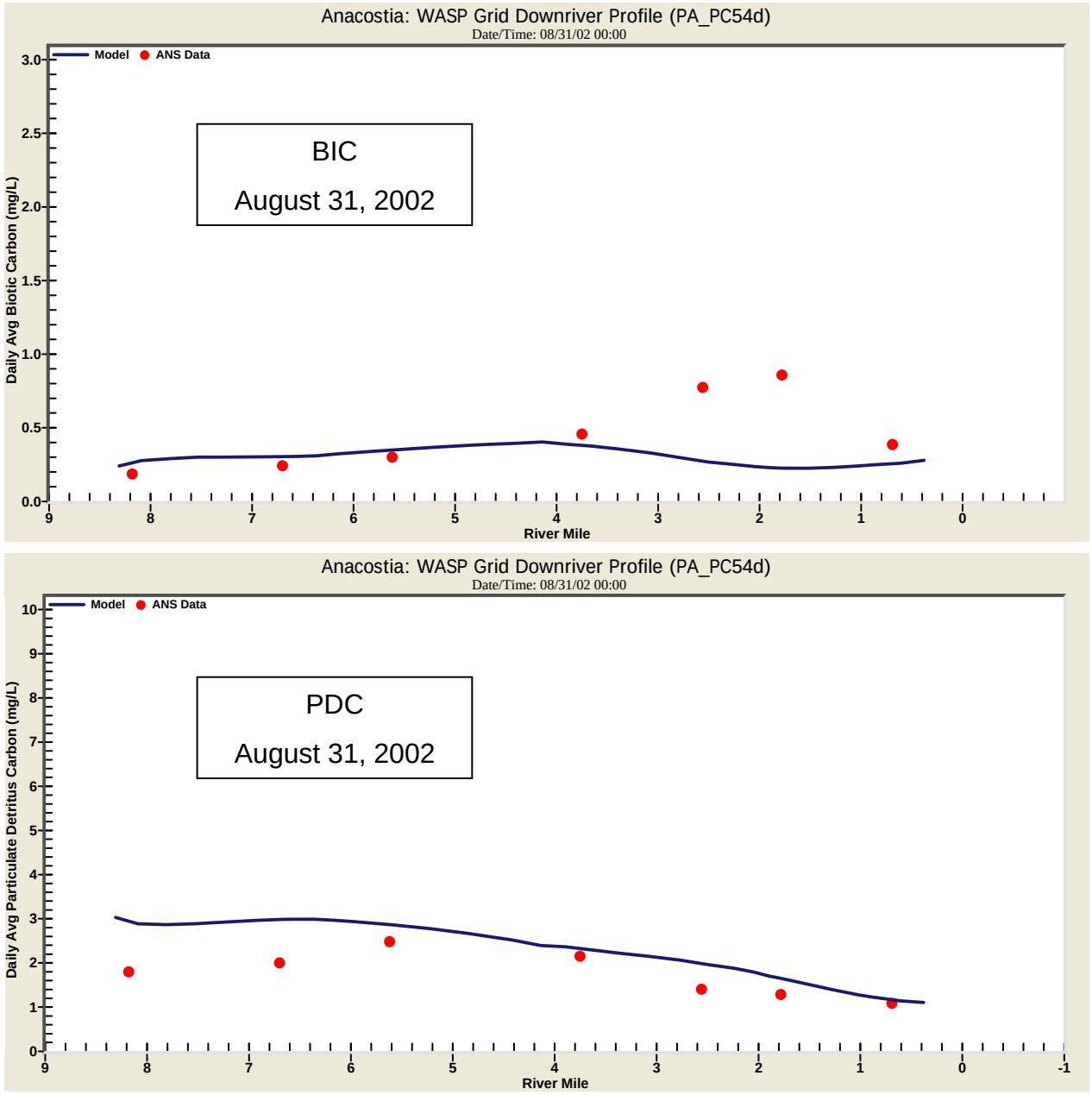

Figure 119. Spatial Profiles of Computed and Observed Daily Average BIC and PDC in Anacostia on August 31, 2002

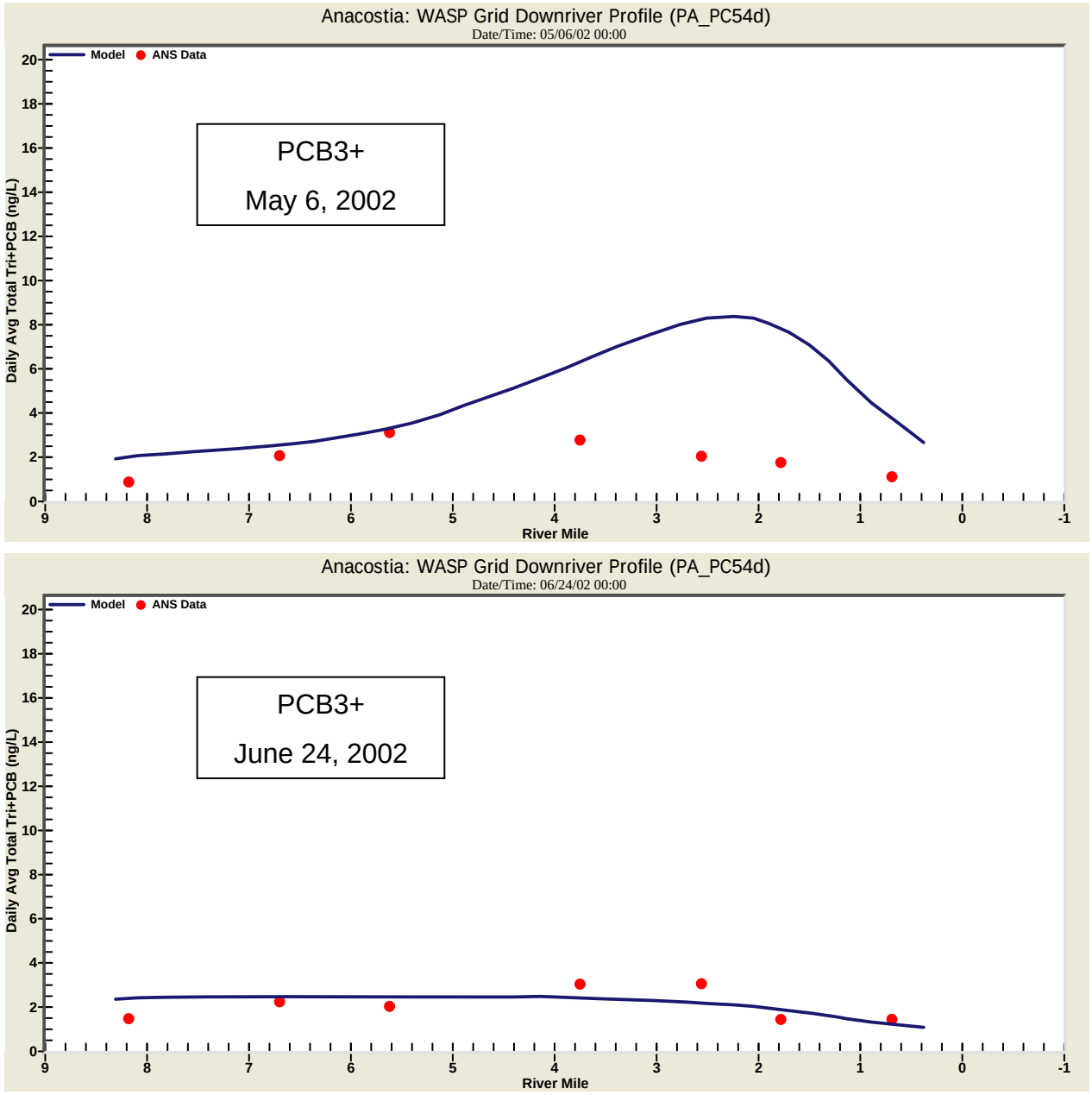

Figure 120. Spatial Profiles of Computed and Observed Daily Average PCB3+ in Anacostia on May 6 and June 24, 2002

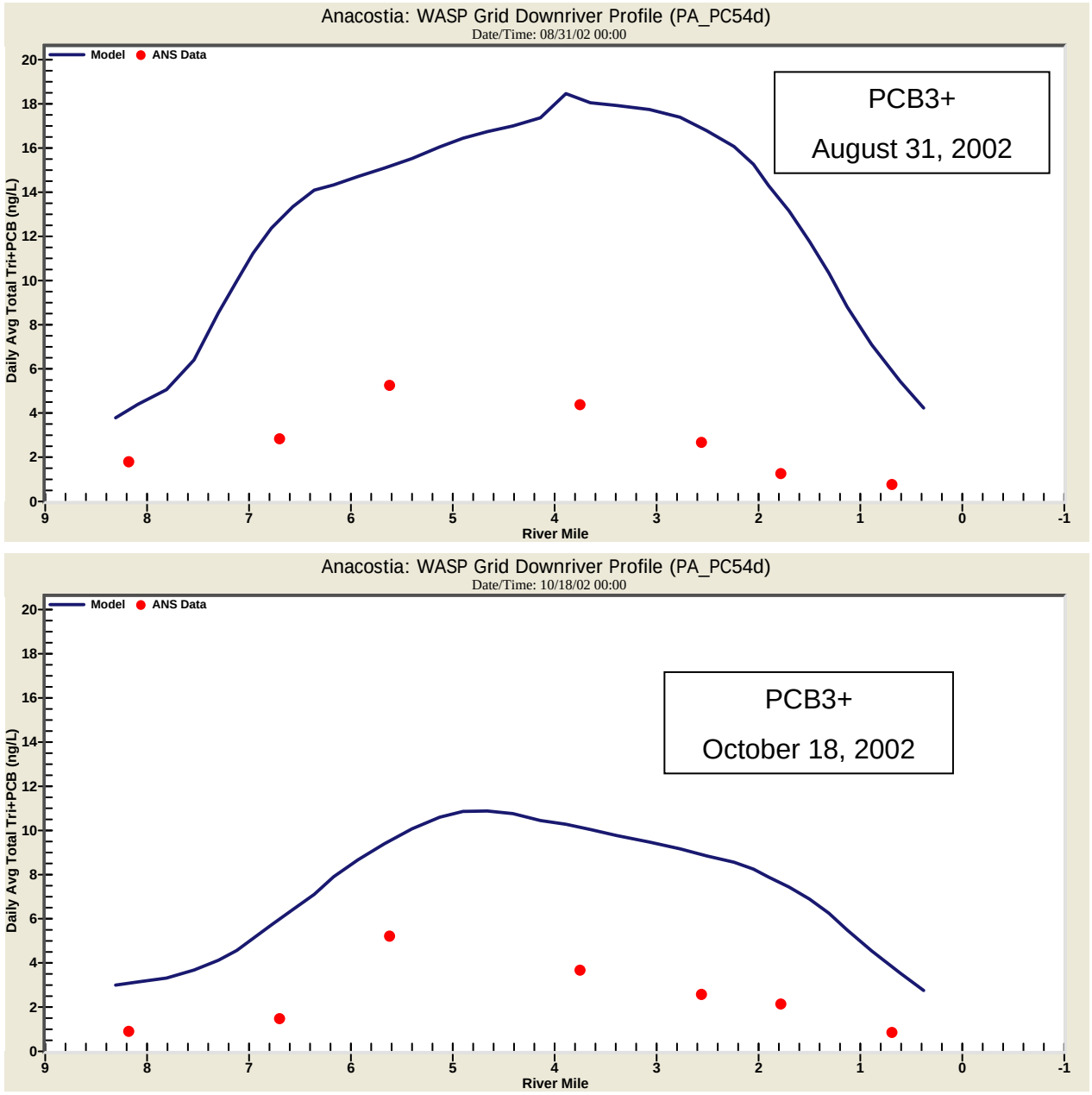

Figure 121. Spatial Profiles of Computed and Observed Daily Average PCB3+ in Anacostia on August 31 and October 18, 2002

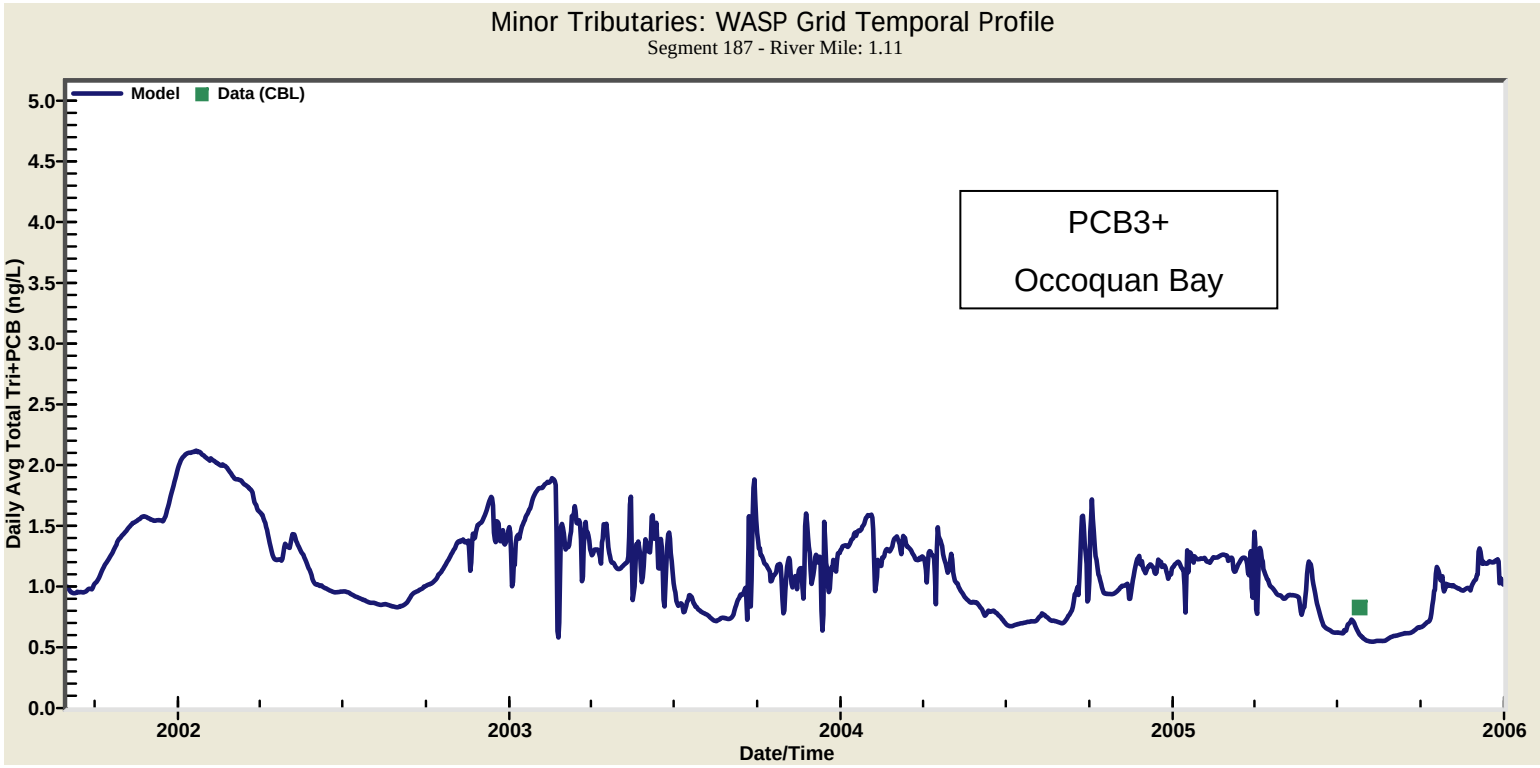

Figure 122. Time Series Plot for Computed and Observed Daily Average PCB3+ in Occoquan Bay

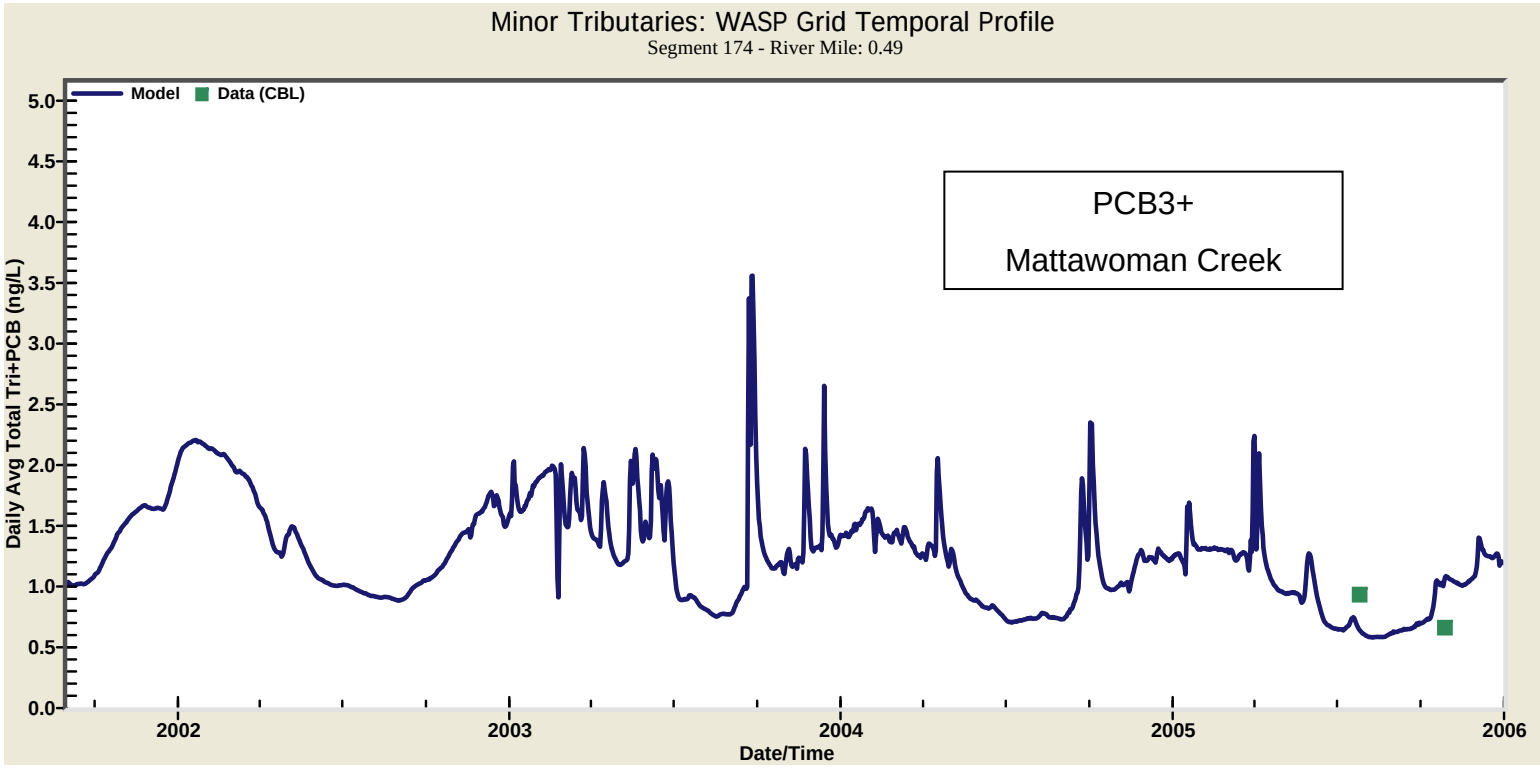

Figure 123. Time Series Plot for Computed and Observed Daily Average PCB3+ in Mattawoman Creek

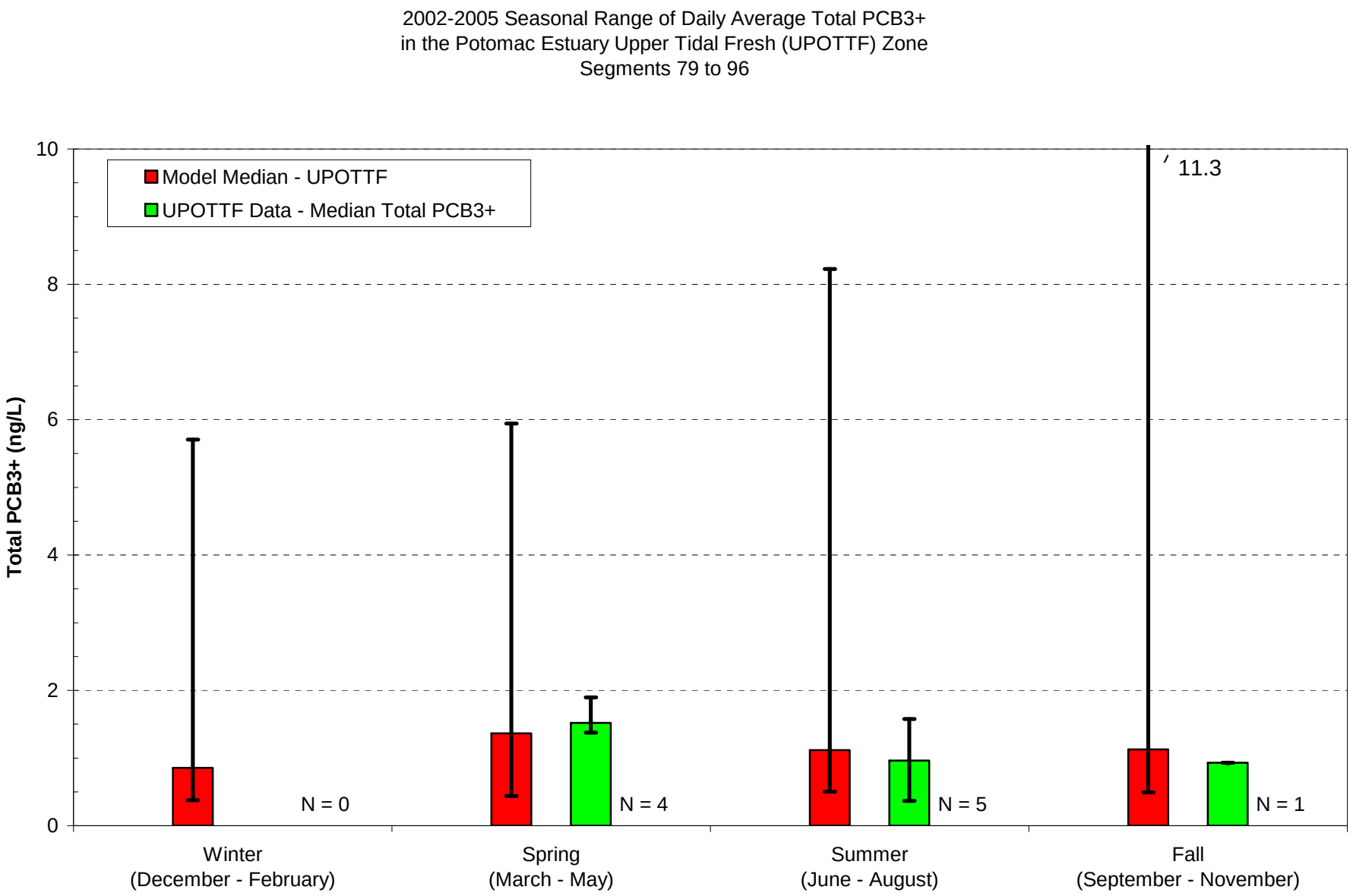

Figure 124. Comparisons Between Computed and Observed Seasonal Medians and Ranges for PCB3+ in UPOTTF

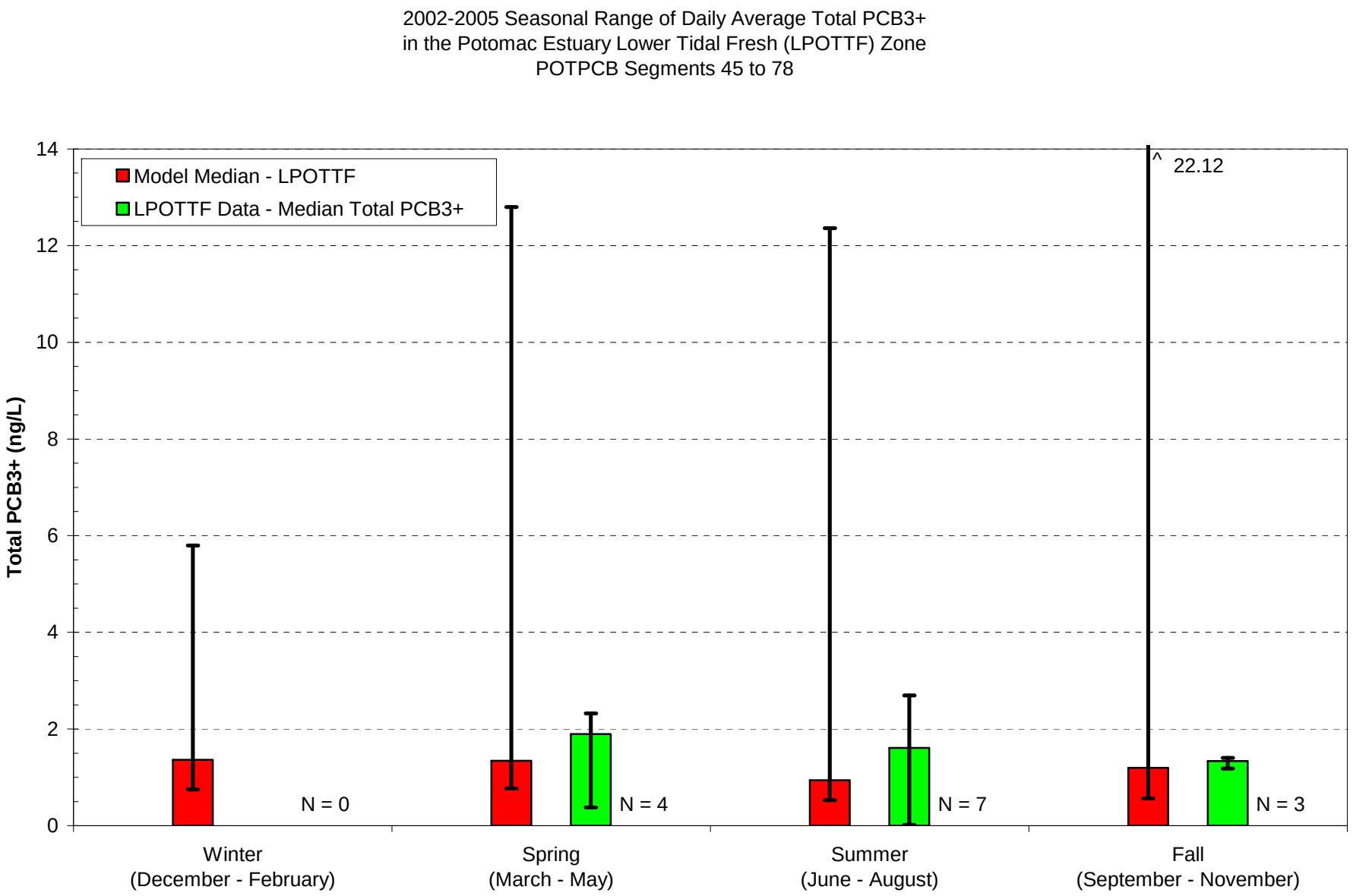

Figure 125. Comparisons Between Computed and Observed Seasonal Medians and Ranges for PCB3+ in LPOTTF

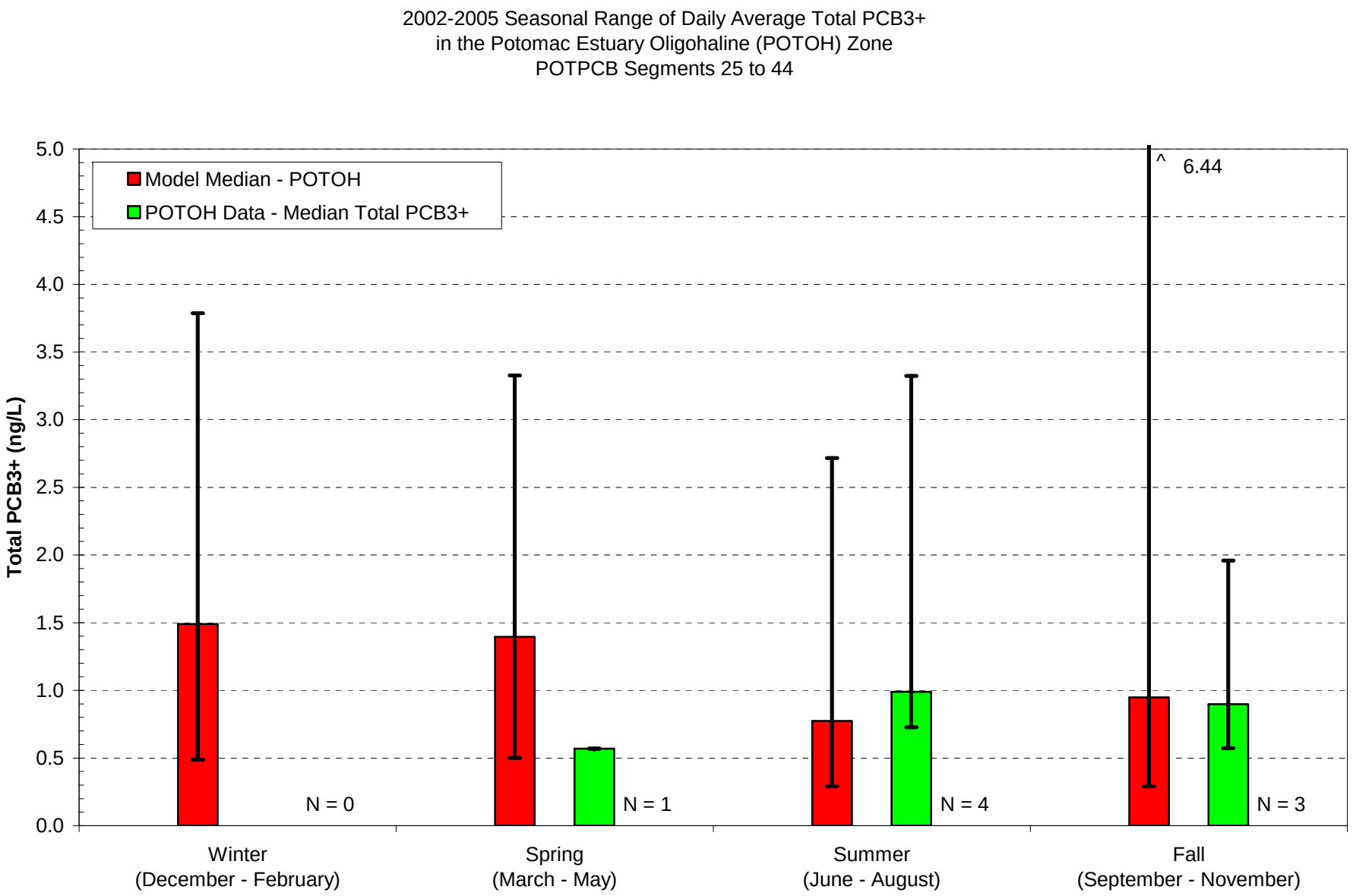

Figure 126. Comparisons Between Computed and Observed Seasonal Medians and Ranges for PCB3+ in POTOH

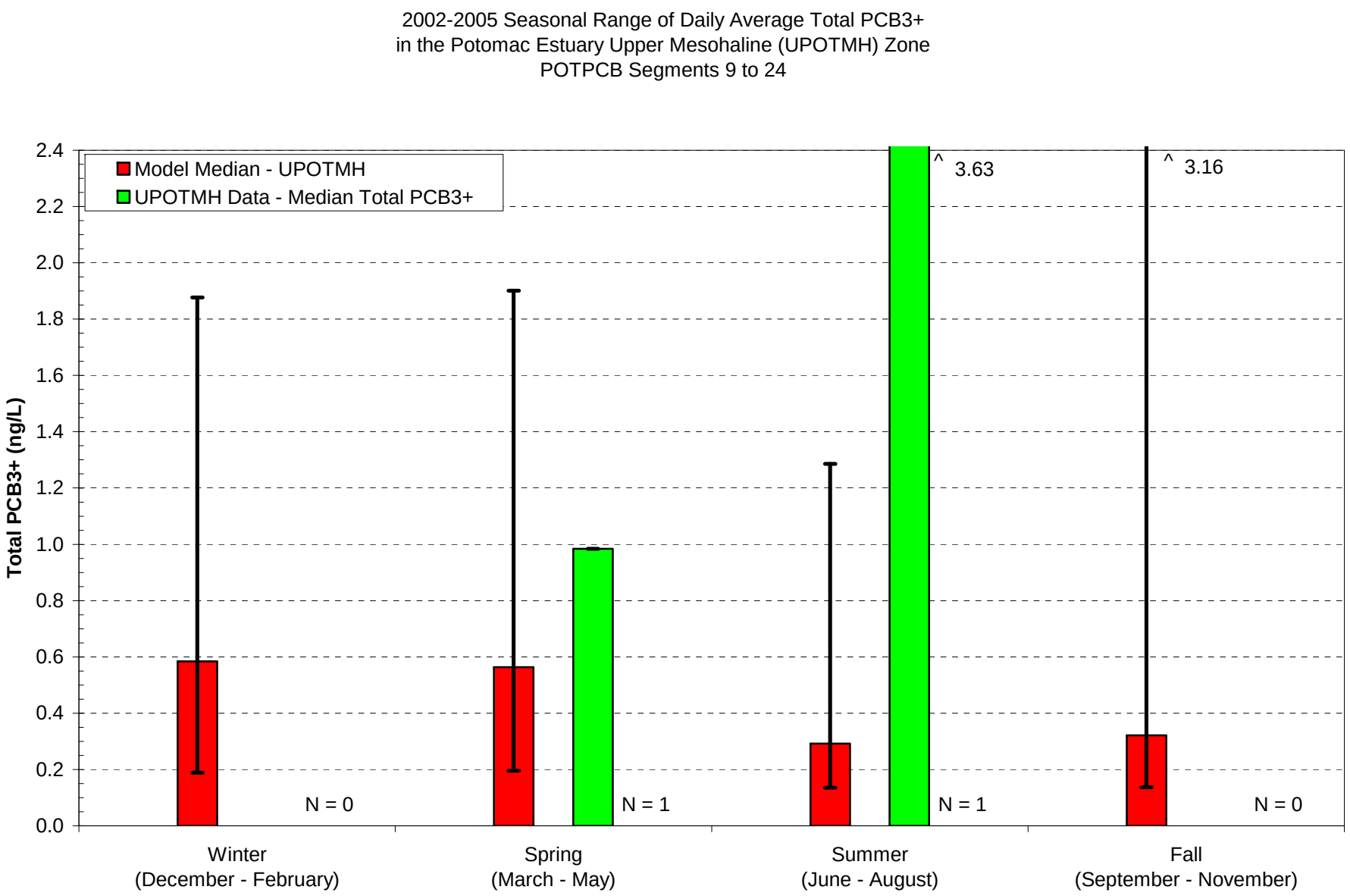

Figure 127. Comparisons Between Computed and Observed Seasonal Medians and Ranges for PCB3+ in UPOTMH

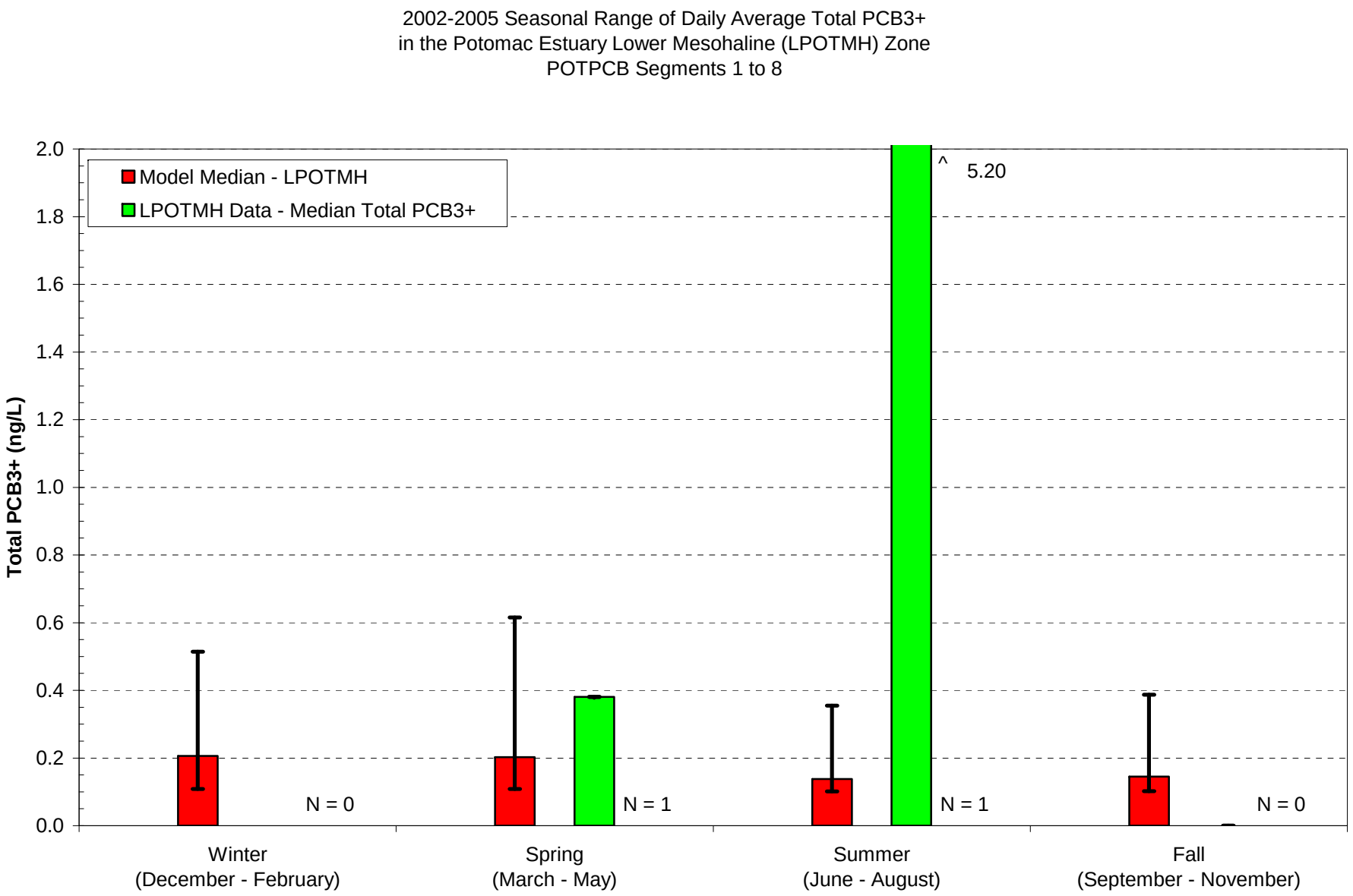

Figure 128. Comparisons Between Computed and Observed Seasonal Medians and Ranges for PCB3+ in LPOTMH

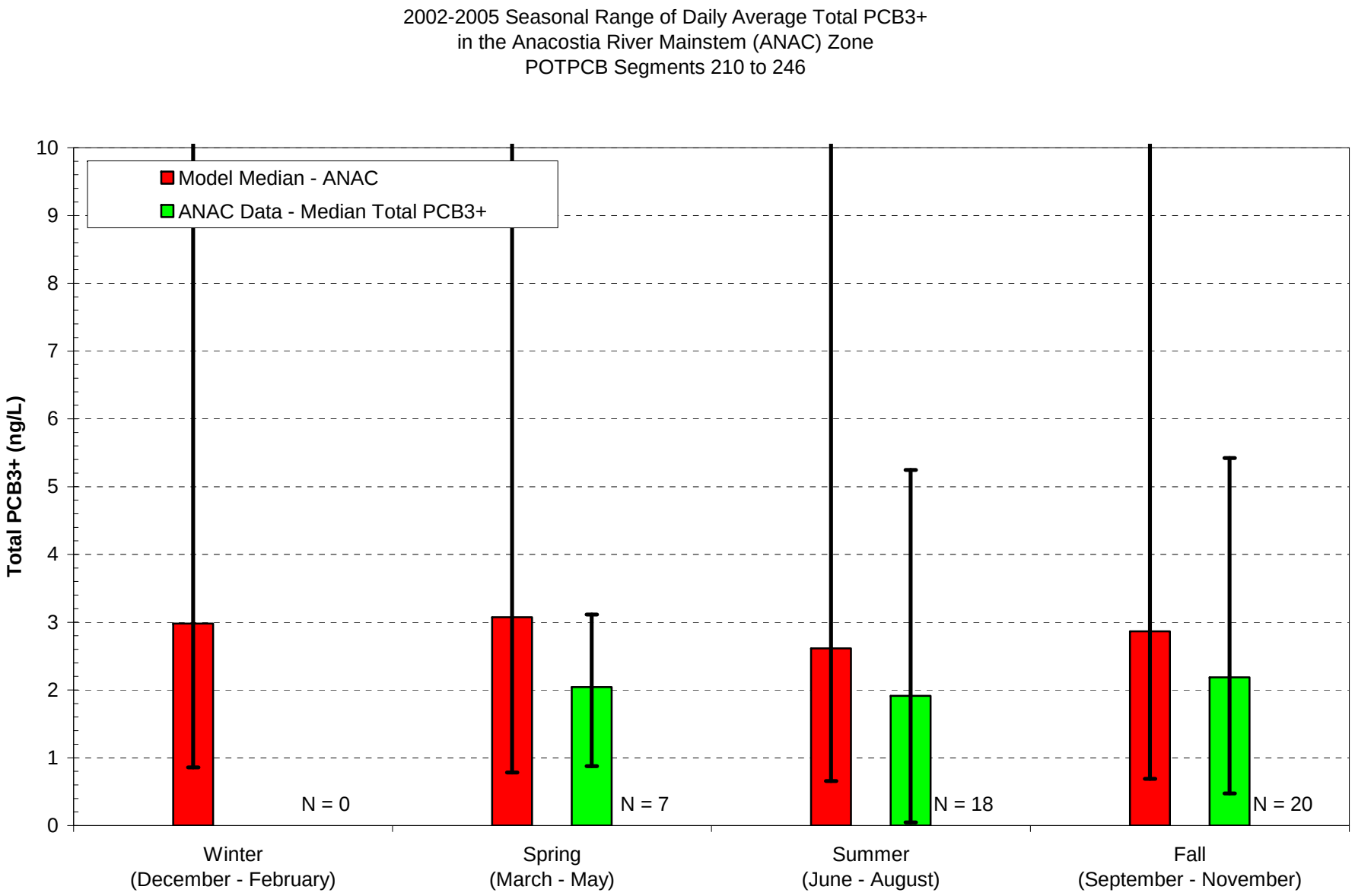

Figure 129. Comparisons Between Computed and Observed Seasonal Medians and Ranges for PCB3+ in ANAC

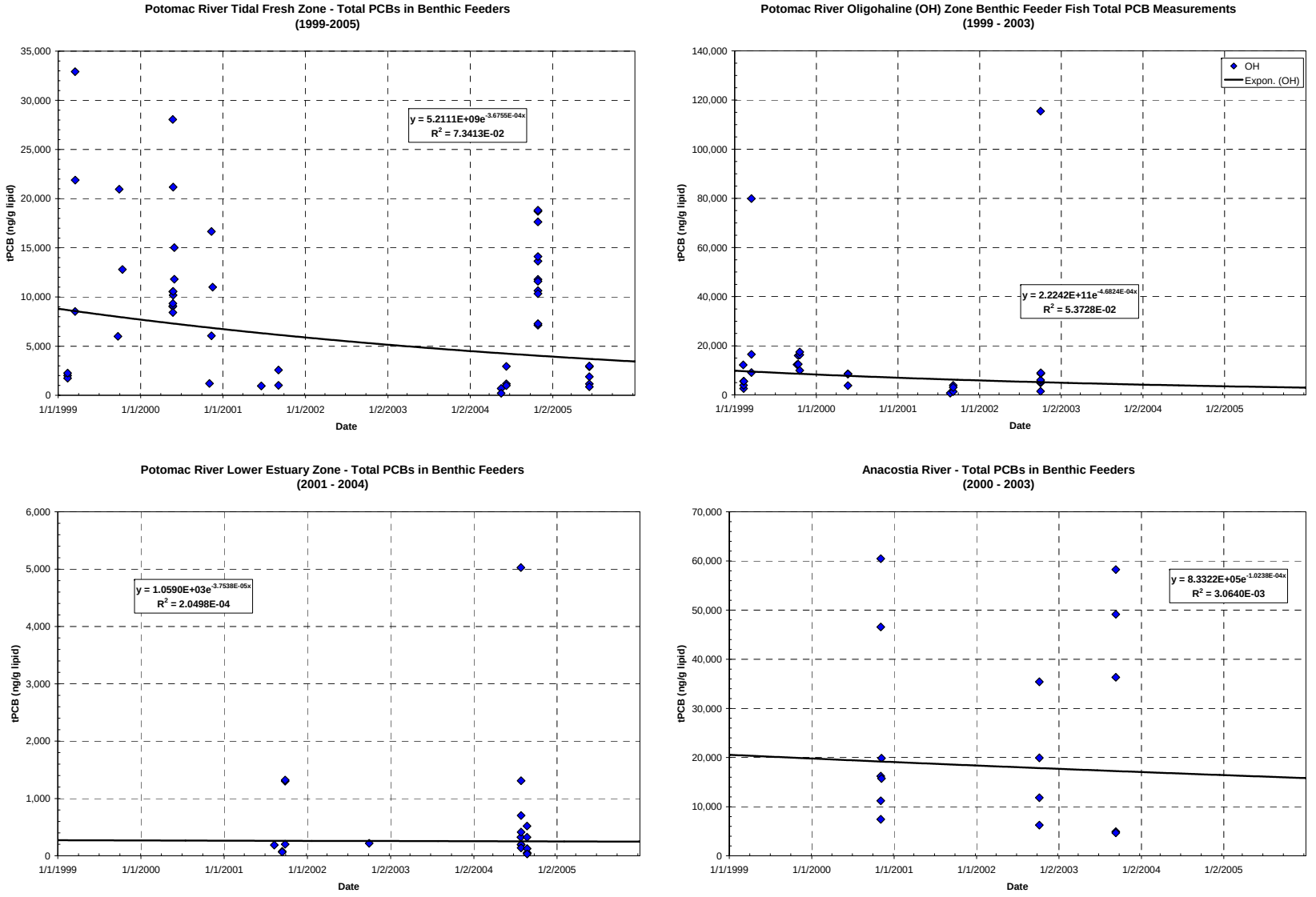

Figure 130. Lipid-Normalized Total PCB Body Burdens in Benthic Feeding Fish Species in Potomac and Anacostia Rivers

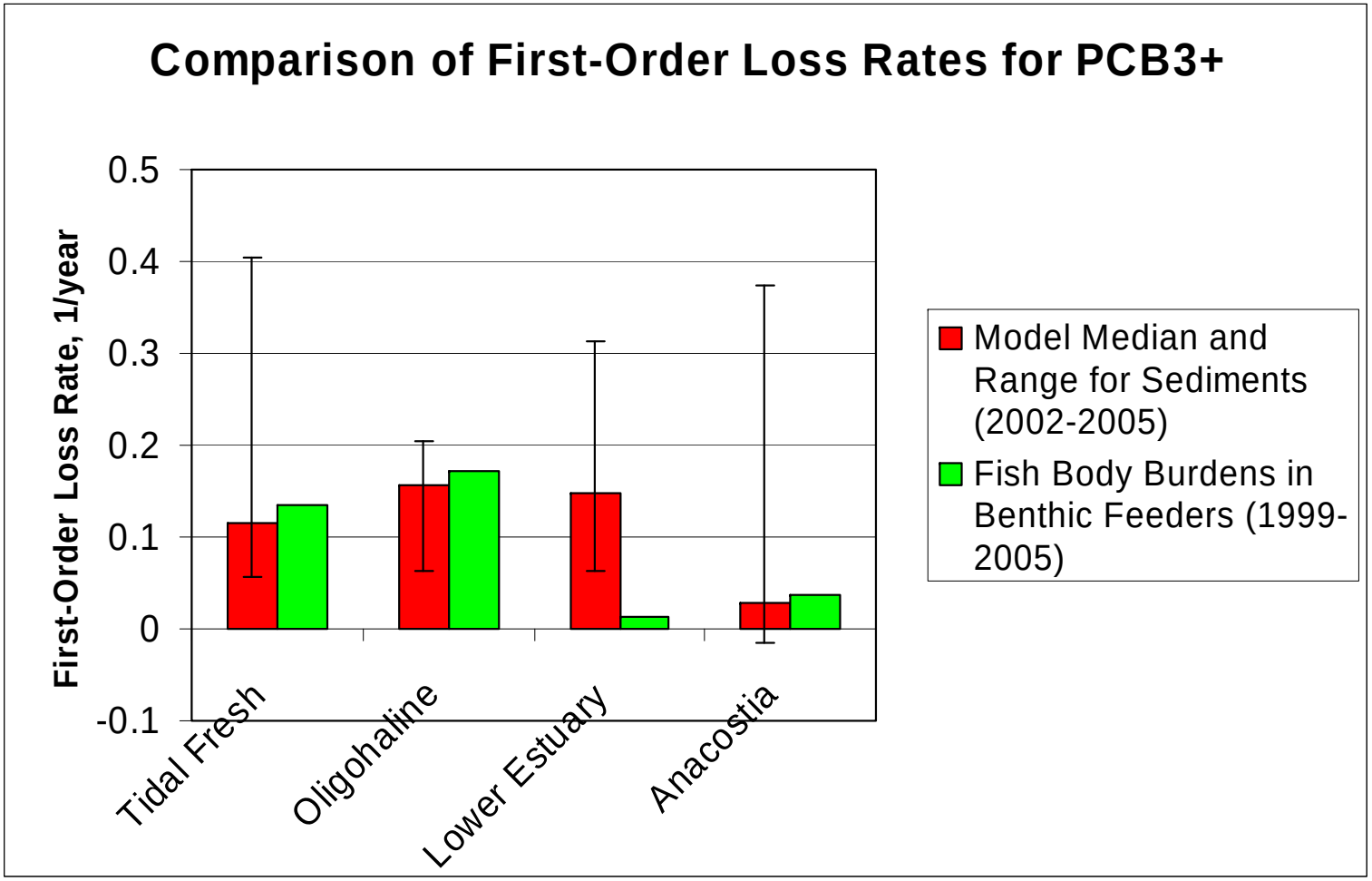

Figure 131. Comparison of Computed and Estimated First-Order Loss Rates for PCB3+

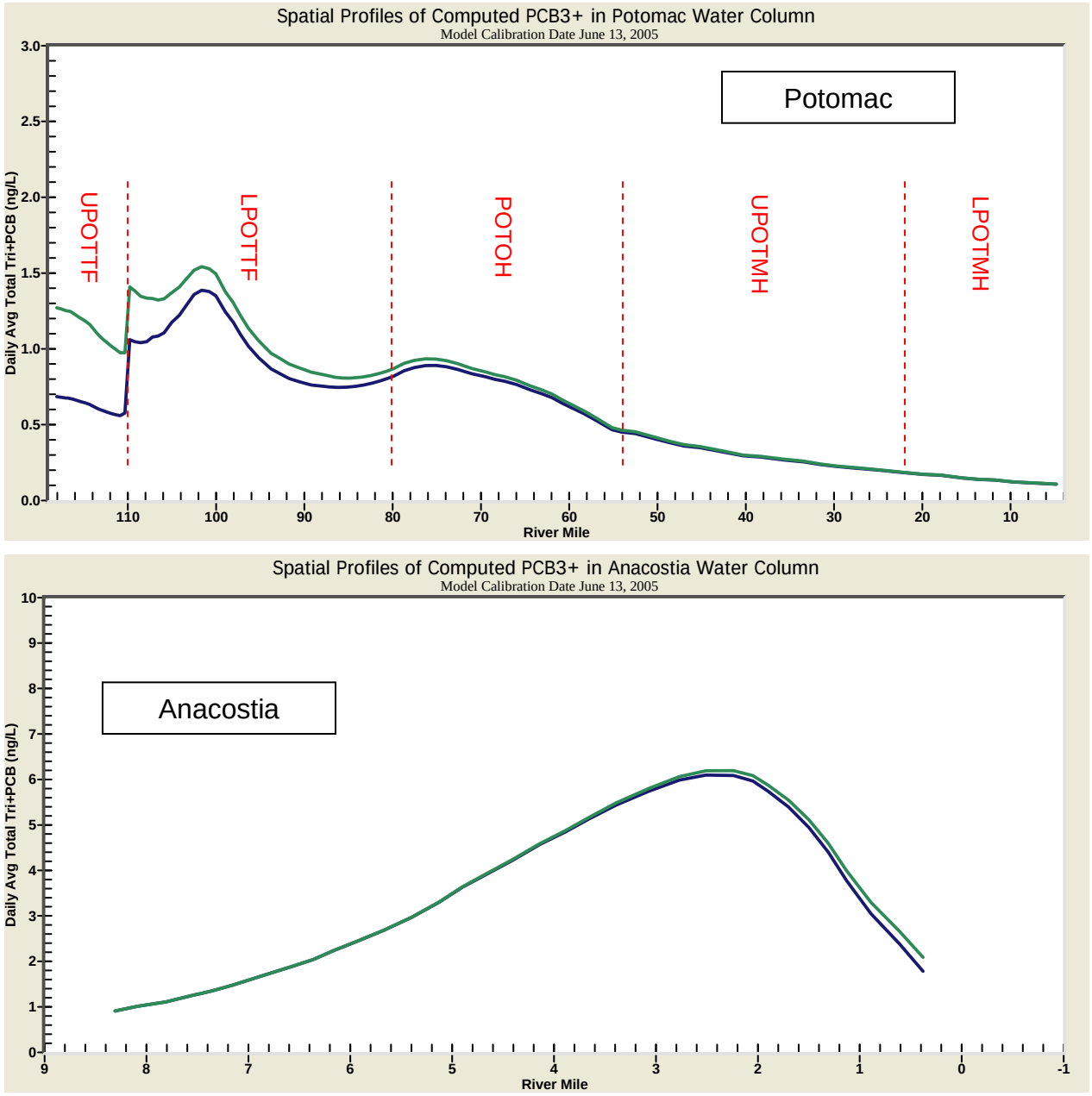

Figure 132. Sensitivity of Model Calibration Results to Plus/Minus 30 Percent Changes in PCB3+ Load at Chain Bridge

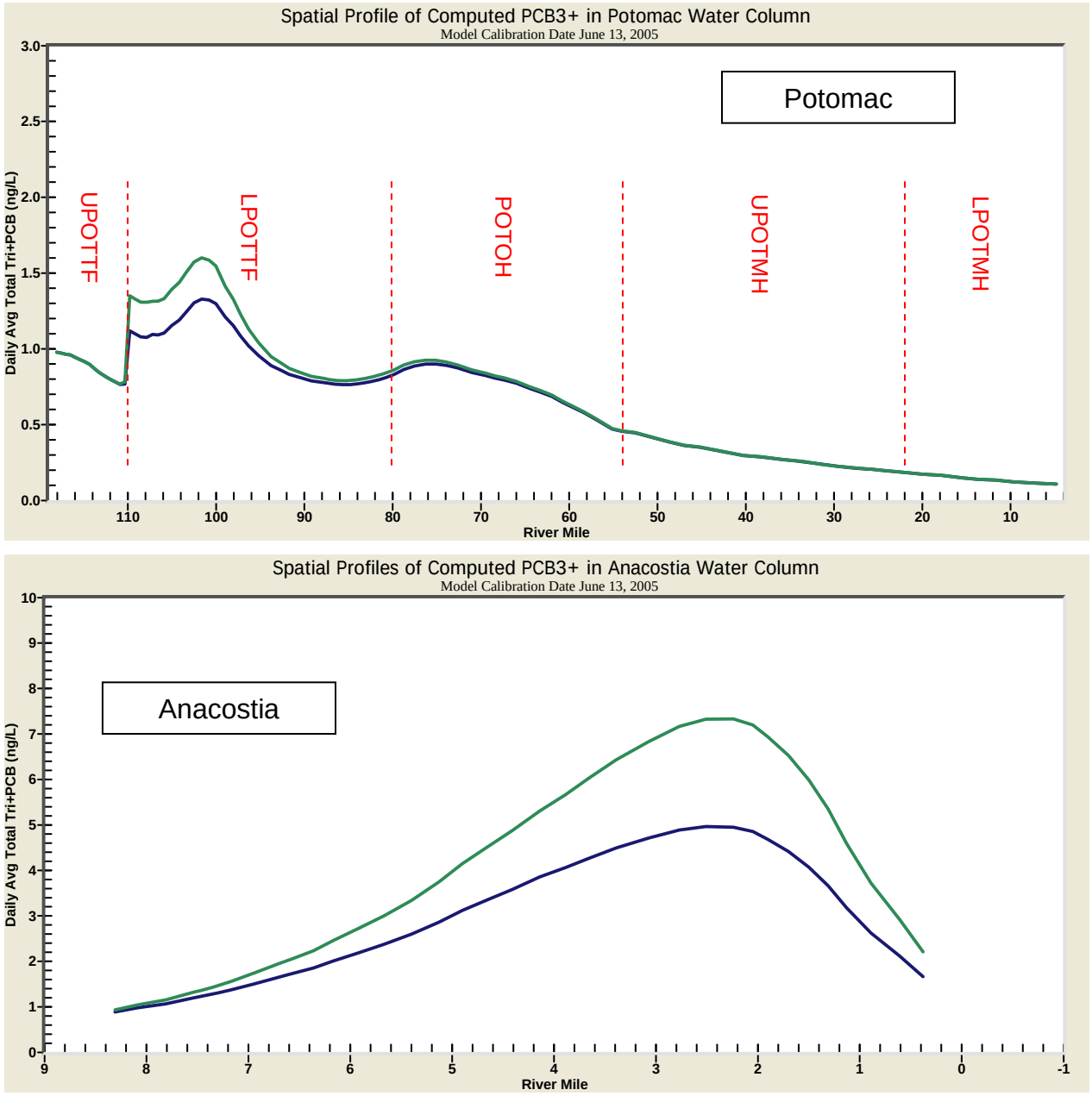

Figure 133. Sensitivity of Model Calibration Results to Plus/Minus 30 Percent Changes in PCB3+ Loads from Direct Drainage

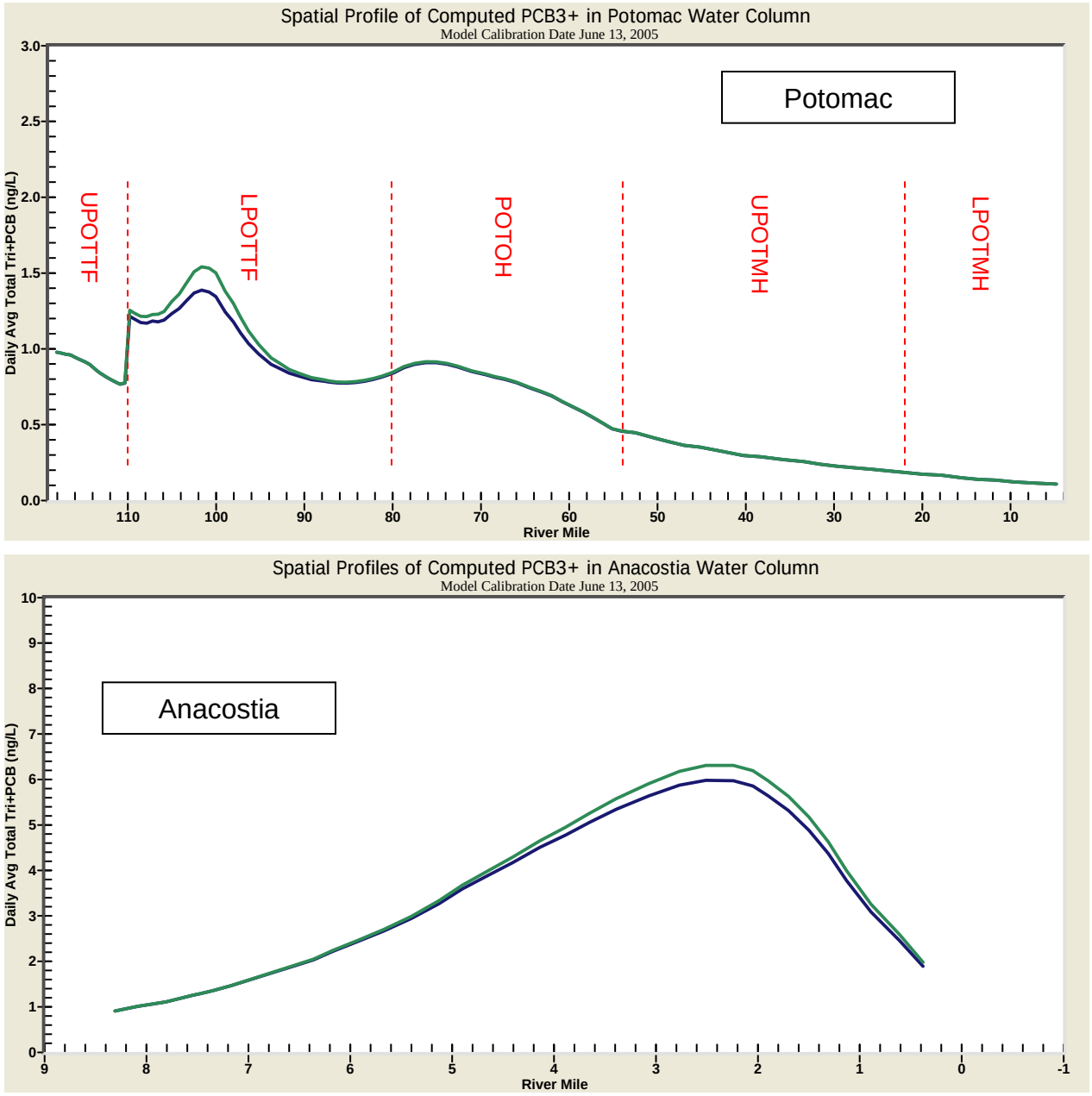

Figure 134. Sensitivity of Model Calibration Results to Plus/Minus 30 Percent Changes in PCB3+ Loads from CSOs

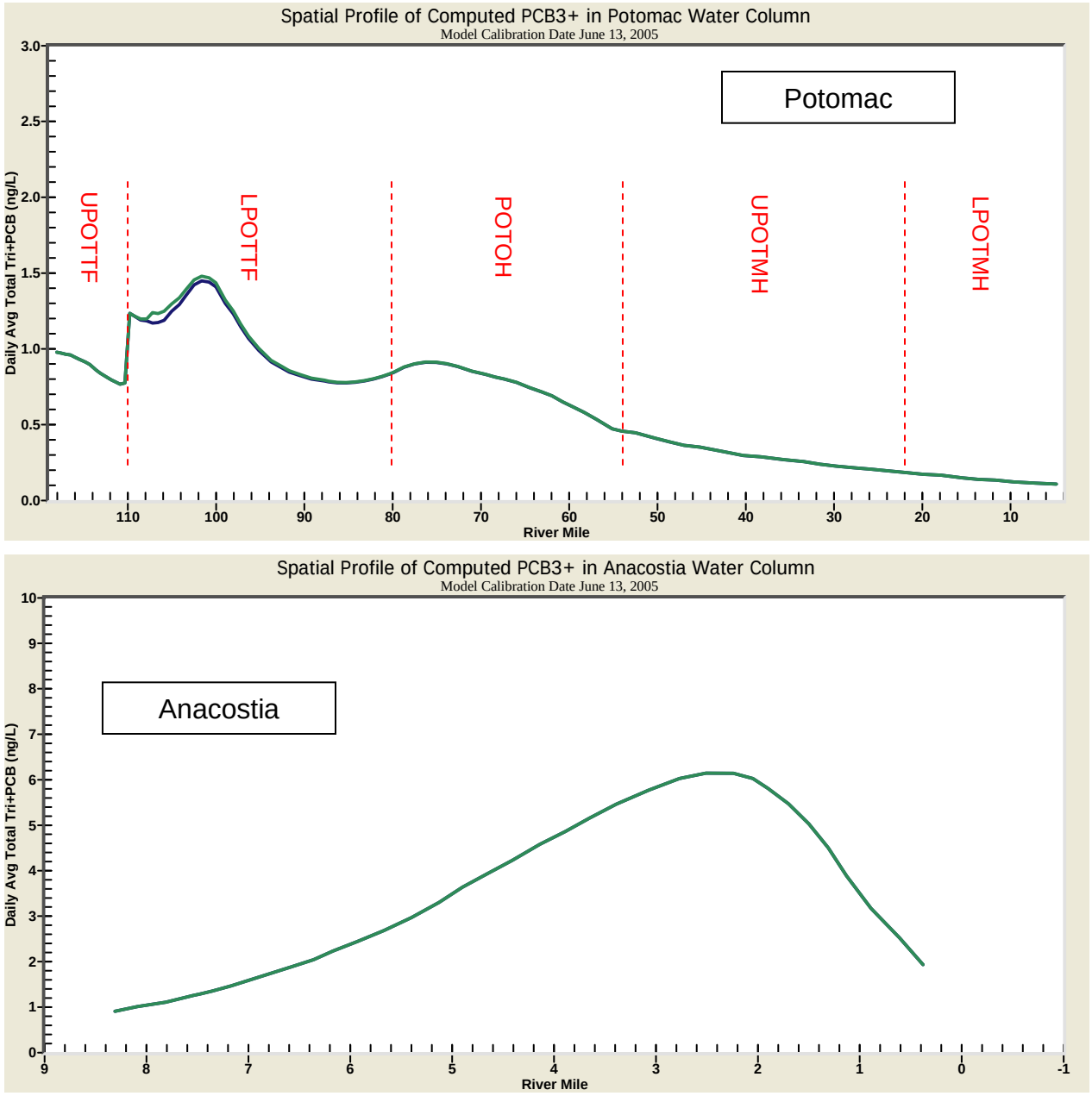

Figure 135. Sensitivity of Model Calibration Results to Plus/Minus 30 Percent Changes in PCB3+ Loads from Point Sources

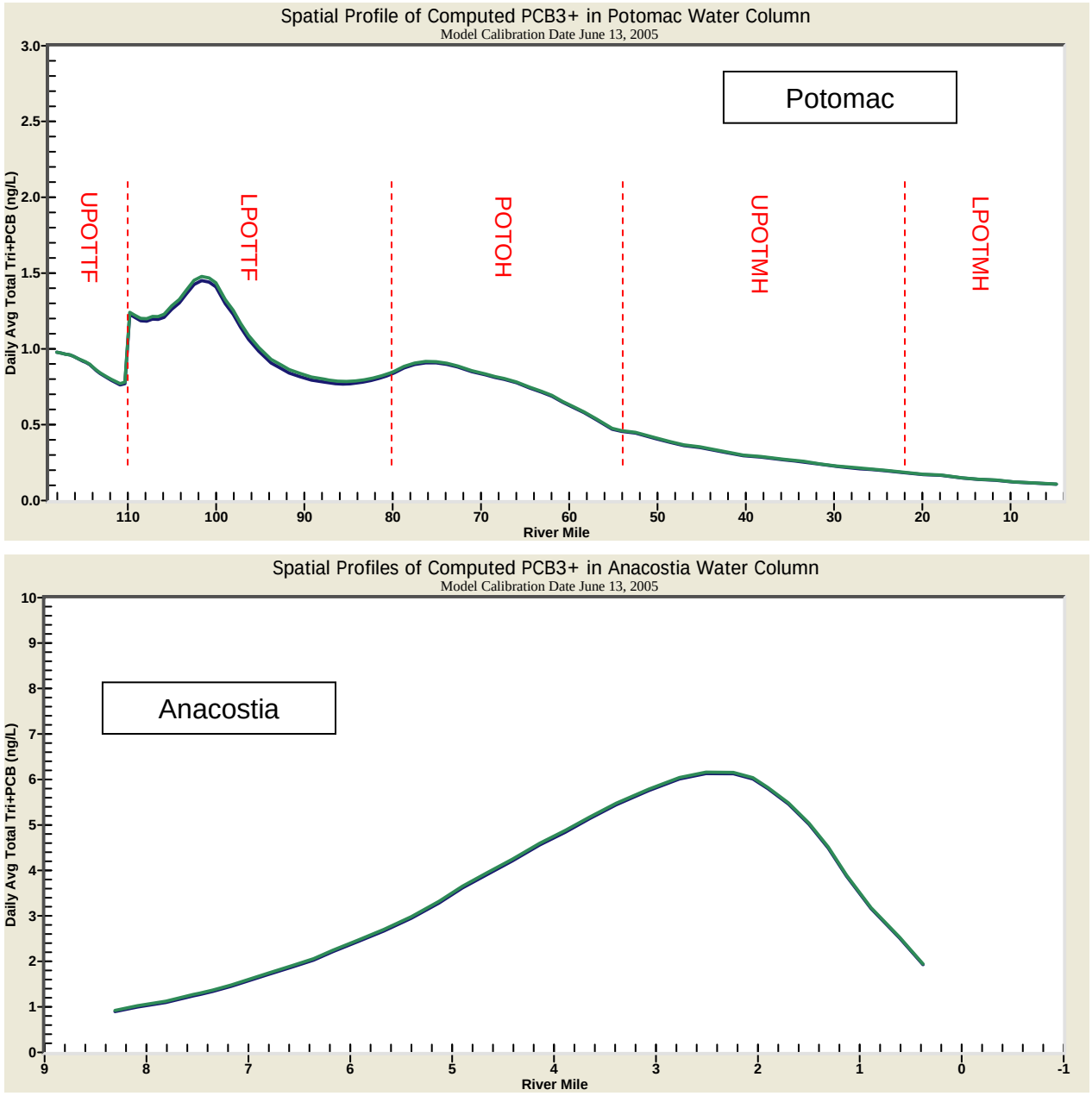

Figure 136. Sensitivity of Model Calibration Results to Plus/Minus 30 Percent Changes in PCB3+ Load from Atm Wet/Dry Deposition

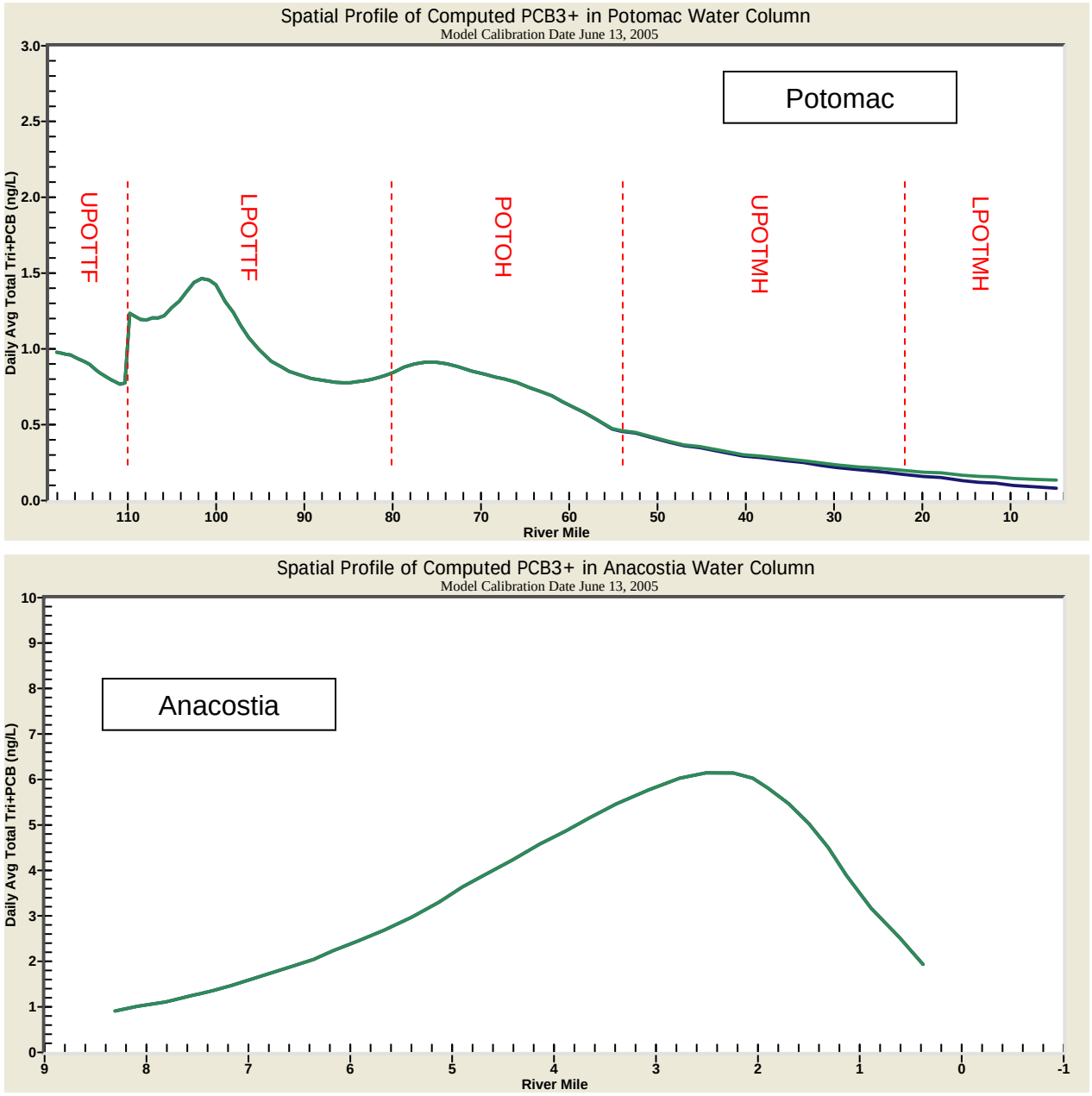

Figure 137. Sensitivity of Model Calibration Results to Plus/Minus 30 Percent Changes in PCB3+ Downstream Boundary Condition

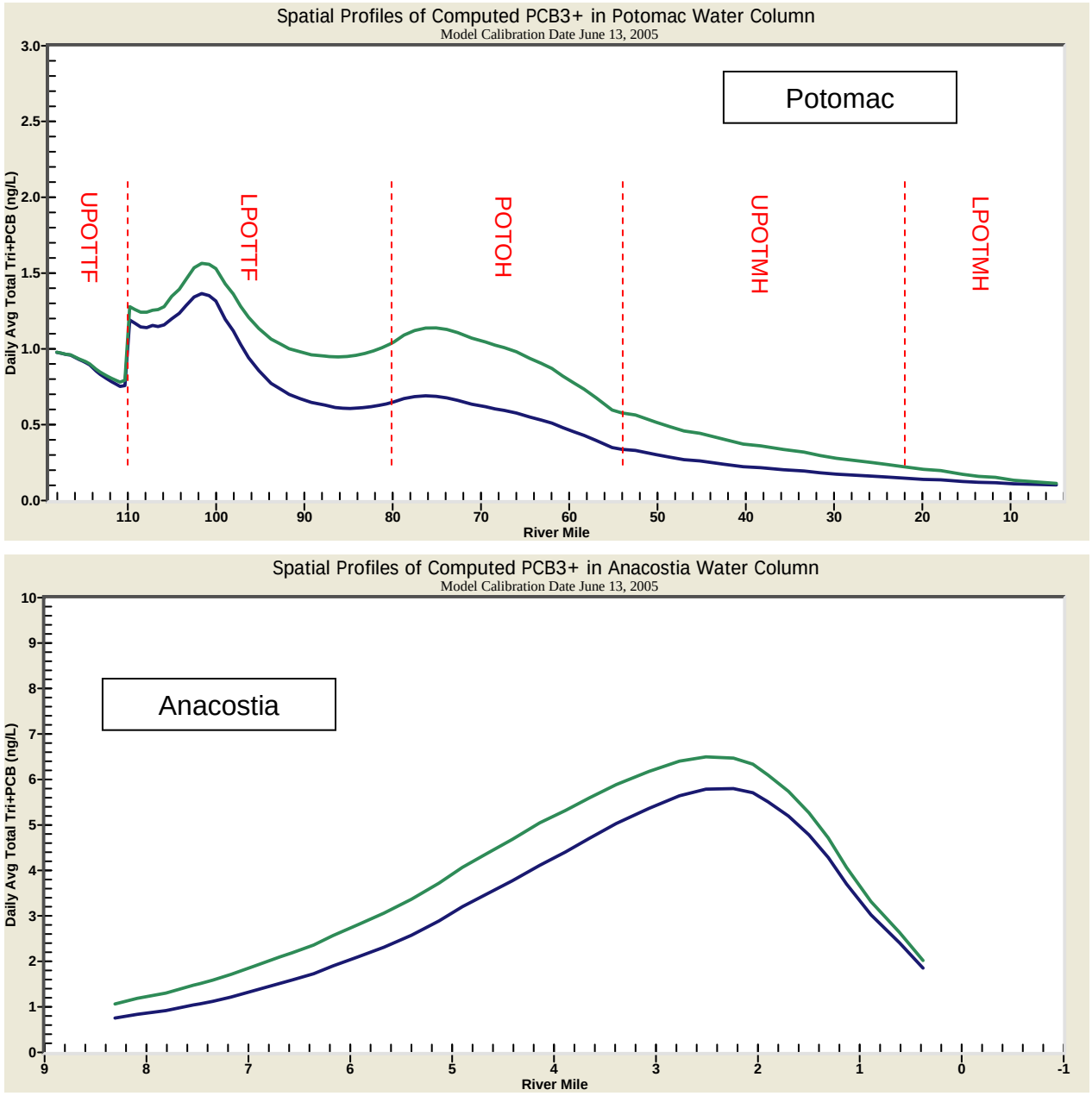

Figure 138. Sensitivity of Model Calibration Results to Plus/Minus 30 Percent Changes in PCB3+ Sediment Initial Conditions

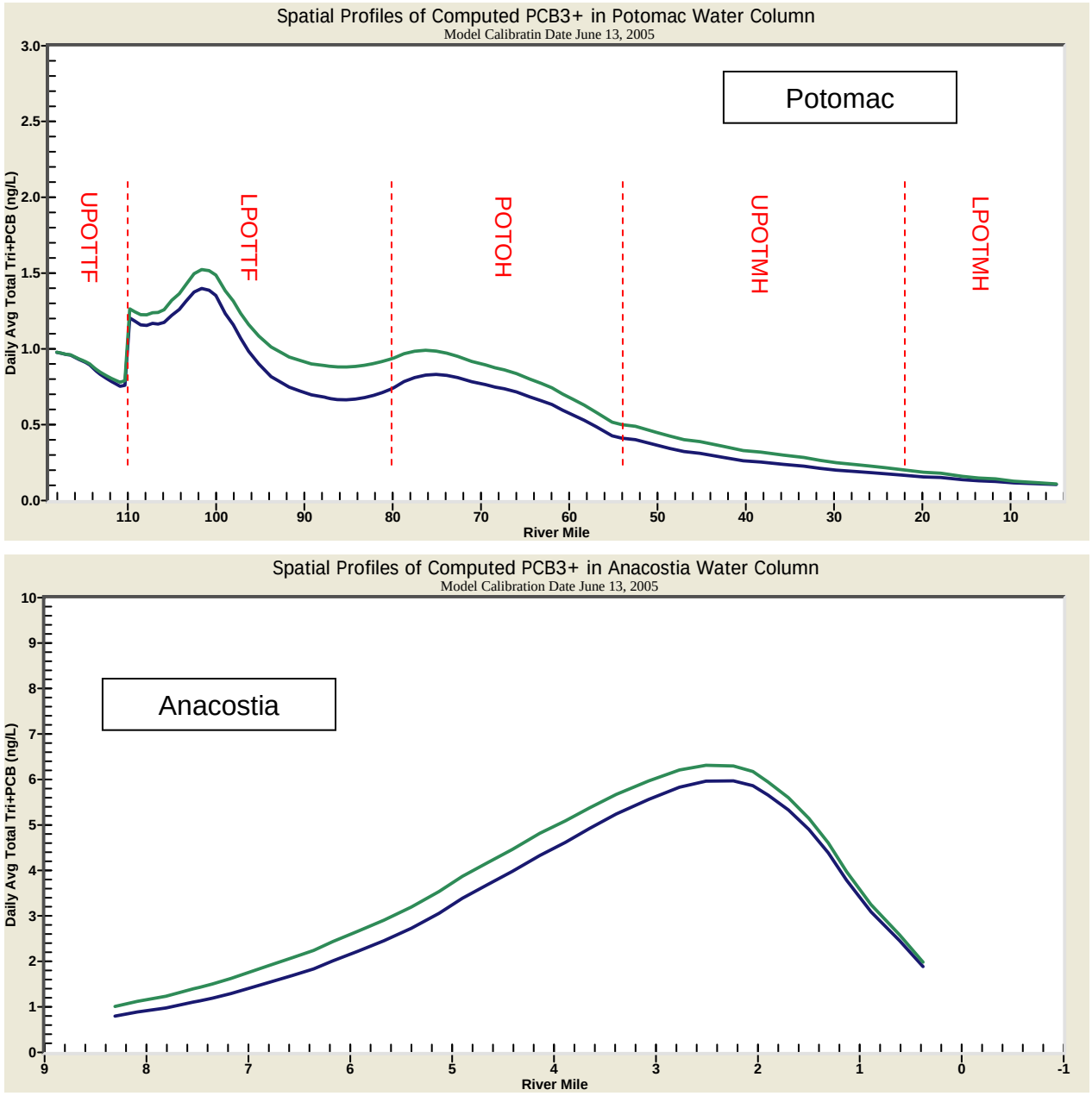

Figure 139. Sensitivity of Model Calibration Results to Plus/Minus 30 Percent Changes in PCB3+ Sediment-Water Mass Transfer Rate

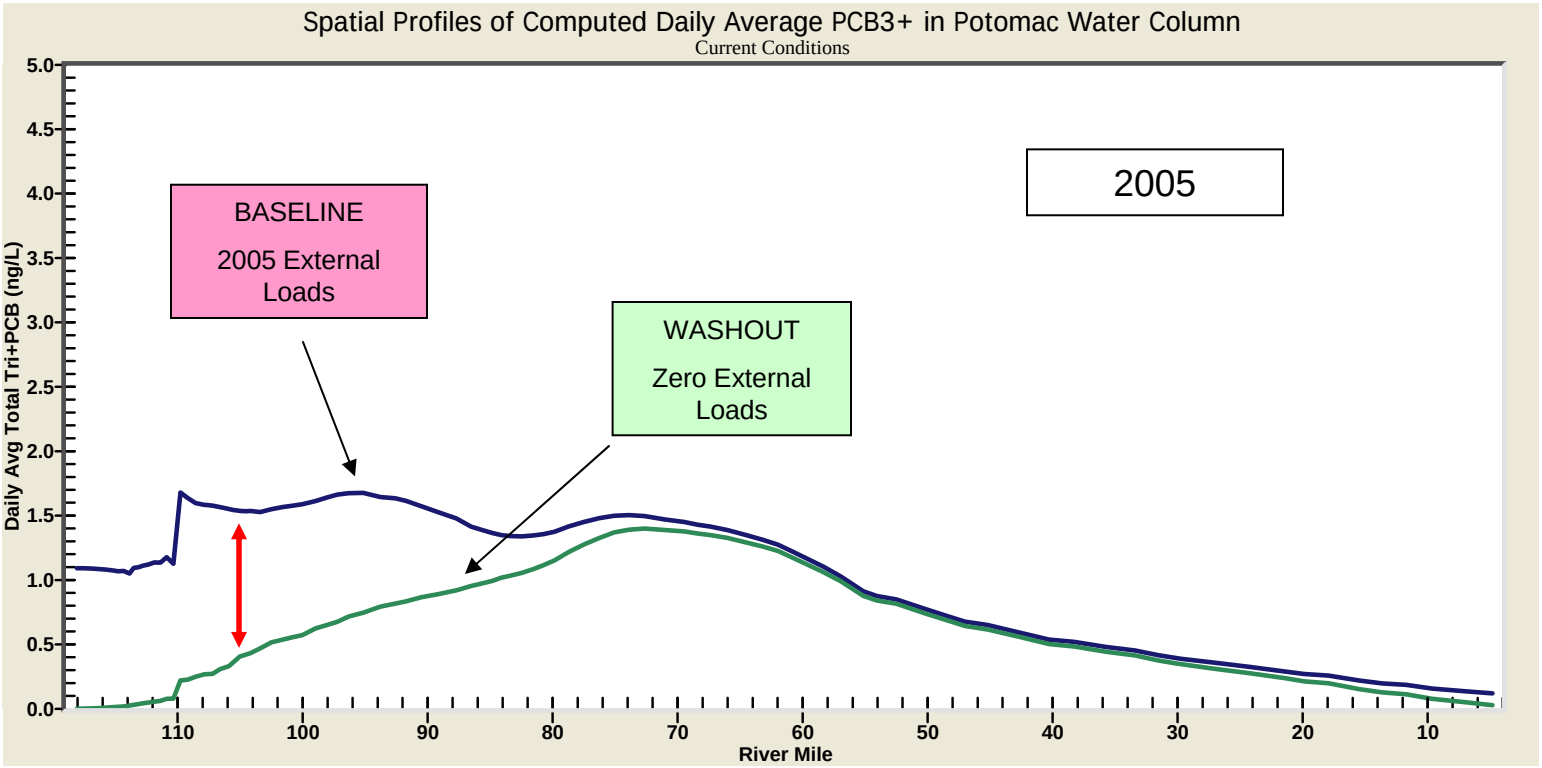

Figure 140. Spatial Profiles of Computed Daily Average PCB3+ in Potomac Water Column in First Year of 100-Year Simulation

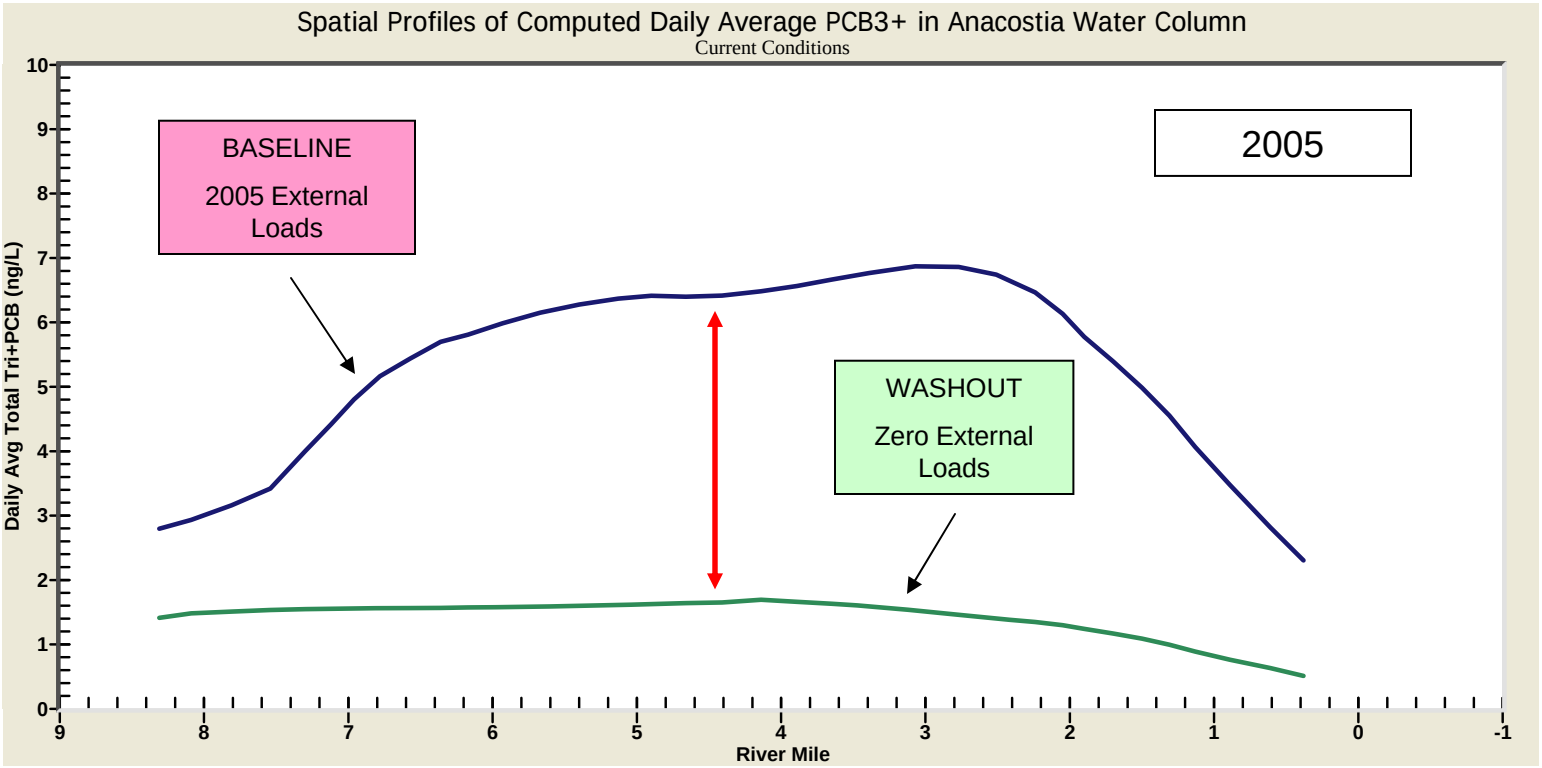

Figure 141. Spatial Profiles of Computed Daily Average PCB3+ in Anacostia Water Column in First Year of 100-Year Simulation

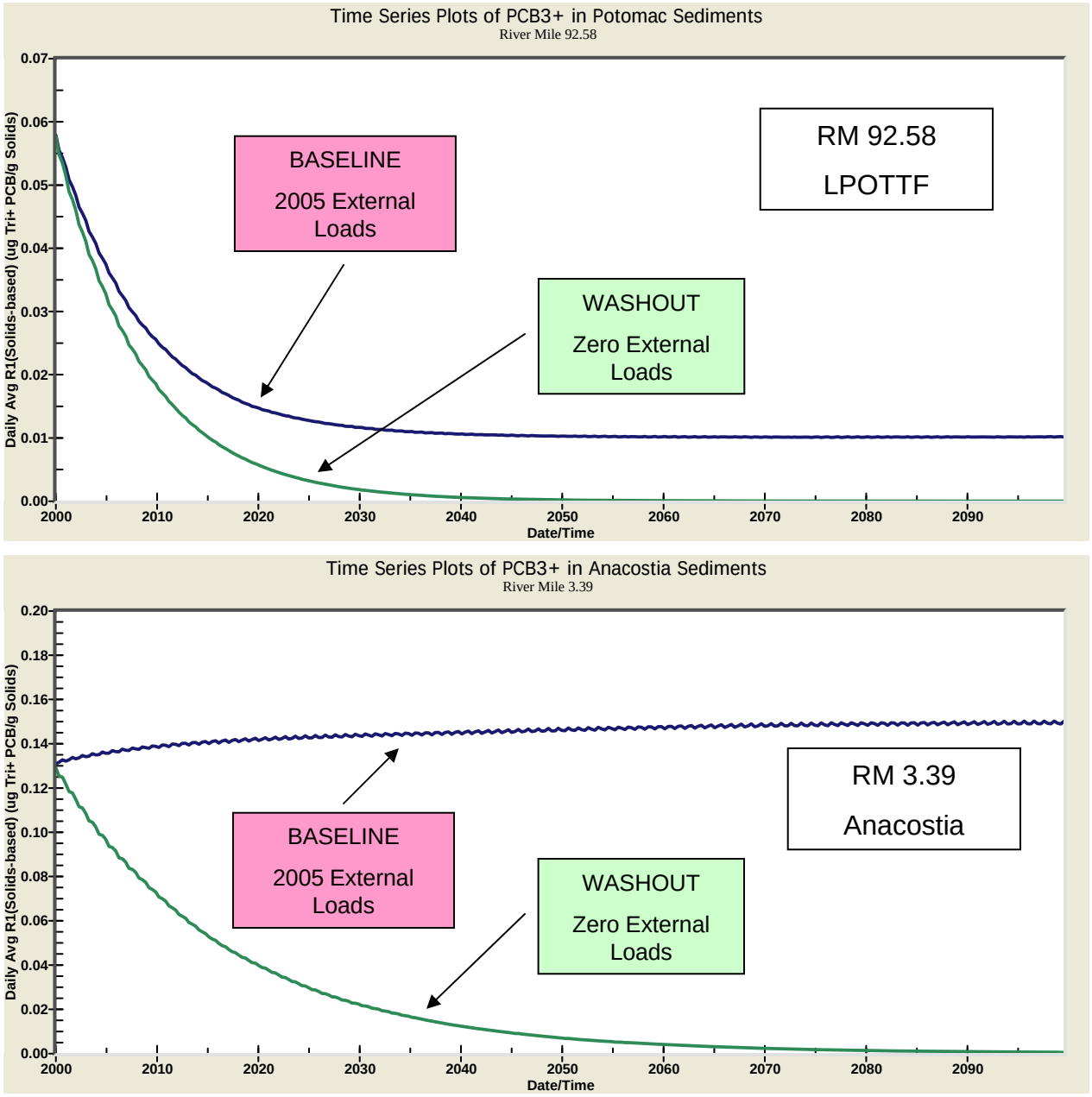

Figure 142. Long-Term Time Series Plots of PCB3+ in Potomac (top) and Anacostia (bottom) Sediments

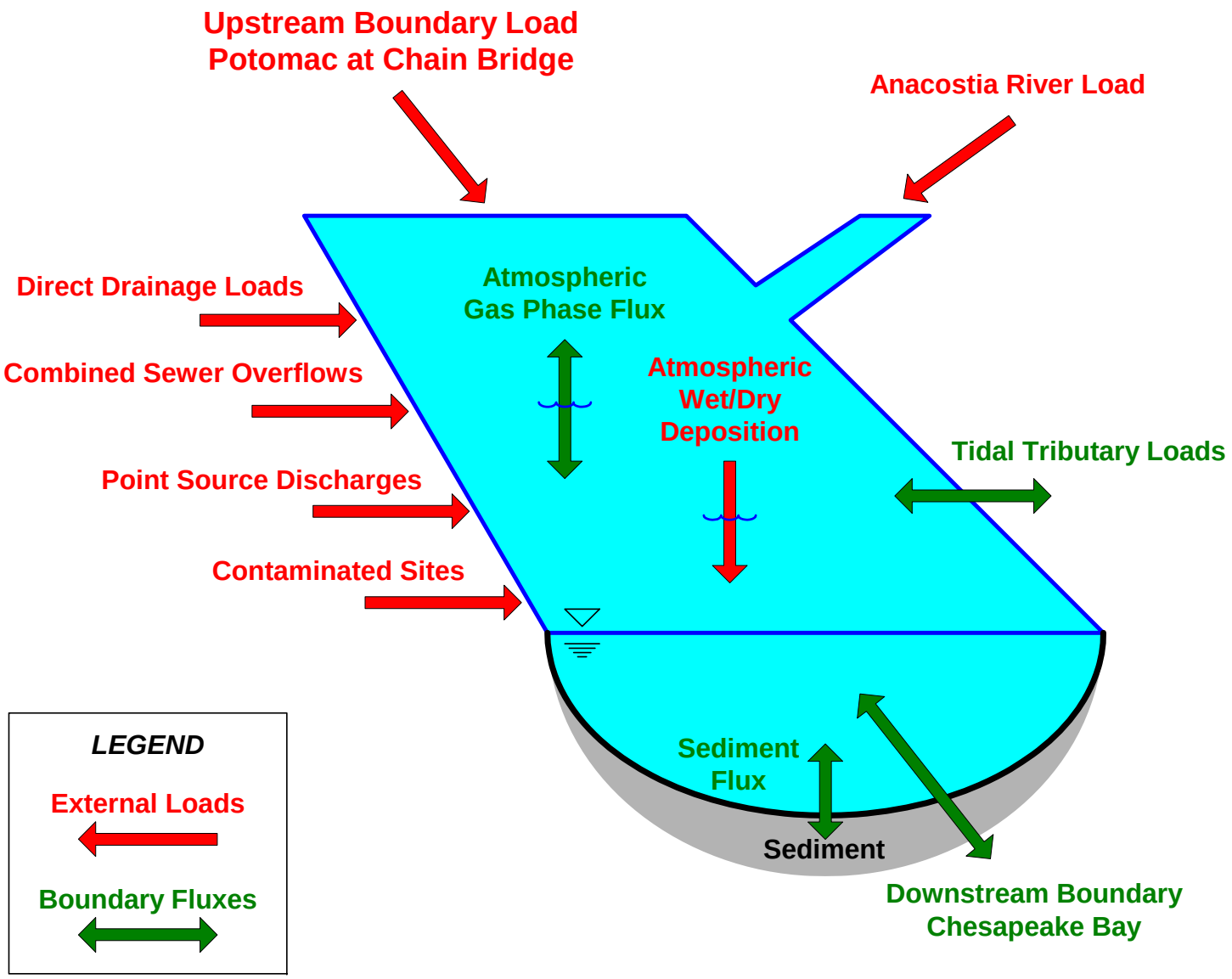

Figure 143. Principal PCB3+ Mass Loads and Fluxes in the Potomac River Estuary

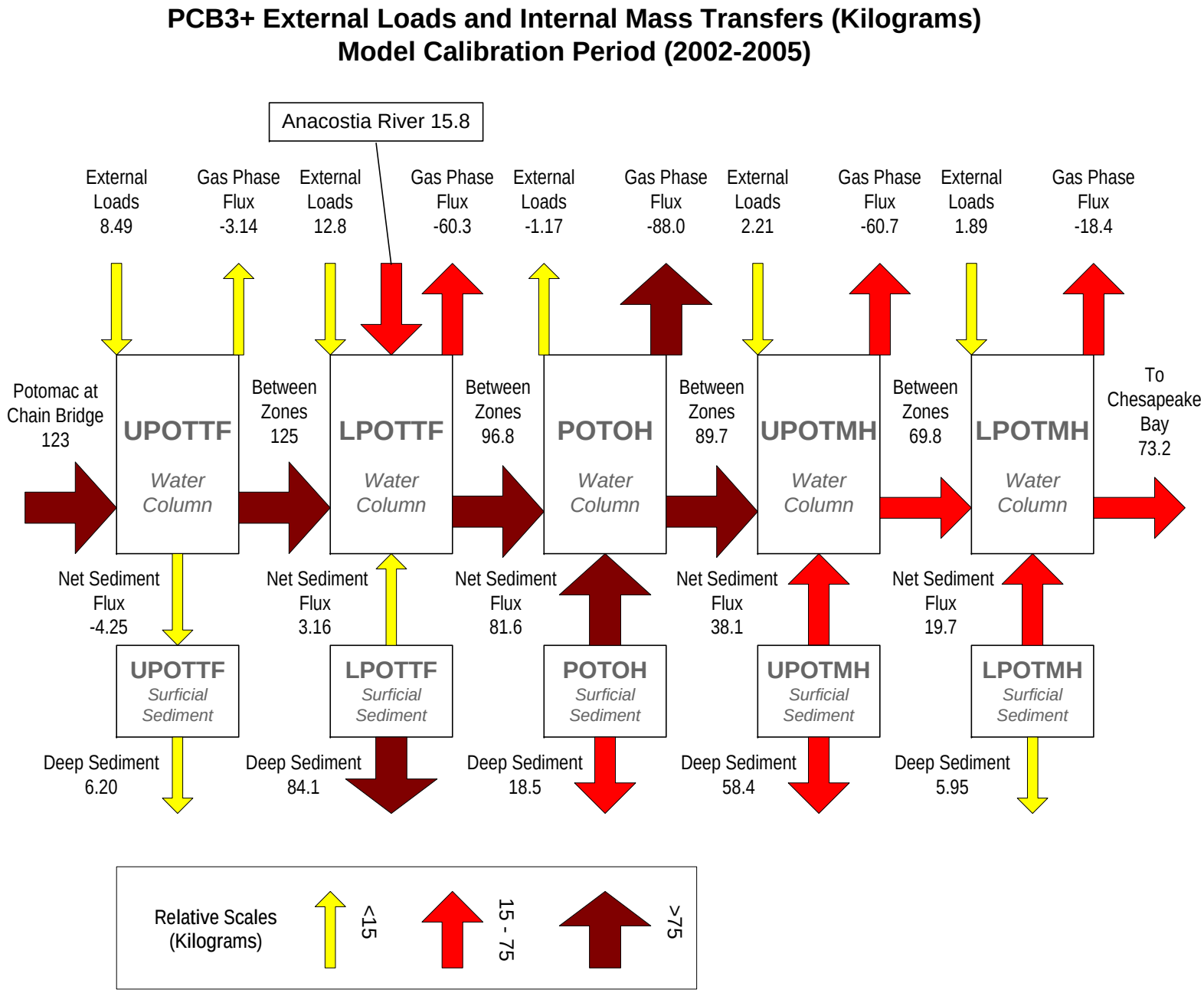

Figure 144. Mass Balance Components for PCB3+ in the Potomac for the Model Calibration Period (2002-2005)

PCB3+ External Loads and Internal Mass Transfers (Kilograms)
Model Calibration Period (2002-2005)

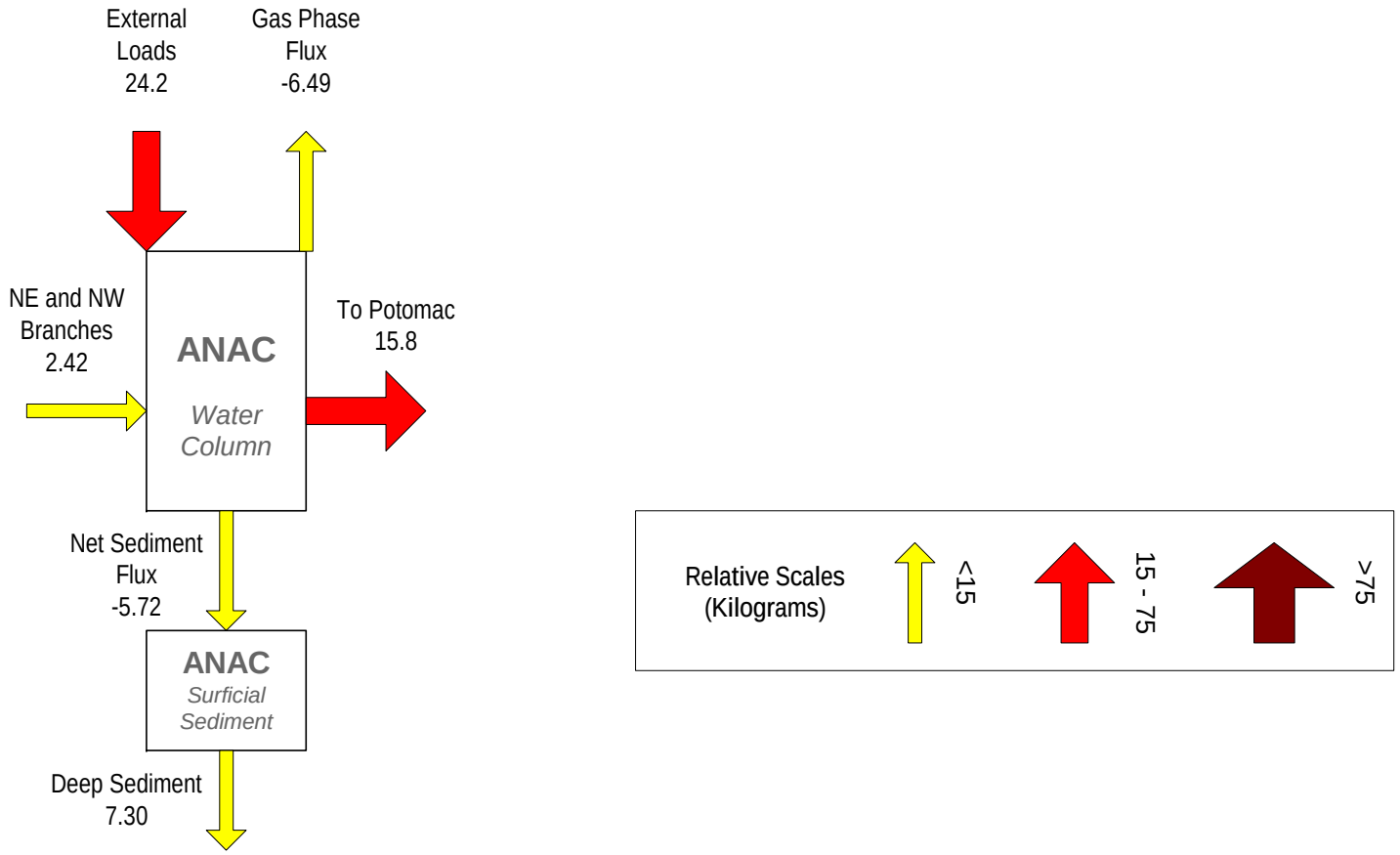

Figure 145. Mass Balance Components for PCB3+ in the Anacostia for the Model Calibration Period (2002-2005)